IRON HOMEOSTATIC SYSTEMS AND

IRON LIMITATION RESPONSES IN BACTERIA

A dissertation

Presented to the Faculty of the Graduate School

of Cornell University

in Partial Fulfillment of the Requirements for the Degree of

Doctor of Philosophy

By

Hualiang Pi

May 2018

IRON HOMEOSTATIC SYSTEMS AND

IRON LIMITATION RESPONSES IN BACTERIA

Hualiang Pi, Ph.D.

Cornell University 2018

Iron is required for most bacteria but its bioavailability is extremely low. So iron acquisition has become a major challenge in bacterial physiology. Iron acquisition includes uptake systems for elemental iron, ferric citrate, and various ferric-siderophore complexes. Iron-mediated regulation takes place at multi-levels: transcriptional, post-transcriptional, and translational. These regulatory systems enable bacteria to achieve homeostatic balance with iron (Chapter 1).

Iron is also toxic at elevated levels. Recent results revealed that Fe(II) exporters play a crucial role in preventing iron overload. These include P_{1B}-type ATPases, cation diffusion facilitators, major facilitator superfamily proteins, and membrane bound ferritin-like proteins (Chapter 2). Among these systems, FrvA is a virulence factor in *Listeria monocytogenes*. The characterization of FrvA as an Fe(II) efflux transporter provides the first direct evidence linking iron efflux to bacterial pathogenesis. Furthermore, FrvA is a high-affinity Fe(II) exporter and its expression imposes severe iron starvation in *Bacillus subtilis* (Chapter 3). Thus it has been employed as an inducible genetic tool to study iron limitation responses.

Iron acquisition and homeostasis systems need to be tightly regulated to ensure sufficiency for biological functions but not excess that would trigger intoxication. The ferric uptake regulator (Fur) monitors intracellular iron levels and plays a central role in maintaining bacterial iron homeostasis. However, it is unclear whether Fur-regulated genes are derepressed coordinately or in a sequential manner upon iron starvation. Here the iron limitation responses were characterized in *B. subtilis* (Chapter 4). In particular, the Fur-regulated genes are induced in three sequential waves in response to iron depletion: (i) cells increase their capacity for iron import from common sources of iron in the environment; (ii) cells turn on high-affinity siderophore-mediated import systems to scavenge iron; (iii) as iron levels decrease further, cells activate an iron-sparing response to remodel their proteome. This graded response correlates with in vivo occupancy of Fur protein and can be explained, at least in part, as a direct effect of differences in operator binding affinity of Fur protein. These results provide insights into the distinct roles of Fur-target genes and contribute to our understanding of bacterial metalloregulatory systems.

BIOGRAPHICAL SKETCH

Hualiang Pi was born in Yuanjiang, Hunan in China. She graduated from Hunan Normal University with a BS in biology education and received a MS degree in biochemistry from University of Oklahoma in December of 2010. After graduation, she worked as a research associate in a structural biology laboratory at University of Oklahoma. In 2011, Hualiang moved with her family to South Bend, Indiana, where she worked in a bioorganic chemistry and biochemistry laboratory at University of Notre Dame.

In 2014, Hualiang decided to pursue a doctorate in microbiology at Cornell University. She joined the research group of Prof. John D. Helmann and worked on bacterial iron homeostasis using *bacillus subtilis* as a model organism. After completion of her PhD degree, she will stay in Helmann laboratory as a postdoctoral associate to finish up two projects while waiting for her next journey.

For Mom, Dad, Qiaobin, Ruby, and Fred

ACKNOWLEDGEMENTS

There are so many people to whom I like to express my sincere appreciation and gratitude.

First, I would like to thank my advisor, Prof. John D Helmann, for his guidance, support and understanding. I greatly appreciate that he has always been helpful, encouraging and positive. He is a fantastic mentor. I have learned a great deal from him ranging from communication skills, experimental design, scientific writing, critical thinking, and many more. I have really enjoyed working with him during this journey.

I would like to thank my committee members: Profs. Ailong Ke and Joseph E Peters for taking the time out of their busy schedule to attend my seminars and committee meetings and offering feedbacks and constructive comments.

I would like to thank all the members in the Helmann lab, especially Drs. Ahmed Gaballa and Pete Chandrangsu, for their help, comments, great ideas, and support. It has always been a pleasure and a wonderful experience to work with each one of them.

Last but very importantly, I would like to thank my parents for their endless love and support. I would like to thank my husband, Dr. Qiaobin Xiao, for always being supportive in all my endeavors. I would like to thank my two amazing kids, Ruby and Fred. They are my inspiration and motivation for everything. Nothing can be more satisfying than watching them grow.

TABLE OF CONTENTS

LIST OF TABLES

LIST OF FIGURES

Chapter 1 Iron acquisition and homeostasis in bacteria

1.1 Abstract

Iron is required for many biological processes but poses toxicity to cells when present in excess. Various iron-mediated stress systems respond to changes in environmental iron availability. Iron limitation induces acquisition systems to scavenge iron from the environment and activates systems to mobilize and prioritize iron utilization; while iron excess induces storage and efflux systems to maintain non-toxic levels of intracellular free labile iron. These responses must be carefully coordinated to ensure effective iron homeostasis. In this chapter, the iron limitation responses are reviewed including various uptake systems and regulatory control mechanisms. The focus is *Escherichia coli* and *Bacillus subtilis* since iron homeostasis has been well studied in these two model organisms.

1.2 Iron, a transition metal essential to life

Iron, a first-row transition metal, is one of the most abundant metals. It exists in two redox states: the soluble reduced ferrous form (Fe^{2+}) and the insoluble oxidized ferric form (Fe^{3+}). Both forms can adopt high or low spin of electronic states and cover a diverse range of redox potentials. For these properties, iron is considered as an ideal choice for incorporation into enzymes as a cofactor, especially during the evolution of early life in anoxic environment (Ilbert & Bonnefoy, 2013), where iron was predominantly in the soluble reduced ferrous form. Iron is essential for almost all organisms and is required for many enzymes that can be categorized into three groups: (i) mono- and di-nuclear iron enzymes, (ii) iron-sulfur cluster proteins, and (iii) heme-containing proteins. These iron-requiring enzymes participate in a wide range of biological functions such as the tricarboxylic acid cycle, N_2 fixation, electron transfer, DNA

synthesis and repair, and gene regulation (Andrews *et al.*, 2003). To survive and propagate, bacterial cells need to maintain intracellular iron levels between 10^{-7} and 10^{-5} M. However, in many natural environments, particularly under physiological pH and aerobic conditions, most of iron is in the insoluble oxidized ferric form and its bioavailability (~10^{-18} M) is extremely low. So iron acquisition is a major challenge in bacterial physiology.

However, excess iron is toxic due to its participation in Fenton chemistry (Imlay, 2003). The redox potential of iron allows ferrous iron to react with dioxygen or peroxide, which generates highly reactive hydroxyl radicals that damage macromolecules such as DNA, proteins and fatty acids, resulting in disruption of metabolic functions and ultimately cell death (Park *et al.*, 2005). Elevated levels of intracellular iron may also be toxic due to the ability of iron to compete with other transition metals (e.g. manganese), for binding to metal-dependent enzymes or regulators, resulting in malfunction and inactivation of these proteins (Imlay, 2014, Barwinska-Sendra & Waldron). Therefore, iron acquisition and homeostasis systems need to be tightly regulated to ensure sufficiency for cell growth but not excess that would trigger intoxication.

1.3 Bacterial iron acquisition systems

To combat iron limitation, bacteria have developed a broad set of acquisition systems to scavenge iron from the environment. Different systems acquire iron from different sources and may function under different environmental conditions. In general there are five type of iron sources: (i) elemental iron (ferrous or ferric iron), (ii) ferric citrate, (iii) ferric siderophore complexes, and (iv) host iron complexes such as heme, heme-containing proteins, transferrin, and lactoferrin. The last group is mainly utilized by pathogenic bacteria and beyond the scope of discussion here. The uptake systems dedicated to various iron sources except the last one are reviewed below in the model organisms *E. coli* and *B. subtilis*.

1.3.1 Elemental iron uptake

Elemental iron uptake systems are ubiquitous in many bacteria and include two major systems: EfeUOB and FeoABC (Kammler *et al.*, 1993, Grosse *et al.*, 2006, Cao *et al.*, 2007). *E. coli* contains both systems, EfeUOB dedicated to ferric iron uptake while FeoAB specific for ferrous iron uptake. However, there is a frameshift mutation in the *efeUOB* operon in some non-pathogenic strains such as *E. coli* K-12 resulting in this system being non-functional (Cao *et al.*, 2007). The membrane component EfeU is a homolog of the high affinity ferric iron permease Ftr1p in *Saccharomyces cerevisiae*. The periplasmic proteins EfeO and EfeB are both required for the function of EfeU and may participate in ferrous iron oxidation. Another system FeoABC, first discovered in *E. coli* K-12, is the major ferrous iron importer under anaerobic-microaerophilic or low pH conditions. FeoA is a small monomeric soluble protein with a SH3 motif; FeoB is the ferrous iron permease with an N-terminal G-protein domain and a C-terminal transmembrane domain; FeoC is a cytoplasmic Fe-S dependent protein and was shown to form a complex with the permease FeoB and may be required for FeoB function.

Unlike the *E. coli* EfeUOB system that imports ferric iron only, the *B. subtilis* EfeUOB (also known as YwbLMN) system transports both ferric and ferrous iron(Miethke *et al.*, 2013). This system is similar to the copper oxidase-dependent ferric iron import system in *Saccharomyces cerevisiae*. Its working model has been proposed: the hemoprotein EfeB serves as a peroxidase and catalyzes ferrous iron oxidation; the lipoprotein EfeO scavenges ferric iron from either EfeB or the environment and transfers the bound ferric iron to the membrane permease EfeU probably through protein-protein interaction; EfeU selectively transports ferric iron into the cytosol with a K_M value of ~9 X 10^{-7} M (Miethke *et al.*, 2013). It is the only known system dedicated to elemental iron transport in *B. subtilis* and is required for cell growth in iron-limiting minimal medium without citrate in *Bacillus* laboratory strains, which are unable to produce the mature siderophore bacillibactin due to an *sfp* null mutation (Ollinger *et al.*, 2006). A recent study discovered that an elemental acquisition factor (efe) might be also involved in iron uptake. This factor is

present under iron-sufficient conditions and its regulation is independent of Fur (Roy & Griffith, 2017). The EfeUOB system is required for its activity (Roy & Griffith, 2017), but this factor is yet characterized and its regulation is unknown.

1.3.2 Ferric citrate uptake

The solubility of ferric iron is very low (10^{-18} M). To achieve iron sufficient for cell growth, bacteria utilize iron chelators as solubilizing agents. The small molecule citrate chelates ferric iron with a relatively high affinity ($10^{-17.7}$ M) and serves as one of the solubilizing agents (Ollinger *et al.*, 2006). Citrate forms multinuclear complexes with ferric iron in neutral aqueous solution, including ferric citrate, ferric di-citrate, diferric di-citrate, and triferric tricitrate (Silva *et al.*, 2009). The ferric citrate import system FecABCDE is well characterized in *E. coli* and is well conserved in many gram-negative bacteria. The structure of the outer-membrane protein FecA bound to citrate alone, ferric citrate, or diferric di-citrate has been determined in *E. coli* (Ferguson *et al.*, 2002, Yue *et al.*, 2003). FecA consists of a β-barrel and a globular domain that serves as a cork or plug. It plays dual roles: it transports ferric citrate into the periplasm and its binding to ferric citrate or diferric di-citrate triggers conformational changes of the complex resulting in transcription induction of the *fecABCDE* operon (Ferguson *et al.*, 2002, Yue *et al.*, 2003). After being translocated into periplasm, ferric citrate is then imported into the cytosol by the ABC (ATP binding cassette) transporter system FecBCDE. FecB is the periplasmic binding protein for ferric citrate; Both FecC and FecD are inner membrane transporters; and FecE is the ATPase responsible for ATP hydrolysis (Harle *et al.*, 1995).

Gram-positive bacteria, such as *B. subtilis*, lack the outer membrane and have no need for the outer-membrane transporters. *B. subtilis* encodes a similar ferric citrate ABC tranport system YfmCDEF (renamed as FecCDEF to reflect its physiological role in ferric citrate uptake, see Chapter 4). FecC (or YfmC) is a substrate binding protein for ferric citrate; both FecD (or YfmD) and FecE (or YfmE) are membrane transporters; and FecF (or YfmF) is the ATPase (Ollinger *et al.*, 2006). This system is required for optimal

growth in iron-starvation minimal medium with supplement of citrate (Ollinger *et al.*, 2006). It is widespread in many gram-positive bacteria with some exceptions such as *Bacillus cereus*. *B. cereus* encodes a unique ferric citrate uptake system FctABC (Fukushima *et al.*, 2012). FctA and FctB are two putative membrane permeases. FctC is a ferric citrate binding protein. FctC binds triferric tricitrate and diferric di-citrate but not ferric di-citrate, ferric citrate, or iron-free citrate. Intriguingly, its preferred substrate is triferric tricitrate even though this complex is present as a minor species (<5%) under various conditions tested (Fukushima *et al.*, 2012). FctC binds triferric tricitrate with a very high affinity (K_d ~0.267 nM), much higher than that of most binding proteins to their substrates (Fukushima *et al.*, 2012). For example, the K_d value of FeuA binding to Fe-bacillibactin is only about 19 nM (Zawadzka *et al.*, 2009).

1.3.3 Ferric-siderophore uptake

The most efficient way to acquire iron is through siderophore-mediated uptake systems. Siderophores are small organic compounds that are synthesized by metabolic pathways in many bacteria, fungi, yeasts, and plants. They chelate ferric iron with extremely high affinity (e.g. ~10^{-34} M for enterobactin to bind ferric iron) (Ollinger *et al.*, 2006). Bacteria produce a wide range of siderophores and over 500 different types have been reported to date. Based on their iron-coordinating functional groups, siderophores can be categorized into three major families: hydroxamates, catecholates, and carboxylates. Some siderophores contain more than one functional group, for example, the fluorescent pyoverdines produced by Pseudomonads have both hydroxamate and carboxylate groups (Cornelis, 2010). Each siderophore has a unique structure and specific systems for iron acquisition. In general siderophore-mediated iron acquisition includes five steps: (i) siderophore biosynthesis, (ii) secretion, (iii) formation of ferric-siderophore complexes, (iv) recognition and uptake of ferric-siderophore complexes, and (v) iron release either by degradation or iron reduction.

Different bacterial species, and even different strains within the same species, may produce different siderophores. Indeed, *E. coli* can synthesize up to four different types of siderophores, including

the hydroxamate aerobactin, the catecholates enterobactin and salmochelin, and the mixed-type yersiniabactin. But only some pathogenic isolates can produce all four and the production of siderophores is modulated by environmental factors such as pH, temperature, and carbon source (Valdebenito *et al.*, 2006). By contrast, *B. subtilis* synthesizes only one siderophore, the catecholate bacillibactin, which is structurally similar to enterobactin. Many enzymes involved in siderophore biosynthesis are non-ribosomal peptide synthetases (NRPS) and each siderophore requires a specific NRPS assembly system. For instance, the assembly machinery for enterobactin involves six enzymes (EntABCDEF), whereas bacillibactin synthesis requires five enzymes (DhbACEBF).

The siderophore transport systems in Gram-negative bacteria differ from those in Gram-positive bacteria. Gram-negative bacteria (e.g. *E. coli*) have two membranes: outer and cytoplasmic membrane. There are no ion gradients across outer membrane and TonB-dependent outer-membrane receptors and transporters mediate iron transport through the outer membrane. TonB, a periplasm-spanning protein, transduces the proton motive force of the cytoplasmic membrane to the outer membrane with assistance of two other inner membrane proteins ExbB and ExbD. Once the ferric-siderophore complex is internalized into the periplasmic space, it is translocated across the cytoplasmic membrane through ABC transport systems. For example, in *E. coli*, enterobactin is secreted by EntS and TolC (Furrer et al., 2002;Bleuel et al., 2005), ferric-bound enterobactin is then transported across the outer membrane by the outer-membrane transporter FepA, and the energy required for FepA activity is provided by the TonB–ExbB–ExbD complex (Guerinot, 1994). Once ferric enterobactin is translocated into the periplasm, it is escorted by a periplasmic binding protein FepB and then transported into cytosol through an ABC transport system (FepCDG) (Guerinot, 1994). Fes, a ferric enterobactin esterase, cleaves the complex into three 2,3-dihydroxybenzoyl-l-serine monomers thereby releasing iron in the cytosol (Brickman & McIntosh, 1992).

In contrast to Gram-negative bacteria, Gram-positive bacteria (e.g. *B. subtilis*) have only one lipid membrane and require none of outer-membrane/periplasmic components or energy transducing system. Ferric-siderophore complexes are recognized by membrane binding proteins and then imported into cytosol by ATP-dependent ABC transport systems (Braun and Hantke, 2011). In *B. subtilis*, the endogenous siderophore bacillibactin is secreted by YmfD, a major facilitator superfamily transporter (Miethke *et al.*, 2008). The ferric-bound siderophore complex is then imported into the cytosol by the FeuABC-YusV system and hydrolyzed by the BesA esterase to release iron (Miethke *et al.*, 2006).

Besides the cognate import systems for the endogenous siderophores, bacteria also encode various uptake systems for xenosiderophores that are produced by other microorganisms in the environment. For examples, *B. subtilis* encodes multiple uptake systems for xenosiderophores: FhuBCGD for ferrioxamine and ferrichrome, FpbNOPQ for petrobactin (also known as YclNOPQ, see Chapter 4), YfiYZA for hydroxamate siderophores including schizokinen, anthrobactin, and corprogen. Besider bacillibactin, the FeuABC-YusV system also imports enterobactin that is produced by many enterobacteria (Fig. 1.1).

Why would bacteria develop so many costly systems just for one single function (Fig. 1.1)? One possibility is that different siderophores may have different scavenging capabilities, which depend on their binding affinity and complex stability. Indeed, enterobactin and bacillibactin exhibit extremely high affinity to iron ($10^{-34.3}$ or $10^{-33.1}$ M, respectively), whereas some hydroxamate siderophores (e.g. ferrioxamine b, ferrichrome, and coprogen) have relatively lower affinity to iron ranging from $10^{-25.2}$ to $10^{-27.5}$ M (Ollinger *et al.*, 2006). The stability of different ferric-siderophore complexes also differs. Ferric enterobactin is known as the most stable siderophore complex with a stability constant of 10^{52} (Ahmed & Holmstrom, 2014). The stability of ferric hydroxamate siderophores (e.g. ferrioxamine b or ferrichrome) is relatively lower ($K \sim 10^{29}$-10^{31}) and that of ferric pyoverdine is even lower ($K \sim 10^{24}$) (Ahmed & Holmstrom, 2014). So this is probably how these different siderophore compounds enable bacteria to combat iron limitation within different ecological niches.

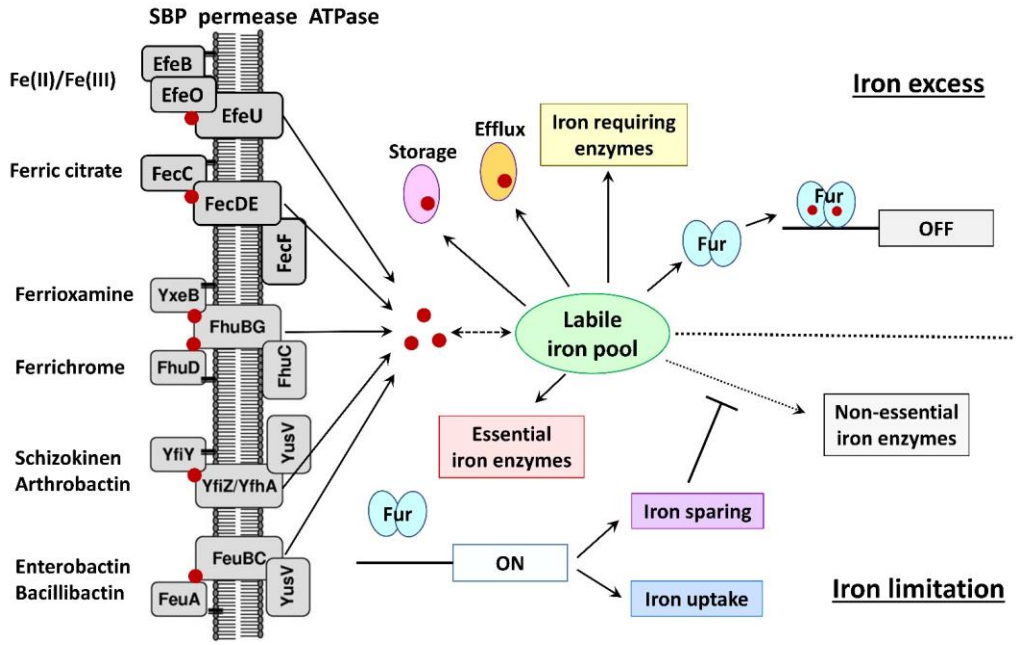

Fig. 1.1 Major iron uptake and homeostatic systems in *B. subtilis*.
When iron is limiting, expression of uptake systems is derepressed to scavenge iron from different iron sources: (i) elemental iron, (ii) ferric citrate, (iii) various ferric-siderophore complexes. Each ABC transporter system consists of a substrate binding protein (SBP), a membrane permease, and a ATPase. To adapt to iron limitation, cell activates the iron sparing response to prioritize iron utilization. This allows access of the limited iron only to the most essential functions by blocking translation of the non-essential iron-requiring enzymes. Under excess iron conditions, all iron-requiring enzymes have access to the labile iron pool. Iron can be either stored for future use or exported by ferrous iron efflux transporter to prevent iron overload. (Modified from (Ollinger *et al.*, 2006))

1.4 Iron-responsive regulatory systems in bacteria

Iron is an essential micronutrient but excess iron is also detrimental. So bacteria require regulatory systems to coordinate pathways for uptake, utilization, storage and efflux. This regulation may take place in multiple levels: transcriptional, post-transcriptional, and translational. The iron-sensing transcription regulators (e.g. ferric uptake regulator, Fur) monitor intracellular iron levels and regulate transcription of systems for iron uptake, storage, and efflux (Fleischhacker & Kiley, 2011, Baichoo *et al.*, 2002). The ‘‘iron-sparing’’ response, mediated by Fur-regulated small RNA, prioritizes iron utilization by translationally inhibiting low priority iron-containing proteins. The RNA binding regulatory role of bacterial aconitase may

provide an additional level of post-transcriptional regulation in response to iron limitation (Pechter *et al.*, 2013, Serio *et al.*, 2006, Alen & Sonenshein, 1999).

1.4.1 Fur, the iron-sensing transcription regulator

Iron-containing transcription regulators are critical in monitoring intracellular iron pools and their affinity to iron defines the borderlines between sufficiency and deficiency (or excess). The ferric uptake regulator Fur was first characterized in *E. coli* as a transcriptional repressor that can be activated by Fe^{2+} and other metal ions *in vitro* but only Fe^{2+} is physiologically relevant (Bagg & Neilands, 1987). Fur is a homodimer and each monomer contains a N-terminal helix-turn-helix motif for DNA binding, a C-terminal dimerization domain, and a metal binding domain with two or three binding sites. In *B. subtilis*, three distinct metal-binding sites were identified (Ma *et al.*, 2012). Site 1 is a structural site with tightly associated Zn(II) that can be only removed by protein denaturation (Mills & Marletta, 2005, Ma *et al.*, 2012). Both site 2 and 3 are Fe(II)-sensing sites with the former playing the major regulatory role (Ma *et al.*, 2012). Dimeric Fur recognizes operators with a DNA consensus sequence known as the Fur box. A classic Fur box is a 19-bp sequence that corresponds to two overlapping 7-1-7 inverted repeat motifs. This 7-1-7 core sequence is the minimal requirement for high-affinity binding by Fur (Baichoo & Helmann, 2002). One Fur dimer binds a 7-1-7 operator while two dimers bind to opposite faces of the DNA helix of the 19-bp Fur box. Both phenomena were observed in different Fur-regulated operator sites *in vitro* (Baichoo & Helmann, 2002). For example, one single dimer binds to the *feuABC* operator site while two dimers occupy the *dhbACEBF* operator region in *B. subtilis*.

Fur is widespread in many bacteria as the key regulator of iron homeostasis. It senses intracellular iron levels and regulates transcription of genes implicated in iron uptake, utilization, storage and efflux in response to iron availability. It is important to note that, in addition to this iron-responsive Fur regulator, other Fur family members play critical roles in peroxide stress (PerR, the peroxide sensor) and maintaining

homeostasis of other metals (Lee & Helmann, 2007), including Mur (Mn(II) sensor) (Troxell & Hassan, 2013), Nur (Ni(II) sensor) (Ahn *et al.*, 2006), and Zur (Zn(II) sensor) (Blindauer, 2015) (Table 1.1). Many bacteria encode multiple Fur paralogs. For instance, *B. subtilis* has three (i.e. Fur, PerR, and Zur) (Lee & Helmann, 2007) and *E. coli* contains two (i.e. Fur and Zur) (Hantke, 2002).

Fur is generally considered as an iron-dependent transcriptional repressor. When iron is replete, Fur binds to its cofactor Fe^{2+} in the cytosol. The resultant holo-Fur binds to its target DNA operators, blocks access of the RNA polymerase to these promoters, and serves as a repressor for its regulated genes. When iron is limiting, Fur loses its cofactor and becomes inactivated. The repression of its regulon is relieved and various homeostasis pathways, particularly numerous iron uptake systems, are induced to scavenge iron and adapt to iron deficiency. There are a few reported examples where holo-Fur functions as a transcriptional activator (Pi *et al.*, 2016, Delany *et al.*, 2004, Nandal *et al.*, 2010), For instance, *E. coli* Fur (Fur_{EC}) positively regulates expression of the iron storage gene *ftnA* through competing against the H-NS repressor under excess iron conditions (Nandal *et al.*, 2010); Fur positively regulates the ferrous iron efflux transporter FrvA in *Listeria mononcytogenes* (Pi *et al.*, 2016). Recently, apo-Fur activation was also proposed as one of its regulation modes (Seo *et al.*, 2014), although there is no experimental validation for this model of activity yet. Nevertheless, the Fur regulon is well characterized in some bacteria, particularly in the two model organisms *E. coli* and *B. subtilis* as exemplified below. These two provide classic examples on the diverse roles that Fur plays to achieve effective iron homeostasis.

1.4.1.1 The Fur regulon in *E. coli* and *B. subtilis*

E. coli Fur (Fur_{EC}) regulates more than 90 genes, ~60 genes of which are involved in siderophore biosynthesis and iron uptake including heme uptake in pathogenic strains. These systems are derepressed to scavenge iron upon iron deprivation. Fur_{EC} also regulates genes involved in iron storage (e.g. bacterioferritin), oxidative stress (e.g. superoxide dismutase, SodB), acid resistance, chemotaxis, and cell

motility (Escolar *et al.*, 1999). In some pathogenic *E. coli* strains, Fur_{EC} regulates transcription of some virulence factors such as colicins, hemolysin, and Shiga-like toxin.

B. subtilis Fur (Fur_{BS}) regulates more than 50 genes, many of which are involved in iron acquisition, including bacillibactin synthesis and transport systems for elemental iron, ferric citrate, bacillibactin/enterobactin, ferrioxamine/ferrichrome, petrobactin, and other xenosiderophores (Ollinger *et al.*, 2006). Fur_{BS} also regulates one of the two heme monooxygenases (i.e. HmoB) (Gaballa & Helmann, 2011). Both monooxygenases are heme-binding proteins. However, neither of them are involved in iron acquisition through heme and their physiological roles remain unclear (Gaballa & Helmann, 2011). In addition, as part of a common strategy against nutrient limitation, cells replace Fe-S protein ferrodoxins with alternative iron-independent flavodoxins to help alleviate iron demand (Merchant & Helmann, 2012). *B. subtilis* encodes two flavodoxins, YkuN and YkuP, and expression of the flavodoxin operon (*ykuNOP*) is under regulation of Fur_{BS} (5, 20).

The Fur regulon may expand further. Recent studies proposed that, besides iron metabolism, the Fur regulatory network may include many other biological processes such as DNA synthesis, energy metabolism, and biofilm formation in *E. coli* and *Vibrio cholerae* (Seo *et al.*, 2014, Davies *et al.*, 2011, Butcher *et al.*, 2011, Chumsakul *et al.*, 2017). This may also apply to the *B. subtilis* Fur regulon under both anaerobic (Chumsakul *et al.*, 2017) and aerobic conditions (see Appendix 2), although future work is needed for validation.

1.4.1.2 The iron sparing response

The early observation that *E. coli fur* mutants were unable to grow on succinate, fumarate or acetate as a sole carbon source suggested a positive regulation by Fur (Hantke, 1987). The mechanism behind this Fur positive regulation has been revealed as part of an “iron-sparing” response, which is mediated by a small RNA RyhB in *E coli* (Masse & Gottesman, 2002). This small RNA RyhB is under negative

regulation of Fur. In the *fur* null mutants, its expression is full derepressed and it represses the translation of succinate dehydrogenase, aconitase, and many other non-essential iron-rich proteins. RhyB functions as an antisense RNA and requires an RNA-binding protein (Hfq) for its activity (Masse & Gottesman, 2002). It binds the complementary regions of its target mRNA through RNA-RNA base pairing and therefore halts translation by blocking the elongating ribosomes on the mRNA. The resultant RhyB-mRNA complex will be then subject to RNA degradation by endoribonucleases (Masse & Gottesman, 2002). When the intracellular iron level is low, bacterial cells activate this adaptive response to reconfigure their proteome and to conserve iron by blocking translation of the non-essential iron-requiring enzymes and permitting access of iron only to the most essential functions.

This iron sparing response is widespread and has been reported in many bacterial species such as *Vibrio cholerae*, *Shigella flexneri*, *Pseudomonas aeruginosa*, and *B. subtilis* (Masse *et al.*, 2007, Gaballa & Helmann, 2011). *Vibrio cholerae* and *Shigella flexneri* encodes a very similar RhyB analog that mediates this response upon iron depletion (Masse *et al.*, 2007). *Pseudomonas aeruginosa* encodes two sRNA analogs (*prrF1* and *prrF2*) for this function (Wilderman *et al.*, 2004). *B. subtilis* encodes a Fur-regulated small RNA FsrA that coordinates this response with the assistance of three putative RNA chaperones (FbpABC) (Gaballa & Helmann, 2011). A similar response was also observed in *Saccharomyces cerevisiae*. Unlike bacteria, *S. cerevisiae* utilize RNA-binding protein to remodel cellular proteome when the intracellular iron is limiting (Puig *et al.*, 2005).

1.4.1.3 The graded response of the Fur regulon

In response to stress stimuli, transcriptional regulators may not activate their regulon all at once, but rather in a stepwise manner. Indeed, the graded response of the zinc uptake regulator Zur has been revealed in the event of zinc limitation (Shin et al., 2011;Shin & Helmann, 2016). Recently, this has also been appreciated in case of iron limitation in *B. subtilis* (Pi & Helmann, 2017). As cells transition from iron

sufficiency to deficiency, the Fur-regulated genes are induced in three sequential waves. First, cells express uptake systems for elemental iron and low chelated iron (e.g. ferric citrate) to prevent iron deficiency. Second, cells turn on high-affinity siderophore-mediated import systems to scavenge iron and express iron-independent flavodoxins to replace iron-requiring ferredoxins. Third, as iron levels decline further, cells activate the iron sparing response to remodel their proteome and conserve iron (Pi & Helmann, 2017). These results illustrate how bacterial cells prioritize their responses to iron limitation and provide important insights into distinct roles of the Fur-target genes and regulation mechanism of this and other metal sensors.

1.4.2 Other iron-responsive transcription regulators

Fur is the master iron regulator in many bacteria, however, some bacteria employ other iron-dependent transcription regulators including Irr, RirA, and DtxR (Table 1.1). Irr, iron response regulator, is also a member of the Fur superfamily. It was first characterized in *Bradyrhizobium japonicum* (Hamza et al., 2000). It is the major transcription control of iron homeostasis in *Rhizobium* and other Alpha-Proteobacteria (Rodionov *et al.*, 2006, Todd *et al.*, 2006, Yang *et al.*, 2006, Small *et al.*, 2009). Unlike Fur that directly senses intracellular iron levels, Irr monitors the status of heme biosynthesis. It directly interacts with ferrochelatase that catalyzes the last step of heme biosynthesis: incorporation of iron into protoporphyrin IX (PPIX, heme precursor). Under high iron conditions when heme levels are also high, Irr interacts with ferrochlatase and heme, which leads to proteolysis of the Irr protein. When iron is limiting and heme levels are also low, Irr does not bind to the PPIX-ferrochelatase complex. Apo-Irr is then released and functions as a regulator for transcription of genes involved in iron uptake, heme utilization, and TCA cycle ((Todd *et al.*, 2006, Small *et al.*, 2009).

Table 1.1 Three families of iron-responsive transcription regulators and their members

Protein	Representative organisms	Cofactor	Function	Reference
Fur family				
Fur	*Escherichia coli* *Bacillus subtilis*	Fe(II)	Iron homeostasis	(Bagg & Neilands, 1987, Ollinger *et al.*, 2006)
Mur	*Sinorhizobium meliloti* *Rhizobium leguminosarum*	Mn(II)	Manganese homeostasis	(Platero *et al.*, 2007, Diaz-Mireles *et al.*, 2004)
Zur	*Escherichia coli* *Bacillus subtilis*	Zn(II)	Zinc homeostasis	(Herbig & Helmann, 2001, Patzer & Hantke, 1998)
PerR	*Bacillus subtilis*	Mn(II) Fe(II)	Peroxide detoxification	(Herbig & Helmann, 2001)
Nur	*Streptomyces coelicolor*	Ni(II)	Nickel homeostasis	(Ahn *et al.*, 2006)
Irr	*Bradyrhizobium japonicum*	Heme	Iron homeostasis	(Hamza *et al.*, 2000)
Rrf2 family				
RirA	*Rhizobium leguminosarum*	Fe-S cluster	Iron homeostasis	(Todd *et al.*, 2002)
NsrR	*Streptomyces coelicolor*	NO	nitric oxide detoxification	(Volbeda *et al.*, 2017)
IscR	*Escherichia coli*	Fe-S cluster	Fe-S cluster biosynthesis	(Schwartz *et al.*, 2001)
CymR	*Staphylococcus aureus*	cysteine	cysteine metabolism	(Soutourina *et al.*, 2009)
RsrR	*Streptomyces venezuelae*	redox changes	NAD(P)H metabolism	(Munnoch *et al.*, 2016)
DtxR family				
DtxR	*Corynebacterium diphtheriae*	Fe(II)	Iron homeostasis	(D'Aquino *et al.*, 2005)
IdeR	*Mycobacterium tuberculosis*	Fe(II)	Iron homeostasis	(Pandey & Rodriguez, 2014)
SirR	*Staphylococcus epidermidis*	Fe(II)	Iron homeostasis	(Massonet *et al.*, 2006)
MntR	*Bacillus subtilis*	Mn(II)	Manganese homeostasis	(Huang *et al.*, 2017)
TroR	*Treponema pallidum*	Mn(II)	Manganese homeostasis	(Posey *et al.*, 1999, Liu *et al.*, 2013)
ScaR	*Streptococcus gordonii*	Mn(II)	Manganese homeostasis	(Jakubovics *et al.*, 2000)
EfaR	*Enterococcus faecalis*	Mn(II)	Manganese homeostasis	(Abrantes *et al.*, 2013)

RirA, rhizobial iron regulator, is another iron-responsive regulator found in the symbiotic Rhizobia. Similar to Fur, RirA functions as a transcription repressor, however, it monitors intracellular Fe-S cluster levels instead of iron levels. It is a member of the Rrf2 transcriptional regulator family (Table 1.1). A classic example of this family is the *E. coli* IscR (iron-sulfur cluster regulator) that monitors status of Fe-S cluster assembly (Schwartz *et al.*, 2001). Other members are also involved in cysteine metabolism, nitric oxide detoxification, and NAD(P)H metabolism (Table 1.1). RirA plays a central role in regulating siderophore biosynthesis and iron uptake systems in *Rhizobium leguminosarum*, Sinorhizobium *melioti*, and *Agrobacterium tumefaciens* (Todd *et al.*, 2002, Viguier *et al.*, 2005, Chao *et al.*, 2005, Ngok-Ngam *et al.*, 2009), although its regulation mechanism is unclear.

DtxR is a family of metalloregulatory proteins found in Gram-positive bacteria with high GC content. It was originally discovered as a diphtheria toxin regulator in *Corynebacterium diphtheriae* (D'Aquino *et al.*, 2005). It shares very low sequence homology to the Fur proteins, however, the DtxR regulon closely resembles that of Fur. Besides production of diphtheria toxin, DtxR regulates siderophore synthesis, iron uptake, and heme oxygenases. It also regulates an AraC family repressor protein RipA that mediates the iron sparing response (Wennerhold & Bott, 2006, Wennerhold *et al.*, 2005). There are also two other members of the DtxR family: IdeR and SirR, which coordinate global iron regulation in *Mycobacteria* (Pandey & Rodriguez, 2014) and *staphylococci* (Massonet *et al.*, 2006), respectively. In addition to these iron-responsive regulators, the DtxR-family proteins also play central roles in manganese homeostasis, including MntR in *B. subtilis* (Huang et al., 2017) and *B. anthracis* (Golynskiy et al., 2006), TroR in *Treponema pallidum* (Posey *et al.*, 1999, Liu *et al.*, 2013), ScaR in *Streptococcus gordonii* (Jakubovics et al., 2000), EfaR in *Enterococcus faecalis* (Abrantes et al., 2013) (Table 1.1).

1.4.3 Aconitase-mediated post-transcriptional regulation

Eukaryotic Iron regulatory RNA binding proteins (IRPs) have been well appreciated as a post-transcriptional regulatory network orchestrating iron metabolism in response to fluctuations in iron availability and oxidative stress in eukaryotes (Eisenstein, 2000, Sanchez *et al.*, 2006, Rouault, 2006, Wallander *et al.*, 2006, Leipuviene & Theil, 2007, Rupani & Connell, 2016). IRPs bind to relatively conserved stem-loop structures known as iron-responsive elements (IREs) in the untranslated region of specific transcripts. There are two families of eukaryotic IRPs, IRP-1 and IRP-2. IRP-1 is identical to the cytosolic aconitase and can function as either an enzyme or iron regulatory RNA binding protein. In contrast, IRP-2 is the major iron sensor with no aconitase activity. Some aconitases (ACNs) are well conserved in bacteria and eukaryotes. It has been reported that ACNs bind to IRE-like stem-loop structures in bacteria as well as the eukaryotic IRE consensus sequences (Tang *et al.*, 2002, Pechter *et al.*, 2013, Serio *et al.*, 2006, Alen & Sonenshein, 1999, Austin & Maier, 2013, Michta *et al.*, 2014, Austin *et al.*, 2015, Tang *et al.*, 2004).

B. subtillis encodes one aconitase (CitB). CitB is bifunctional, serving as an aconitase enzyme in the Krebs citric acid cycle and an RNA binding regulatory protein. When intracellular iron is sufficient, CitB is in the 4Fe-4S cluster holo-form and functions as an active enzyme; under iron deficiency or oxidative stress conditions, the labile 4Fe-4S cluster is dissembled and apo-form of CitB becomes a RNA binding protein with no aconitase activity. It can bind either 5’ UTR or 3’ UTR of mRNAs to block initiation of translation or promote mRNA stability, respectively. A few targets were identified for CitB: *citZ* (citrate synthase), *gerE* (a transcriptional regulator involved in sporulation), *qoxD* (iron-containing cytochrome aa3 oxidase), and *feuABC* (iron uptake system) (Pechter *et al.*, 2013, Serio *et al.*, 2006, Alen & Sonenshein, 1999).

E. coli has two aconitases, AcnA and AcnB. AcnA is very similar to the human IRP1 with 53% sequence identity while AcnB has very low similarity to AcnA or the eukaryotic IRPs. Both AcnA and AcnB can bind to an IRE-like sequence in the 3' UTR of their own mRNA to promote mRNA stability (Tang & Guest, 1999, Benjamin & Masse, 2014). In *Salmonella enterica* serovar Typhimurium, AcnB tunes the production of FliC by interacting with the *ftsH* transcript (encodes an ATP-dependent protease) in response to oxidative stress (Rupani & Connell, 2016).

Interestingly, Fur positively regulates ACNs through the iron sparing response as shown in both *E. coli* and *B. subtilis*. Future work is needed to further dissect the ACN regulons, to define their physiological functions in bacterial iron homeostasis and oxidative stress, and to characterize the correlation among the Fur transcriptional regulation, the small-RNA-mediated iron sparing response, and the ACN post-transcriptional regulation. These would be of immense significance to the bacterial iron physiology field.

1.5 Summary

It is of critical importance that bacterial cells control the balance of iron due to the nature of this micronutrient: essential but toxic. Numerous strategies have been employed not only to ensure sufficient quantity to support growth but also to prevent iron intoxication (Fig. 1.1). Summarized below are the five crucial strategies.

(i) Iron import systems enable bacteria to scavenge iron from different sources in the environment (e.g. elemental iron, low-affinity chelated iron (ferric citrate), high-affinity chelated iron (siderophore and xenosiderophores)), and host iron complexes and enable bacteria to combat iron limitation within different ecological niches;

(ii) Iron sparing responses allow cells to prioritize iron utilization and permit functionality of the essential iron-requiring enzymes when iron is scarce;

(iii) Iron storage systems sequestrate excess iron from the cytosol to alleviate toxicity and also provide a source of iron that can be mobilized in times of iron limitation (Chapter 2);

(iv) Iron efflux systems export excess iron from the cytosol and prevent iron intoxication (Chapter 2 and 3);

(v) Iron responsive regulatory systems coordinate expression of these iron homeostatic systems above in response to iron availability.

1.6 References

Abrantes, M.C., J. Kok & F. Lopes Mde, (2013) EfaR is a major regulator of Enterococcus faecalis manganese transporters and influences processes involved in host colonization and infection. *Infection and immunity* **81**: 935-944.

Ahmed, E. & S.J. Holmstrom, (2014) Siderophores in environmental research: roles and applications. *Microbial biotechnology* **7**: 196-208.

Ahn, B.E., J. Cha, E.J. Lee, A.R. Han, C.J. Thompson & J.H. Roe, (2006) Nur, a nickel-responsive regulator of the Fur family, regulates superoxide dismutases and nickel transport in Streptomyces coelicolor. *Molecular microbiology* **59**: 1848-1858.

Alen, C. & A.L. Sonenshein, (1999) Bacillus subtilis aconitase is an RNA-binding protein. *Proc Natl Acad Sci U S A* **96**: 10412-10417.

Andrews, S.C., A.K. Robinson & F. Rodriguez-Quinones, (2003) Bacterial iron homeostasis. *FEMS microbiology reviews* **27**: 215-237.

Austin, C.M. & R.J. Maier, (2013) Aconitase-mediated posttranscriptional regulation of Helicobacter pylori peptidoglycan deacetylase. *Journal of bacteriology* **195**: 5316-5322.

Austin, C.M., G. Wang & R.J. Maier, (2015) Aconitase Functions as a Pleiotropic Posttranscriptional Regulator in Helicobacter pylori. *Journal of bacteriology* **197**: 3076-3086.

Bagg, A. & J.B. Neilands, (1987) Ferric uptake regulation protein acts as a repressor, employing iron (II) as a cofactor to bind the operator of an iron transport operon in Escherichia coli. *Biochemistry* **26**: 5471-5477.

Baichoo, N. & J.D. Helmann, (2002) Recognition of DNA by Fur: a reinterpretation of the Fur box consensus sequence. *Journal of bacteriology* **184**: 5826-5832.

Baichoo, N., T. Wang, R. Ye & J.D. Helmann, (2002) Global analysis of the Bacillus subtilis Fur regulon and the iron starvation stimulon. *Molecular microbiology* **45**: 1613-1629.

Barwinska-Sendra, A. & K.J. Waldron, The Role of Intermetal Competition and Mis-Metalation in Metal Toxicity. In: Advances in Microbial Physiology. Academic Press, pp.

Benjamin, J.A. & E. Masse, (2014) The iron-sensing aconitase B binds its own mRNA to prevent sRNA-induced mRNA cleavage. *Nucleic acids research* **42**: 10023-10036.

Blindauer, C.A., (2015) Advances in the molecular understanding of biological zinc transport. *Chemical communications (Cambridge, England)* **51**: 4544-4563.

Butcher, B.G., P.A. Bronstein, C.R. Myers, P.V. Stodghill, J.J. Bolton, E.J. Markel, M.J. Filiatrault, B. Swingle, A. Gaballa, J.D. Helmann, D.J. Schneider & S.W. Cartinhour, (2011) Characterization of the Fur regulon in Pseudomonas syringae pv. tomato DC3000. *Journal of bacteriology* **193**: 4598-4611.

Cao, J., M.R. Woodhall, J. Alvarez, M.L. Cartron & S.C. Andrews, (2007) EfeUOB (YcdNOB) is a tripartite, acid-induced and CpxAR-regulated, low-pH Fe2+ transporter that is cryptic in Escherichia coli K-12 but functional in E. coli O157:H7. *Molecular microbiology* **65**: 857-875.

Chao, T.C., J. Buhrmester, N. Hansmeier, A. Puhler & S. Weidner, (2005) Role of the regulatory gene rirA in the transcriptional response of Sinorhizobium meliloti to iron limitation. *Applied and environmental microbiology* **71**: 5969-5982.

Chumsakul, O., D.P. Anantsri, T. Quirke, T. Oshima, K. Nakamura, S. Ishikawa & M.M. Nakano, (2017) Genome-Wide Analysis of ResD, NsrR, and Fur Binding in Bacillus subtilis during Anaerobic Fermentative Growth by In Vivo Footprinting. *Journal of bacteriology* **199**.

Cornelis, P., (2010) Iron uptake and metabolism in pseudomonads. *Applied microbiology and biotechnology* **86**: 1637-1645.

D'Aquino, J.A., J. Tetenbaum-Novatt, A. White, F. Berkovitch & D. Ringe, (2005) Mechanism of metal ion activation of the diphtheria toxin repressor DtxR. *Proceedings of the National Academy of Sciences of the United States of America* **102**: 18408-18413.

Davies, B.W., R.W. Bogard & J.J. Mekalanos, (2011) Mapping the regulon of Vibrio cholerae ferric uptake regulator expands its known network of gene regulation. *Proc Natl Acad Sci U S A* **108**: 12467-12472.

Delany, I., R. Rappuoli & V. Scarlato, (2004) Fur functions as an activator and as a repressor of putative virulence genes in Neisseria meningitidis. *Molecular microbiology* **52**: 1081-1090.

Diaz-Mireles, E., M. Wexler, G. Sawers, D. Bellini, J.D. Todd & A.W. Johnston, (2004) The Fur-like protein Mur of Rhizobium leguminosarum is a Mn(2+)-responsive transcriptional regulator. *Microbiology* **150**: 1447-1456.

Eisenstein, R.S., (2000) Iron regulatory proteins and the molecular control of mammalian iron metabolism. *Annu Rev Nutr* **20**: 627-662.

Escolar, L., J. Perez-Martin & V. de Lorenzo, (1999) Opening the iron box: transcriptional metalloregulation by the Fur protein. *Journal of bacteriology* **181**: 6223-6229.

Ferguson, A.D., R. Chakraborty, B.S. Smith, L. Esser, D. van der Helm & J. Deisenhofer, (2002) Structural basis of gating by the outer membrane transporter FecA. *Science (New York, N.Y.)* **295**: 1715-1719.

Fleischhacker, A.S. & P.J. Kiley, (2011) Iron-containing transcription factors and their roles as sensors. *Current opinion in chemical biology* **15**: 335-341.

Fukushima, T., A.K. Sia, B.E. Allred, R. Nichiporuk, Z. Zhou, U.N. Andersen & K.N. Raymond, (2012) Bacillus cereus iron uptake protein fishes out an unstable ferric citrate trimer. *Proceedings of the National Academy of Sciences of the United States of America* **109**: 16829-16834.

Gaballa, A. & J.D. Helmann, (2011) Bacillus subtilis Fur represses one of two paralogous haem-degrading monooxygenases. *Microbiology* **157**: 3221-3231.

Golynskiy, M.V., W.A. Gunderson, M.P. Hendrich & S.M. Cohen, (2006) Metal binding studies and EPR spectroscopy of the manganese transport regulator MntR. *Biochemistry* **45**: 15359-15372.

Grosse, C., J. Scherer, D. Koch, M. Otto, N. Taudte & G. Grass, (2006) A new ferrous iron-uptake transporter, EfeU (YcdN), from Escherichia coli. *Molecular microbiology* **62**: 120-131.

Hamza, I., Z. Qi, N.D. King & M.R. O'Brian, (2000) Fur-independent regulation of iron metabolism by Irr in Bradyrhizobium japonicum. *Microbiology* **146**: 669-676.

Hantke, K., (1987) Selection procedure for deregulated iron transport mutants (fur) in Escherichia coli K 12: fur not only affects iron metabolism. *Molecular & general genetics : MGG* **210**: 135-139.

Hantke, K., (2002) Members of the Fur protein family regulate iron and zinc transport in E. coli and characteristics of the Fur-regulated fhuF protein. *Journal of molecular microbiology and biotechnology* **4**: 217-222.

Harle, C., I. Kim, A. Angerer & V. Braun, (1995) Signal transfer through three compartments: transcription initiation of the Escherichia coli ferric citrate transport system from the cell surface. *The EMBO journal* **14**: 1430-1438.

Herbig, A.F. & J.D. Helmann, (2001) Roles of metal ions and hydrogen peroxide in modulating the interaction of the Bacillus subtilis PerR peroxide regulon repressor with operator DNA. *Molecular microbiology* **41**: 849-859.

Huang, X., J.H. Shin, A. Pinochet-Barros, T.T. Su & J.D. Helmann, (2017) Bacillus subtilis MntR coordinates the transcriptional regulation of manganese uptake and efflux systems. *Molecular microbiology* **103**: 253-268.

Ilbert, M. & V. Bonnefoy, (2013) Insight into the evolution of the iron oxidation pathways. *Biochimica et Biophysica Acta (BBA) - Bioenergetics* **1827**: 161-175.

Imlay, J.A., (2003) Pathways of oxidative damage. *Annu Rev Microbiol* **57**: 395-418.

Imlay, J.A., (2014) The mismetallation of enzymes during oxidative stress. *The Journal of biological chemistry* **289**: 28121-28128.

Jakubovics, N.S., A.W. Smith & H.F. Jenkinson, (2000) Expression of the virulence-related Sca (Mn2+) permease in Streptococcus gordonii is regulated by a diphtheria toxin metallorepressor-like protein ScaR. *Molecular microbiology* **38**: 140-153.

Kammler, M., C. Schon & K. Hantke, (1993) Characterization of the ferrous iron uptake system of Escherichia coli. *Journal of bacteriology* **175**: 6212-6219.

Lee, J.W. & J.D. Helmann, (2007) Functional specialization within the Fur family of metalloregulators. *Biometals : an international journal on the role of metal ions in biology, biochemistry, and medicine* **20**: 485-499.

Leipuviene, R. & E.C. Theil, (2007) The family of iron responsive RNA structures regulated by changes in cellular iron and oxygen. *Cellular and molecular life sciences : CMLS* **64**: 2945-2955.

Liu, Y., W. Li, Y. Wei, Y. Jiang & X. Tan, (2013) Efficient preparation and metal specificity of the regulatory protein TroR from the human pathogen Treponema pallidum. *Metallomics : integrated biometal science* **5**: 1448-1457.

Ma, Z., M.J. Faulkner & J.D. Helmann, (2012) Origins of specificity and cross-talk in metal ion sensing by Bacillus subtilis Fur. *Mol Microbiol* **86**: 1144-1155.

Masse, E. & S. Gottesman, (2002) A small RNA regulates the expression of genes involved in iron metabolism in Escherichia coli. *Proc Natl Acad Sci U S A* **99**: 4620-4625.

Masse, E., H. Salvail, G. Desnoyers & M. Arguin, (2007) Small RNAs controlling iron metabolism. *Current opinion in microbiology* **10**: 140-145.

Massonet, C., V. Pintens, R. Merckx, J. Anné, E. Lammertyn & J. Van Eldere, (2006) Effect of iron on the expression of sirR and sitABC in biofilm-associated Staphylococcus epidermidis. *BMC Microbiology* **6**: 103.

Merchant, S.S. & J.D. Helmann, (2012) Elemental economy: microbial strategies for optimizing growth in the face of nutrient limitation. *Advances in microbial physiology* **60**: 91-210.

Michta, E., W. Ding, S. Zhu, K. Blin, H. Ruan, R. Wang, W. Wohlleben & Y. Mast, (2014) Proteomic approach to reveal the regulatory function of aconitase AcnA in oxidative stress response in the antibiotic producer Streptomyces viridochromogenes Tu494. *PloS one* **9**: e87905.

Miethke, M., O. Klotz, U. Linne, J.J. May, C.L. Beckering & M.A. Marahiel, (2006) Ferri-bacillibactin uptake and hydrolysis in Bacillus subtilis. *Molecular microbiology* **61**: 1413-1427.

Miethke, M., C.G. Monteferrante, M.A. Marahiel & J.M. van Dijl, (2013) The Bacillus subtilis EfeUOB transporter is essential for high-affinity acquisition of ferrous and ferric iron. *Biochimica et biophysica acta* **1833**: 2267-2278.

Miethke, M., S. Schmidt & M.A. Marahiel, (2008) The major facilitator superfamily-type transporter YmfE and the multidrug-efflux activator Mta mediate bacillibactin secretion in Bacillus subtilis. *Journal of bacteriology* **190**: 5143-5152.

Mills, S.A. & M.A. Marletta, (2005) Metal binding characteristics and role of iron oxidation in the ferric uptake regulator from Escherichia coli. *Biochemistry* **44**: 13553-13559.

Munnoch, J.T., M.T. Martinez, D.A. Svistunenko, J.C. Crack, N.E. Le Brun & M.I. Hutchings, (2016) Characterization of a putative NsrR homologue in Streptomyces venezuelae reveals a new member of the Rrf2 superfamily. *Scientific reports* **6**: 31597.

Nandal, A., C.C. Huggins, M.R. Woodhall, J. McHugh, F. Rodriguez-Quinones, M.A. Quail, J.R. Guest & S.C. Andrews, (2010) Induction of the ferritin gene (ftnA) of Escherichia coli by Fe(2+)-Fur is mediated by reversal of H-NS silencing and is RyhB independent. *Molecular microbiology* **75**: 637-657.

Ngok-Ngam, P., N. Ruangkiattikul, A. Mahavihakanont, S.S. Virgem, R. Sukchawalit & S. Mongkolsuk, (2009) Roles of Agrobacterium tumefaciens RirA in iron regulation, oxidative stress response, and virulence. *Journal of bacteriology* **191**: 2083-2090.

Ollinger, J., K.B. Song, H. Antelmann, M. Hecker & J.D. Helmann, (2006) Role of the Fur regulon in iron transport in Bacillus subtilis. *Journal of bacteriology* **188**: 3664-3673.

Pandey, R. & G.M. Rodriguez, (2014) IdeR is required for iron homeostasis and virulence in Mycobacterium tuberculosis. *Molecular microbiology* **91**: 98-109.

Park, S., X. You & J.A. Imlay, (2005) Substantial DNA damage from submicromolar intracellular hydrogen peroxide detected in Hpx- mutants of Escherichia coli. *Proc Natl Acad Sci U S A* **102**: 9317-9322.

Patzer, S.I. & K. Hantke, (1998) The ZnuABC high-affinity zinc uptake system and its regulator Zur in Escherichia coli. *Molecular microbiology* **28**: 1199-1210.

Pechter, K.B., F.M. Meyer, A.W. Serio, J. Stulke & A.L. Sonenshein, (2013) Two roles for aconitase in the regulation of tricarboxylic acid branch gene expression in Bacillus subtilis. *Journal of bacteriology* **195**: 1525-1537.

Pi, H. & J.D. Helmann, (2017) Sequential induction of Fur-regulated genes in response to iron limitation in Bacillus subtilis. *Proc Natl Acad Sci U S A*.

Pi, H., S.J. Patel, J.M. Arguello & J.D. Helmann, (2016) The Listeria monocytogenes Fur-regulated virulence protein FrvA is an Fe(II) efflux P1B4 -type ATPase. *Molecular microbiology* **100**: 1066-1079.

Platero, R., V. de Lorenzo, B. Garat & E. Fabiano, (2007) Sinorhizobium meliloti fur-like (Mur) protein binds a fur box-like sequence present in the mntA promoter in a manganese-responsive manner. *Applied and environmental microbiology* **73**: 4832-4838.

Posey, J.E., J.M. Hardham, S.J. Norris & F.C. Gherardini, (1999) Characterization of a manganese-dependent regulatory protein, TroR, from Treponema pallidum. *Proc Natl Acad Sci U S A* **96**: 10887-10892.

Puig, S., E. Askeland & D.J. Thiele, (2005) Coordinated remodeling of cellular metabolism during iron deficiency through targeted mRNA degradation. *Cell* **120**: 99-110.

Rodionov, D.A., M.S. Gelfand, J.D. Todd, A.R. Curson & A.W. Johnston, (2006) Computational reconstruction of iron- and manganese-responsive transcriptional networks in alpha-proteobacteria. *PLoS computational biology* **2**: e163.

Rouault, T.A., (2006) The role of iron regulatory proteins in mammalian iron homeostasis and disease. *Nature chemical biology* **2**: 406-414.

Roy, E.M. & K.L. Griffith, (2017) Characterization of a Novel Iron Acquisition Activity That Coordinates the Iron Response with Population Density under Iron-Replete Conditions in Bacillus subtilis. *Journal of bacteriology* **199**.

Rupani, D.N. & G.J. Connell, (2016) Transferrin receptor mRNA interactions contributing to iron homeostasis. *RNA (New York, N.Y.)* **22**: 1271-1282.

Sanchez, M., B. Galy, T. Dandekar, P. Bengert, Y. Vainshtein, J. Stolte, M.U. Muckenthaler & M.W. Hentze, (2006) Iron regulation and the cell cycle: identification of an iron-responsive element in the 3'-untranslated region of human cell division cycle 14A mRNA by a refined microarray-based screening strategy. *The Journal of biological chemistry* **281**: 22865-22874.

Schwartz, C.J., J.L. Giel, T. Patschkowski, C. Luther, F.J. Ruzicka, H. Beinert & P.J. Kiley, (2001) IscR, an Fe-S cluster-containing transcription factor, represses expression of Escherichia coli genes encoding Fe-S cluster assembly proteins. *Proceedings of the National Academy of Sciences* **98**: 14895-14900.

Seo, S.W., D. Kim, H. Latif, E.J. O'Brien, R. Szubin & B.O. Palsson, (2014) Deciphering Fur transcriptional regulatory network highlights its complex role beyond iron metabolism in Escherichia coli. *Nature communications* **5**: 4910-4910.

Serio, A.W., K.B. Pechter & A.L. Sonenshein, (2006) Bacillus subtilis aconitase is required for efficient late-sporulation gene expression. *Journal of bacteriology* **188**: 6396-6405.

Silva, A.M., X. Kong, M.C. Parkin, R. Cammack & R.C. Hider, (2009) Iron(III) citrate speciation in aqueous solution. *Dalton transactions (Cambridge, England : 2003)*: 8616-8625.

Small, S.K., S. Puri & M.R. O'Brian, (2009) Heme-dependent metalloregulation by the Iron Response Regulator (Irr) Protein in Rhizobium and other Alpha-Proteobacteria. *Biometals : an international journal on the role of metal ions in biology, biochemistry, and medicine* **22**: 89-97.

Soutourina, O., O. Poupel, J.Y. Coppee, A. Danchin, T. Msadek & I. Martin-Verstraete, (2009) CymR, the master regulator of cysteine metabolism in Staphylococcus aureus, controls host sulphur source utilization and plays a role in biofilm formation. *Molecular microbiology* **73**: 194-211.

Tang, Y. & J.R. Guest, (1999) Direct evidence for mRNA binding and post-transcriptional regulation by Escherichia coli aconitases. *Microbiology* **145 (Pt 11)**: 3069-3079.

Tang, Y., J.R. Guest, P.J. Artymiuk, R.C. Read & J. Green, (2004) Post-transcriptional regulation of bacterial motility by aconitase proteins. *Molecular microbiology* **51**: 1817-1826.

Tang, Y., M.A. Quail, P.J. Artymiuk, J.R. Guest & J. Green, (2002) Escherichia coli aconitases and oxidative stress: post-transcriptional regulation of sodA expression. *Microbiology* **148**: 1027-1037.

Todd, J.D., G. Sawers, D.A. Rodionov & A.W. Johnston, (2006) The Rhizobium leguminosarum regulator IrrA affects the transcription of a wide range of genes in response to Fe availability. *Molecular genetics and genomics : MGG* **275**: 564-577.

Todd, J.D., M. Wexler, G. Sawers, K.H. Yeoman, P.S. Poole & A.W. Johnston, (2002) RirA, an iron-responsive regulator in the symbiotic bacterium Rhizobium leguminosarum. *Microbiology* **148**: 4059-4071.

Troxell, B. & H.M. Hassan, (2013) Transcriptional regulation by Ferric Uptake Regulator (Fur) in pathogenic bacteria. *Frontiers in cellular and infection microbiology* **3**: 59.

Valdebenito, M., A.L. Crumbliss, G. Winkelmann & K. Hantke, (2006) Environmental factors influence the production of enterobactin, salmochelin, aerobactin, and yersiniabactin in Escherichia coli strain Nissle 1917. *International journal of medical microbiology : IJMM* **296**: 513-520.

Viguier, C., O.C. P, P. Clarke & M. O'Connell, (2005) RirA is the iron response regulator of the rhizobactin 1021 biosynthesis and transport genes in Sinorhizobium meliloti 2011. *FEMS microbiology letters* **246**: 235-242.

Volbeda, A., E.L. Dodd, C. Darnault, J.C. Crack, O. Renoux, M.I. Hutchings, N.E. Le Brun & J.C. Fontecilla-Camps, (2017) Crystal structures of the NO sensor NsrR reveal how its iron-sulfur cluster modulates DNA binding. *Nat Commun* **8**: 15052.

Wallander, M.L., E.A. Leibold & R.S. Eisenstein, (2006) Molecular control of vertebrate iron homeostasis by iron regulatory proteins. *Biochimica et biophysica acta* **1763**: 668-689.

Wennerhold, J. & M. Bott, (2006) The DtxR regulon of Corynebacterium glutamicum. *Journal of bacteriology* **188**: 2907-2918.

Wennerhold, J., A. Krug & M. Bott, (2005) The AraC-type regulator RipA represses aconitase and other iron proteins from Corynebacterium under iron limitation and is itself repressed by DtxR. *The Journal of biological chemistry* **280**: 40500-40508.

Wilderman, P.J., N.A. Sowa, D.J. FitzGerald, P.C. FitzGerald, S. Gottesman, U.A. Ochsner & M.L. Vasil, (2004) Identification of tandem duplicate regulatory small RNAs in Pseudomonas aeruginosa involved in iron homeostasis. *Proc Natl Acad Sci U S A* **101**: 9792-9797.

Yang, J., I. Sangwan, A. Lindemann, F. Hauser, H. Hennecke, H.M. Fischer & M.R. O'Brian, (2006) Bradyrhizobium japonicum senses iron through the status of haem to regulate iron homeostasis and metabolism. *Molecular microbiology* **60**: 427-437.

Yue, W.W., S. Grizot & S.K. Buchanan, (2003) Structural evidence for iron-free citrate and ferric citrate binding to the TonB-dependent outer membrane transporter FecA. *Journal of molecular biology* **332**: 353-368.

Zawadzka, A.M., R.J. Abergel, R. Nichiporuk, U.N. Andersen & K.N. Raymond, (2009) Siderophore-mediated iron acquisition systems in Bacillus cereus: Identification of receptors for anthrax virulence-associated petrobactin. *Biochemistry* **48**: 3645-3657.

Chapter 2 Ferrous Iron Efflux Systems in Bacteria

2.1 Abstract

Bacteria require iron for growth, with only a few reported exceptions. In many environments, iron is a limiting nutrient for growth and high affinity uptake systems play a central role in iron homeostasis. However, iron can also be detrimental to cells when it is present in excess, particularly under aerobic conditions, due to its participation in Fenton chemistry, which generates highly reactive hydroxyl radicals. Recent results have revealed a critical role for iron efflux transporters in protecting bacteria from iron intoxication. Systems that efflux iron are widely distributed amongst bacteria and fall into several categories: P_{1B}-type ATPases, cation diffusion facilitator (CDF) proteins, major facilitator superfamily (MFS) proteins, and membrane bound ferritin-like proteins. Here, we review the emerging role of iron export in both iron homeostasis and as part of the adaptive response to oxidative stress.

2.2 Introduction

Iron is critical for cell growth and survival. However, when present in excess, it is also detrimental to cells. Under aerobic conditions, iron toxicity is closely related to oxidative stress through Fenton chemistry (Imlay, 2003). Hydrogen peroxide (H_2O_2) reacts with ferrous iron (Fe^{2+}) to generate highly reactive hydroxyl radicals that damage macromolecules such as DNA, proteins and fatty acids, resulting in disruption of cell metabolism and ultimately cell death (Park *et al.*, 2005). Therefore, the toxicity of reactive oxygen species (ROS) is generally thought to be exacerbated by conditions that elevate the

---

This chapter is adapted from Pi H & Helmann JD. *Metallomics*, 2017,9, 840-851.

intracellular iron pool. Conversely, high levels of intracellular iron may also be toxic independent of ROS, presumably due to the ability of iron to compete with other transition metals, such as manganese, for binding to metal-dependent enzymes or regulators, resulting in mismetallation and inactivation of these proteins (Imlay, 2014, Barwinska-Sendra & Waldron). ROS such as H_2O_2 and superoxide radical can disrupt iron-sulfur clusters and mononuclear iron centers of iron-enzymes, thereby leading to iron release (Anjem & Imlay, 2012, Jang & Imlay, 2007). Therefore, iron intoxication may also be exacerbated by an elevation in ROS. Clearly, the toxicity of iron and ROS are closely intertwined, with each potentially increasing the toxicity of the other.

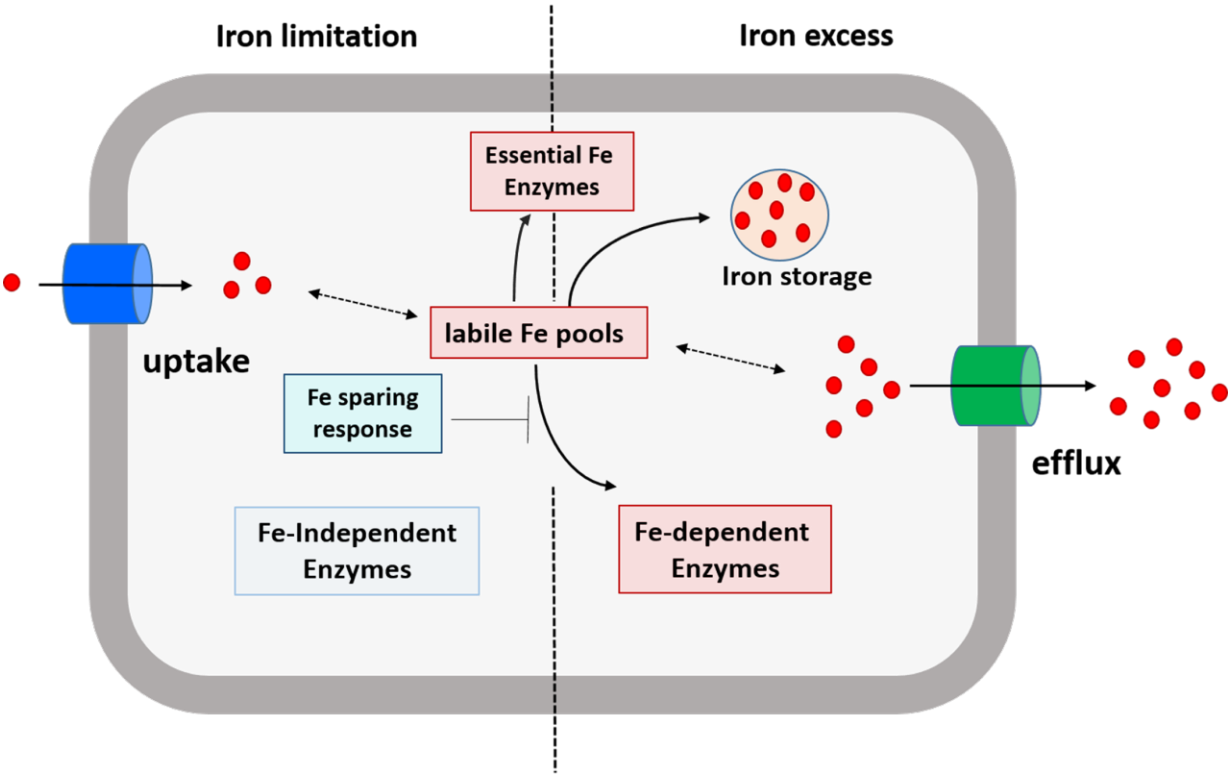

Fig. 2.1 Iron homeostasis in bacteria.

Under iron deficient conditions (left), high affinity iron uptake systems are induced to scavenge iron from the surroundings to maintain the cell's labile iron pool. When iron is limiting, it is selectively partitioned to the most essential functions and incorporation into lower priority iron enzymes is translationally inhibited as part of an iron sparing response. In many cases, iron-independent enzymes may be derepressed to replace functions that would otherwise depend on iron. Under iron excess conditions, the cell will have a full complement of iron-requiring enzymes, and iron in excess of immediate needs will be either stored for future use or exported by Fe^{2+} efflux transporters to prevent iron overload.

Bacteria adapt to environmental stresses by activation of specific transcriptional programs. In the case of iron homeostasis, bacteria monitor intracellular iron levels using metal-sensing (metalloregulatory) proteins (Waldron *et al.*, 2009, Chandrangsu *et al.*, 2017). The ferric uptake regulator (Fur) protein is the most widespread bacterial iron sensor (Fleischhacker & Kiley, 2011a), but it can be replaced by functionally analogous proteins such as IdeR (in actinomycetes) (Rodriguez *et al.*, 2002, Sritharan, 2016) and Irr (in alpha- proteobacteria) (Rodionov *et al.*, 2006, Todd *et al.*, 2006, Yang *et al.*, 2006). Fur helps to maintain iron homeostasis by regulating genes implicated in iron uptake, storage, and efflux (Helmann, 2014a). Typically, Fur is considered to function as an Fe^{2+}-activated transcriptional repressor for most of its targets, but there are increasing examples where Fur functions as a transcriptional activator or where it binds DNA in the absence of bound iron (Seo *et al.*, 2014a, Delany *et al.*, 2004b, Yu & Genco, 2012).

Iron-sensing regulators such as Fur play a central role in the control of iron homeostasis (Andrews *et al.*, 2003). The *Escherichia coli* Fur regulon illustrates the diverse roles that Fur may play. *E. coli* Fur (Fur_{EC}) binds to DNA when associated with Fe^{2+} and serves to repress the expression of target operons (McHugh *et al.*, 2003). This repression is relieved under iron-limited conditions, and this results in the derepression of iron uptake systems, including the synthesis of the high-affinity iron-chelating compound siderophore known as enterobactin and its cognate import system (Hunt *et al.*, 1994). Fur also helps bacteria to remodel their proteomes to prioritize the utilization of iron, in a process known as "iron-sparing" (Fig. 2.1). (Masse & Gottesman, 2002, Masse *et al.*, 2007, Masse *et al.*, 2005) In *E. coli*, the loss of Fur_{EC} DNA-binding activity (under low iron conditions) results in expression of the RyhB small RNA (sRNA) that represses translation of non-essential iron-enzymes (Masse & Gottesman, 2002, Masse *et al.*, 2007, Masse *et al.*, 2005). Fur also participates in the regulation of gene expression under conditions of iron excess. For example, Fur_{EC} positively regulates expression of the iron storage protein ferritin by occluding the binding of the H-NS transcriptional repressor (Nandal *et al.*, 2010). In general, adaptation to iron excess often involves expression of iron storage functions (including heme-containing bacterioferritins,

ferritins, and Dps-family mini-ferritins) but may additionally require iron efflux systems (Fig. 2.1). In light of the central role of Fur in coordinating iron homeostasis, it is not surprising that some iron efflux systems are induced by Fur in response to iron excess (Faulkner *et al.*, 2012, Pi *et al.*, 2016).

Bacteria also adapt to oxidative stress by the induction of specific defensive genes. For example, H_2O_2 induces a specific peroxide-stress response that is regulated by the OxyR repressor in *E. coli* (Storz & Altuvia, 1994) and by the PerR repressor in *Bacillus subtilis* (Herbig & Helmann, 2001). In both model organisms, a rise in intracellular H_2O_2 triggers the induction of defensive enzymes such as catalase and alkyl hydroperoxide reductase, which can directly detoxify H_2O_2. In addition, cells scavenge excess iron from the cytosol by sequestration into mini-ferritin proteins, including Dps in *E. coli* (Calhoun & Kwon, 2011) and the Dps ortholog MrgA in *B. subtilis* (Chen & Helmann, 1995). The co-regulation of H_2O_2 degradation enzymes and iron-sequestering proteins further highlights the central role of iron in peroxide intoxication. In addition to scavenging iron, peroxide stress also frequently modulates metal uptake and efflux systems (Faulkner & Helmann, 2011). In *E. coli*, H_2O_2 induces an OxyR-activated Mn^{2+} uptake system (MntH) (Anjem *et al.*, 2009, Kehres *et al.*, 2000), and in *B. subtilis* H_2O_2 induces a PerR-regulated iron efflux system, PfeT (Gaballa & Helmann, 2002b, Guan *et al.*, 2015a). PfeT is a member of the P_{1B4}-type ATPases, and recent results indicate that several close homologs also function as Fe^{2+} efflux pumps (Pi *et al.*, 2016, Patel *et al.*, 2016, VanderWal *et al.*, 2017, Turner *et al.*, 2017). Fe^{2+} efflux pumps have now been documented in a wide variety of Bacteria, and include P_{1B}-type ATPases, cation diffusion facilitator (CDF) proteins, major facilitator superfamily (MFS) proteins, and membrane bound ferritin-like proteins. Here, we summarize the emerging role of these ferrous iron efflux pumps in helping ameliorate the deleterious effects of excess iron and peroxide (Table 2.1).

2.3 P-type ATPases

The P-type ATPases are a large group of transmembrane proteins that transport ions and lipids across cellular membranes, energetically driven by ATP hydrolysis (Kuhlbrandt, 2004). Five subgroups of

P-type ATPases have been defined based on sequence homology and substrate specificity (Chan *et al.*, 2010). These are the P_1-type (K^+ and transition metal transporters), P_2-type (Ca^{2+}, Na^+/K^+, and H^+/K^+ pumps), P_3-type (H^+ pumps), P_4-type (phospholipid transporters), and P_5-type ATPases (unknown substrate). The P_2-type ATPases have been well studied and are more prevalent in eukaryotes than in prokaryotes. The majority of P_3-type ATPases are H^+ pumps found in plants and fungi. Some of the P_4-type ATPases have been revealed to be phospholipid transporters (Lenoir *et al.*, 2007, Lopez-Marques *et al.*, 2010). No specific substrate has yet been identified for the P_5-type ATPases that are only found in eukaryotes.

Table 2.1 Fe^{2+} efflux transporters in bacteria.

Protein	Organism	Function	Category	Substrate specificity*	Transcription regulation	References
PfeT	*Bacillus subtilis*	Fe^{2+} efflux	P_{1B4}-type ATPase	$Fe^{2+\,a,\,b}$, $Co^{2+\,a}$	PerR & Fur	36
FrvA	*Listeria monocytogenes*	Fe^{2+} efflux	P_{1B4}-type ATPase	$Fe^{2+\,a,\,b}$, $Co^{2+\,a}$, $Zn^{2+\,a}$	PerR & Fur	27
CtpD	*Mycobacterium tuberculosis*	Fe^{2+} efflux	P_{1B4}-type ATPase	$Fe^{2+\,a,\,b}$, $Co^{2+\,a}$	Unknown	37
PmtA	group A *Streptococcus*	Fe^{2+} efflux	P_{1B4}-type ATPase	$Fe^{2+\,b}$	PerR	38, 39
Nia	*Sinorhizobium meliloti*	Fe^{2+} or Ni^{2+} efflux	P_{1B5}-type ATPase	$Fe^{2+\,a,\,b}$, $Ni^{2+\,a,\,b}$	Unknown	73
FieF or YiiP	*Escherichia coli*	Fe^{2+} or Zn^{2+} efflux	CDF family	$Fe^{2+\,b}$, $Zn^{2+\,a}$, $Cd^{2+\,a}$,	Unknown	92-94
AitP	*Pseudomonas aeruginosa*	Fe^{2+} or Co^{2+} efflux	CDF family	$Fe^{2+\,b}$	Unknown	97
FeoE	*Shewanella oneidensis*	Fe^{2+} efflux	CDF family	$Fe^{2+\,b}$	Unknown	101
IceT	*Salmonella typhimurium*	Fe^{2+} citrate or citrate efflux	MFS family	$Fe^{2+\,b}$	BaeSR	120
MbfA	*Agrobacterium tumefaciens*	Fe^{2+} efflux	Membrane bound ferritin	$Fe^{2+\,b}$	Irr	125
MbfA	*Bradyrhizobium japonicum*	Fe^{2+} efflux	Membrane bound ferritin	$Fe^{2+\,b}$	Irr	127

*Note: the substrate specificity of the transporters is either based on biochemical measurements (a), inferred from physiology studies (b), or both (a, b).

The P_1-type ATPases exist predominately in prokaryotes but are omnipresent across all domains of life (Thever & Saier, 2009): P_{1A}-ATPases are involved in K^+ transport whereas P_{1B}-ATPases are important for maintaining transition metal homeostasis. P_{1B}-ATPases are known to transport Cu^+ (Gonzalez-Guerrero *et al.*, 2008, Fan & Rosen, 2002), Ag^+ (Mandal *et al.*, 2002), Zn^{2+} (Liu *et al.*, 2006), Cd^{2+} (Nucifora *et al.*, 1989), Cu^{2+} (Mana-Capelli *et al.*, 2003), Co^{2+} (Zielazinski *et al.*, 2012) and Fe^{2+} (Guan *et al.*, 2015a, Pi *et al.*, 2016, Patel *et al.*, 2016). The structure of a typical P_{1B}-ATPase includes a transmembrane domain with 6-8 helices, a soluble actuator domain, and an ATP-binding domain (Smith *et al.*, 2014) (Fig 2.2). The P_{1B}-ATPases can be further divided into seven subclasses based on sequence similarity and metal substrate specificity (Smith *et al.*, 2014). The P_{1B4}-type ATPases were originally assigned a role in Co^{2+} export, based on the properties of some of the first characterized members (Arguello, 2003). However, P_{1B4}-type ATPases have recently been found to function instead, or in addition, as Fe^{2+} efflux transporters including *Bacillus subtilis* PfeT (Guan *et al.*, 2015a), *Listeria monocytogenes* FrvA (Pi *et al.*, 2016), *Mycobacterium tuberculosis* CtpD (Patel *et al.*, 2016), and group A *Streptococcus* PmtA (Turner *et al.*, 2017, VanderWal *et al.*, 2017).

2.3.1 PfeT in *Bacillus subtilis*

B. subtilis is a Gram-positive soil microorganism and encodes two transcriptional regulators critical for iron homeostasis, Fur_{Bs} and PerR. Fur_{Bs} is a global transcriptional regulator of iron homeostasis analogous to Fur_{EC} (Ollinger *et al.*, 2006) and PerR mediates the adaptive response to peroxide stress by regulating genes involved in iron storage and peroxide detoxification(Herbig & Helmann, 2001). The regulons for both Fur_{Bs} and PerR have been well defined (Baichoo *et al.*, 2002, Fuangthong *et al.*, 2002a). Fur_{Bs} senses intracellular iron sufficiency and represses genes that are involved in siderophore synthesis and uptake (Lee & Helmann, 2007, Ollinger *et al.*, 2006). Fur_{Bs} also regulates an iron sparing response

mediated by the small non-coding RNA FsrA (Fig. 1) and its coregulators FbpA, FbpB and FbpC (Gaballa *et al.*, 2008, Smaldone *et al.*, 2012a, Smaldone *et al.*, 2012b). This system, analogous to RyhB in *E. coli*, blocks the translation of non-essential iron-containing enzymes such as aconitase and succinate dehydrogenase (Gaballa *et al.*, 2008, Smaldone *et al.*, 2012a, Smaldone *et al.*, 2012b). PerR regulates peroxide detoxification enzymes (catalase, alkyl hydroperoxide reductase), iron sequestration (MrgA) and the P_{1B4}-type ATPase (PfeT). Although the Fur and PerR regulons are largely non-overlapping, *pfeT* is the exception and is regulated by both proteins (Faulkner *et al.*, 2012). The result is that *pfeT* is induced by either peroxide stress or by iron excess (unpublished data, Pinochet-Barros A & Helmann JD).

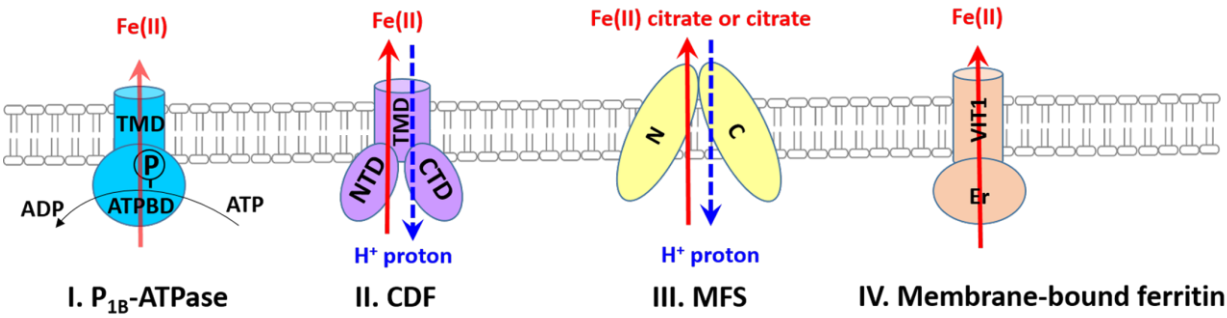

Fig. 2.2 Ferrous iron efflux systems in bacteria.

Four different groups of transporters can function as Fe^{2+} efflux pumps. I. P_{1B}-ATPase; II. Cation diffusion facilitator (CDF); III. Major facilitator superfamily (MFS); IV. Membrane-bound ferritin. A typical P_{1B}-ATPase consists of a transmembrane domain (TMD) that has 6-8 helices, a soluble actuator domain (not shown), and an ATP-binding domain (ATP-BD) (Smith *et al.*, 2014). A CDF transporter contains a N-terminal domain (NTD), a transmembrane domain (TMD) that has 6 helices, a histine-rich interconnecting loop (IL) between TM4 and TM5 (not shown), and a C-terminal cytoplasmic domain (CTD) (Haney *et al.*, 2005). The common structural fold (MFS fold) of a MFS transporter is composed of two distinct domains, N domain and C domain. Each domain has six consecutive transmembrane helices (Yan, 2015). A membrane-bound ferritin transporter has two major domains, N-terminal ferritin-like or Er domain (Er) and C-terminal membrane-embedded vacuolar iron transporter domain (VIT1).

PfeT is one of three P_{1B} ATPases encoded by *B. subtilis*. CopA is a P_{1B1}-ATPase that functions as a Cu^+ efflux transporter and, appropriate to its function, is regulated by the CsoR Cu^+ sensor (Smaldone &

Helmann, 2007). CadA is a P_{1B2}-ATPase that confers resistance to Cd^{2+}, Zn^{2+}, and Co^{2+} and is regulated by the divalent cation sensor CzrA (Moore *et al.*, 2005). PfeT (formerly named as ZosA) is a P_{1B4}-type ATPase and was discovered as a transporter induced by H_2O_2 that plays a role in protecting cells against oxidative stress (Gaballa & Helmann, 2002b). Initial results indicated that deletion of *pfeT* enhanced Zn^{2+} tolerance, as monitored in cells lacking the CadA efflux system (Gaballa & Helmann, 2002b). This led to the proposal that PfeT might function as a Zn^{2+} importer under oxidative stress conditions, consistent with the idea that Zn^{2+} has a role in protecting cells against oxidative damage (Gaballa & Helmann, 2002b). As a result, PfeT was originally named for this proposed role as ZosA ($\underline{Z}n^{2+}$ uptake under $\underline{o}$xidative $\underline{s}$tress) (Gaballa & Helmann, 2002b).

Contrary to this model, most P_{1B}-type ATPases function in metal export rather than import, which motivated a reinvestigation of the role of PfeT. Further study revealed that a *pfeT* null mutant is sensitive to Fe^{2+} and Fe^{3+}, particularly under acidic media conditions, but not to Zn^{2+} or Co^{2+}. Moreover, a *pfeT* null mutant accumulates elevated levels of intracellular Fe^{2+}, as judged by sensitivity to the Fe^{2+}-activated antibiotic streptonigrin and by direct chemical measurement (Guan *et al.*, 2015a). Biochemical studies confirmed that the ATPase activity of PfeT is induced the most by Fe^{2+}, with modest induction by Co^{2+} but not with other metals, including Zn^{2+}. In addition to H_2O_2, *pfeT* is strongly and specifically induced by iron, but not by other metals. Together, these findings indicate that PfeT function as a peroxide- and iron-induced ferrous efflux transporter (Guan *et al.*, 2015a). The ability of PfeT to protect against H_2O_2 is secondary to that of the detoxification enzymes catalase and alkyl hydroperoxide reductase. However, PfeT plays a dominant role in protecting cells from iron overload with the MrgA miniferritin playing a secondary role (Guan *et al.*, 2015a). The revelation that PfeT functions in Fe^{2+} efflux, in turn, prompted a re-evaluation of the roles of several other P_{1B4}-type ATPases in bacterial iron homeostasis.

2.3.2 FrvA in *Listeria monocytogenes*

L. monocytogenes is the causative agent of the foodborne disease listeriosis, which is associated with central nervous system infections and bacteremia. FrvA (Lmo0641) is a P_{1B4}-ATPase originally described as a Fur-regulated virulence factor (McLaughlin *et al.*, 2012). FrvA was proposed to function as a heme exporter that was suggested to be induced by iron deficiency and to be under negative regulation of both Fur and PerR (McLaughlin *et al.*, 2012, Rea *et al.*, 2005). However, a different transcriptome study showed a downregulation of *frvA* in a *fur* null mutant (Ledala *et al.*, 2010), indicating a positive regulatory role of Fur in *frvA* expression.

To resolve these contradictory reports of iron regulation, and to test if FrvA might function in Fe^{2+} efflux, the mutant phenotype was reinvestigated and the FrvA protein was purified for biochemical studies (Pi *et al.*, 2016). As predicted based on studies of *pfeT*, a *frvA* null mutant was sensitive to iron intoxication, but not to other metals or heme. Like *B. subtilis pfeT*, *frvA* is positively regulated by Fur in response to high Fe^{2+} levels and is repressed by PerR (Pi *et al.*, 2016, Rea *et al.*, 2005). Biochemical studies indicate the FrvA ATPase activity is stimulated most strongly by Fe^{2+} with weaker stimulation in the presence of Co^{2+} or Zn^{2+}. Based on the Fe^{2+} concentration dependence of ATPase activity, FrvA seems to have a higher affinity for Fe^{2+} than *B. subtilis* PfeT. Consistent with this, not only does FrvA complement the iron-sensitive phenotype of a *B. subtilis pfeT* null mutant, its expression depletes the cytosol of iron (even under iron-rich conditions) thereby leading to derepression of the Fur regulon (Pi *et al.*, 2016). These results support the hypothesis that FrvA functions as a Fe^{2+} efflux transporter that protects cells from Fe^{2+} intoxication (Pi *et al.*, 2016).

FrvA is required for virulence in murine and insect (*Galleria mellonella*) infection models (McLaughlin *et al.*, 2012). The *frvA* null mutant strain shows strong attenuation in virulence, but is still able to invade and propagate inside antigen-presenting cells (McLaughlin *et al.*, 2013), suggesting an

important link between iron homeostasis and virulence, but it is not clear at which stage(s) of the *L. monocytogenes* life cycle FrvA is important. The phagocytic vacuole is generally considered to be an iron-limited environment. One possibility is that the expression of high affinity iron uptake systems by iron limitation during infection or in the phagocytic vacuole can contribute to iron overload upon escape of cells into the relatively iron-rich cytosol. Alternatively, the imposition of oxidative damage from host immune cells may trigger iron release from listerial iron enzymes and this may lead to iron overload. The points in the infection cycle where FrvA plays a critical role are not yet clearly defined and provide an interesting avenue for future research.

2.3.3 CtpD in *Mycobacterium tuberculosis*

M. tuberculosis is an obligate pathogen and the causative agent of human tuberculosis. Nearly one-third of the world's population is infected with *M. tuberculosis,* which can persist in a latent state for decades and then later emerge (in ~10% of cases) as an active lung infection. *M. tuberculosis* encodes a total of 11 P-type ATPases, which have been suggested to be possible targets for therapeutic intervention (Novoa-Aponte & Soto Ospina, 2014). Of these, two encode P_{1B4}-ATPases: CtpD (Rv1469) and CtpJ (Rv3743) (Patel *et al.*, 2016). CtpD, but not CtpJ, was found to be important for survival in macrophages and the mouse lung (Patel *et al.*, 2016). Biochemical studies had previously highlighted the activity of these two P_{1B4}-ATPases with Co^{2+}, but it was not clear why *M. tuberculosis* would encode two such proteins, nor was it understood why Co^{2+} efflux would be important for survival in the host.

In light of the finding that PfeT functions as an Fe^{2+} efflux transporter, the roles of CtpD and CtpJ were reinvestigated. Biochemical studies indicated that the ATPase activity of CtpD is most strongly activated by Fe^{2+}. Although Co^{2+} also activates ATPase activity, the maximal activity (V_{max}) is 10-fold lower than with ferrous iron (Patel *et al.*, 2016). CtpD also binds Fe^{2+} with 3-fold higher affinity than Co^{2+}. In contrast, the CtpJ ATPase activity is activated by both Fe^{2+} and Co^{2+}, and has a slightly higher affinity for

Co^{2+} than Fe^{2+}. To better understand their roles *in vivo*, metal accumulation and sensitivity was monitored for strains lacking either *ctpD* or *ctpJ*. The *ctpD* mutant strain did not accumulate Co^{2+} and was impaired in growth in iron-amended medium, consistent with a primary role in resistance to iron intoxication (Patel *et al.*, 2016). Mutation of *ctpJ* led to a significant increase in Co^{2+} accumulation and expression was induced by Co^{2+}, consistent with a primary role in Co^{2+} resistance (Patel *et al.*, 2016). However, the *ctpJ* mutant was also growth impaired in the presence of excess iron. Thus, these two paralogous transporters seem to have overlapping metal selectivity, but largely distinct physiological roles. Further studies are needed to understand the molecular mechanism of substrate specificity, but based on X-ray absorption spectroscopy (XAS) analysis, it is likely that distinct metal coordination geometry plays an important role (Patel *et al.*, 2016).

During infection, *M. tuberculosis* propagates in the host macrophages, which are considered iron-poor environments. Just as noted for *L. monocytogenes*, it is not yet clear where in the infection process cells experience iron intoxication. Further studies are needed to better understand the conditions that lead to induction of *ctpD*. In prior work *ctpD* was not induced by metals such as Co^{2+}, Zn^{2+}, and Ni^{2+}, but its cognate substrate Fe^{2+} was not tested (Raimunda *et al.*, 2014a). CtpD might be induced by Fe^{2+} and, by analogy with its orthologs, this might involve an iron-sensing transcription factor. IdeR, a member of DtxR family, is the major iron-dependent transcriptional regulator in *M. tuberculosis* (Rodriguez *et al.*, 2002, Sritharan, 2016). IdeR represses transcription of genes involved in iron uptake and siderophore biosynthesis and activates expression of genes encoding iron-storage proteins such as bacterioferritin and a ferritin-like protein (Rodriguez *et al.*, 2002, Sritharan, 2016). Since *M. tuberculosis* is primarily a pathogen of the mammalian respiratory system it might frequently encounter oxidative stress. Thus, it is also possible that *ctpD* might be induced in response to H_2O_2 stress. Future work to monitor the expression of *ctpD in vitro* in response to specific stresses and *in vivo* during the course of infection will be needed to elucidate the physiological role of CtpD during the infection process.

2.3.4 PmtA in group A *Streptococcus*

Group A *Streptococcus* (GAS), a human pathogen, is the causative agent of a wide range of diseases, from mild skin infection to life-threatening diseases such as necrotizing fasciitis (Olsen *et al.*, 2009). GAS encodes a P_{1B4}-type ATPase under regulation of PerR, and was therefore named a PerR-regulated metal transporter (PmtA). In a *perR* null mutant, high level expression of PmtA is associated with derepression of genes normally responsive to cellular zinc status due to repression by AdcR (Brenot *et al.*, 2007), a Zn^{2+}-dependent repressor. This simplest interpretation of this result is that PmtA may function as a Zn^{2+} efflux transporter. Consistent with this notion, a *perR* null mutant has an increased resistance to Zn^{2+}, and this depends on PmtA (Brenot *et al.*, 2007). However, it is unclear why cells would efflux Zn^{2+} in response to H_2O_2 stress, nor is there any evidence that PmtA is important for Zn^{2+} resistance in wild-type cells, which presumably relies on the Zn^{2+}-inducible CzcD efflux pump to ameliorate Zn^{2+}-toxicity.

By analogy with PfeT and its orthologs, an alternative interpretation is that the primary role of PmtA is as a H_2O_2-inducible Fe^{2+}-efflux pump and that activity with Zn^{2+} may only be revealed when it is constitutively overexpressed in a *perR* null mutant. Two recent studies have confirmed the primary role of PmtA as an Fe^{2+}-efflux pump (Turner *et al.*, 2017, VanderWal *et al.*, 2017). PmtA is important for resistance to iron intoxication, and a *pmtA* null mutant accumulates elevated levels of intracellular iron. As expected, expression of *pmtA* is strongly induced by Fe^{2+}. Although a *pmtA* null mutant shows similar sensitivity to peroxide stress as a wild type strain in the absence of excess Fe^{2+}, it exhibits significantly increased susceptibility to peroxide stress when treated with Fe^{2+}. Since GAS is catalase negative, PmtA might be a frontline defense against peroxide stress. PmtA is also a critical virulence factor and is required for survival during infection in both intramuscular and subcutaneous mouse models (VanderWal *et al.*, 2017), which again links iron efflux and peroxide resistance to pathogen virulence.

2.3.5 Nia in *Sinorhizobium meliloti*

In addition to the P_{1B4}-ATPases featured above, it is possible that P_{1B}-ATPases of other groups may also have physiologically relevant activity with iron. One example is Nia, a P_{1B5}-ATPase with a C-terminal hemerythrin domain. Since hemerythrin domains bind O_2 via a diiron active site, this suggests a possible role in O_2-sensing (Xiong *et al.*, 2000, Karlsen *et al.*, 2005). Nia is encoded by the symbiotic plasmid A of *Sinorhizobium meliloti*, a nitrogen fixing microbe in the *Rhizobiales* lineage that has a symbiotic relationship with legumes in which it establishes nodules associated with roots.

Consistent with a possible role in Fe^{2+} efflux, a *nia* null mutant accumulates Fe^{2+} under excess metal conditions (Zielazinski *et al.*, 2013). However, Nia also functions with Ni^{2+} and a *nia* null mutant accumulates Ni^{2+} when in excess. The precise physiological role of Nia is not yet resolved. Biochemical assays suggest that Nia interacts with both Fe^{2+} and Ni^{2+} (but not Co^{2+}). However, a *nia* null mutant showed moderate sensitivity to Ni^{2+}, but not to Fe^{2+}, under the conditions tested (Zielazinski *et al.*, 2013). Expression of *nia* was moderately induced by Fe^{2+} (3-fold), Ni^{2+} (3-fold), and Co^{2+} (2-fold), but not by other metals. Interestingly, *nia* was most strongly induced (20-fold) in root nodules, thought to be a microaerobic, iron-rich environment (Becker *et al.*, 2004). These results lead to a model in which Nia is expressed in nitrogen-fixing root nodules, in response to either iron excess or microaerobic conditions. The C-terminal hemerythrin domain may also participate in or regulate transport activity, perhaps in response to O_2 (Zielazinski *et al.*, 2013). More work needs to be done to characterize the details of *nia* gene regulation and to more clearly define the physiological role of Nia during the *S. meliloti* -plant symbiosis.

2.4 Cation diffusion facilitator (CDF) proteins

Cation diffusion facilitators (CDFs) are a family of membrane-bound proteins that export and thereby confer tolerance to heavy metal ions (Haney *et al.*, 2005, Kolaj-Robin *et al.*, 2015). CDF proteins

are ubiquitous in bacteria, archaea, and eukaryotes (Nies, 2003). Collectively, bacterial CDF proteins have been implicated in transport of a wide range of metal ions (Zn^{2+}, Cd^{2+}, Co^{2+}, Ni^{2+}, Fe^{2+} and Mn^{2+}) with some transporters able to transport multiple metals (Munkelt *et al.*, 2004, Lu & Fu, 2007, Cubillas *et al.*, 2014, Raimunda & Elso-Berberian, 2014, Rosch *et al.*, 2009). Phylogenetic analysis of the CDF transporters defines three major groups corresponding to substrate specificity: 1) manganese efflux, 2) iron/zinc efflux, 3) zinc and other metals (but not manganese or iron) efflux (Montanini *et al.*, 2007).

A typical bacterial CDF contains an N-terminal domain (NTD), 6 transmembrane helices (TM), a histidine-rich interconnecting loop (IL) between TM4 and TM5, and a C-terminal cytoplasmic domain (CTD) (Haney *et al.*, 2005) (Fig 2.2). However, the detailed mechanisms of metal selectivity are unknown. Some studies suggest the cytoplasmic domain or the IL loop is important for metal specificity (Blindauer & Schmid, 2010, Podar *et al.*, 2012, Kawachi *et al.*, 2008), but other studies highlight the role of residues in the TM3 helix on metal selectivity (Lin *et al.*, 2009). For the *E. coli* FieF transporter, evidence supports a role for a tetrahedral metal-binding site formed between TM2 and TM5 in metal selectivity (Hoch *et al.*, 2012). So far, there is no unifying model that can account for metal selectivity of CDF proteins.

2.4.1 FieF in *E. coli*: Zn^{2+} vs. Fe^{2+} efflux

There are two CDF transporters in *E coli*: ZitB and FieF (also named as YiiP). ZitB is the secondary zinc efflux system that is critical for maintaining zinc homeostasis only when the zinc efflux ATPase ZntA is absent (Grass *et al.*, 2001). FieF has been studied for more than a decade, but its physiological function has been controversial. In 2004, the first two reports of its structural analysis were built on the assumption that FieF acts as a zinc efflux protein (Chao & Fu, 2004, Wei *et al.*, 2004). In fact, prior studies had demonstrated that *fieF* is induced by either zinc or iron (Grass *et al.*, 2001). However, ectopic expression

of FieF does not restore zinc tolerance in a zinc-sensitive strain, suggesting it might not play a role in zinc homeostasis (Grass *et al.*, 2001).

Physiological studies suggest that the major physiological role of FieF may be in iron tolerance. Indeed, FieF is important for full resistance to iron intoxication in a *fur* null mutant, where iron homeostasis is disrupted and iron uptake systems are constitutively expressed (Grass *et al.*, 2005). Ectopic expression of FieF leads to reduced accumulation of iron in a *fieF* null mutant. Moreover, reconstitution of FieF in proteoliposomes showed that it mediates iron transport *in vitro* (Grass *et al.*, 2005). These results all support the assignment of FieF (ferrous iron efflux) as an iron efflux transporter. However, this notion has been challenged by others. For example, FieF was shown to selectively bind zinc and cadmium with high affinity, but not iron or other metals tested (Wei & Fu, 2005). Based on the site-directed fluorescence resonance energy transfer (FRET) measurements, Lu *et al*. proposed an autoregulation model of transport activity in response to intracellular zinc levels (Lu *et al.*, 2009). Currently, FieF (YiiP) is referred to as a Zn^{2+} transporter in most published papers.

Ever since its structure was solved in 2007 (Lu & Fu, 2007), FieF has been considered as a prototype for bacterial CDF proteins, which makes it more frustrating that its physiological role has remained controversial. The regulation of *fieF* expression has not been well defined, but it does not appear to be regulated by Fur (Grass *et al.*, 2005). The physiological studies of FieF are certainly supportive of a role in Fe(II) efflux. This inference is further supported by the observation that the FieF homologs MamM and MamB form a heterodimeric CDF protein required for Fe(II) import into vesicles in support of magnetosome formation in the magnetotatic bacterium *Magnetospirillum gryphiswaldense* (Nies, 2011, Uebe *et al.*, 2011).

2.4.2 AitP in *Pseudomonas aeruginosa*

Pseudomonas aeruginosa is Gram-negative, opportunistic pathogen that is highly antibiotic resistant. *P. aeruginosa* encodes three paralogous CDF efflux systems: CzcD (PA0397), AitP (PA1297), and YiiP (PA3963). Of these, the alternative iron transport protein (AitP) most likely functions physiologically in Fe^{2+} efflux. Deletion of *aitP* leads to an increased sensitivity to both Fe^{2+} and Co^{2+}, increased intracellular accumulation of both ions, and decreased survival in presence of H_2O_2 (Salusso & Raimunda, 2017). The observed sensitivity to H_2O_2 is most consistent with a role in Fe^{2+} efflux, as noted above for P-type ATPases. In contrast with AitP, the CzcD and YiiP proteins were inferred to function physiologically in Zn^{2+} resistance, although this role is largely masked in wild-type cells by the activity of the Zn^{2+} efflux P-type ATPase, ZntA (Pederick *et al.*, 2015). All the three transporters are critical for virulence in a plant infection model (Salusso & Raimunda, 2017). However, it remains unclear why this organism requires multiple classes of Zn^{2+} efflux proteins or under what conditions the three proteins are physiologically important during the infection process.

2.4.3 FeoE in *Shewanella oneidensis* MR-1

Shewanella oneidensis MR-1 is a facultative anaerobe in the γ-proteobacterium family that is capable of respiration using metals (e.g. manganese, lead, uranium and ferric iron) as electron acceptors (Hau & Gralnick, 2007). *S. oneidensis* cells are usually pink or red, reflective of a high iron content in hemoproteins and cytochromes (Meyer *et al.*, 2004). When Fe^{3+} is used as a terminal electron acceptor, cells generate a large amount of soluble Fe^{2+} which could potentially lead to iron intoxication. FeoE, a CDF protein, is required for cell growth during anaerobic iron respiration, and deletion of *feoE* increased susceptibility to Fe^{2+} intoxication, consistent with a physiological role in Fe^{2+} efflux (Bennett *et al.*, 2015). Further work is required to understand how *feoE* expression is regulated. It is unclear, for example,

whether FeoE is induced in response to excess iron. Fur is the primary regulator that modulates iron acquisition in *S. oneidenis* (Yang *et al.*, 2008), and is a candidate for an iron-responsive transcription factor that could be involved.

2.5 Major facilitator superfamily (MFS)

The major facilitator superfamily **(**MFS) of membrane transporters function with a wide scope of small molecules such as ions, nucleosides, amino acids, small peptides, and lipids (Yan, 2015). They can be categorized into three groups: uniporters that transport a single substrate, symporters that transport a substrate coupled with another ion (generally a proton), and antiporters that transport two substrates in opposite directions (Forrest *et al.*, 2011, Quistgaard *et al.*, 2016). All the MFS transporters share a canonical structural fold composed of two distinct domains [Fig 2.2], each consisting of six transmembrane helices. The substrate binding site is located at the interface between these two domains (Yan, 2015).

The mechanism of transport by MFS proteins is not clear, but several related models have been proposed. The first, an alternate-access model, was proposed more than five decades ago (Jardetzky, 1966). This model speculates that the transporters undergo a conformational change that alternates between a form where substrate can bind from one side of the membrane to one where it can only bind from the other side. This has been validated by many structural studies such as the xylose/H^+ symporter XylE and for LacY (Quistgaard *et al.*, 2013, Kumar *et al.*, 2015, Kumar *et al.*, 2014). The second, a rocker-switch model, postulates that conformational changes are accomplished through rocker-switch-type rotation between the N and C domain. This model is supported by some open-conformation structures (Dang *et al.*, 2010) but not by the structures in occluded states (Yin *et al.*, 2006, Newstead *et al.*, 2011, Yan *et al.*, 2013, Fukuda *et al.*, 2015). A third, clamp-and-switch model, provides a two-step transport mechanism: a clamping step that mediates occlusion of the binding site and a switching step that mediates the exposure of the binding site. This model postulates four conformational states: inward open, outward

open, inward-facing occlusion, and outward-facing occlusion (Quistgaard *et al.*, 2016). This model is in a good agreement with studies of some MFS transporters (Deng *et al.*, 2015, Nomura *et al.*, 2015), but more structural analyses combined with biochemical and computational analyses are needed to further understand the transport mechanism of MFS transporters.

2.5.1 IceT (iron and citrate efflux transporter) in *Salmonella enterica sv.* Typhimurium

Salmonella enterica sv. Typhimurium is a Gram-negative pathogen commonly found in the gastrointestinal tract. IceT (MdtD) is a member of the MFS superfamily in *S. enterica*. The *mdtABCD baeSR* operon encodes IceT and two other systems: a RND (resistance-nodulation-division) drug efflux system MdtABC and a two-component regulatory system BaeSR that regulates antibiotic resistance and efflux (Baranova & Nikaido, 2002, Leblanc *et al.*, 2011, Nagakubo *et al.*, 2002). IceT is proposed to be an iron-citrate efflux transporter and it can export either iron citrate or citrate alone (Frawley *et al.*, 2013). The *iceT* null mutant shows increased susceptibility to the antibiotic streptonigrin (SN), the activity of which is modulated by the level of intracellular free iron (Yeowell & White, 1982). This result suggests that the mutation of *iceT* leads to an increase in intracellular labile iron pools. Consistent with this result, induction of IceT expression leads to reduced levels of intracellular iron (Frawley *et al.*, 2013).

Although the *mdtABCD baeSR* operon is not induced directly by high Fe^{2+} (Bjarnason *et al.*, 2003), it is induced by disruption of iron homeostasis in a *fur* null mutant where iron uptake systems are constitutively expressed, supportive of a physiological role for IceT in iron efflux. Although IceT confers resistance to peroxide stress in a *fur* null mutant, the *mdtABCD baeSR* operon is not induced by H_2O_2 or superoxide-generating reagents such as paraquat (Frawley *et al.*, 2013). However, it is induced by nitric oxide, which is also known to interact with the labile iron pool (Frawley *et al.*, 2013). The significance of

the regulation of IceT, together with its co-transcribed ABC transporter, by the BaeSR two-component system is not understood, nor is it yet clear whether or not IceT is important for pathogenesis.

2.6 Membrane bound ferritin A (MbfA) in *Agrobacterium tumefaciens* and *Bradyrhizobium japonicum*

Agrobacterium tumefaciens belongs to the *Rhizobiales* lineage and is the causative agent of the economically important plant disease, crown gall. MbfA was originally described as membrane-bound ferritin A, and is a member of the erythrin-vacuolar iron transport (Er-VIT1) ferritin-like superfamily. MbfA has two major domains: an N-terminal ferritin-like or Er domain (Er) and C-terminal membrane-embedded vacuolar iron transporter domain (VIT1) (Fig 2.2). The Er domain has a di-iron binding site and the VIT1 domain shows sequence homology to *Arabidopsis* VIT1, which is responsible for transferring iron into vacuoles (Kim *et al.*, 2006). Ferritin is an cytosolic iron storage protein ubiquitous in prokaryotes and eukaryotes (Arosio *et al.*, 2017), however, MbfA is not a *bona fide* ferritin and its physiological function was not immediately apparent.

Plant hosts often produce reactive oxygen species as a defense mechanism in response to microbial infection. Initial studies revealed that MbfA confers resistance to H_2O_2 stress, suggesting that it may play an important role in plant-pathogen interaction (Ruangkiattikul *et al.*, 2012). Moreover, MbfA expression was induced in response to high iron conditions as sensed by the iron response regulator protein, Irr (Ruangkiattikul *et al.*, 2012). However, these results could not distinguish between a role for MbfA in sequestration of iron (through its ferritin domain) or iron efflux. A follow up study revealed that MbfA is important for resistance to iron intoxication under acidic conditions (pH 5.5), which enhances iron solubility thereby promoting toxicity (Johnson *et al.*, 2012). Compared to wild-type, a *mbfA* null mutant had a modest increase in intracellular total iron as well as labile iron (Ruangkiattikul *et al.*, 2012). Since *mbfA* expression is induced by high iron under acidic conditions(Ruangkiattikul *et al.*, 2012), and reduces

intracellular iron levels, MbfA was postulated to function as an iron efflux transporter (Ruangkiattikul *et al.*, 2012).

Bradyrhizobium japonicum also encodes an MbfA protein implicated in iron efflux (Sankari & O'Brian, 2014). *B. japonicum* is a nitrogen-fixing endosymbiotic microbe that, like *A. tumefaciens,* belongs to the *Rhizobiales* lineage. As in *A. tumefaciens*, iron homeostasis in *B. japonicum* is also under control of Irr (Hamza *et al.*, 2000), which regulates iron uptake, storage, and utilization (Rudolph *et al.*, 2006). MbfA in *B. japonicum* is specifically induced by high iron and confers resistance to iron intoxication and H_2O_2 stress. Moreover, an *mbfA* null mutant accumulates significantly high levels of iron. Collectively, these data support the idea that MbfA functions physiologically as an iron efflux transporter (Sankari & O'Brian, 2014). Interestingly, the N-terminal ferritin-like domain located on the cytoplasmic side of inner membrane is required for iron transport activity and stress resistance. The purified ferritin domain forms a dimer in solution, which suggests that MbfA may dimerize to form a functional channel (Sankari & O'Brian, 2014). By mediating the efflux of Fe^{2+}, MbfA functions cooperatively with bacterioferritin (Bfr), which functions in iron sequestration, to prevent iron intoxication (Sankari & O'Brian, 2016). Mutation of either *mbfA* or *bfr* increases Fe^{2+} sensitivity, but a double *mbfA bfr* mutant is extremely sensitive to iron (Sankari & O'Brian, 2016).

2.7 Conclusions

Efflux systems play a central role in the resistance of bacteria to heavy metals, but their role in iron homeostasis has been relatively slow to emerge. This is perhaps a reflection of the fact that iron limitation is a far more prevalent challenge for bacteria than iron intoxication (Hood & Skaar, 2012), due in part to the very low solubility of iron under aerobic conditions of near neutral pH. Recent results, however, have greatly expanded our appreciation of the central importance of iron efflux systems and their contribution to virulence in human pathogens (Pi *et al.*, 2016, Patel *et al.*, 2016, VanderWal *et al.*,

2017). This implies that iron intoxication imposes a selective pressure during infection, although how this arises is not yet clear. For example, iron intoxication may arise from an uncontrolled influx of iron into the cell from the outside. Indeed, it is thought that macrophages impose Zn^{2+} and Cu^{+} toxicity on engulfed bacteria by import of metals into the phagolysosome (Flannagan *et al.*, 2015). However, iron is not known to be imported into the phagocytic vacuole. Iron overload may also result when bacteria exposed to an iron limited environment, and therefore expressing high affinity uptake systems, transition to an iron-rich environment. The sudden influx of iron may then be best accommodated by storage or efflux. Alternatively, or in addition, iron intoxication may arise from within the cell. For example, oxidative stress may lead to the release of iron from abundant iron-sulfur and mononuclear iron enzymes, thereby leading to an increase in cytosolic iron levels.

Iron intoxication may also be present in specific environments. For example, acidophilic bacteria grow in low pH environments where iron concentrations may be 10^{18} times higher than that found in pH neutral environments (Osorio *et al.*, 2008). In the case of iron-respiring bacteria, high local concentrations of Fe^{2+} may be produced by reduction of Fe^{3+}-containing minerals (Bennett *et al.*, 2015). Further work is needed to better define the prevalence of iron intoxication in natural environment settings and the role of iron efflux in these environments.

With the identification of the several families of iron efflux systems noted here, the stage is now set for further structural, biochemical and genetic studies to address their mechanisms of metal selectivity. It is presently unclear how these efflux transporters discriminate Fe^{2+} from competing substrates and how, at a structural level, efflux is coupled to substrate binding and energy consumption. It is also unclear why some cells rely on ATP-dependent P-type transporters and others utilize CDF proteins, which are coupled to the proton motive force. It is notable that in several cases efflux pumps were initially assigned a role for substrates others than Fe^{2+} (PfeT, FrvA, CtpD), and in other cases (FieF, Nia) the most relevant physiological substrate is still unclear. This highlights the fact that metal selectivity cannot be easily

predicted from protein sequence alone, and biochemical assays need to be interpreted in context of the physiology of the organisms. In several of the cases described, the most compelling evidence to assign function has emerged from a careful analysis of mutant phenotypes combined with detailed analysis of regulation to infer those conditions that specifically induce expression.

2.8 References

Andrews, S.C., A.K. Robinson & F. Rodriguez-Quinones, (2003) Bacterial iron homeostasis. *FEMS microbiology reviews* **27**: 215-237.

Anjem, A. & J.A. Imlay, (2012) Mononuclear iron enzymes are primary targets of hydrogen peroxide stress. *The Journal of biological chemistry* **287**: 15544-15556.

Anjem, A., S. Varghese & J.A. Imlay, (2009) Manganese import is a key element of the OxyR response to hydrogen peroxide in Escherichia coli. *Molecular microbiology* **72**: 844-858.

Arguello, J.M., (2003) Identification of ion-selectivity determinants in heavy-metal transport P1B-type ATPases. *The Journal of membrane biology* **195**: 93-108.

Arosio, P., L. Elia & M. Poli, (2017) Ferritin, cellular iron storage and regulation. *IUBMB life*.

Baichoo, N., T. Wang, R. Ye & J.D. Helmann, (2002) Global analysis of the Bacillus subtilis Fur regulon and the iron starvation stimulon. *Molecular microbiology* **45**: 1613-1629.

Baranova, N. & H. Nikaido, (2002) The baeSR two-component regulatory system activates transcription of the yegMNOB (mdtABCD) transporter gene cluster in Escherichia coli and increases its resistance to novobiocin and deoxycholate. *Journal of bacteriology* **184**: 4168-4176.

Barwinska-Sendra, A. & K.J. Waldron, The Role of Intermetal Competition and Mis-Metalation in Metal Toxicity. In: Advances in Microbial Physiology. Academic Press, pp.

Becker, A., H. Berges, E. Krol, C. Bruand, S. Ruberg, D. Capela, E. Lauber, E. Meilhoc, F. Ampe, F.J. de Bruijn, J. Fourment, A. Francez-Charlot, D. Kahn, H. Kuster, C. Liebe, A. Puhler, S. Weidner & J. Batut,

(2004) Global changes in gene expression in Sinorhizobium meliloti 1021 under microoxic and symbiotic conditions. *Molecular plant-microbe interactions : MPMI* **17**: 292-303.

Bennett, B.D., E.D. Brutinel & J.A. Gralnick, (2015) A Ferrous Iron Exporter Mediates Iron Resistance in Shewanella oneidensis MR-1. *Applied and environmental microbiology* **81**: 7938-7944.

Bjarnason, J., C.M. Southward & M.G. Surette, (2003) Genomic profiling of iron-responsive genes in Salmonella enterica serovar typhimurium by high-throughput screening of a random promoter library. *Journal of bacteriology* **185**: 4973-4982.

Blindauer, C.A. & R. Schmid, (2010) Cytosolic metal handling in plants: determinants for zinc specificity in metal transporters and metallothioneins. *Metallomics : integrated biometal science* **2**: 510-529.

Brenot, A., B.F. Weston & M.G. Caparon, (2007) A PerR-regulated metal transporter (PmtA) is an interface between oxidative stress and metal homeostasis in Streptococcus pyogenes. *Molecular microbiology* **63**: 1185-1196.

Calhoun, L.N. & Y.M. Kwon, (2011) Structure, function and regulation of the DNA-binding protein Dps and its role in acid and oxidative stress resistance in Escherichia coli: a review. *Journal of applied microbiology* **110**: 375-386.

Chan, H., V. Babayan, E. Blyumin, C. Gandhi, K. Hak, D. Harake, K. Kumar, P. Lee, T.T. Li, H.Y. Liu, T.C. Lo, C.J. Meyer, S. Stanford, K.S. Zamora & M.H. Saier, Jr., (2010) The p-type ATPase superfamily. *J Mol Microbiol Biotechnol* **19**: 5-104.

Chandrangsu, P., C. Rensing & J.D. Helmann, (2017) Metal homeostasis and resistance in bacteria. *Nature reviews. Microbiology*.

Chao, Y. & D. Fu, (2004) Thermodynamic studies of the mechanism of metal binding to the Escherichia coli zinc transporter YiiP. *The Journal of biological chemistry* **279**: 17173-17180.

Chen, L. & J.D. Helmann, (1995) Bacillus subtilis MrgA is a Dps(PexB) homologue: evidence for metalloregulation of an oxidative-stress gene. *Molecular microbiology* **18**: 295-300.

Cubillas, C., P. Vinuesa, M.L. Tabche, A. Davalos, A. Vazquez, I. Hernandez-Lucas, D. Romero & A. Garcia-de los Santos, (2014) The cation diffusion facilitator protein EmfA of Rhizobium etli belongs to a novel subfamily of Mn(2+)/Fe(2+) transporters conserved in alpha-proteobacteria. *Metallomics : integrated biometal science* **6**: 1808-1815.

Dang, S., L. Sun, Y. Huang, F. Lu, Y. Liu, H. Gong, J. Wang & N. Yan, (2010) Structure of a fucose transporter in an outward-open conformation. *Nature* **467**: 734-738.

Delany, I., R. Rappuoli & V. Scarlato, (2004) Fur functions as an activator and as a repressor of putative virulence genes in Neisseria meningitidis. *Molecular microbiology* **52**: 1081-1090.

Deng, D., P. Sun, C. Yan, M. Ke, X. Jiang, L. Xiong, W. Ren, K. Hirata, M. Yamamoto, S. Fan & N. Yan, (2015) Molecular basis of ligand recognition and transport by glucose transporters. *Nature* **526**: 391-396.

Fan, B. & B.P. Rosen, (2002) Biochemical characterization of CopA, the Escherichia coli Cu(I)-translocating P-type ATPase. *The Journal of biological chemistry* **277**: 46987-46992.

Faulkner, M.J. & J.D. Helmann, (2011) Peroxide stress elicits adaptive changes in bacterial metal ion homeostasis. *Antioxidants & redox signaling* **15**: 175-189.

Faulkner, M.J., Z. Ma, M. Fuangthong & J.D. Helmann, (2012) Derepression of the Bacillus subtilis PerR peroxide stress response leads to iron deficiency. *Journal of bacteriology* **194**: 1226-1235.

Flannagan, R.S., B. Heit & D.E. Heinrichs, (2015) Antimicrobial Mechanisms of Macrophages and the Immune Evasion Strategies of Staphylococcus aureus. *Pathogens (Basel, Switzerland)* **4**: 826-868.

Fleischhacker, A.S. & P.J. Kiley, (2011) Iron-containing transcription factors and their roles as sensors. *Current opinion in chemical biology* **15**: 335-341.

Forrest, L.R., R. Kramer & C. Ziegler, (2011) The structural basis of secondary active transport mechanisms. *Biochimica et biophysica acta* **1807**: 167-188.

Frawley, E.R., M.L. Crouch, L.K. Bingham-Ramos, H.F. Robbins, W. Wang, G.D. Wright & F.C. Fang, (2013) Iron and citrate export by a major facilitator superfamily pump regulates metabolism and stress

resistance in Salmonella Typhimurium. *Proceedings of the National Academy of Sciences of the United States of America* **110**: 12054-12059.

Fuangthong, M., A.F. Herbig, N. Bsat & J.D. Helmann, (2002) Regulation of the Bacillus subtilis fur and perR genes by PerR: not all members of the PerR regulon are peroxide inducible. *Journal of bacteriology* **184**: 3276-3286.

Fukuda, M., H. Takeda, H.E. Kato, S. Doki, K. Ito, A.D. Maturana, R. Ishitani & O. Nureki, (2015) Structural basis for dynamic mechanism of nitrate/nitrite antiport by NarK. *Nature communications* **6**: 7097.

Gaballa, A., H. Antelmann, C. Aguilar, S.K. Khakh, K.B. Song, G.T. Smaldone & J.D. Helmann, (2008) The Bacillus subtilis iron-sparing response is mediated by a Fur-regulated small RNA and three small, basic proteins. *Proceedings of the National Academy of Sciences of the United States of America* **105**: 11927-11932.

Gaballa, A. & J.D. Helmann, (2002) A peroxide-induced zinc uptake system plays an important role in protection against oxidative stress in Bacillus subtilis. *Molecular microbiology* **45**: 997-1005.

Gonzalez-Guerrero, M., E. Eren, S. Rawat, T.L. Stemmler & J.M. Arguello, (2008) Structure of the two transmembrane Cu+ transport sites of the Cu+ -ATPases. *The Journal of biological chemistry* **283**: 29753-29759.

Grass, G., B. Fan, B.P. Rosen, S. Franke, D.H. Nies & C. Rensing, (2001) ZitB (YbgR), a member of the cation diffusion facilitator family, is an additional zinc transporter in Escherichia coli. *Journal of bacteriology* **183**: 4664-4667.

Grass, G., M. Otto, B. Fricke, C.J. Haney, C. Rensing, D.H. Nies & D. Munkelt, (2005) FieF (YiiP) from Escherichia coli mediates decreased cellular accumulation of iron and relieves iron stress. *Archives of microbiology* **183**: 9-18.

Guan, G., A. Pinochet-Barros, A. Gaballa, S.J. Patel, J.M. Arguello & J.D. Helmann, (2015) PfeT, a P1B4 -type ATPase, effluxes ferrous iron and protects Bacillus subtilis against iron intoxication. *Molecular microbiology* **98**: 787-803.

Hamza, I., Z. Qi, N.D. King & M.R. O'Brian, (2000) Fur-independent regulation of iron metabolism by Irr in Bradyrhizobium japonicum. *Microbiology (Reading, England)* **146 (Pt 3)**: 669-676.

Haney, C.J., G. Grass, S. Franke & C. Rensing, (2005) New developments in the understanding of the cation diffusion facilitator family. *Journal of industrial microbiology & biotechnology* **32**: 215-226.

Hau, H.H. & J.A. Gralnick, (2007) Ecology and biotechnology of the genus Shewanella. *Annual review of microbiology* **61**: 237-258.

Helmann, J.D., (2014) Specificity of metal sensing: iron and manganese homeostasis in Bacillus subtilis. *The Journal of biological chemistry* **289**: 28112-28120.

Herbig, A.F. & J.D. Helmann, (2001) Roles of metal ions and hydrogen peroxide in modulating the interaction of the Bacillus subtilis PerR peroxide regulon repressor with operator DNA. *Molecular microbiology* **41**: 849-859.

Hoch, E., W. Lin, J. Chai, M. Hershfinkel, D. Fu & I. Sekler, (2012) Histidine pairing at the metal transport site of mammalian ZnT transporters controls Zn2+ over Cd2+ selectivity. *Proceedings of the National Academy of Sciences of the United States of America* **109**: 7202-7207.

Hood, M.I. & E.P. Skaar, (2012) Nutritional immunity: transition metals at the pathogen–host interface. *Nat Rev Micro* **10**: 525-537.

Hunt, M.D., G.S. Pettis & M.A. McIntosh, (1994) Promoter and operator determinants for fur-mediated iron regulation in the bidirectional fepA-fes control region of the Escherichia coli enterobactin gene system. *Journal of bacteriology* **176**: 3944-3955.

Imlay, J.A., (2003) Pathways of oxidative damage. *Annual review of microbiology* **57**: 395-418.

Imlay, J.A., (2014) The mismetallation of enzymes during oxidative stress. *The Journal of biological chemistry* **289**: 28121-28128.

Jang, S. & J.A. Imlay, (2007) Micromolar intracellular hydrogen peroxide disrupts metabolism by damaging iron-sulfur enzymes. *The Journal of biological chemistry* **282**: 929-937.

Jardetzky, O., (1966) Simple allosteric model for membrane pumps. *Nature* **211**: 969-970.

Johnson, D.B., T. Kanao & S. Hedrich, (2012) Redox Transformations of Iron at Extremely Low pH: Fundamental and Applied Aspects. *Frontiers in microbiology* **3**: 96.

Karlsen, O.A., L. Ramsevik, L.J. Bruseth, O. Larsen, A. Brenner, F.S. Berven, H.B. Jensen & J.R. Lillehaug, (2005) Characterization of a prokaryotic haemerythrin from the methanotrophic bacterium Methylococcus capsulatus (Bath). *The FEBS journal* **272**: 2428-2440.

Kawachi, M., Y. Kobae, T. Mimura & M. Maeshima, (2008) Deletion of a histidine-rich loop of AtMTP1, a vacuolar Zn(2+)/H(+) antiporter of Arabidopsis thaliana, stimulates the transport activity. *The Journal of biological chemistry* **283**: 8374-8383.

Kehres, D.G., M.L. Zaharik, B.B. Finlay & M.E. Maguire, (2000) The NRAMP proteins of Salmonella typhimurium and Escherichia coli are selective manganese transporters involved in the response to reactive oxygen. *Molecular microbiology* **36**: 1085-1100.

Kim, S.A., T. Punshon, A. Lanzirotti, L. Li, J.M. Alonso, J.R. Ecker, J. Kaplan & M.L. Guerinot, (2006) Localization of iron in Arabidopsis seed requires the vacuolar membrane transporter VIT1. *Science (New York, N.Y.)* **314**: 1295-1298.

Kolaj-Robin, O., D. Russell, K.A. Hayes, J.T. Pembroke & T. Soulimane, (2015) Cation Diffusion Facilitator family: Structure and function. *FEBS letters* **589**: 1283-1295.

Kuhlbrandt, W., (2004) Biology, structure and mechanism of P-type ATPases. *Nature reviews. Molecular cell biology* **5**: 282-295.

Kumar, H., J.S. Finer-Moore, H.R. Kaback & R.M. Stroud, (2015) Structure of LacY with an alpha-substituted galactoside: Connecting the binding site to the protonation site. *Proceedings of the National Academy of Sciences of the United States of America* **112**: 9004-9009.

Kumar, H., V. Kasho, I. Smirnova, J.S. Finer-Moore, H.R. Kaback & R.M. Stroud, (2014) Structure of sugar-bound LacY. *Proceedings of the National Academy of Sciences of the United States of America* **111**: 1784-1788.

Leblanc, S.K., C.W. Oates & T.L. Raivio, (2011) Characterization of the induction and cellular role of the BaeSR two-component envelope stress response of Escherichia coli. *Journal of bacteriology* **193**: 3367-3375.

Ledala, N., M. Sengupta, A. Muthaiyan, B.J. Wilkinson & R.K. Jayaswal, (2010) Transcriptomic response of Listeria monocytogenes to iron limitation and Fur mutation. *Applied and environmental microbiology* **76**: 406-416.

Lee, J.W. & J.D. Helmann, (2007) Functional specialization within the Fur family of metalloregulators. *Biometals : an international journal on the role of metal ions in biology, biochemistry, and medicine* **20**: 485-499.

Lenoir, G., P. Williamson & J.C. Holthuis, (2007) On the origin of lipid asymmetry: the flip side of ion transport. *Current opinion in chemical biology* **11**: 654-661.

Lin, H., D. Burton, L. Li, D.E. Warner, J.D. Phillips, D.M. Ward & J. Kaplan, (2009) Gain-of-function mutations identify amino acids within transmembrane domains of the yeast vacuolar transporter Zrc1 that determine metal specificity. *The Biochemical journal* **422**: 273-283.

Liu, J., S.J. Dutta, A.J. Stemmler & B. Mitra, (2006) Metal-binding affinity of the transmembrane site in ZntA: implications for metal selectivity. *Biochemistry* **45**: 763-772.

Lopez-Marques, R.L., L.R. Poulsen, S. Hanisch, K. Meffert, M.J. Buch-Pedersen, M.K. Jakobsen, T.G. Pomorski & M.G. Palmgren, (2010) Intracellular targeting signals and lipid specificity determinants

of the ALA/ALIS P4-ATPase complex reside in the catalytic ALA alpha-subunit. *Molecular biology of the cell* **21**: 791-801.

Lu, M., J. Chai & D. Fu, (2009) Structural basis for autoregulation of the zinc transporter YiiP. *Nature structural & molecular biology* **16**: 1063-1067.

Lu, M. & D. Fu, (2007) Structure of the zinc transporter YiiP. *Science (New York, N.Y.)* **317**: 1746-1748.

Mana-Capelli, S., A.K. Mandal & J.M. Arguello, (2003) Archaeoglobus fulgidus CopB is a thermophilic Cu2+-ATPase: functional role of its histidine-rich-N-terminal metal binding domain. *The Journal of biological chemistry* **278**: 40534-40541.

Mandal, A.K., W.D. Cheung & J.M. Arguello, (2002) Characterization of a thermophilic P-type Ag+/Cu+-ATPase from the extremophile Archaeoglobus fulgidus. *The Journal of biological chemistry* **277**: 7201-7208.

Masse, E. & S. Gottesman, (2002) A small RNA regulates the expression of genes involved in iron metabolism in Escherichia coli. *Proc Natl Acad Sci U S A* **99**: 4620-4625.

Masse, E., H. Salvail, G. Desnoyers & M. Arguin, (2007) Small RNAs controlling iron metabolism. *Current opinion in microbiology* **10**: 140-145.

Masse, E., C.K. Vanderpool & S. Gottesman, (2005) Effect of RyhB small RNA on global iron use in Escherichia coli. *Journal of bacteriology* **187**: 6962-6971.

McHugh, J.P., F. Rodriguez-Quinones, H. Abdul-Tehrani, D.A. Svistunenko, R.K. Poole, C.E. Cooper & S.C. Andrews, (2003) Global iron-dependent gene regulation in Escherichia coli. A new mechanism for iron homeostasis. *The Journal of biological chemistry* **278**: 29478-29486.

McLaughlin, H.P., M. Bahey-El-Din, P.G. Casey, C. Hill & C.G. Gahan, (2013) A mutant in the Listeria monocytogenes Fur-regulated virulence locus (frvA) induces cellular immunity and confers protection against listeriosis in mice. *Journal of medical microbiology* **62**: 185-190.

McLaughlin, H.P., Q. Xiao, R.B. Rea, H. Pi, P.G. Casey, T. Darby, A. Charbit, R.D. Sleator, S.A. Joyce, R.E. Cowart, C. Hill, P.E. Klebba & C.G. Gahan, (2012) A putative P-type ATPase required for virulence and resistance to haem toxicity in Listeria monocytogenes. *PloS one* **7**: e30928.

Meyer, T.E., A.I. Tsapin, I. Vandenberghe, L. de Smet, D. Frishman, K.H. Nealson, M.A. Cusanovich & J.J. van Beeumen, (2004) Identification of 42 possible cytochrome C genes in the Shewanella oneidensis genome and characterization of six soluble cytochromes. *Omics : a journal of integrative biology* **8**: 57-77.

Montanini, B., D. Blaudez, S. Jeandroz, D. Sanders & M. Chalot, (2007) Phylogenetic and functional analysis of the Cation Diffusion Facilitator (CDF) family: improved signature and prediction of substrate specificity. *BMC genomics* **8**: 107.

Moore, C.M., A. Gaballa, M. Hui, R.W. Ye & J.D. Helmann, (2005) Genetic and physiological responses of Bacillus subtilis to metal ion stress. *Molecular microbiology* **57**: 27-40.

Munkelt, D., G. Grass & D.H. Nies, (2004) The chromosomally encoded cation diffusion facilitator proteins DmeF and FieF from Wautersia metallidurans CH34 are transporters of broad metal specificity. *Journal of bacteriology* **186**: 8036-8043.

Nagakubo, S., K. Nishino, T. Hirata & A. Yamaguchi, (2002) The putative response regulator BaeR stimulates multidrug resistance of Escherichia coli via a novel multidrug exporter system, MdtABC. *Journal of bacteriology* **184**: 4161-4167.

Nandal, A., C.C. Huggins, M.R. Woodhall, J. McHugh, F. Rodriguez-Quinones, M.A. Quail, J.R. Guest & S.C. Andrews, (2010) Induction of the ferritin gene (ftnA) of Escherichia coli by Fe(2+)-Fur is mediated by reversal of H-NS silencing and is RyhB independent. *Molecular microbiology* **75**: 637-657.

Newstead, S., D. Drew, A.D. Cameron, V.L. Postis, X. Xia, P.W. Fowler, J.C. Ingram, E.P. Carpenter, M.S. Sansom, M.J. McPherson, S.A. Baldwin & S. Iwata, (2011) Crystal structure of a prokaryotic

homologue of the mammalian oligopeptide-proton symporters, PepT1 and PepT2. *The EMBO journal* **30**: 417-426.

Nies, D.H., (2003) Efflux-mediated heavy metal resistance in prokaryotes. *FEMS microbiology reviews* **27**: 313-339.

Nies, D.H., (2011) How iron is transported into magnetosomes. *Molecular microbiology* **82**: 792-796.

Nomura, N., G. Verdon, H.J. Kang, T. Shimamura, Y. Nomura, Y. Sonoda, S.A. Hussien, A.A. Qureshi, M. Coincon, Y. Sato, H. Abe, Y. Nakada-Nakura, T. Hino, T. Arakawa, O. Kusano-Arai, H. Iwanari, T. Murata, T. Kobayashi, T. Hamakubo, M. Kasahara, S. Iwata & D. Drew, (2015) Structure and mechanism of the mammalian fructose transporter GLUT5. *Nature* **526**: 397-401.

Novoa-Aponte, L. & C.Y. Soto Ospina, (2014) Mycobacterium tuberculosis P-type ATPases: possible targets for drug or vaccine development. *BioMed research international* **2014**: 296986.

Nucifora, G., L. Chu, T.K. Misra & S. Silver, (1989) Cadmium resistance from Staphylococcus aureus plasmid pI258 cadA gene results from a cadmium-efflux ATPase. *Proceedings of the National Academy of Sciences of the United States of America* **86**: 3544-3548.

Ollinger, J., K.B. Song, H. Antelmann, M. Hecker & J.D. Helmann, (2006) Role of the Fur regulon in iron transport in Bacillus subtilis. *Journal of bacteriology* **188**: 3664-3673.

Olsen, R.J., S.A. Shelburne & J.M. Musser, (2009) Molecular mechanisms underlying group A streptococcal pathogenesis. *Cellular microbiology* **11**: 1-12.

Osorio, H., V. Martinez, P.A. Nieto, D.S. Holmes & R. Quatrini, (2008) Microbial iron management mechanisms in extremely acidic environments: comparative genomics evidence for diversity and versatility. *BMC microbiology* **8**: 203.

Park, S., X. You & J.A. Imlay, (2005) Substantial DNA damage from submicromolar intracellular hydrogen peroxide detected in Hpx- mutants of Escherichia coli. *Proceedings of the National Academy of Sciences of the United States of America* **102**: 9317-9322.

Patel, S.J., B.E. Lewis, J.E. Long, S. Nambi, C.M. Sassetti, T.L. Stemmler & J.M. Arguello, (2016) Fine-tuning of Substrate Affinity Leads to Alternative Roles of Mycobacterium tuberculosis Fe2+-ATPases. *The Journal of biological chemistry* **291**: 11529-11539.

Pederick, V.G., B.A. Eijkelkamp, S.L. Begg, M.P. Ween, L.J. McAllister, J.C. Paton & C.A. McDevitt, (2015) ZnuA and zinc homeostasis in Pseudomonas aeruginosa. *Scientific reports* **5**: 13139.

Pi, H., S.J. Patel, J.M. Arguello & J.D. Helmann, (2016) The Listeria monocytogenes Fur-regulated virulence protein FrvA is an Fe(II) efflux P1B4 -type ATPase. *Molecular microbiology* **100**: 1066-1079.

Podar, D., J. Scherer, Z. Noordally, P. Herzyk, D. Nies & D. Sanders, (2012) Metal selectivity determinants in a family of transition metal transporters. *The Journal of biological chemistry* **287**: 3185-3196.

Quistgaard, E.M., C. Low, F. Guettou & P. Nordlund, (2016) Understanding transport by the major facilitator superfamily (MFS): structures pave the way. *Nature reviews. Molecular cell biology* **17**: 123-132.

Quistgaard, E.M., C. Low, P. Moberg, L. Tresaugues & P. Nordlund, (2013) Structural basis for substrate transport in the GLUT-homology family of monosaccharide transporters. *Nature structural & molecular biology* **20**: 766-768.

Raimunda, D. & G. Elso-Berberian, (2014) Functional characterization of the CDF transporter SMc02724 (SmYiiP) in Sinorhizobium meliloti: Roles in manganese homeostasis and nodulation. *Biochimica et biophysica acta* **1838**: 3203-3211.

Raimunda, D., J.E. Long, T. Padilla-Benavides, C.M. Sassetti & J.M. Arguello, (2014) Differential roles for the Co(2+) /Ni(2+) transporting ATPases, CtpD and CtpJ, in Mycobacterium tuberculosis virulence. *Molecular microbiology* **91**: 185-197.

Rea, R., C. Hill & C.G. Gahan, (2005) Listeria monocytogenes PerR mutants display a small-colony phenotype, increased sensitivity to hydrogen peroxide, and significantly reduced murine virulence. *Applied and environmental microbiology* **71**: 8314-8322.

Rodionov, D.A., M.S. Gelfand, J.D. Todd, A.R. Curson & A.W. Johnston, (2006) Computational reconstruction of iron- and manganese-responsive transcriptional networks in alpha-proteobacteria. *PLoS computational biology* **2**: e163.

Rodriguez, G.M., M.I. Voskuil, B. Gold, G.K. Schoolnik & I. Smith, (2002) ideR, An essential gene in mycobacterium tuberculosis: role of IdeR in iron-dependent gene expression, iron metabolism, and oxidative stress response. *Infection and immunity* **70**: 3371-3381.

Rosch, J.W., G. Gao, G. Ridout, Y.D. Wang & E.I. Tuomanen, (2009) Role of the manganese efflux system mntE for signalling and pathogenesis in Streptococcus pneumoniae. *Molecular microbiology* **72**: 12-25.

Ruangkiattikul, N., S. Bhubhanil, J. Chamsing, P. Niamyim, R. Sukchawalit & S. Mongkolsuk, (2012) Agrobacterium tumefaciens membrane-bound ferritin plays a role in protection against hydrogen peroxide toxicity and is negatively regulated by the iron response regulator. *FEMS microbiology letters* **329**: 87-92.

Rudolph, G., G. Semini, F. Hauser, A. Lindemann, M. Friberg, H. Hennecke & H.M. Fischer, (2006) The Iron control element, acting in positive and negative control of iron-regulated Bradyrhizobium japonicum genes, is a target for the Irr protein. *Journal of bacteriology* **188**: 733-744.

Salusso, A. & D. Raimunda, (2017) Defining the Roles of the Cation Diffusion Facilitators in Fe2+/Zn2+ Homeostasis and Establishment of Their Participation in Virulence in Pseudomonas aeruginosa. *Frontiers in cellular and infection microbiology* **7**: 84.

Sankari, S. & M.R. O'Brian, (2014) A bacterial iron exporter for maintenance of iron homeostasis. *The Journal of biological chemistry* **289**: 16498-16507.

Sankari, S. & M.R. O'Brian, (2016) Synthetic Lethality of the bfr and mbfA Genes Reveals a Functional Relationship between Iron Storage and Iron Export in Managing Stress Responses in Bradyrhizobium japonicum. *PloS one* **11**: e0157250.

Seo, S.W., D. Kim, H. Latif, E.J. O'Brien, R. Szubin & B.O. Palsson, (2014) Deciphering Fur transcriptional regulatory network highlights its complex role beyond iron metabolism in Escherichia coli. *Nature communications* **5**: 4910.

Smaldone, G.T., H. Antelmann, A. Gaballa & J.D. Helmann, (2012a) The FsrA sRNA and FbpB protein mediate the iron-dependent induction of the Bacillus subtilis lutABC iron-sulfur-containing oxidases. *Journal of bacteriology* **194**: 2586-2593.

Smaldone, G.T. & J.D. Helmann, (2007) CsoR regulates the copper efflux operon copZA in Bacillus subtilis. *Microbiology (Reading, England)* **153**: 4123-4128.

Smaldone, G.T., O. Revelles, A. Gaballa, U. Sauer, H. Antelmann & J.D. Helmann, (2012b) A global investigation of the Bacillus subtilis iron-sparing response identifies major changes in metabolism. *Journal of bacteriology* **194**: 2594-2605.

Smith, A.T., K.P. Smith & A.C. Rosenzweig, (2014) Diversity of the metal-transporting P1B-type ATPases. *Journal of biological inorganic chemistry : JBIC : a publication of the Society of Biological Inorganic Chemistry* **19**: 947-960.

Sritharan, M., (2016) Iron Homeostasis in Mycobacterium tuberculosis: Mechanistic Insights into Siderophore-Mediated Iron Uptake. *Journal of bacteriology* **198**: 2399-2409.

Storz, G. & S. Altuvia, (1994) OxyR regulon. *Methods in enzymology* **234**: 217-223.

Thever, M.D. & M.H. Saier, Jr., (2009) Bioinformatic characterization of p-type ATPases encoded within the fully sequenced genomes of 26 eukaryotes. *The Journal of membrane biology* **229**: 115-130.

Todd, J.D., G. Sawers, D.A. Rodionov & A.W. Johnston, (2006) The Rhizobium leguminosarum regulator IrrA affects the transcription of a wide range of genes in response to Fe availability. *Molecular genetics and genomics : MGG* **275**: 564-577.

Turner, A.G., C.Y. Ong, K.Y. Djoko, N.P. West, M.R. Davies, A.G. McEwan & M.J. Walker, (2017) The PerR-Regulated P1B-4-Type ATPase (PmtA) Acts as a Ferrous Iron Efflux Pump in Streptococcus pyogenes. *Infection and immunity* **85**.

Uebe, R., K. Junge, V. Henn, G. Poxleitner, E. Katzmann, J.M. Plitzko, R. Zarivach, T. Kasama, G. Wanner, M. Posfai, L. Bottger, B. Matzanke & D. Schuler, (2011) The cation diffusion facilitator proteins MamB and MamM of Magnetospirillum gryphiswaldense have distinct and complex functions, and are involved in magnetite biomineralization and magnetosome membrane assembly. *Molecular microbiology* **82**: 818-835.

VanderWal, A.R., N. Makthal, A. Pinochet-Barros, J.D. Helmann, R.J. Olsen & M. Kumaraswami, (2017) Iron Efflux by PmtA Is Critical for Oxidative Stress Resistance and Contributes Significantly to Group A Streptococcus Virulence. *Infection and immunity* **85**.

Waldron, K.J., J.C. Rutherford, D. Ford & N.J. Robinson, (2009) Metalloproteins and metal sensing. *Nature* **460**: 823-830.

Wei, Y. & D. Fu, (2005) Selective metal binding to a membrane-embedded aspartate in the Escherichia coli metal transporter YiiP (FieF). *The Journal of biological chemistry* **280**: 33716-33724.

Wei, Y., H. Li & D. Fu, (2004) Oligomeric state of the Escherichia coli metal transporter YiiP. *The Journal of biological chemistry* **279**: 39251-39259.

Xiong, J., D.M. Kurtz, Jr., J. Ai & J. Sanders-Loehr, (2000) A hemerythrin-like domain in a bacterial chemotaxis protein. *Biochemistry* **39**: 5117-5125.

Yan, H., W. Huang, C. Yan, X. Gong, S. Jiang, Y. Zhao, J. Wang & Y. Shi, (2013) Structure and mechanism of a nitrate transporter. *Cell reports* **3**: 716-723.

Yan, N., (2015) Structural Biology of the Major Facilitator Superfamily Transporters. *Annual review of biophysics* **44**: 257-283.

Yang, J., I. Sangwan, A. Lindemann, F. Hauser, H. Hennecke, H.M. Fischer & M.R. O'Brian, (2006) Bradyrhizobium japonicum senses iron through the status of haem to regulate iron homeostasis and metabolism. *Molecular microbiology* **60**: 427-437.

Yang, Y., D.P. Harris, F. Luo, L. Wu, A.B. Parsons, A.V. Palumbo & J. Zhou, (2008) Characterization of the Shewanella oneidensis Fur gene: roles in iron and acid tolerance response. *BMC genomics* **9 Suppl 1**: S11.

Yeowell, H.N. & J.R. White, (1982) Iron requirement in the bactericidal mechanism of streptonigrin. *Antimicrobial agents and chemotherapy* **22**: 961-968.

Yin, Y., X. He, P. Szewczyk, T. Nguyen & G. Chang, (2006) Structure of the multidrug transporter EmrD from Escherichia coli. *Science (New York, N.Y.)* **312**: 741-744.

Yu, C. & C.A. Genco, (2012) Fur-mediated activation of gene transcription in the human pathogen Neisseria gonorrhoeae. *Journal of bacteriology* **194**: 1730-1742.

Zielazinski, E.L., G.E. Cutsail, 3rd, B.M. Hoffman, T.L. Stemmler & A.C. Rosenzweig, (2012) Characterization of a cobalt-specific P(1B)-ATPase. *Biochemistry* **51**: 7891-7900.

Zielazinski, E.L., M. Gonzalez-Guerrero, P. Subramanian, T.L. Stemmler, J.M. Arguello & A.C. Rosenzweig, (2013) Sinorhizobium meliloti Nia is a P(1B-5)-ATPase expressed in the nodule during plant symbiosis and is involved in Ni and Fe transport. *Metallomics : integrated biometal science* **5**: 1614-1623.

Chapter 3. The *Listeria monocytogenes* Fur-regulated virulence protein FrvA is an Fe(II) efflux P_{1B4}-type ATPase

3.1 Summary

Listeria monocytogenes FrvA (Lmo0641) is critical for virulence in the mouse model and is an ortholog of the *Bacillus subtilis* Fur- and PerR-regulated Fe(II) efflux P_{1B4}-type ATPase PfeT. Previously, FrvA was suggested to protect against heme toxicity. Here, we demonstrate that an *frvA* mutant is sensitive to iron intoxication, but not to other metals. Expression of *frvA* is induced by high iron and this induction requires Fur. FrvA functions *in vitro* as a divalent cation specific ATPase most strongly activated by ferrous iron. When expressed in *B. subtilis*, FrvA increases resistance to iron toxicity both in wild-type and in a *pfeT* null strain. FrvA is a high affinity Fe(II) exporter and its induction imposes severe iron limitation in *B. subtilis* resulting in derepression of both Fur- and PerR-regulated genes. FrvA also recognizes Co(II) and Zn(II) as substrates and can complement *B. subtilis* strains defective in the endogenous export systems for these cations. Building on these results, we conclude that FrvA functions in the efflux of Fe(II), and not heme, during listerial infection.

3.2 Introduction

Listeria monocytogenes is a model intracellular pathogen that invades mammalian cells by phagocytosis, ultimately escaping the phagocytic vacuole to proliferate in host cytosol and spread from cell to cell (Cossart, 2011). Despite intensive study, the roles of many genes critical for virulence have remained unclear. Our attention was drawn to the Fur-regulated virulence determinant *frvA* (*lmo0641*)

This chapter is adapted from Pi, H., S.J. Patel, J.M. Arguello & J.D. Helmann. *Molecular microbiology* 2016, 100: 1066-1079. The ATPase assays were done by S.J.P. The primary change has been to merge Supplemental information from the cited publication into the main body of this chapter to comply with the formatting requirements.

which encodes a protein homologous to the *Bacillus subtilis* P_{1B4}-type ATPase PfeT (Guan *et al.*, 2015b). The FrvA protein is critical for virulence, although the nature of the virulence defect is not yet clear (McLaughlin *et al.*, 2012). The Δ*frvA* strain is highly attenuated, but is still able to invade and replicate in a macrophage cell line. Inoculation into mice induces cellular immunity suggesting that this strain could be useful for vaccine development (McLaughlin *et al.*, 2013).

FrvA is a member of the P_{1B4} subfamily of metal transport ATPases as it shares their invariant transmembrane metal binding site (Argüello, 2003, McLaughlin *et al.*, 2012). In general, P_{1B}-ATPases drive cytoplasmic metal ion efflux, and members of the P_{1B4} subfamily are most closely associated with efflux of Co(II) (Argüello, 2003, Raimunda *et al.*, 2014b, Raimunda *et al.*, 2012, Smith *et al.*, 2014, Zielazinski *et al.*, 2012). Previous studies have highlighted the role of Cu(I) and Zn(II) efflux P-type ATPases in resistance to metal ion toxicity and in virulence (Argüello *et al.*, 2011, Djoko *et al.*, 2015, German *et al.*, 2013). Similarly, some P_{1B4}-type ATPases, including FrvA, are known to be critical for virulence (McLaughlin *et al.*, 2012, Raimunda *et al.*, 2014b). However, the nature of the substrate transported by the corresponding proteins during infection is not established, and it would be surprising for Co(II) efflux to be relevant to pathogenesis.

The *B. subtilis* PfeT protein (formerly ZosA) is a prototypic member of the P_{1B4}-class of ATPases and was originally ascribed a function in Zn(II) homeostasis (Gaballa & Helmann, 2002a). Recently, we demonstrated that the primary function of PfeT is efflux of Fe(II) to prevent iron overload (Guan *et al.*, 2015b). We therefore reasoned that FrvA (and perhaps other P_{1B4} ATPases) might also function in Fe(II) efflux. If correct, this would provide evidence that the role of metal efflux ATPases in bacterial virulence includes the export of Fe(II). However, this model contrasts with a previous report that FrvA likely functions as a heme exporter as inferred from an increase in accumulated ^{59}Fe when cells were exposed to ^{59}Fe-labeled heme (McLaughlin *et al.*, 2012).

The physiological role of proteins is often revealed by a careful analysis of their patterns of expression. The *frvA* (*lmo0641*) gene was first highlighted as a member of the PerR regulon (Rea *et al.*, 2005), consistent with the PerR regulation of the *B. subtilis* homolog (Fuangthong & Helmann, 2003, Gaballa & Helmann, 2002a, Helmann *et al.*, 2003). The *frvA* gene is highly derepressed in a *perR* null mutant and the promoter region is associated with candidate Per box sequences (Rea *et al.*, 2005). These results are consistent with PerR acting as a repressor of *frvA* and further suggest that *frvA* is induced by hydrogen peroxide. It is likely that FrvA is coordinately induced with other PerR-regulated genes including catalase and the *hemA* operon (Rea *et al.*, 2005), encoding enzymes of heme biosynthesis, as also observed in *B. subtilis* (Chen *et al.*, 1995, Fuangthong *et al.*, 2002b). The presumed rationale for derepression of the *hemA* operon is that high level expression of catalase, a heme-containing enzyme, increases the cellular demand for heme. Indeed, expression of catalase in a *B. subtilis perR* mutant contributes to iron deficiency due to the high demand imposed for its heme cofactor (Faulkner *et al.*, 2012, Ma *et al.*, 2012). The proposed role of FrvA in heme export (McLaughlin *et al.*, 2012) would seem inconsistent with its apparent co-induction with heme biosynthesis functions.

In addition to PerR, FrvA is also known to be regulated by Fur, the ferric uptake repressor. FrvA was named as a Fur-regulated virulence determinant in studies that sought to identify additional ferric uptake regulator (Fur) regulated genes by searching the *L. monocytogenes* genome for candidate Fur binding sites (McLaughlin *et al.*, 2012). Fur generally functions as an Fe(II)-dependent repressor, which led to the expectation that FrvA would be derepressed under iron limitation conditions. Indeed, RT-PCR analyses revealed an increased level of transcripts for all 12 tested Fur regulon genes (including *frvA*) in a Δ*fur* strain (McLaughlin *et al.*, 2012). However, an opposite result was noted in a prior transcriptomic study in which it was observed that *frvA* was expressed at a 5.6-fold *lower* level in a *fur* mutant under iron replete conditions (Ledala *et al.*, 2010). Thus, the role of Fur in regulation of *frvA* is presently unclear.

The current model, in which FrvA functions as a Fur-regulated heme exporter induced by iron deficiency (McLaughlin *et al.*, 2012), is counterintuitive: why would cells efflux heme under conditions of iron starvation when iron uptake functions (including heme import) are derepressed (Lechowicz & Krawczyk-Balska, 2015, Sheldon & Heinrichs, 2015)? We instead favor a model in which FrvA functions, like PfeT, as an Fe(II) efflux pump that is induced by conditions of iron excess.

Here, we have re-investigated the role of FrvA and demonstrate that this gene is indeed induced by elevated levels of available iron, consistent with a role in iron detoxification, and this induction requires Fur. Moreover, physiological studies monitoring the effects of FrvA expression in *B. subtilis* demonstrate a striking ability of this protein to deplete the bacterial cell of iron as well as an ability to export other divalent cations. These results correlate with biochemical studies showing a strong Fe(II)-dependent activation of the purified FrvA ATPase. These results are integrated with previously published studies in *L. monocytogenes* to support a role for iron efflux in the growth and dissemination of this model intracellular pathogen.

3.3 Results and discussion

3.3.1 An *L. monocytogenes frvA* mutant is sensitive to iron intoxication

A *B. subtilis pfeT* mutant strain is sensitive to iron overload, as monitored by the zone of growth inhibition in a disk diffusion assay (Guan *et al.*, 2015b), and prior work suggests that an *L. monocytogenes frvA* mutant may have a similar phenotype (McLaughlin *et al.*, 2012, Rea *et al.*, 2005). We therefore compared the sensitivity to high concentrations of metal ions for the *L. monocytogenes* EGDe wild-type strain (WT) and an isogenic *frvA* null mutant with and without complementation by an ectopic copy of *frvA*. The *frvA* mutant strain was more sensitive to iron intoxication than WT as apparent from a >15% increase in the diameter of growth inhibition as well as a large zone of reduced cell density surrounding the iron-loaded filter disk (**Fig. 3.1** and **Fig. 3.2**). This increase in iron sensitivity is metal specific; there was

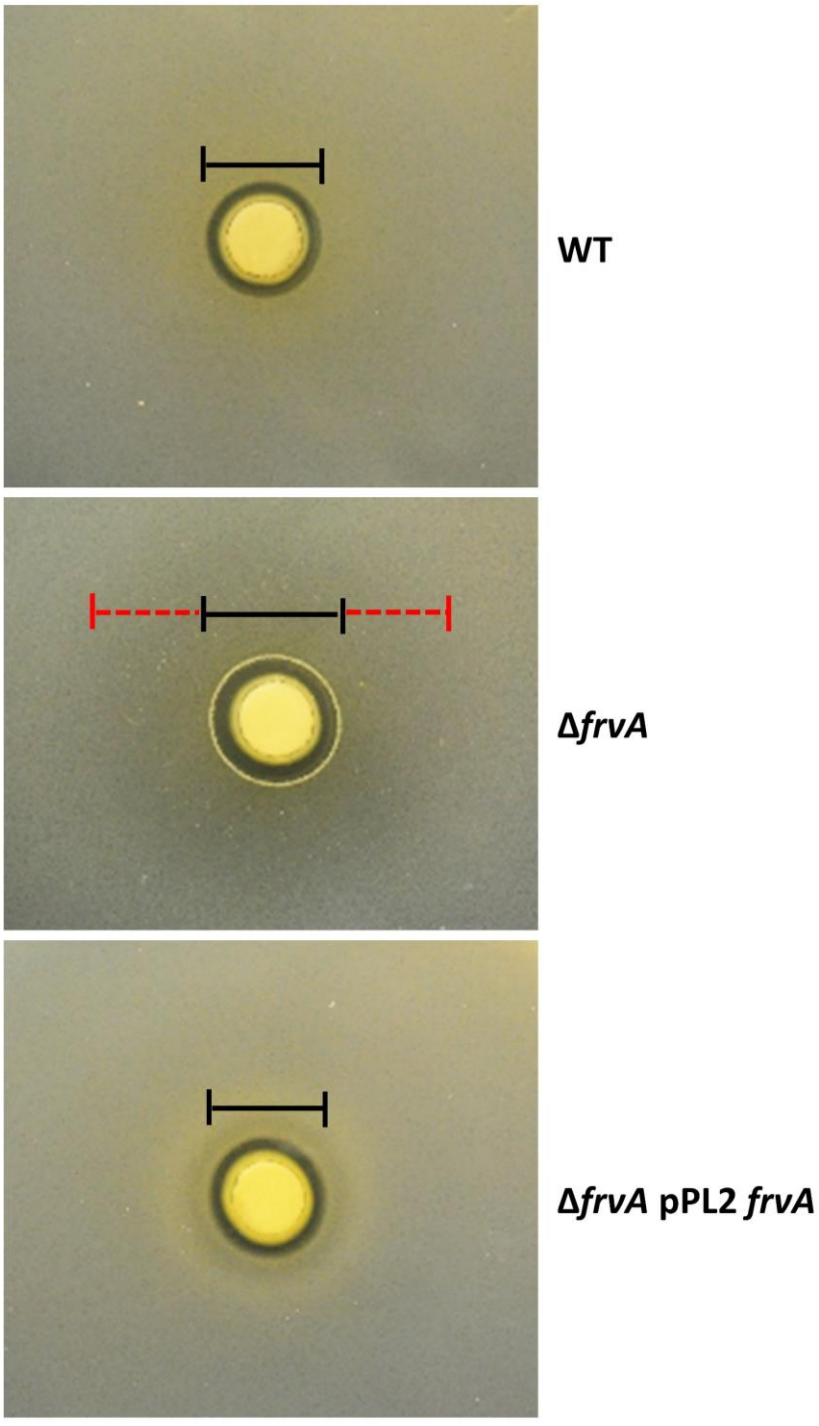

Fig. 3.1 An *frvA* mutant is sensitive to iron intoxication in *Listeria monocytogenes*.
Representative photographs of a disk diffusion assay with wild-type EGDe (WT), an isogenic *frvA* null mutant(Δ*frvA*), and *frvA* complemented strain (Δ*frvA* pPL2 *frvA*) on BHI plates with 10 µl of 1 M $FeSO_4$ added onto the filter paper disk. Black lines indicate the clearance zone and red dashed lines indicate the sensitivity zone. Δ*frvA* null mutant has a bigger clearance zone (2 ± 0.3 mm difference) and a large sensitivity zone with reduced cell density (28 ± 1 mm).

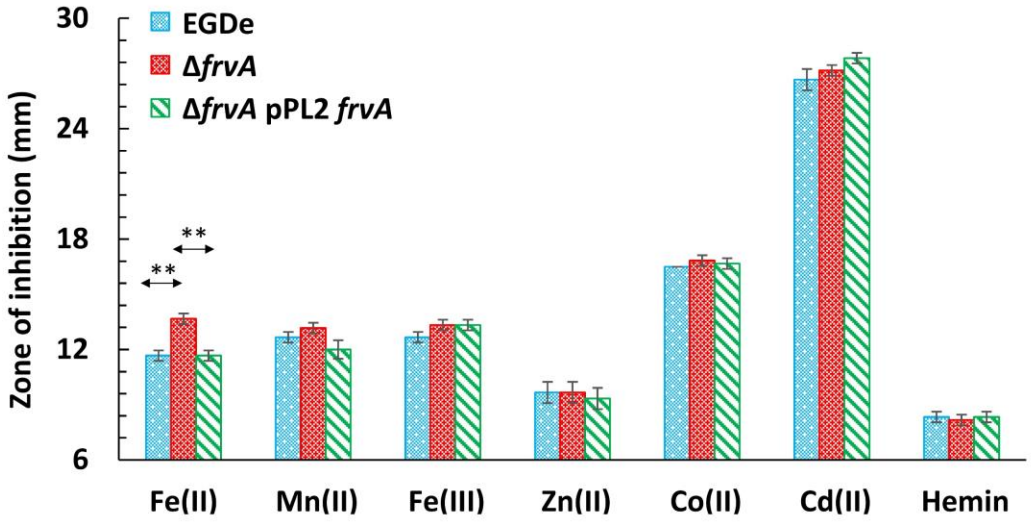

Fig. 3.2 An *frvA* mutant is sensitive to iron intoxication but not other metals in *Listeria monocytogenes*. Sensitivity of wild-type EGDe, an isogenic frvA null mutant(ΔfrvA), and frvA complemented strain (ΔfrvA pPL2 frvA) to different metal ion stress as measured by a disk diffusion assay. 10 µl of 1 M metal ion as indicated or 10 mM hemin was added onto the paper disk. The results are expressed as the diameter (mean ± SD; n=3) of the clearance zone (mm). **P<0.01 indicate statistically significant difference between the indicated groups.

no significant increase in sensitivity to other tested metals or to hemin (**Fig. 3.2**). These results are consistent with the hypothesis that FrvA functions as a Fe(II) efflux pump.

3.3.2 *L. monocytogenes frvA* is regulated by Fur in response to bioavailable iron

Prior studies have suggested the *frvA* promoter region contains a binding site for the iron-sensing transcription factor, Fur. However, reports are conflicted as to the role of Fur with one study presenting results suggesting that *frvA* is repressed by Fur (McLaughlin *et al.*, 2012, Rea *et al.*, 2005) and another including data consistent with activation by Fur (Ledala *et al.*, 2010). We therefore set out to determine if *frvA* is induced by iron and/or heme, and whether or not this induction is mediated by Fur acting as a repressor or an activator.

If FrvA functions in Fe(II) efflux, one would expect that expression would be induced by Fe(II). Indeed, *frvA* mRNA levels are elevated ~8-fold within 5 minutes of treatment with iron (**Fig. 3.3A**). Induction by iron was rapid with the highest mRNA levels at 5 min after treatment and lower levels at

later times tested. In contast, induction by heme (a preferred iron source for *L. monocytogenes*) was more modest with the highest level at 15 min after treatment, a delay consistent with the idea that heme is first imported into the cell and then iron is released intracellularly, ultimately leading to iron stress. This induction was specific for iron since treatment of cells with high levels of Zn(II), known to strongly induce Zn(II) efflux in *B. subtilis* (Ma *et al.*, 2014), did not lead to induction of *frvA* (**Fig. 3.3A**).

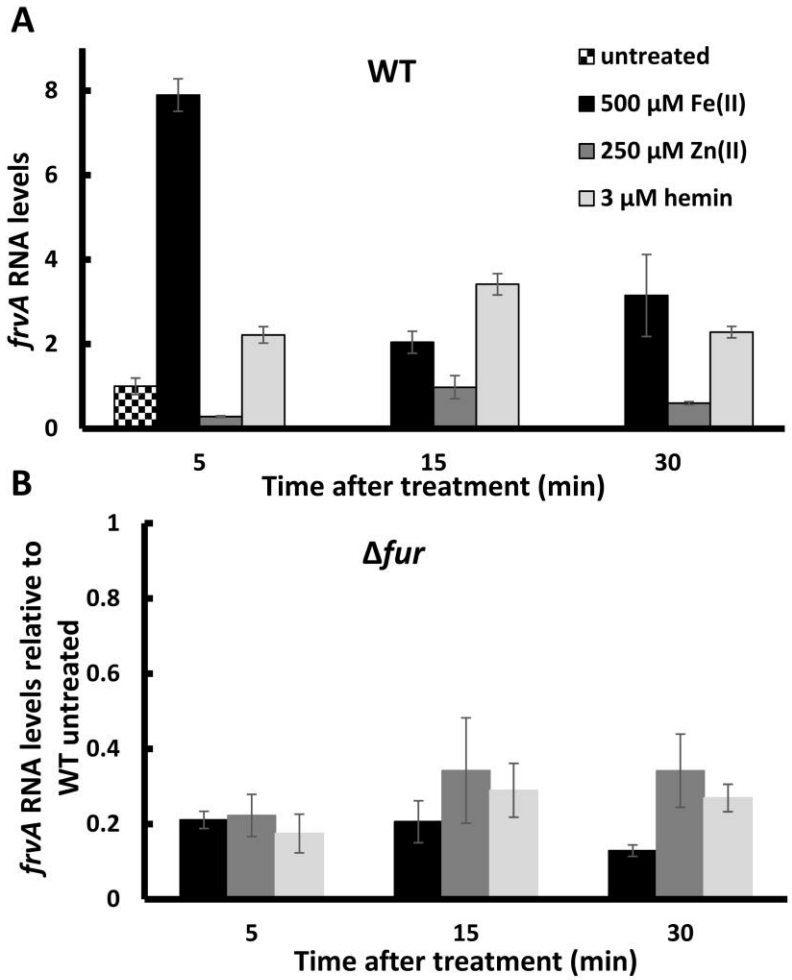

Fig. 3.3 Induction of *Listeria monocytogenes frvA* by Fe(II) and hemin.
L. monocytogenes wild-type EGDe (A) and an isogenic null mutant EGDe Δ*fur* (B) were grown at 37^{0}C in BHI medium overnight and subcultured with 1:100 ratio into fresh BHI medium to an OD_{600} of 0.4. Cells were treated with 500 µM $FeSO_4$, 250 µM $ZnCl_2$, or 3 µM hemin, respectively. Aliquots of 5 ml of cells were harvested at different time points as indicated and total RNA from both treated and untreated samples was extracted and used for reverse transcription and the subsequent quantitative real time-PCR to evaluate mRNA expression levels for *frvA*. The expression levels of *frvA* in WT untreated cells are set as 1 in both Fig. 3.2A and 3.2B. *L. monocytogenes* 16S rRNA was used as a housekeeping control gene. The data are expressed as the mean ± SD (n=3).

To address the role of Fur in gene regulation we repeated these measurements using a *fur* null mutant (**Fig. 3.3B**). The basal level of *frvA* expression was lower in the *fur* mutant strain (nearly 5-fold below the level in WT), and no further increase was noted within 5 min of treatment (and only modest changes were noted thereafter). These results indicate that Fur functions as a positive regulator required for the induction of *frvA* in response to elevated Fe(II) levels. The participation of Fur in the regulation of *frvA* is further evidence in support of an iron- rather than heme-related function since Fur senses Fe(II) directly. As noted previously, *frvA* is also repressed by PerR (Rea *et al.*, 2005), suggesting that this gene is also likely induced in response to peroxide stress.

A direct role for Fur in positive regulation of frvA is also congruent with a prior transcriptomic study in which *frvA* was expressed at a 5.6-fold lower level in the *fur* mutant (almost identical to that noted here) under iron replete conditions (Ledala *et al.*, 2010). In contrast, in this same study genes encoding predicted iron uptake proteins (based on homology to the characterized iron uptake functions of *B. subtilis;* (Ollinger *et al.*, 2006) were, as expected, derepressed between 3- and 15-fold in the *fur* mutant compared to the wild-type strain. Moreover, the predicted iron uptake functions were up-regulated in medium depleted of iron, whereas *frvA* was not. These results suggest that Fur binds DNA in response to elevated intracellular iron and serves to repress genes for iron uptake and activate *frvA*.

3.3.3 Expression of *frvA* complements the iron-sensitivity of a *B. subtilis pfeT* null mutant

To further investigate the function of FrvA, we have used a heterologous expression strategy taking advantage of the detailed knowledge of the *B. subtilis* PerR, Fur and other metal ion responsive regulons (Faulkner & Helmann, 2011, Helmann, 2014b). As shown previously, a mutant strain lacking PfeT (32% identical to FrvA) is sensitive to iron intoxication (Guan *et al.*, 2015b). We integrated an IPTG-inducible copy of the *frvA* gene into the *amyE* locus of the *B. subtilis pfeT* null mutant, and checked the effect of *frvA* induction on resistance to iron intoxication using a growth curve assay. In LBC medium (LB medium amended with 3.4 mM citrate trisodium dihydrate) amended with 4 mM Fe(II), the *pfeT* null

mutant is severely compromised in growth whereas the WT strain grows well after an extended lag phase, as previously reported (Guan *et al.*, 2015b). The severe growth defect, which is dependent on added iron, is complemented by either PfeT or FrvA (**Fig. 3.4**). Significant complementation is observed in this assay

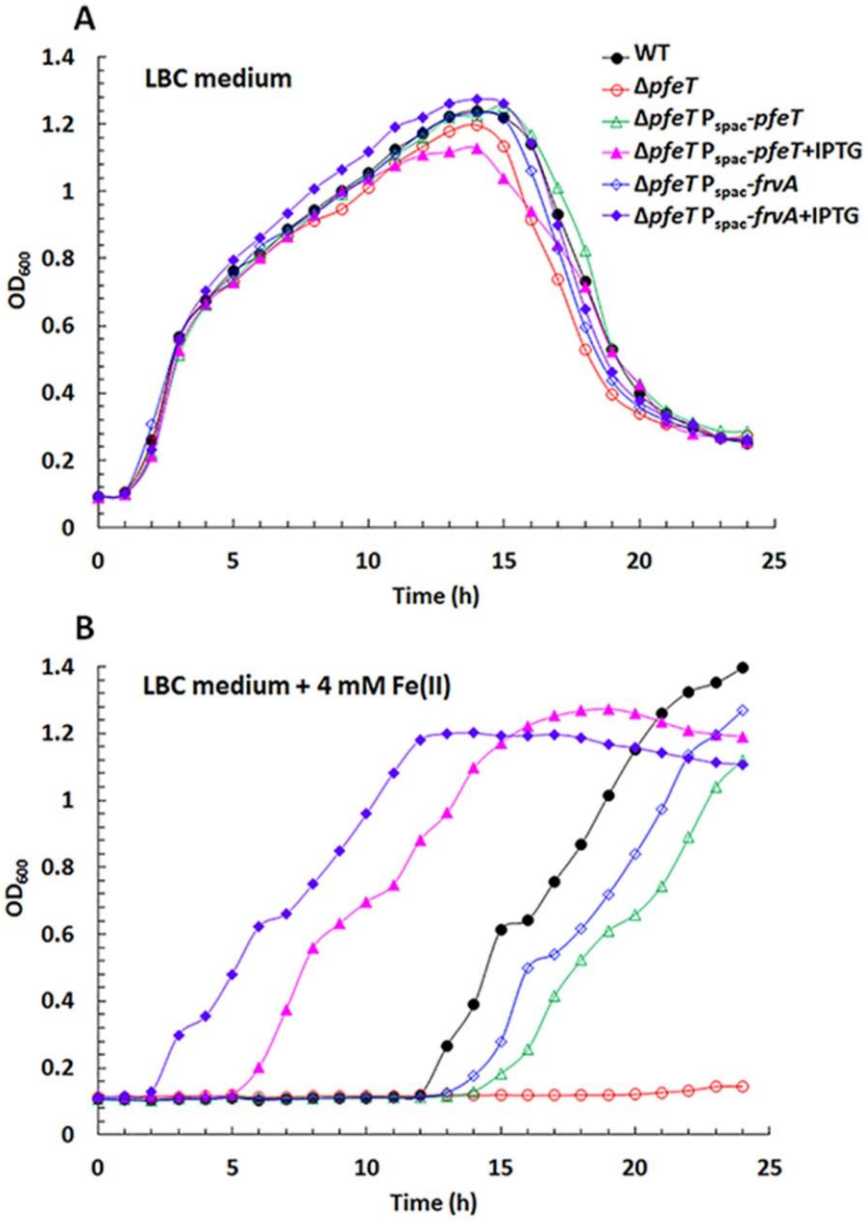

Fig. 3.4 Induction of *L. monocytogenes* FrvA complements a *pfeT* deletion of *B. subtilis*.
A. Representative growth curves of strains WT (CU1065), Δ*pfeT*, Δ*pfeT* P_{spac}-*pfeT*, and Δ*pfeT* P_{spac}-*frvA* grown in LBC medium with no added iron.
B. Representative growth curves of the same strains as panel (A) in LBC medium amended with 4 mM $FeSO_4$. For IPTG treated cells, 1 mM IPTG was added to cell cultures 30 min before 2 µl of cell culture was inoculated to 200 µl of growth medium.

even in the absence of added IPTG, indicating that even the low level of expression in uninduced cells is sufficient to provide protection against iron intoxication. Consistent with prior results, the growth lag upon exposure to toxic levels of iron can be eliminated if PfeT is induced prior to sub-culturing, and similar results are noted for FrvA. Complementation of the *pfeT* null mutant is also apparent in a spot dilution assay to monitor the ability of cells to grow under conditions of iron intoxication. In this assay, the *pfeT* mutant is unable to grow on LBC medium with 4 mM Fe(II) and grows as very small colonies on plates amended with 3 mM Fe(II). Mutant strains expressing either PfeT or FrvA from an IPTG-inducible promoter plate at high efficiency and grow as well as WT under these conditions (**Fig. 3.5**). To further characterize the effects of FrvA on iron intoxication, a disk diffusion assay was used to evaluate the sensitivity of strains to high Fe(II). The *pfeT* null mutant displays an elevated sensitivity to Fe(II) compared to the WT cells (**Fig. 3.6A**). Induction of FrvA or PfeT by IPTG in the null mutant restored a similar level of resistance to Fe(II) as for WT cells (**Fig. 3.6B and 3.6C**). These results demonstrate that *frvA* complements the *pfeT* null mutation in *B. subtilis.*

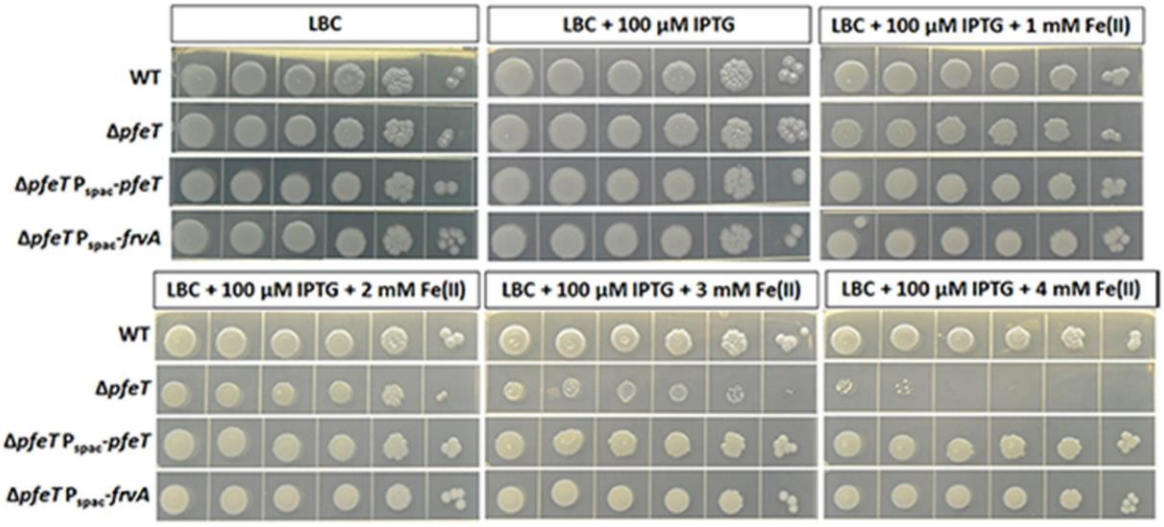

Fig. 3.5 *L. monocytogenes frvA* complements a *B. subtilis pfeT* mutant.
Representative photographs of a spot dilution assay with WT (CU1065), Δ*pfeT*, *pfeT* P_{spac}-*pfeT*, and *pfeT* P_{spac}-*frvA* on LBC agar amended with 100 µM IPTG and various concentrations of FeSO4 as indicated. Spots represent undiluted original cell culture on the left to 10-5 dilution on the right in 10-fold decrements.

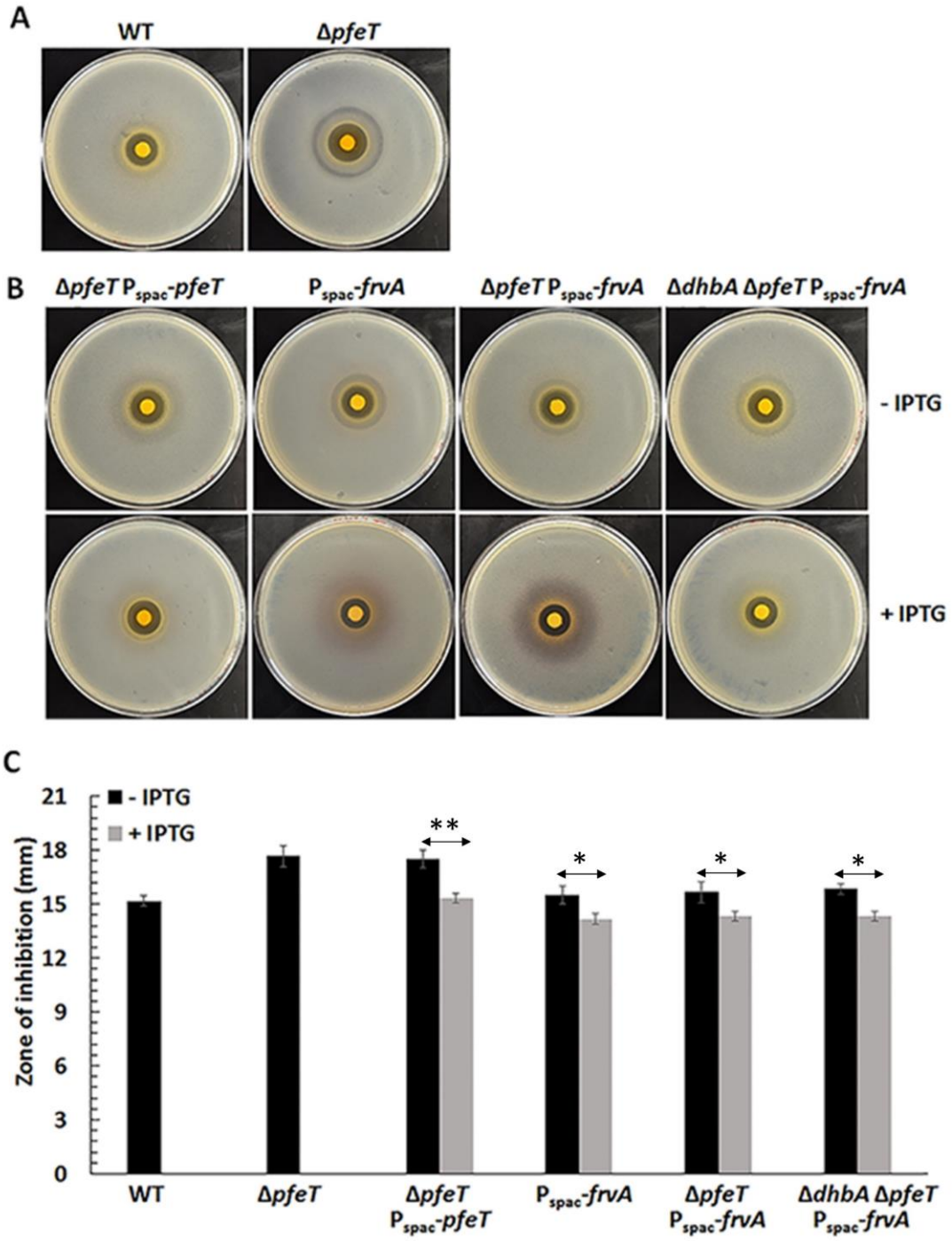

Fig. 3.6 Induction of *L. monocytogenes* FrvA leads to iron starvation and induces the Fur regulon.
Representative photographs of a disk diffusion assay with (A) WT and *pfeT* null mutant as shown previously (Guan *et al.*, 2015) and (B) Δ*pfeT* P_{spac}-*pfeT*, P_{spac}-*frvA*, Δ*pfeT* P_{spac}-*frvA*, and Δ*dhbA* Δ*pfeT* P_{spac}-*frvA* strains, each grown without (top) or with (bottom) IPTG induction. The plates contained LBC medium with 10 µl of 1 M $FeSO_4$ added onto he filter paper disk.
C. The data are expressed as the diameter (mean ± SD; n=3) of the clearance zone (mm). *P<0.05 and **P<0.01 indicate statistically significant difference between the indicated groups.

3.3.4 Induction of FrvA imposes iron limitation and induces the Fur regulon

In the course of these complementation studies, we were surprised to note that induction of FrvA (but not PfeT) resulted in a readily visible purple halo around the inhibition zone (**Fig. 3.6B**). This color is reminiscent of the Fe(III)-complex formed by *B. subtilis* siderophores (Ito & Neilands, 1958, Peters & Warren, 1968), suggesting that FrvA may be imposing iron starvation on the cells despite the presence of high or even toxic levels of iron in the medium. Most laboratory strains of *B. subtilis* (strain 168 and its derivatives) encode the catecholate siderophore bacillibactin, but are unable to synthesize the mature siderophore due to a null mutation of *sfp* (sfp^0) (May *et al.*, 2001). Instead, *B. subtilis* 168 strains produce 2, 3-dihydroxybenzoate (DHBA) and its derivative, dihydroxybenzoylglycine (DHBG), precursors of bacillibactin which form purple colored ferric complexes (Ito & Neilands, 1958, Peters & Warren, 1968). As predicted, the purple color disappeared after introduction of a *dhbA* null mutation to the *frvA* complemented strain (**Fig. 3.6B**). These observations indicate that induction of FrvA imposes iron limitation and induces the Fur regulon. To further test this hypothesis, we measured the effect of FrvA induction on expression of a *dhbA-lacZ* reporter fusion (**Fig. 3.7**). In LB medium, this reporter fusion is largely repressed by Fur. However, β-galactosidase levels increased ~25-fold upon induction of *frvA*. Together, these results

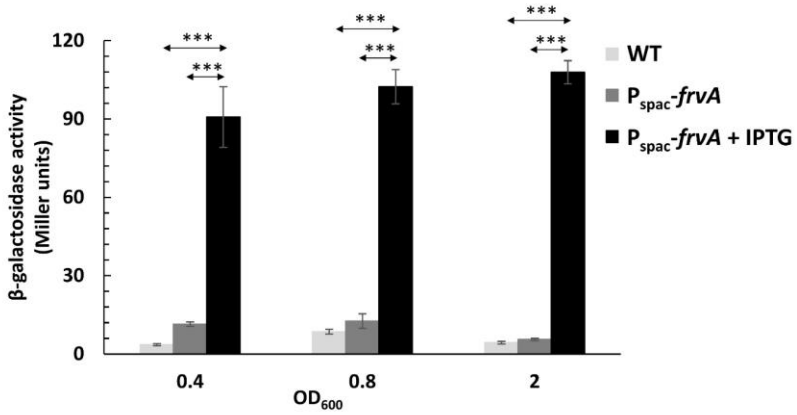

Fig. 3.7 Induction of *dhbA* is increased in cells expressing FrvA.
Wild-type strain CU1065 and CU1065 P_{spac}-*frvA* (without and with 1 mM IPTG induction) carrying a *dhbA-cat-lacZ* reporter fusion were grown to different growth points as indicated in LB medium and assayed for β-galactosidase activity.

indicate that induction of FrvA (but not PfeT) leads to iron limitation sufficient to derepress the Fur-regulated *dhb* operon (Baichoo *et al.*, 2002, Bsat & Helmann, 1999). One possible explanation for this result is that FrvA may be a higher affinity Fe(II) efflux transporter compared to PfeT. Indeed, we find that induction of FrvA, but not PfeT, slightly increases the Fe(II) tolerance of WT cells despite the fact that these cells already express PfeT (**Fig. 3.6C**).

3.3.5 FrvA is a divalent metal ion activated ATPase selective for Fe(II)

The metal ion selectivity of P_{1B}-type ATPases can be inferred from biochemical studies that monitor the metal-dependency of ATPase activation (Argüello *et al.*, 2011). We therefore purified FrvA after overexpression in *E. coli* and assayed metal ion-activated ATPase activity in detergent micelles as described previously for PfeT. Of the metal ions tested, the highest level of ATPase activity was observed with Fe(II), with lower levels of activity with Co(II) and Zn(II) (**Fig. 3.8A**). The overall pattern of metal ion activation of FrvA by metals shows similarities with that reported for PfeT (Guan *et al.*, 2015b), although the latter protein was not significantly activated by Zn(II). In addition, the apparent $K_{1/2}$ for activation of FrvA by Fe(II) (116±24 μM) was substantially lower than for PfeT (520±120 μM) (**Fig. 3.8C**). Similarly, the $K_{1/2}$ for Co(II) (**Fig. 3.8B**) was also ~3-4-fold lower than measured for PfeT (Guan *et al.*, 2015b), but quite similar to that observed in *Mycobacterium smegmatis* CtpJ (Raimunda et al. 2012). These differences in relative metal selectivity and $K_{1/2}$ are likely associated with differences in the second spheres of metal coordination present in the compared proteins. The physiological implications of these observations are not straightforward since alternative forms of Fe(II), rather than the hydrated metal, might be relevant *in vivo*. Nevertheless, this lower $K_{1/2}$ for activation of the ATPase is consistent with the inference that FrvA may have a higher affinity for Fe(II) *in vivo* when compared to PfeT.

To monitor the effects of FrvA on intracellular metal ion levels we grew cells in LB medium and, using inductively coupled plasma mass spectrometry (ICP-MS), we monitored the intracellular levels of Mn(II), Fe(II), and Zn(II) in both WT and the WT strain carrying an IPTG-inducible copy of *frvA*. Even in the

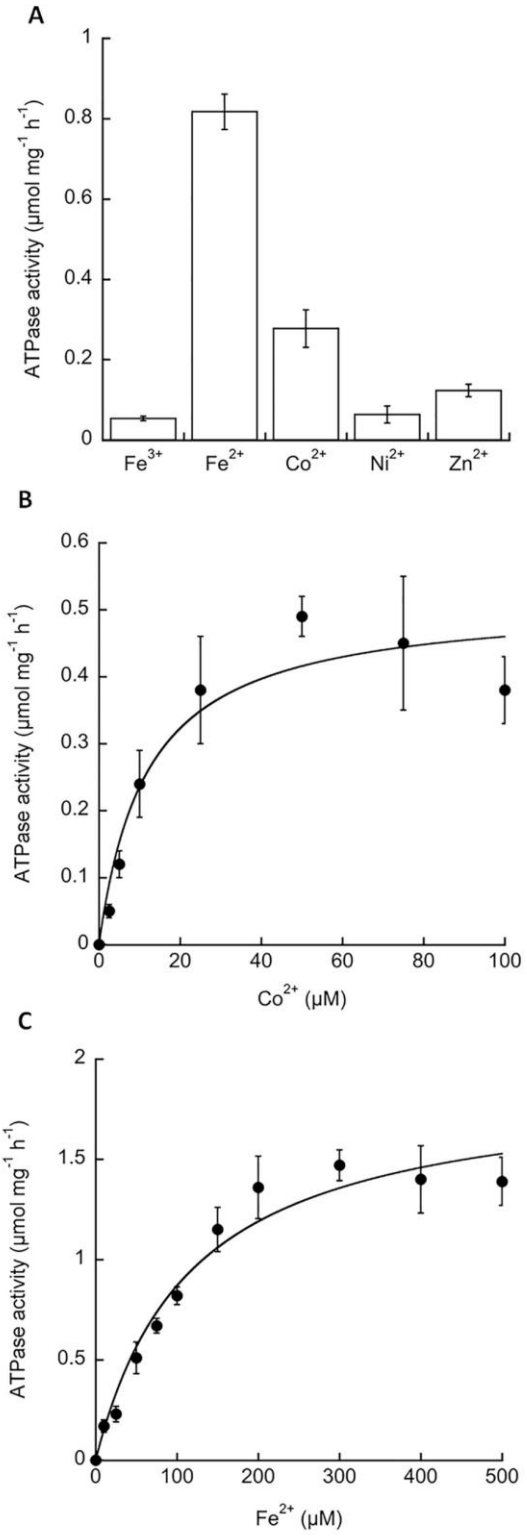

Fig. 3.8 Activation of FrvA ATPase activity by metal ions.

A. FrvA was purified and its ATPase activity (µmol mg^{-1} h^{-1}) was measured *in vitro* in the presence of 100 µM of metal ions as indicated.

B. Kinetic characterization of the FrvA ATPase activity in the presence of various concentrations of Co(II) reveals a V_{max} = 0.51 ± 0.05 µmol mg^{-1} h^{-1} and $K_{1/2}$ = 12 ± 4 µM.

C. Kinetic characterization of the FrvA ATPase activity in the presence of various concentration of Fe(II) reveals a V_{max} = 1.88 ± 0.14 µmol mg^{-1} h^{-1} and $K_{1/2}$ = 116 ± 24 µM.

Data are expressed as the mean ± SD (n=3).

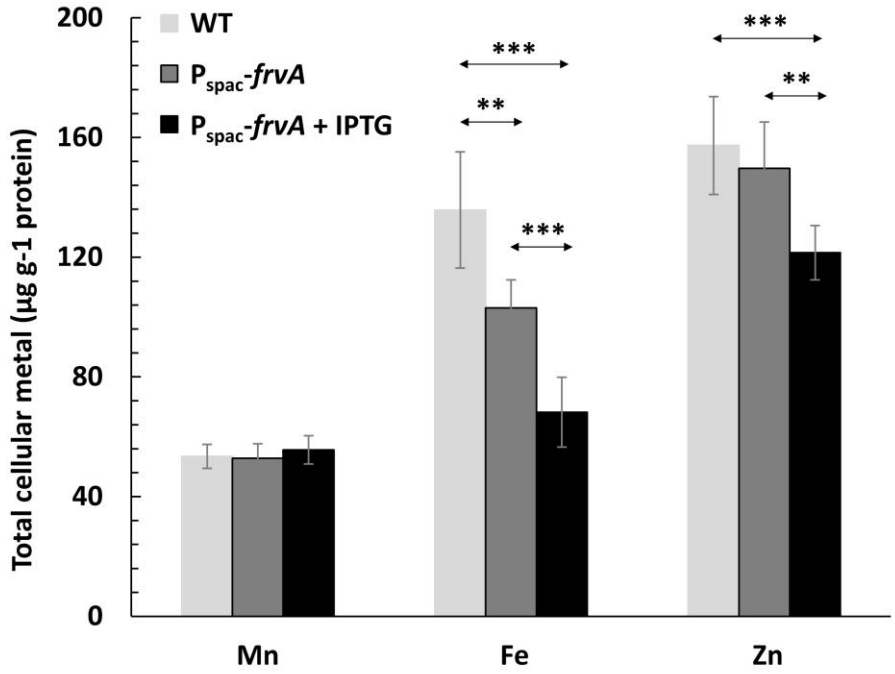

Fig. 3.9 Measurements of intracellular metal ion concentrations by ICP-MS.
Cells were grown in LB medium to an OD_{600} of about 0.1 and supplemented with 1 mM IPTG where indicated, then harvested after two additional hours. Levels of intracellular Mn, Fe and Zn were analyzed by inductively coupled plasma mass spectrometry (ICP-MS). Strains included in the study were WT and P_{spac}-*frvA* (with or without IPTG induction). The total concentration of ions was expressed as µg ion per gram of protein content (mean ± SD; n=9). **P<0.01 and ***P<0.001 indicate statistically significant difference between the indicated groups.

uninduced cells, the presence of the *frvA* gene led to a reduction in intracellular Fe(II) levels, but did not affect Mn(II) or Zn(II) levels (**Fig. 3.9**). This is consistent with the finding that *frvA* can partially complement a *pfeT* mutant strain for growth under conditions of iron intoxication even when it is not induced (**Figs. 3.4 and 3.6**), presumably due to leaky expression from the P_{spac} promoter. When *frvA* is induced, there is a further reduction of Fe(II) levels and under these conditions Zn(II) levels also decline (**Fig. 3.9**). This suggests that, at least when overproduced, FrvA can export Zn(II) from cells, consistent with the weak but demonstrable activation of FrvA ATPase activity by added Zn(II) (**Fig. 3.8A**).

3.3.6 FrvA can increase tolerance to Co(II) and Zn(II) in efflux-defective mutants

We previously demonstrated that artificial induction of PfeT could increase the Co(II) tolerance of a *B. subtilis* mutant lacking the endogenous Co(II) efflux system, CzcD (Guan *et al.*, 2015b). Here we have confirmed this effect, and also tested FrvA for the ability to increase Co(II) tolerance as measured in both a zone of inhibition assay (**Fig. 3.10A**) and a spot dilution assay (**Fig. 3.10B**). Indeed, a low-level induction of FrvA (with 25 µM IPTG to avoid iron deprivation) does increase Co(II) resistance in a *B. subtilis czcD* mutant strain, suggesting that FrvA can also serve to efflux Co(II).

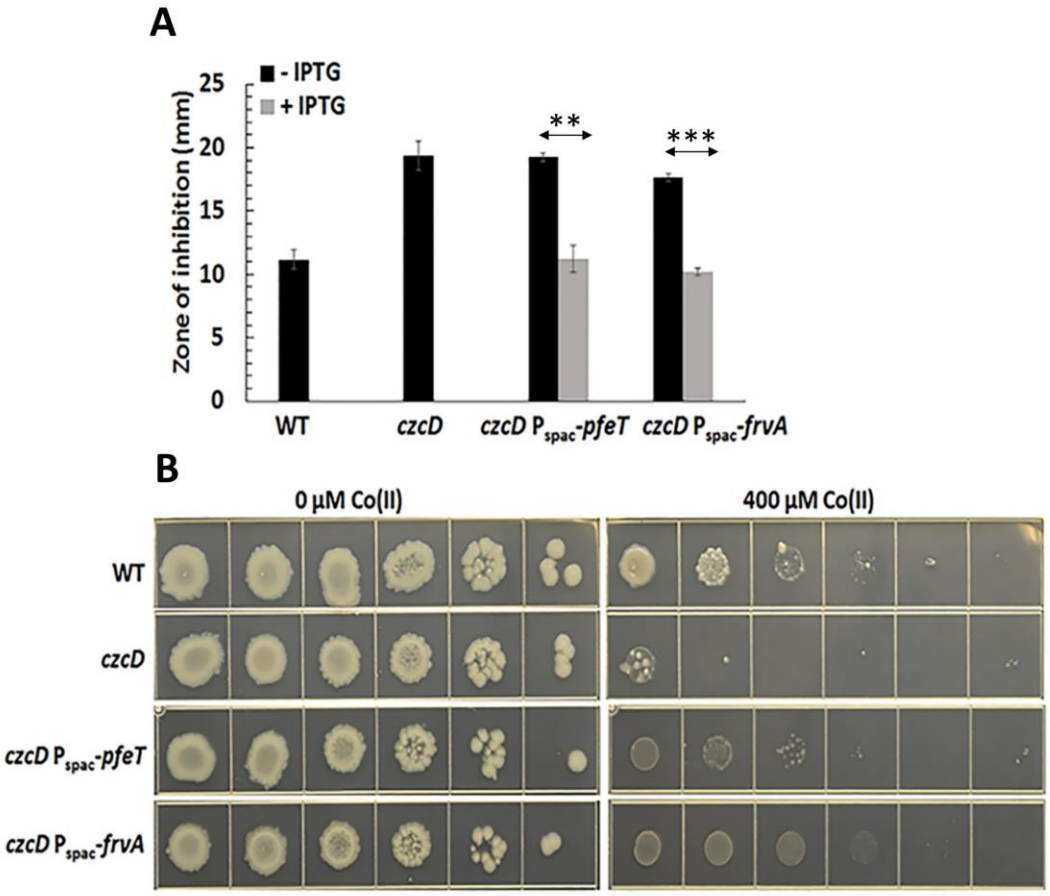

Fig. 3.10 Induction of FrvA increases Co(II) resistance in a *B. subtilis czcD* mutant.
A. Disk diffusion assay of strains WT, *czcD*, *czcD* P_{spac}-*pfeT* and *czcD* P_{spac}-*frvA*. 10 µl of 100mM CoCl2 was added onto filter paper disk. The data are expressed as the mean ± SD (n=3) in mm.
B. Representative photographs of a spot dilution assay with same strains as Fig 3.7A on LB agar plates. 25 µM and 1 mM IPTG were used to induce FrvA and PfeT, respectively. **P<0.01 and ***P<0.001 indicate statistically significant difference between the indicated groups.

In contrast with PfeT, FrvA ATPase activity was activated (albeit weakly; **Fig. 3.8A**) by Zn(II). This motivated us to test whether or not FrvA might function *in vivo* in Zn(II) export, as suggested by the ICP-MS measurements of intracellular metal levels (**Fig. 3.9**). We therefore introduced an IPTG-inducible copy of *frvA* into a *cadA czcD* double mutant known to be highly sensitive to Zn(II) intoxication (Ma *et al.*, 2014). In this background, induction of FrvA but not PfeT significantly increased Zn(II) tolerance (**Fig. 3.11A**). As expected, induction of FrvA or PfeT in the WT background (containing the Zn(II)-inducible CadA and CzcD efflux pumps) did not lead to any further increase in Zn(II) tolerance and may even lead to a slight increase in Zn(II) sensitivity. To further characterize the contribution of FrvA to Zn(II) tolerance, we treated cells with 250 μM $ZnCl_2$ and monitored metal ion levels over time using ICP-MS. Within five min after Zn(II) addition, there is a significant increase in intracellular Zn(II) in the *cadA czcD* double mutant. Induction of FrvA can prevent this accumulation of intracellular Zn(II) upon shift to zinc excess (**Fig. 3.11B**).

Collectively, these results indicate that FrvA can export Co(II) and Zn(II), in addition to Fe(II), when induced. However, as noted previously for PfeT (Guan *et al.*, 2015b), this does not imply that this is a normal *in vivo* activity of FrvA. *L. monocytogenes* encodes predicted Zn(II) and Co(II) efflux transporters that are likely orthologs of CzcD (Lmo2575; 56% identity) and CadA (Lmo1100; 34% identity) and these would likely obscure any role for FrvA in efflux *in vivo* (Jesse *et al.*, 2014). Moreover, it is unclear whether FrvA would be expressed under conditions of Zn(II) or Co(II) toxicity. Indeed, PerR regulated genes may be repressed under conditions of excess Zn(II) or Co(II) (Chen *et al.*, 1993, Moore *et al.*, 2005), and excess Zn(II) failed to induce *frvA in vivo* (**Fig. 3.3**). An ability of P_{1B4} subfamily ATPases to efflux Zn(II) is supported by the observation that derepression of the FrvA homolog PmtA in a *Streptococcus pyogenes perR* mutant leads to induction of genes regulated by the Zn(II)-sensing repressor AdcR (Brenot *et al.*, 2007, Sanson *et al.*, 2015). This can now be understood as likely reflecting depletion of cytosolic Zn(II) pools by the constitutively expressed PmtA.

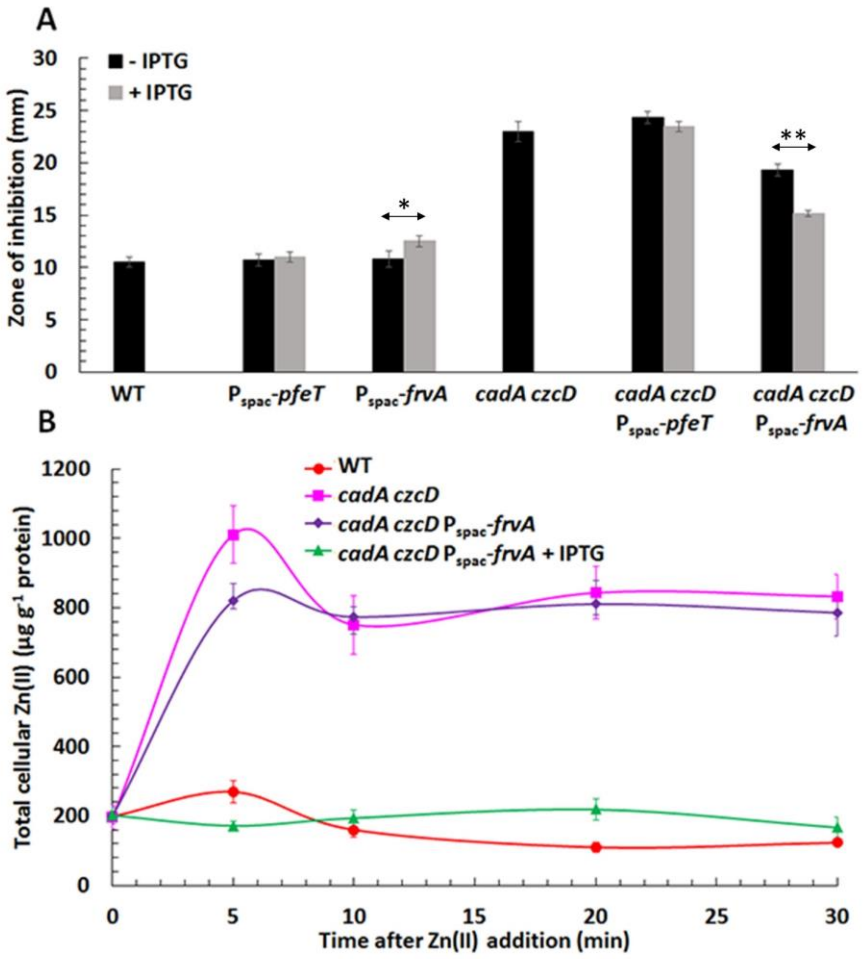

Fig. 3.11 Induction of FrvA increases Zn(II) resistance in a *B. subtilis* strain lacking Zn(II) efflux systems. A. Disk diffusion assay of strains WT, P_{spac}-*pfeT*, P_{spac}-*frvA*, *cadA czcD*, *cadA czcD* P_{spac}-*pfeT*, and *cadA czcD* P_{spac}-*frvA*. For IPTG treated cells, 1mM IPTG was added to both soft agar and LB agar plates. 10 µl of 100mM $ZnCl_2$ was added onto the filter paper disk. The data are expressed as the mean ± SD (n=3). *P<0.05 and **P<0.01 indicate statistically significant difference between the indicated groups.
B. Levels of intracellular Zn monitored by ICP-MS for WT, *cadA czcD*, and *cadA czcD* P_{spac}-*frvA* (without and with 1mM IPTG induction) before and at the time points indicated after addition of 250 µM $ZnCl_2$ to LB medium. The data are expressed as the mean ± SD (n=3).

3.3.7 Induction of FrvA leads to protoporphyrin IX accumulation

Although the preceding biochemical and physiological results strongly suggest that FrvA functions in Fe(II) efflux, we sought to further test the suggestion that FrvA might play a role in heme export (McLaughlin *et al.*, 2012). As noted above, an *L. monocytogenes frvA* mutant was not more sensitive to

heme than WT (**Fig. 3.2**). Next, we tested whether induction of FrvA would protect *B. subtilis* from heme toxicity. In these experiments we failed to note any increase in heme tolerance in the induced cells (data not shown), however *B. subtilis* (unlike *L. monocytogenes*) is not known to import heme and the mechanism of heme toxicity is not understood in this system. We hypothesized that if FrvA does have a robust heme efflux activity it might lead to a measurable reduction in intracellular heme pools. Therefore, we measured intracellular heme levels using a fluorescence-based assay. In this assay, iron chelated by heme is removed by heating in 2 M oxalic acid and the resultant protoporphyrin IX (PPIX) is measured by fluorescence. To avoid contamination from heme in the medium, we grew cells using a metal-limiting minimal medium (MLMM) with 80 nM Mn(II) (Chen *et al.*, 1993). Unexpectedly, IPTG-induced *frvA* complemented cells contained more than 2-fold *more* total PPIX than the WT (**Fig. 3.12A**). To determine whether this increase was due to higher levels of heme or to higher levels of the PPIX precursor, we extracted the tetrapyrroles from cells and monitored PPIX and heme separately using fluorescence assays optimized for PPIX and heme detection (**Fig. 3.12B and C**). These results indicate that FrvA induction leads to elevated levels of PPIX, but not to a significant change in heme levels. Since FrvA did not reduce, under any tested condition, the level of heme in the cell we suggest that FrvA has no significant heme efflux activity under these conditions.

Since induction of FrvA depletes cells of Fe(II) leading to induction of the Fur regulon, we speculated that Fe(II) depletion might also lead to induction of the PerR regulon, including the *hemA* biosynthesis operon, and this might account for the elevation of intracellular PPIX levels. To test this notion, we repeated the study using the same MLMM amended with 10 µM Mn(II), a concentration sufficient to activate the PerR repressor even under conditions of low Fe(II) availability (Chen *et al.*, 1995, Fuangthong *et al.*, 2002b, Helmann, 2014b). As predicted, in this Mn(II) amended medium heme overproduction was no longer observed (**Fig. 3.12A**). We confirmed these results using qRT-PCR which revealed that induction of FrvA leads to ~5-7-fold derepression of *hemA* (the first gene of the *hemAXCDBL*

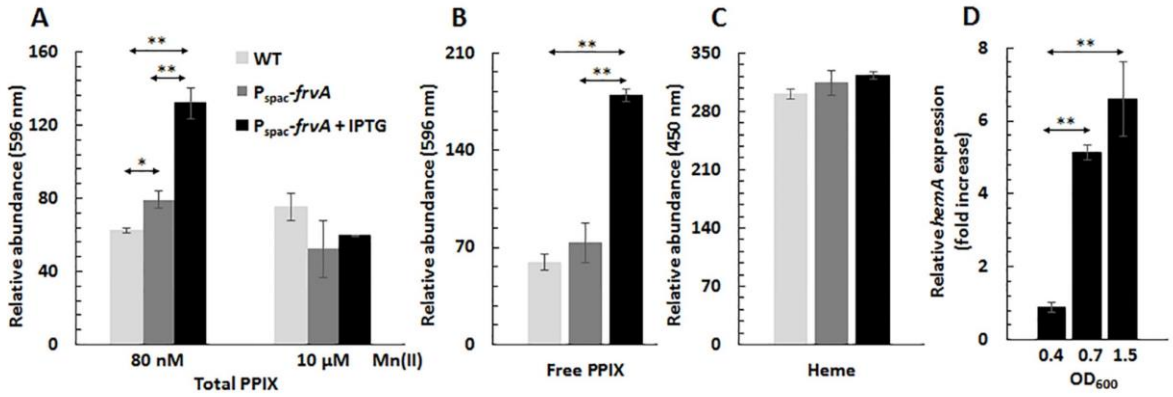

Fig. 3.12 Effects of FrvA on *B. subtilis* heme biosynthesis.

A. Overnight culture of WT and P_{spac}-*frvA* were subcultured (1:100 ratio) in MOPS metal-limiting minimal medium (MLMM; (Chen *et al.*, 1993)) supplemented with 80 nM or 10 µM $MnCl_2$. FrvA was induced with 1 mM IPTG at mid-log phase (OD_{600}=0.25) for 3 h. Total protoporphyrin IX (PPIX) was extracted by 2M oxalic acid. The fluorescence emission of PPIX was scanned from 560 to 680 nm after excitation at 400 nm and fluorescence intensity at 596 nm (peak) was normalized and plotted.

B. Measurements of PPIX in the same strains listed as Fig. 3.9A by acidic acetone extraction. The fluorescence emission of PPIX was scanned from 500 to 650 nm after excitation at 410 nm and fluorescence intensity at 596 nm (peak) was normalized and plotted.

C. Measurements of heme in the same strains listed as Fig. 3.9A by acidic acetone extraction. The fluorescence emission of heme was scanned from 400 to 500 nm after excitation at 380 nm and fluorescence intensity at 450 nm (peak) was normalized and plotted.

D. Strain CU1065 P_{spac}-*frvA* was grown in LB medium in the absence or presence of 1 mM IPTG. Total RNA was extracted from cells harvested at different growth points as indicated (n=3) and used for reverse transcription and the subsequent quantitative real-time PCR to evaluate mRNA expression levels for *hemA*. The *hemA* mRNA levels in cells with 1 mM IPTG were presented as fold increase relatively to those of uninduced cells.

The data are expressed as the mean ± SD (n=3). *P<0.05 and **P<0.01 indicate statistically significant difference between the indicated groups.

operon) at mid-logarithmic and stationary phases (OD_{600}= 0.7 and 1.5, respectively) (**Fig. 3.12D**). Therefore, we conclude that FrvA depletes intracellular Fe(II) leading to derepression of the PerR-regulated heme biosynthesis operon and upregulation of heme biosynthesis. Despite upregulation of PPIX biosynthesis, there is no detectable increase in cellular heme levels. This may be due to a restriction of the activity of ferrochelatase imposed by the ability of FrvA to deplete the cytosol of iron. We conclude that induction of FrvA can derepress the PerR regulon, likely due to iron depletion from the cytosol. PerR binds Fe(II)

with substantially higher affinity than Fur (K_a >10^8 M^{-1} for PerR vs. 1.2 x 10^6 M^{-1} for Fur) (Ma *et al.*, 2011, Ma *et al.*, 2012), which further highlights the extent to which FrvA can impose iron limitation on *B. subtilis*.

3.4 Concluding Remarks

We propose, based on the evidence provided here, that the critical role of FrvA in virulence is resistance to Fe(II) intoxication. The inclusion of FrvA as a member of the PerR regulon suggests that this gene is upregulated in response to oxidative stress, which is likely to be adaptive since hydrogen peroxide toxicity results largely from its reaction with Fe(II) to generate toxic hydroxyl radicals via Fenton chemistry (Imlay, 2013).

The inclusion of FrvA as part of the Fur regulon has led to some confusion since published results are conflicting as to whether *frvA* transcription is increased or decreased in *fur* mutant strains (Ledala *et al.*, 2010, McLaughlin *et al.*, 2012). We demonstrate here that *frvA* is positively regulated by Fur, and that this provides a mechanism for the induction of *frvA* in response to high Fe(II) levels. The basis for the attenuated virulence of the *frvA* mutant strain is still unresolved (McLaughlin *et al.*, 2013, McLaughlin *et al.*, 2012). We favor a model in which this role is based on Fe(II) efflux. Based on its inclusion in the PerR regulon, one might expect that FrvA could function in the activated macrophage. However, *frvA* does not appear to be upregulated (and is actually downregulated) in the macrophage phagosome (Chatterjee *et al.*, 2006). This may reflect the fact that this is generally considered to be an Fe(II) restricted environment due to the action of host NRAMP1 (Wessling-Resnick, 2015). In contrast, the host cytosol is often considered an iron replete environment. However, the iron status of these compartments may change upon infection or depending on the nutritional status of the host cell. For example, internalization of *L. monocytogenes* in macrophages has been linked to upregulation of the major cellular Fe(II) exporter, ferroportin (Haschka *et al.*, 2015). Moreover, supplementation of cultured phagocytes with iron salts led to an increase in intracellular proliferation of *L. monocytogenes* suggesting that the cytosol may be an

iron-restricted environment, perhaps due to the induction of ferroportin. In contrast, iron supplementation led to increased killing of an *L. monocytogenes llo* mutant unable to escape from the phagocytic vacuole, consistent with a model in which cells employ iron intoxication as a killing mechanism (Haschka *et al.*, 2015). It is therefore presently unclear at which stage(s) (invasion, escape from the vacuole, intercellular translocation, and dissemination) FrvA is likely to play the most important role, but we speculate that this role is correlated in general with the transition of cells from iron-limited to iron replete environments.

There are several reasons to question the previously proposed role of FrvA in heme efflux (McLaughlin *et al.*, 2012). First, the evidence in support of this notion derives from the elevated accumulation of ^{59}Fe from heme in *frvA* mutant cells, and this cannot distinguish between a role in Fe(II) efflux or heme efflux and, indeed, *frvA* mutants are sensitive to elevated Fe(II) (**Figs. 3.1, 3.2**), consistent with prior findings (McLaughlin *et al.*, 2012). Second, the coordination of Co(II) by the invariant transmembrane residues present in P_{1B4}-ATPases, as verified by X-ray spectroscopy and site directed mutagenesis (Zielazinski *et al.*, 2012), defines a divalent ion binding site poorly suited to accommodate the bulky heme group. Third, *L. monocytogenes* can efficiently acquire iron from heme through the combined actions of hemolysin and the HupDCG heme import system (Klebba *et al.*, 2012, Lechowicz & Krawczyk-Balska, 2015). The importance of this pathway is evident from the 100-fold attenuation in virulence of *hupDCG* mutant cells in the mouse model. Once imported, heme is degraded to liberate Fe(II) (Lechowicz & Krawczyk-Balska, 2015). If iron-limited cells encounter a heme rich environment it can be imagined that the highly efficient import of heme could lead to transient iron overload leading to induction of FrvA to help alleviate iron toxicity. While some imported heme may be directly shuttled into heme proteins, as shown for *Staphylococcus aureus* (Hammer & Skaar, 2011), this has not been demonstrated in *L. monocytogenes,* and the major fate of imported heme under iron limitation conditions is presumed to be degradation and Fe(II) release (Lechowicz & Krawczyk-Balska, 2015, Hammer & Skaar,

2011). It is possible that heme overload might occur under specific conditions in which heme degradation is inhibited or in which the rate of heme uptake exceeds that of degradation. In this situation *L. monocytogenes* may export excess heme using a system (Lmo2580, 48% identity to HrtA; Lmo2581, 30% identity to HrtB) orthologous to the *S. aureus* HrtAB heme exporter (Anzaldi & Skaar, 2010), although this remains to be tested.

The finding that *B. subtilis* PfeT functions physiologically as a Fe(II) exporter (Guan *et al.*, 2015b), and that the *L. monocytogenes* FrvA protein has a very similar activity, suggests that Fe(II) efflux may be important in other human pathogens. Notably, the *Mycobacterium tuberulosis* CtpD protein is also a member of the P_{1B4} subfamily of metal-activated ATPases, is known to be activated *in vitro* by Co(II) (which is structurally similar to Fe(II)) and is important for survival in the mouse lung (Raimunda *et al.*, 2014b). The results reported here provide evidence for the notion that Fe(II) efflux is an important, although only recently appreciated, contributor to bacterial iron homeostasis. Previous results have highlighted the role of cation diffusion facilitator proteins in efflux of Fe(II) in *E. coli* (FieF) (Grass *et al.*, 2005) and, more recently, during Fe(III) respiration in *Shewanella oneidensis* (FeoE) (Bennett *et al.*, 2015). *Salmonella enterica* encodes a major facilitator superfamily (MFS) protein, IceT, that exports iron-citrate complexes (Frawley *et al.*, 2013), but the physiological role of this system is unclear. Indeed, IceT seems to be induced by nitric oxide (which may lead to elevated iron toxicity) rather than specifically by iron overload, and also effluxes citrate alone, suggesting a possible role in curtailing activity of the TCA cycle. The characterization of *L. monocytogenes* FrvA as an Fe(II) efflux ATPase provides direct evidence linking iron efflux to bacterial pathogenesis.

3.5 Experimental Procedures

3.5.1 Bacterial strains, plasmids, and growth conditions

All *B. subtilis* strains are derivatives of strain CU1065 (WT). Strains and plasmids used in the study are listed in Table S1. *E. coli* DH5α was used for standard cloning procedures. Bacteria were grown in LB medium (*B. subtilis*) or BHI medium (*L. monocytogenes*) with vigorous shaking or on solid LB (*B. subtilis*) or BHI (*L. monocytogenes*) agar with appropriate antibiotic selection at 37°C. LBC medium (LB medium supplemented with 3.4 mM of citrate trisodium dihydrate) was used to reduce iron precipitation in iron intoxication experiments (Guan *et al.*, 2015). Antibiotics were used for selection at the following concentration: ampicillin (amp, 100 μg ml^{-1}), spectinomycin (spec, 100 μg ml^{-1}), chloramphenicol (cm, 10 μg ml^{-1}), tetracycline (tet, 5μg ml^{-1}), kanamycin (kan, 15 μg ml^{-1}), neomycin (neo, 8 μg ml^{-1}), and macrolide lincosoamide-streptogramin B (MLS, 1 μg ml^{-1} erythromycin and 25 μg ml^{-1} lincomycin).

3.5.2 Strain constructions

The *frvA* gene, amplified from *L. monocytogenes* 10403S chromosomal DNA, was cloned into plasmid pPL82 (Quisel et al., 2001) after digestion with HindIII and XbaI. The sequence of the insert was confirmed by DNA sequencing (Cornell DNA sequencing facility). Primer pairs used for PCR amplification, confirmation and sequencing are listed in Table S2. The recombinant plasmid was transformed into *B. subtilis* and integrated into the *amyE* locus. Chromosomal DNA transformation was conducted as described previously (Harwood & Cutting, 1990). SPβ606 lysate was prepared from strain HB606 by heating at 50°C for 15 min and transduced to strain HB19208 (*amyE*::P_{spac}-*frvA*) to make *lacZ* reporter strain HB19253 (HB19208 SPβ P_{dhbA}-*cat-lacZ*).

3.5.3 RNA extraction and qRT-PCR

To monitor *frvA* induction, *L. monocytogenes* EGDe and EGDe Δ*fur* was grown at 37^0C in BHI medium overnight and subcultured with 1:100 ratio into fresh BHI medium to an OD_{600} of 0.4. Cells were treated with Fe(II), Zn(II), or hemin at the indicated concentrations. Aliquots of 5 ml of cells were harvested at

different time points as indicated and total RNA from both treated and untreated samples was extracted using RNeasy Mini Kit following the manufacturer's instructions (Qiagen Sciences, Germantown, MD).

To monitor *hemA* induction, strains were grown in LB medium overnight and subcultured at 1% into fresh LB medium in the presence or absence of 1mM IPTG where indicated. Aliquots of 2 mL of cells were harvested at different growth phases as indicated and total RNA from each sample was extracted using RNeasy Mini Kit according to the manufacturer's instructions.

All RNA samples were treated with Turbo-DNA free™ DNase (Ambion™) and precipitated with ethanol and sodium acetate at -80^{0}C overnight. RNA samples were washed with 70% ethanol and dissolved in RNase-free water then quantified by NanoDrop spectrophotometer. 200 ng of total RNA from each sample was used for cDNA synthesis with TaqMan reverse transcription reagent (Applied Biosystems, Foster City, CA). Primers used for cDNA synthesis are listed in Table S2. Qualitative PCR (qPCR) was then conducted using iQ SYBR green supermix in an Applied Biosystems 7300 Real Time PCR System. 16S rRNA (*L. monocytogenes*) or 23S rRNA (*B. subtilis*) was used as an internal housekeeping control gene.

3.5.4 Growth curves

Strains were grown overnight in LB medium and then subcultured at 1% into LB medium to an OD_{600} of 0.4. For IPTG treated cells, 1mM IPTG was added to cell cultures 30 min before 2 µl of cell culture was inoculated to 200 µl of LBC medium or LBC medium supplemented with 4 mM $FeSO_4$ (Guan *et al.*, 2015). Cell Growth (OD_{600}) was monitored every 15 min for 25 h using a Bioscreen growth analyzer (Growth Curves USA, Piscataway, NJ) at 37°C with continuous shaking. Data shown were representative growth curves and experiments were performed at least three times with at least three biological replicates.

3.5.5 Disk diffusion assays

All strains tested were grown overnight in LB medium (*B. subtilis*) or BHI medium (*L. monocytogenes*) then subcultured at 1% into fresh medium to an OD_{600} of 0.4. Aliquots of 100 µl (*B. subtilis*) or 150 µl (*L. monocytogenes*) of cell cultures were mixed with 4 ml of 0.75% LB (*B. subtilis*) or BHI (*L. monocytogenes*)

soft agar and poured onto LB (*B. subtilis*) or BHI (*L. monocytogenes*) agar plates. The plates were dried for 10 to 15 min in laminar flow hood at room temperature. Filter paper disks (6.5 mm in diameter) soaked with 10 µl of desired chemicals were placed on the top of the agar plates, and the plates were incubated at 37°C for 16 to 18 h. The diameter of the zone of clearance was measured. The data shown are the mean and standard deviation of three biological replicates. For IPTG-treated cells, indicated concentration of IPTG was added to both the soft agar and the LB agar plates.

3.5.6 β-Galactosidase assays

To check the effects of *frvA* induction on *dhbA* expression, the WT strain and HB19208 harboring a *dhbA-cat-lacZ* reporter fusion were grown overnight in LB medium and then subcultured at 1% into fresh LB medium to different growth phases as indicated in the presence or absence of 1 mM IPTG and assayed for β-galactosidase as described previously (Chen et al., 1993, Miller, 1972).

3.5.7 Measurements of intracellular metal ion concentrations by ICP-MS

For experiments performed in Fig. 3.6, cells were grown in LB medium to an OD_{600} of about 0.1 and 1 mM IPTG was added into the cell culture where indicated. Aliquots of 4 ml of cell culture were harvested after two additional hours of incubation. For experiments performed in Fig. 3.8B, cells were grown in LB medium to an OD_{600} of 0.4 in the presence or absence of 1 mM IPTG where indicated and then 250 uM $ZnCl_2$ were added to cell cultures. Aliquots of 4 ml cell culture were harvested at different time points before and after addition of 250 µM $ZnCl_2$.

All samples were prepared as described previously (Guan et al., 2015). Briefly, samples were washed once with buffer 1 (1X PBS buffer, 0.1 M EDTA) then twice with buffer 2 (1X chelex-treated PBS buffer). Cell pellets were resuspended in 400 µl buffer 3 (1X chelex-treated PBS buffer, 75 mM NaN_3, 1% Triton X-100) and incubated at 37°C for 90 min for cell lysis. Lysed samples were centrifuged and subject to Bradford assay to quantify the total protein content. Then, samples were mixed with 600 µl buffer 4 (5% HNO_3, 0.1% (v/v) Triton X-100) and heated in a 95°C sand bath for 30 min. Samples were centrifuged

and supernatants were diluted in 1% HNO_3. Levels of intracellular Zn, Fe and Mn were analyzed by Perkin-Elmer ELAN DRC II ICP-MS. Gallium was used as an internal standard. The total concentration of metal ions was calculated as the average of three biological replicates (± standard deviation) and expressed as µg ion per gram of protein.

3.5.8 Fluorescence heme assay

For experiments performed in Fig. 3.9A, strains were grown overnight in LB medium and then subcultured with 1:100 ratio in MOPS minimum medium amended with 80 nM or 10 µM of $MnCl_2$ (Fig. 3.9A). At OD_{600} ~0.3, 1 mM IPTG was added to induce FrvA expression. After three additional hours of incubation, OD_{600} was recorded for each sample and aliquots of 4 ml of cell culture were harvested. Wild type cells and uninduced HB19208 cells (*amyE*::P_{spac}-*frvA*) were included as controls. All samples were washed once with PBS buffer. Cell pellets were resuspended in 400 µl chelex-treated PBS buffer containing 75 mM NaN_3 and 1% Triton X-100 and incubated at 37°C for 90 min to lyse the cells. Lysed cells were mixed with 500 µl of 2 M oxalic acid and heated in a 95°C sand bath for 30 min to remove iron from heme. The fluorescence emission of the resultant protoporphyrin IX was scanned from 560 nm to 680 nm with excitation at 400 nm as described (Sinclair *et al.*, 2001). Fluorescence intensity at 596 nm (peak) was normalized and plotted. Data shown represent the mean and standard deviation of three biological replicates.

For experiments performed in Fig. 3.12B & C, strains were grown overnight in LB medium and then subcultured with 1:100 ratio in fresh LB medium with or without 1mM IPTG induction to an OD_{600} of 0.5. OD_{600} was recorded and aliquots of 5 ml of cell culture were harvested. Cell pellets were resuspended in 1 mL 50 mM TRIS buffer (pH7.4) containing 100 µg/mL of lysozyme and were incubated in 37°C for 30 min to lyse the cells. Cell debris was removed by centrifugation. Protoporphyrin IX and heme were extracted from 500 µl of the clear lysates using 500 µl acidic acetone (20% 1.6 M HCl v/v). Precipitate was removed by centrifugation and the supernatant was analyzed by fluorescence spectroscopy. The fluorescence emission of protoporphyrin IX was scanned from 500 nm to 680 nm with excitation at 410 nm as described

(Mielcarek *et al*., 2015). Fluorescence intensity at 596 nm (peak) was normalized and plotted. The fluorescence emission of heme was scanned from 400 nm to 500 nm with excitation at 380 nm as described (Mielcarek *et al*., 2015). Fluorescence intensity at 450 nm (peak) was normalized and plotted.

3.5.9 Spot dilution assays

All strains tested were grown overnight in LB medium and then inoculated at 1% into fresh LB medium to an OD_{600} of 0.4. A serial of 10-fold dilutions were prepared for each strain and aliquots of 5 µl cell dilutions were spotted on LB plates amended with different concentrations of metal ions as indicated. Data shown represent the efficiency of plating of cell culture from 1, 10^{-1}, 10^{-2}, 10^{-3}, 10^{-4}, and 10^{-5}-fold serial dilutions (from left to right). Different concentrations of IPTG as indicated were amended in the LB agar plates to induce either PfeT or FrvA expression. The plates were incubated at 37°C for 16-18 hours. Data shown are representative photographs from three individual experiments.

3.5.10 FrvA expression and purification

L. monocytogenes frvA cDNA was amplified using genomic DNA as template and primers that introduced a Tobacco etch virus (TEV) protease site coding sequence at the amplicon 3' ends. The PCR product was cloned into the pBAD-TOPO/His vector (Invitrogen) that introduces a C-terminal 6xHis tag. The plasmid was introduced into *E. coli* Top10 chemically competent cells. For FrvA-TEV-6xHis expression, cells were grown at 37°C in ZYP-505 media supplemented with 0.05% arabinose and 100 µg ml^{-1} ampicillin (Studier, 2005). Affinity purification of membrane proteins and removal of the 6xHis tag was performed as previously described (Raimunda *et al.*, 2014b, Raimunda *et al.*, 2012). Solubilized lipid/detergent micellar forms of FrvA proteins were stored at −20°C in buffer C containing 25 mM Tris, pH 8.0, 50 mM NaCl, 0.01% n-dodecyl-β-d-maltopyranoside, 0.01% asolectin and 20% glycerol until use. The 6xHis tag was cleaved from the FrvA-6xHis fusion protein by treatment with 6xHis-tagged TEV protease (Rosadini *et al.*, 2011) at 5:1 FrvA:TEV weight ratio for 1 h at 22°C in buffer C plus 1 mM Tris(2-carboxyethyl)phosphine (TCEP) and

0.5 mM EDTA. TEV-6xHis was removed by affinity purification with Ni-NTA resin. Protein determinations were performed in accordance to Bradford (Bradford, 1976). Protein purity was assessed by Coomassie brilliant blue staining of overloaded SDS-PAGE gels and by immunostaining of Western blots with rabbit anti-6xHis polyclonal primary antibody (GenScript) and goat anti-rabbit IgG secondary antibody coupled to horseradish peroxidase. Prior to ATPase activity determinations, proteins (1 mg ml^{-1}) were treated with 0.5 mM EDTA and 0.5 mM tetrathiomolybdate for 45 min at room temperature. Chelators were removed using Ultra-30 Centricon (Millipore) filtration devices.

3.5.11 ATPase assays

The ATPase activity of isolated FrvA was measured as previously described (Guan *et al*., 2015). The assay was performed at 37°C in a medium containing 50 mM Tris (pH 7.4), 50 mM NaCl, 3 mM $MgCl_2$, 3 mM ATP, 0.01% asolectin, 0.01% n-dodecyl-β-d-maltopyranoside, 2.5 mM TCEP, 20 µg ml^{-1} purified protein, and freshly prepared transition metal ions at the desired concentrations. Fe^{2+} and Zn^{2+} were included in the assay media as the sulfate salts, whereas Co^{2+} and Ni^{2+} were included as their chloride salts. Fe^{3+} was added as $FeCl_3$, where TCEP was not included in the assay media. ATPase activity was stopped after 20 min incubation and released P_i determined (Lanzetta *et al.*, 1979). ATPase activity measured in the absence of transition metals was subtracted from plotted values. Curves of ATPase activity versus metal concentrations were fit to $v = V_{max}[metal]/([metal] + K_{1/2})$. The reported standard errors for V_{max} and $K_{1/2}$ are asymptotic standard errors reported by the fitting software KaleidaGraph (Synergy).

Table 3.1 Strains and plasmids used in this study

Strain	**Genotype**	**Reference**
CU1065	*trpC2 attSPβ*	Lab stock
10403S	*Listeria monocytogenes* wild-type strain	Lab stock
EGDe	*Listeria monocytogenes* wild-type strain	(McLaughlin *et al.*, 2012)
EGDe Δ*fur*	EGDe derivative with *fur* deleted	(McLaughlin *et al.*, 2012)
Δ*frvA*	EGDe derivative with *frvA* deleted	(McLaughlin *et al.*, 2012)
Δ*frvA* pPL2 *frvA*	Δ*frvA with* pPL2 *frvA* integrated at tRNA Arg-attB' site	(McLaughlin *et al.*, 2012)
HB17802	*pfeT*::*spc*	(Guan *et al.*, 2015b)
HB17852	*pfeT::spc amyE::*P_{spac}*- pfeT*::*cm*	(Guan *et al.*, 2015b)
HB19208	*amyE::*P_{spac}*- frvA*::*cm*	This study
HB19204	*pfeT::spc amyE::*P_{spac}*- frvA*::*cm*	This study
HB19205	*pfeT::spc dhbA::mls amyE::*P_{spac}*- frvA*::*cm*	This study
HB606	CU1065 *SPβc2Δ2::Tn917::ϕ(dhbA'-cat-lacZ) (mls & neo)*	(Baichoo *et al.*, 2002)
HB19253	*AmyE::Pspac-frvA SPβc2Δ2::Tn917::ϕ(dhbA'-cat-lacZ) (mls & neo)*	This study
HB8125	CU1065 *SPβc2Δ2::Tn917::ϕ(cadA'-cat-lacZ) (mls & neo)*	(Gaballa & Helmann, 2003)
HB19257	*cadA:kan czcD::tet SPβc2Δ2::Tn917::ϕ(cadA'-cat-lacZ) (mls & neo)*	This study
HB19259	*cadA:kan czcD::tet AmyE::Pspac-frvA SPβc2Δ2::Tn917::ϕ(cadA'-cat-lacZ) (mls & neo)*	This study
HB11394	*czcD::tet*	(Ma *et al.*, 2014)
HB17833	*czcD::tet amyE::*P_{spac}*- pfeT*::*cm*	(Guan *et al.*, 2015b)
HB19227	*czcD::tet amyE::*P_{spac}*- frvA*::*cm*	This study
HB17814	*AmyE::*P_{spac}*-pfeT::cm*	(Guan *et al.*, 2015b)
HB11395	*cadA::kan czcD::tet*	Ma *et al*., 2014
HB17845	*cadA::kan czcD::tet amyE::*P_{spac}*- pfeT*::*cm*	(Guan *et al.*, 2015b)
HB19229	*cadA::kan czcD::tet amyE::*P_{spac}*-frvA*::*cm*	This study
Plasmid	**Description**	**Reference**
pPL82	Expression of gene under P_{spac} promoter	(Quisel *et al.*, 2001)
pBAD	Arabinose-induced expression of protein	Thermo-Fisher

Table 3.2 Primer oligonucleotides

Number	Name	Sequence
6437	frvA-HindIII	GCCGAAGCTTTGGAGAGGATGAGCATAA
6438	frvA-XbaI	CCGTCTAGATCACTTTTTCCGGTTAGAT
6439	frvA_seq_1	GTGTTCCAATCGATGGAGTGA
6440	frvA_seq_2	CTTGAAGGGCTTTGATCGTAC
5782	pPL82-check-for	AAGAAAGATATCCTAACAGCACA
5783	pPL82-check-rev	ACGATCTTTCAGCCGACTCA
6441	frvA_pBAD_1	ATGAAAGATTGGATGAAGCAGAATTG
6442	frvA_pBAD_2	GGACTGAAAATACAGGTTTTCGCCGCTG
6804	EGDe_16s_rRNA_Fw	GGCTAACTACGTGCCAGCAG
6805	EGDe_16s_rRNA_Rv	ACTCTCCTCTTCTGCACTCCAG
6806	frvA_RTPCR_FW	GAGCTACAACTGGATGATATGGT
6807	frvA_RTPCR_RV	CTACTTACATTGACCGTTCCACC
6697	hemA_RT_FW	TTATGCGGTAGTCGACCAGCTT
6698	hemA_RT_RV	ATCACCATAGAATCAAGTCCGCA
4368	23S-RT-F	AAAGGCACAAGGGAGCTTGACTGC
4369	23S-RT-R	ATGAGCCGACATCGAGGTGCCAAA

3.6 REFERENCES

Anzaldi, L.L. & E.P. Skaar, (2010) Overcoming the heme paradox: heme toxicity and tolerance in bacterial pathogens. *Infection and immunity* **78**: 4977-4989.

Argüello, J.M., (2003) Identification of ion-selectivity determinants in heavy-metal transport P_{1B}-type ATPases. *The Journal of membrane biology* **195**: 93-108.

Argüello, J.M., M. Gonzalez-Guerrero & D. Raimunda, (2011) Bacterial transition metal P_{1B}-ATPases: transport mechanism and roles in virulence. *Biochemistry* **50**: 9940-9949.

Baichoo, N., T. Wang, R. Ye & J.D. Helmann, (2002) Global analysis of the *Bacillus subtilis* Fur regulon and the iron starvation stimulon. *Mol Microbiol* **45**: 1613-1629.

Bennett, B.D., E.D. Brutinel & J.A. Gralnick, (2015) A Ferrous Iron Exporter Mediates Iron Resistance in *Shewanella oneidensis* MR-1. *Applied and environmental microbiology* **81**: 7938-7944.

Bradford, M.M., (1976) A rapid and sensitive method for the quantitation of microgram quantities of protein utilizing the principle of protein-dye binding. *Analytical biochemistry* **72**: 248-254.

Brenot, A., B.F. Weston & M.G. Caparon, (2007) A PerR-regulated metal transporter (PmtA) is an interface between oxidative stress and metal homeostasis in *Streptococcus pyogenes*. *Mol Microbiol* **63**: 1185-1196.

Bsat, N. & J.D. Helmann, (1999) Interaction of *Bacillus subtilis* Fur (Ferric Uptake Repressor) with the *dhb* Operator *In Vitro* and *In Vivo. J Bacteriol* **181**: 4299-4307.

Chatterjee, S.S., H. Hossain, S. Otten, C. Kuenne, K. Kuchmina, S. Machata, E. Domann, T. Chakraborty & T. Hain, (2006) Intracellular gene expression profile of *Listeria monocytogenes*. *Infection and immunity* **74**: 1323-1338.

Chen, L., L.P. James & J.D. Helmann, (1993) Metalloregulation in *Bacillus subtilis*: Isolation and Characterization of Two Genes Differentially Repressed by Metal Ions. *Journal of Bacteriology* **175**: 5428-5437.

Chen, L., L. Keramati & J.D. Helmann, (1995) Coordinate regulation of *Bacillus subtilis* peroxide stress genes by hydrogen peroxide and metal ions. *Proc Natl Acad Sci U S A* **92**: 8190-8194.

Cossart, P., (2011) Illuminating the landscape of host-pathogen interactions with the bacterium Listeria monocytogenes. *Proc Natl Acad Sci U S A* **108**: 19484-19491.

Djoko, K.Y., C.L. Ong, M.J. Walker & A.G. McEwan, (2015) The Role of Copper and Zinc Toxicity in Innate Immune Defense against Bacterial Pathogens. *J Biol Chem* **290**: 18954-18961.

Faulkner, M.J. & J.D. Helmann, (2011) Peroxide stress elicits adaptive changes in bacterial metal ion homeostasis. *Antioxidants & redox signaling* **15**: 175-189.

Faulkner, M.J., Z. Ma, M. Fuangthong & J.D. Helmann, (2012) Derepression of the *Bacillus subtilis* PerR peroxide stress response leads to iron deficiency. *J Bacteriol* **194**: 1226-1235.

Frawley, E.R., M.L. Crouch, L.K. Bingham-Ramos, H.F. Robbins, W. Wang, G.D. Wright & F.C. Fang, (2013) Iron and citrate export by a major facilitator superfamily pump regulates metabolism and stress resistance in *Salmonella* Typhimurium. *Proc Natl Acad Sci U S A* **110**: 12054-12059.

Fuangthong, M. & J.D. Helmann, (2003) Recognition of DNA by three ferric uptake regulator (Fur) homologs in *Bacillus subtilis*. *J Bacteriol* **185**: 6348-6357.

Fuangthong, M., A.F. Herbig, N. Bsat & J.D. Helmann, (2002) Regulation of the *Bacillus subtilis fur* and *perR* genes by PerR: not all members of the PerR regulon are peroxide inducible. *J Bacteriol* **184**: 3276-3286.

Gaballa, A. & J.D. Helmann, (2002) A peroxide-induced zinc uptake system plays an important role in protection against oxidative stress in *Bacillus subtilis*. *Mol. Microbiol.* **45**: 997-1005.

Gaballa, A. & J.D. Helmann, (2003) *Bacillus subtilis* CPx-type ATPases: characterization of Cd, Zn, Co and Cu efflux systems. *Biometals* **16**: 497-505.

German, N., D. Doyscher & C. Rensing, (2013) Bacterial killing in macrophages and amoeba: do they all use a brass dagger? *Future Microbiol* **8**: 1257-1264.

Grass, G., M. Otto, B. Fricke, C.J. Haney, C. Rensing, D.H. Nies & D. Munkelt, (2005) FieF (YiiP) from *Escherichia coli* mediates decreased cellular accumulation of iron and relieves iron stress. *Archives of microbiology* **183**: 9-18.

Guan, G., A. Pinochet-Barros, A. Gaballa, S.J. Patel, J.M. Arguello & J.D. Helmann, (2015) PfeT, a P -type ATPase, effluxes ferrous iron and protects *Bacillus subtilis* against iron intoxication. *Mol Microbiol* **98**: 787-803.

Hammer, N.D. & E.P. Skaar, (2011) Molecular mechanisms of *Staphylococcus aureus* iron acquisition. *Annual review of microbiology* **65**: 129-147.

Harwood, C.R. & S.M. Cutting, (1990) Molecular Biological Methods for Bacillus. John Wiley and Sons, Ltd.

Haschka, D., M. Nairz, E. Demetz, S. Wienerroither, T. Decker & G. Weiss, (2015) Contrasting regulation of macrophage iron homeostasis in response to infection with *Listeria monocytogenes* depending on localization of bacteria. *Metallomics: integrated biometal science* **7**: 1036-1045.

Helmann, J.D., (2014) Specificity of Metal Sensing: Iron and Manganese Homeostasis in *Bacillus subtilis*. *J Biol Chem* **289**: 28112-28120.

Helmann, J.D., M.F. Wu, A. Gaballa, P.A. Kobel, M.M. Morshedi, P. Fawcett & C. Paddon, (2003) The global transcriptional response of *Bacillus subtilis* to peroxide stress is coordinated by three transcription factors. *J Bacteriol* **185**: 243-253.

Imlay, J.A., (2013) The molecular mechanisms and physiological consequences of oxidative stress: lessons from a model bacterium. *Nature reviews. Microbiology* **11**: 443-454.

Ito, T. & J.B. Neilands, (1958) Products of "Low-iron Fermentation" with *Bacillus subtilis*: Isolation, Characterization and Synthesis of 2,3-Dihydroxybenzoylglycine. *Journal of the American Chemical Society* **80**: 4645-4647.

Jesse, H.E., I.S. Roberts & J.S. Cavet, (2014) Metal ion homeostasis in *Listeria monocytogenes* and importance in host-pathogen interactions. *Advances in microbial physiology* **65**: 83-123.

Klebba, P.E., A. Charbit, Q. Xiao, X. Jiang & S.M. Newton, (2012) Mechanisms of iron and haem transport by *Listeria monocytogenes*. *Mol Membr Biol* **29**: 69-86.

Lanzetta, P.A., L.J. Alvarez, P.S. Reinach & O.A. Candia, (1979) An improved assay for nanomole amounts of inorganic phosphate. *Analytical biochemistry* **100**: 95-97.

Lechowicz, J. & A. Krawczyk-Balska, (2015) An update on the transport and metabolism of iron in *Listeria monocytogenes*: the role of proteins involved in pathogenicity. *Biometals* **28**: 587-603.

Ledala, N., M. Sengupta, A. Muthaiyan, B.J. Wilkinson & R.K. Jayaswal, (2010) Transcriptomic response of Listeria monocytogenes to iron limitation and Fur mutation. *Applied and environmental microbiology* **76**: 406-416.

Ma, Z., P. Chandrangsu, T.C. Helmann, A. Romsang, A. Gaballa & J.D. Helmann, (2014) Bacillithiol is a major buffer of the labile zinc pool in *Bacillus subtilis*. *Mol Microbiol* **94**: 756-770.

Ma, Z., M.J. Faulkner & J.D. Helmann, (2012) Origins of specificity and cross-talk in metal ion sensing by *Bacillus subtilis* Fur. *Mol Microbiol* **86**: 1144-1155.

Ma, Z., J.W. Lee & J.D. Helmann, (2011) Identification of altered function alleles that affect Bacillus subtilis PerR metal ion selectivity. *Nucleic acids research* **39**: 5036-5044.

May, J.J., T.M. Wendrich & M.A. Marahiel, (2001) The *dhb* operon of *Bacillus subtilis* encodes the biosynthetic template for the catecholic siderophore 2,3-dihydroxybenzoate-glycine-threonine trimeric ester bacillibactin. *J Biol Chem* **276**: 7209-7217.

McLaughlin, H.P., M. Bahey-El-Din, P.G. Casey, C. Hill & C.G. Gahan, (2013) A mutant in the *Listeria monocytogenes* Fur-regulated virulence locus (*frvA*) induces cellular immunity and confers protection against listeriosis in mice. *J Med Microbiol* **62**: 185-190.

McLaughlin, H.P., Q. Xiao, R.B. Rea, H. Pi, P.G. Casey, T. Darby, A. Charbit, R.D. Sleator, S.A. Joyce, R.E. Cowart, C. Hill, P.E. Klebba & C.G. Gahan, (2012) A putative P-type ATPase required for virulence and resistance to haem toxicity in *Listeria monocytogenes. PloS one* **7**: e30928.

Mielcarek A, Blauenburg B, Miethke M, Marahiel MA (2015) Molecular Insights into Frataxin-Mediated Iron Supply for Heme Biosynthesis in *Bacillus subtilis*. PLoS ONE 10(3): e0122538. doi:10.1371/journal.pone.0122538

Moore, C.M., A. Gaballa, M. Hui, R.W. Ye & J.D. Helmann, (2005) Genetic and physiological responses of *Bacillus subtilis* to metal ion stress. *Mol Microbiol* **57**: 27-40.

Ollinger, J., K.B. Song, H. Antelmann, M. Hecker & J.D. Helmann, (2006) Role of the Fur regulon in iron transport in *Bacillus subtilis*. *J Bacteriol* **188**: 3664-3673.

Peters, W.J. & R.A. Warren, (1968) Itoic acid synthesis in *Bacillus subtilis*. *J Bacteriol* **95**: 360-366.

Quisel, J.D., W.F. Burkholder & A.D. Grossman, (2001) In vivo effects of sporulation kinases on mutant Spo0A proteins in *Bacillus subtilis*. *J Bacteriol* **183**: 6573-6578.

Raimunda, D., J.E. Long, T. Padilla-Benavides, C.M. Sassetti & J.M. Argüello, (2014) Differential roles for the Co(2+) /Ni(2+) transporting ATPases, CtpD and CtpJ, in *Mycobacterium tuberculosis* virulence. *Mol Microbiol* **91**: 185-197.

Raimunda, D., J.E. Long, C.M. Sassetti & J.M. Argüello, (2012) Role in metal homeostasis of CtpD, a Co^{2+} transporting P_{1B4}-ATPase of *Mycobacterium smegmatis*. *Mol Microbiol* **84**: 1139-1149.

Rea, R., C. Hill & C.G. Gahan, (2005) *Listeria monocytogenes* PerR mutants display a small-colony phenotype, increased sensitivity to hydrogen peroxide, and significantly reduced murine virulence. *Applied and environmental microbiology* **71**: 8314-8322.

Rosadini, C.V., J.D. Gawronski, D. Raimunda, J.M. Argüello & B.J. Akerley, (2011) A novel zinc binding system, ZevAB, is critical for survival of nontypeable *Haemophilus influenzae* in a murine lung infection model. *Infection and immunity* **79**: 3366-3376.

Sanson, M., N. Makthal, A.R. Flores, R.J. Olsen, J.M. Musser & M. Kumaraswami, (2015) Adhesin competence repressor (AdcR) from S*treptococcus pyogenes* controls adaptive responses to zinc limitation and contributes to virulence. *Nucleic acids research* **43**: 418-432.

Sheldon, J.R. & D.E. Heinrichs, (2015) Recent developments in understanding the iron acquisition strategies of gram positive pathogens. *FEMS microbiology reviews* **39**: 592-630.

Sinclair, P.R., N. Gorman & J.M. Jacobs, (2001) Measurement of heme concentration. *Curr Protoc Toxicol* **Chapter 8**: Unit 8 3.

Smith, A.T., K.P. Smith & A.C. Rosenzweig, (2014) Diversity of the metal-transporting P_{1B}-type ATPases. *Journal of biological inorganic chemistry: JBIC: a publication of the Society of Biological Inorganic Chemistry* **19**: 947-960.

Studier, F.W., (2005) Protein production by auto-induction in high density shaking cultures. *Protein Expr Purif* **41**: 207-234.

Wessling-Resnick, M., (2015) Nramp1 and Other Transporters Involved in Metal Withholding during Infection. *J Biol Chem* **290**: 18984-18990.

Zielazinski, E.L., G.E. Cutsail, 3rd, B.M. Hoffman, T.L. Stemmler & A.C. Rosenzweig, (2012) Characterization of a cobalt-specific P_{1B}-ATPase. *Biochemistry* **51**: 7891-7900.

Chapter 4. Sequential Induction of Fur-Regulated Genes in Response to Iron Limitation in *Bacillus subtilis*

4.1 Abstract

Bacterial cells modulate transcription in response to changes in iron availability. The ferric uptake regulator (Fur) senses intracellular iron availability and plays a central role in maintaining iron homeostasis in *Bacillus subtilis*. Here we utilized FrvA, a high affinity Fe^{2+} efflux transporter from *Listeria monocytogenes*, as an inducible genetic tool to deplete intracellular iron. We then characterized the responses of the Fur, FsrA, and PerR regulons as cells transition from iron sufficiency to deficiency. Our results indicate that the Fur regulon is derepressed in three distinct waves. First, uptake systems for elemental iron (*efeUOB*), ferric citrate (*fecCDEF*), and petrobactin (*fpbNOPQ*) are induced to prevent iron deficiency. Second, *B. subtilis* synthesizes its own siderophore bacillibactin (*dhbACEBF*) and turns on bacillibactin (*feuABC*) and hydroxamate siderophore (*fhuBCGD*) uptake systems to scavenge iron from the environment and flavodoxins (*ykuNOP*) to replace ferredoxins. Third, as iron levels decline further, an "iron sparing" response (*fsrA*, *fbpAB*, and *fbpC*) is induced to block the translation of abundant iron-utilizing proteins and thereby permit the most essential iron-dependent enzymes access to the limited iron pools. ChIP experiments demonstrate that *in vivo* occupancy of Fur correlates with derepression of each operon, and the graded response observed here results, at least in part, from higher affinity binding of Fur to the "late" induced genes.

This chapter is adapted from Pi, H. & J.D. Helmann. *Proc Natl Acad Sci U S A.* 2017;114(48):12785-12790. The primary change has been to merge Supplemental information from the cited publication into the main body of this chapter to comply with the formatting requirements.

4.2 Significance Statement

Fur is a key regulator of bacterial iron homeostasis and regulates the derepression of iron acquisition systems when iron is limited. However, it is unclear whether Fur regulated genes are derepressed coordinately or in a sequential manner. Here, we describe a graded response for the *Bacillus subtilis* Fur regulon as the intracellular iron pool is gradually depleted. Three distinct sets of genes are sequentially expressed and the induction order can be explained, at least in part, by differences in Fur affinity to its target operator sites. These results provide insights into the distinct roles of Fur target genes and contribute to our understanding of bacterial metalloregulatory systems.

4.3 Introduction

Iron is indispensable for cell growth and survival for most bacteria. In many natural environments, particularly under neutral pH and aerobic conditions, iron limitation is a big challenge for bacteria due to the extremely low solubility and bioavailability of the Fe^{3+} ion. However, iron can be also toxic to cells when present in excess due to its participation in Fenton chemistry, which generates reactive oxygen radicals resulting in macromolecular damage and cell death (Imlay, 2003, Park *et al.*, 2005). Therefore, bacteria require regulatory systems to maintain iron homeostasis. The ferric uptake regulator (Fur) senses intracellular iron levels and plays a critical role in bacterial iron homeostasis by virtue of its ability to regulate transcription of genes involved in iron uptake, storage, and efflux (Helmann, 2014, Fleischhacker & Kiley, 2011).

The Fur regulon has been well characterized in *B. subtilis* and includes more than 50 genes, many of which are implicated in iron uptake, endogenous siderophore (bacillibactin) synthesis and uptake, and xenosiderophore uptake (siderophore made by other organisms) (Baichoo *et al.*, 2002). Under iron sufficient conditions, Fur binds to Fe^{2+} in the cytosol and the resultant holo-Fur binds to its target DNA

operators and functions as a repressor; under iron limited conditions, apo-Fur dissociates from DNA and the repression by Fur is relieved. Derepression of the Fur regulon leads to expression of numerous iron uptake systems to scavenge iron and adapt to iron deficiency. These include transporters for the import of elemental iron (EfeUOB), ferric citrate (YmfCDEF, renamed as FecCDEF to reflect their physiological role in ferric citrate import), hydroxamate siderophores (ferrioxamine and ferrichrome) (FhuBCGD-YxeB), and petrobactin (YclNOPQ, renamed as FpbNOPQ to reflect their role in ferric petrobactin import) (Zawadzka *et al.*, 2009).

In addition, *B. subtilis* synthesizes its own siderophore, bacillibactin (BB) (DhbACEBF), and a cognate uptake system (FeuABC-YusV), both of which are under Fur regulation (Baichoo *et al.*, 2002, Ollinger *et al.*, 2006, Miethke *et al.*, 2006). A phosphopantetheinyl transferase (encoded by *sfp*) is also required for BB biosynthesis (May *et al.*, 2001, Quadri *et al.*, 1998). Most laboratory strains of *B. subtilis* (those derived from the legacy strain *B. subtilis* 168 (Zeigler *et al.*, 2008)) carry an *sfp* null mutation (sfp^0) (Quadri *et al.*, 1998, May *et al.*, 2001) and can only produce the BB precursor 2,3-dihydroxybenzoic acid (DHBA) and its glycine conjugate (DHBG) (collectively assigned as DHB(G)). The DHB(G) compounds bind to Fe^{3+} with modest affinity while BB binds to Fe^{3+} with very high affinity (Ollinger *et al.*, 2006, Dertz *et al.*, 2006). BB uptake shares the same pathway as enterobactin (FeuABC-YusV) (Miethke *et al.*, 2006) and is under two levels of regulation: iron-dependent repression by Fur and substrate-specific activation by Btr (bacillibactin transport regulator), an AraC family transcriptional activator (Smaldone *et al.*, 2012, Gaballa & Helmann, 2007). In addition to its prototypic role as an Fe^{2+}-sensing repressor, emerging evidence indicates that in some cases apo-Fur (without its coregulator Fe^{2+}-bound) also binds DNA and both forms of Fur may also function as transcriptional activators (Seo *et al.*, 2014, Delany *et al.*, 2004, Yu & Genco, 2012).

To adapt to iron limitation, bacteria also reconfigure their proteome to reduce synthesis of abundant, iron-utilizing proteins that are not essential for growth (an “iron-sparing” response) and they

express alternative, iron-independent versions of some proteins. Together, these responses enable the cell to prioritize utilization of iron (Masse *et al.*, 2005, Gaballa *et al.*, 2008, Smaldone *et al.*, 2012). In *B. subtilis*, Fur regulates FsrA, a noncoding Fur-regulated small RNA, which mediates the iron-sparing response with the help of three putative RNA chaperones (FbpABC) (Smaldone *et al.*, 2012, Gaballa *et al.*, 2008). FsrA and its coregulators block the translation of low-priority iron-utilizing enzymes such as aconitase and succinate dehydrogenase and enable high-priority iron-dependent proteins to utilize the limited iron (Gaballa *et al.*, 2008, Smaldone *et al.*, 2012). In addition, cells may substitute iron-independent flavodoxin for ferrodoxin, an abundant iron-sulfur protein involved in electron transfer reactions. Expression of flavodoxins (YkuNOP) is under regulation of Fur (Lawson *et al.*, 2004, Baichoo *et al.*, 2002).

Another transcriptional regulator that plays an important role in *B*. *subtilis* iron homeostasis is PerR, which modulates the adaptive response to peroxide stress, including peroxide detoxification, heme biosynthesis, and iron storage genes (Lee & Helmann, 2006, Faulkner & Helmann, 2011, Zuber, 2009, Chen & Helmann, 1995, Herbig & Helmann, 2001, Fuangthong *et al.*, 2002). PerR also regulates *pfeT*, a P_{1B4}-type ATPase recently characterized as an Fe^{2+} efflux transporter (Guan *et al.*, 2015). Expression of *pfeT* is induced under two conditions, oxidative stress and excess iron (Guan *et al.*, 2015). A homolog of PfeT in *L*. *monocytogenes*, FrvA, has been identified as a high affinity Fe^{2+} exporter and its expression imposes severe iron limitation that leads to derepression of Fur and PerR regulons in *B. subtilis* (Pi *et al.*, 2016).

In this study, we utilized *L. monocytogenes* FrvA as an inducible genetic tool to deplete intracellular iron. By monitoring the transcription of Fur-regulated genes as cells transition from iron sufficiency to deficiency we determined that the Fur regulon is derepressed in three distinguishable waves. The first wave comprises uptake systems for elemental iron (*efeUOB*), ferric citrate (*fecCDEF*), and petrobactin (*fpbNOPQ*); in the second wave, *B. subtilis* synthesizes its own siderophore bacillibactin (*dhbACEBF*) and turns on bacillibactin uptake (*feuABC*) along with hydroxamate siderophore uptake (*fhuBCGD*) and flavodoxins (*ykuNOP*); last, as iron levels decrease further, the iron sparing response (*fsrA*,

fbpAB, and *fbpC*) is induced to prioritize iron utilization. Furthermore, the stepwise induction of Fur-regulated genes correlates with operator occupancy *in vivo* and can be explained, at least in part, by differences in protein-DNA binding affinity.

4.4 Results

4.4.1 Expression of FrvA imposes iron deprivation and inhibits cell growth of *B. subtilis.*

Due to the high activity and redundancy of iron import systems, iron starvation can be difficult to achieve under laboratory conditions without the use of chelating agents such as dipyridyl. Here, we explored the use of the Fe^{2+} efflux transporter FrvA as a genetic tool to study iron limitation responses in *B. subtilis*. The resulting gradual depletion of intracellular iron levels may more closely mimic the natural situation wherein intracellular iron is depleted by growth.

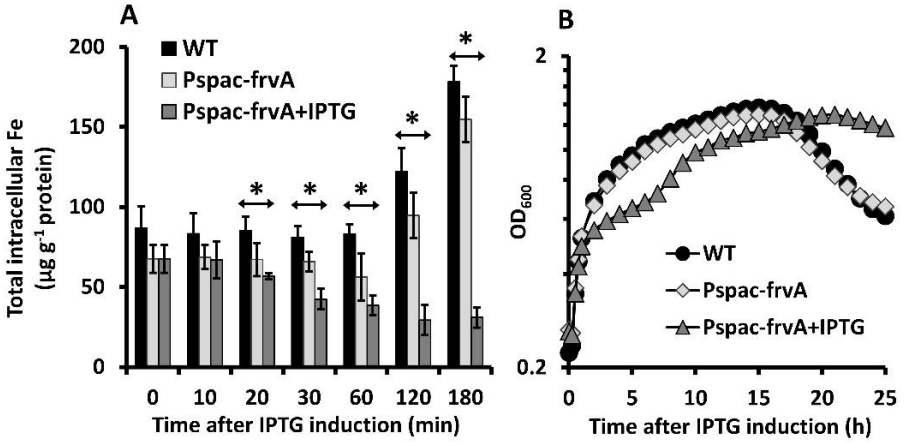

Fig. 4.1 Induction of *L. monocytogenes* FrvA imposes iron deprivation and inhibits cell growth of *B. subtilis.*

A. Levels of intracellular metals (Fe, Mn, and Co) were monitored for three hours after 1 mM IPTG addition by inductively coupled plasma mass spectrometry (ICP-MS). The total concentration of ions was expressed as μg ion per gram of protein (mean ± SD; n=3). Significant differences between WT and induced P_{spac}-*frvA* cells are determined by two-tailed *t*-test as indicated: *, $P < 0.01$.

B. Representative growth curves of the same strains as panel (A) in LB medium amended with 10 μM $FeSO_4$. For IPTG treated cells, 1 mM IPTG was added to cell culture when OD_{600} reaches ~0.25. Experiments were performed at least three times with three biological replicates.

To validate its use as an iron depletion system, we monitored the effects of FrvA expression on intracellular metal levels using inductively coupled plasma mass spectrometry (ICP-MS). The uninduced cells harboring an IPTG-inducible ectopic copy of *frvA* (WT P_{spac}-*frvA*) displayed a slightly reduced level of intracellular iron compared to WT, presumably due to the leaky expression of FrvA from the P_{spac} promoter. When FrvA expression was induced by IPTG, intracellular iron levels declined with a 2-fold decrease after 30 min of treatment. This decline continued gradually over time (Fig. 4.1A). By contrast, intracellular iron levels in both WT and uninduced cells increased significantly (about 2-fold) after 2 h (Fig. 4.1A), probably due in part to high iron demand as the growing cells enter into late logarithmic phase (transition phase) growth, which is generally characterized by increased respiratory activity (Mueller & Taber, 1989). The intracellular level of other metals such as Mn and Co was not significantly changed during the course of the experiment (Fig. 4.2).

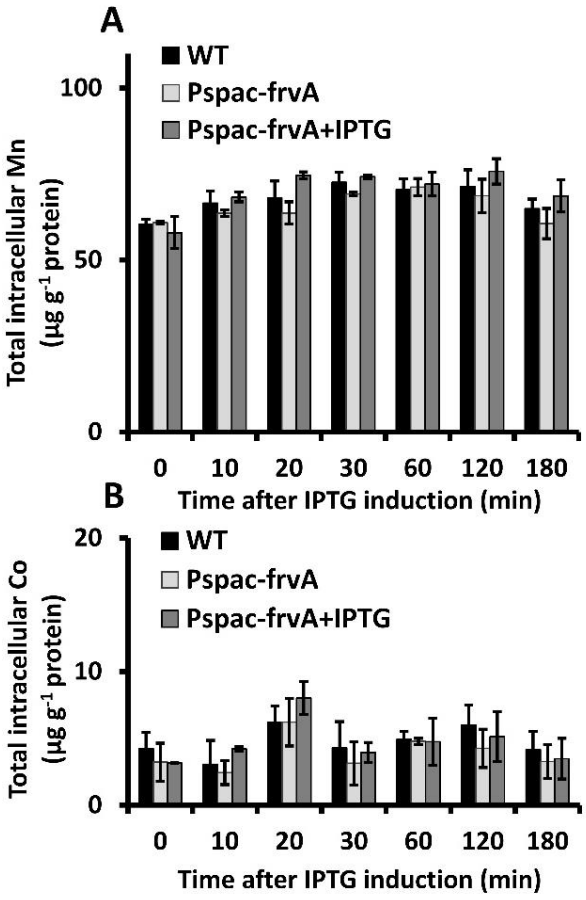

Fig. 4.2 Expression of FrvA has no effects on intracellular Mn and Co levels.

Levels of intracellular Mn (A) and Co (B) were monitored for three hours after IPTG addition by inductively coupled plasma mass spectrometry (ICP-MS). The total concentration of ions was expressed as μg ion per gram of protein (mean ± SD; n=3). Mn and Co levels were not significantly changed over the course of the experiment.

To evaluate the effects of FrvA expression on cell growth, we grew cells to early exponential phase (OD_{600}~0.25) in LB medium amended with 10 µM of $FeSO_4$, induced expression of FrvA with 1 mM of IPTG, and monitored growth. The uninduced cells grew as well as WT in the first three hours and displayed very minor growth inhibition afterwards, presumably due to leaky expression of FrvA from the P_{spac} promoter (Fig. 4.1B) (Pi *et al.*, 2016). In contrast, when FrvA is induced cell growth was inhibited beginning ~2 h after IPTG treatment (Fig. 4.1B). Thus, there is a substantial period of time (between ~30 to 90 min after induction) where iron levels are significantly reduced (more than 2-fold reduction of total intracellular iron) with little if any apparent growth inhibition. Therefore, we chose this period of time to characterize the graded response of the Fur regulon, when iron levels are declining, but growth has not yet been strongly affected.

4.4.2 Fur-regulated genes are derepressed in a stepwise fashion

To provide a global overview of the transcriptional changes as cells transition from iron sufficiency to iron deficiency we analyzed changes in RNA levels at 20, 30, 60, and 120 min after FrvA induction using oligonucleotide-based microarrays (Fig. 4.3). In this analysis, most Fur-regulated operons were expressed at a low level prior to induction, as expected for cells grown in LB supplemented with 10 µM iron. In a direct comparison of mRNA levels between cells carrying the P_{spac}-*frvA* construct grown with and without IPTG induction, the majority of the Fur regulon was derepressed (at least transiently) between 20 and 60 min after induction. In many cases, the maximal fold induction was comparable to that noted in a comparison of the *fur* mutant to WT (in strains lacking P_{spac}-*frvA*). In general, it appeared that some genes were induced at earlier time points, while induction of other genes was only evident at late time points, suggesting that the Fur regulon might be derepressed in a gradual manner in response to iron availability. Consistent with our prior study (Pi *et al.*, 2016), induction of the PerR regulon in response to iron limitation is also apparent in our microarray experiments at late timepoints (3 h) and also in cultures with IPTG added at the time of sub-culture (steady state) (Fig. 4.4A). This derepression is noted for peroxide

detoxification enzymes (*katA*, *ahpC*, and *ahpF*) and a miniferritin that may function in iron storage (*mrgA*). These results were further confirmed by qPCR (Fig. 4.4B).

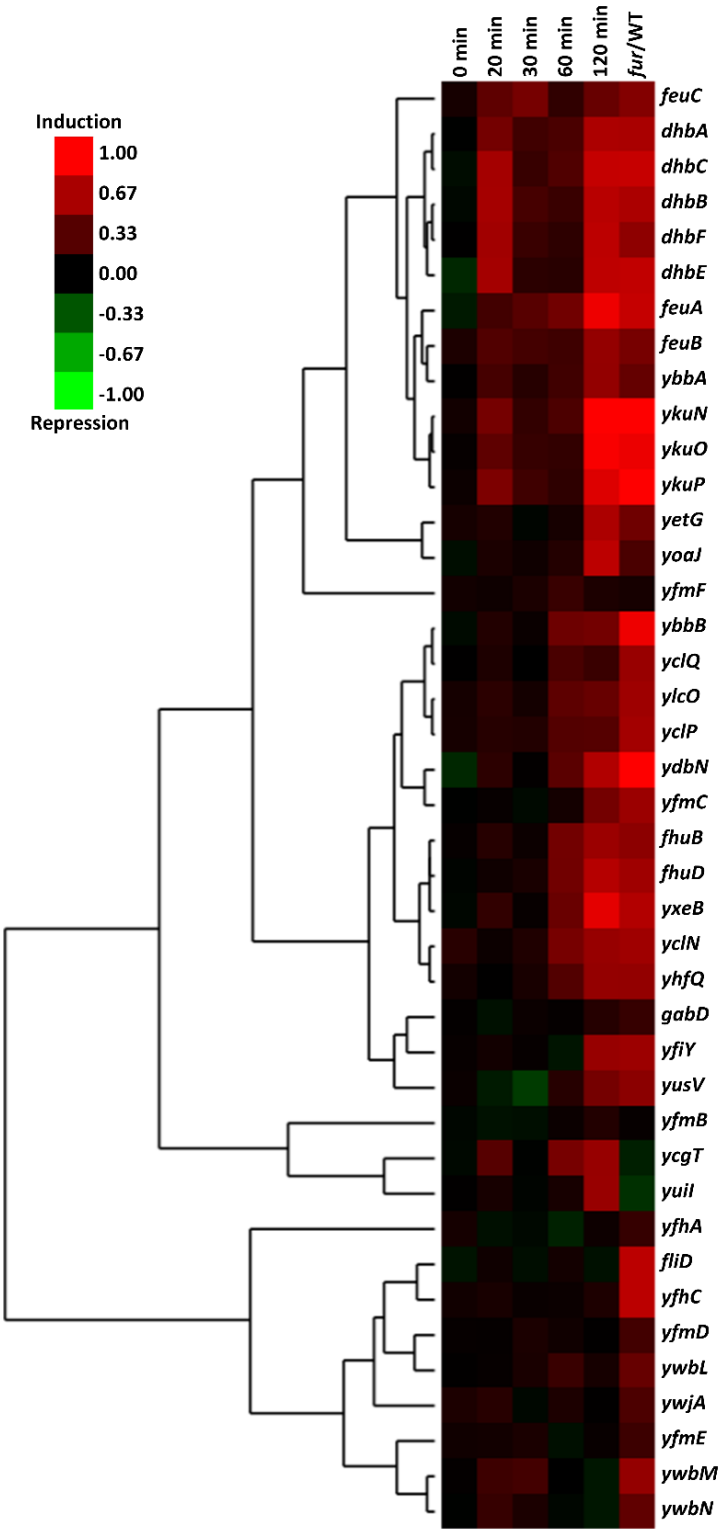

Fig. 4.3 Most of Fur-regulated genes are derepressed in response to iron depletion.

Cells (WT P_{spac}-*frvA*) were grown in LB medium amended with 10 µM $FeSO_4$ to an OD_{600} of ~0.25 and expression of FrvA was induced with 1 mM IPTG. Aliquots of 40 ml of cell culture were harvested at different time-points and total RNA was extracted using an acidic phenol-based method. All RNA samples were treated with Turbo-DNA free™ DNase and 20 µg of total RNA was used for cDNA synthesis followed by cDNA labeling with either Alexa Fluor® 647 (uninduced or WT) or Alexa Fluor® 555 (induced or *fur* null). 250 pmol of cDNA was then subjected to hybridization onto microarray slides. Hierarchical clustering was used to generate a heat map of induction (red) of known Fur-regulated genes at different time points as indicated on the top. Full-derepression of each Fur-regulated gene was shown in the last column where the transcriptome of a *fur* null mutant was compared to that of WT.

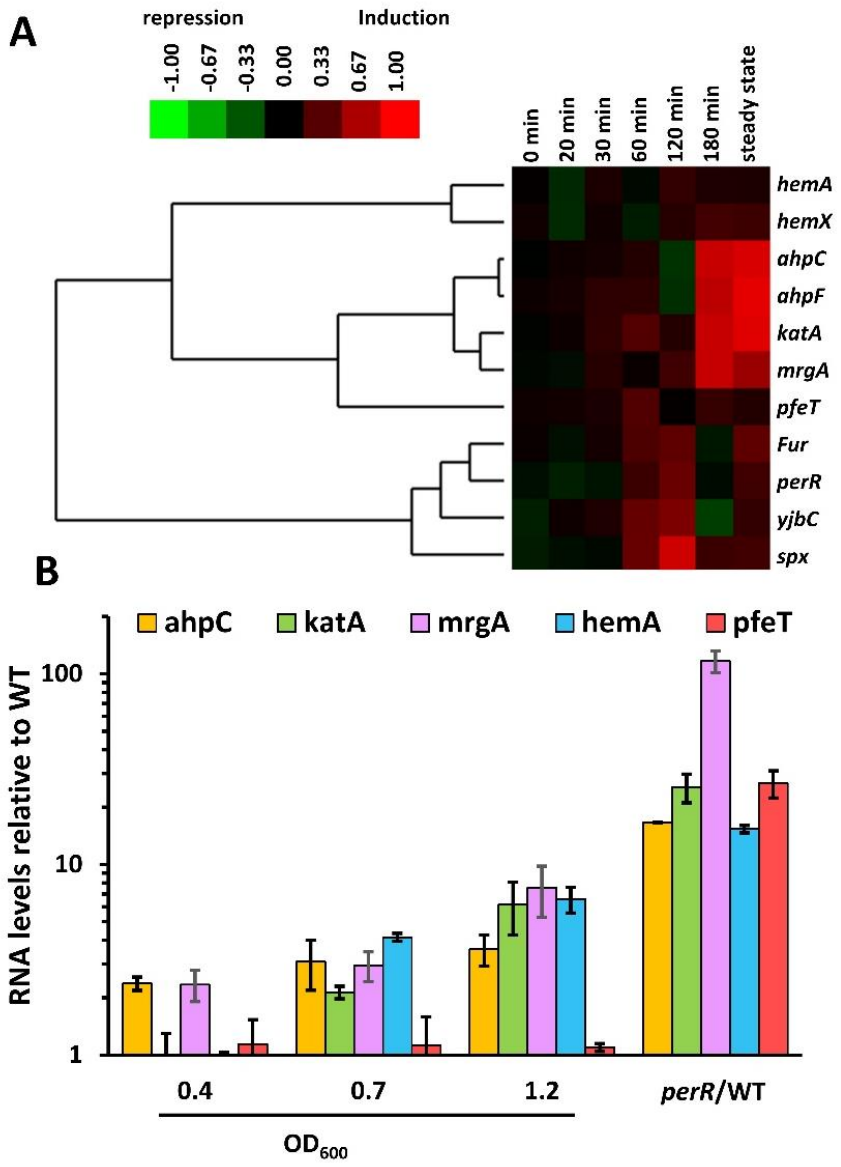

Fig. 4.4 Severe iron deprivation induces some PerR-regulated genes.

A. Hierarchical clustering was used to generate a heat map of induction (red) of known PerR-regulated genes at different time points as indicated on the top. Evident induction of some genes is shown in the last column, marked as "steady state", where expression of FrvA was induced by 1 mM IPTG from the beginning of the inoculum that leads to severe iron limitation and cells were harvested around OD_{600} ~0.6.

B. Overnight cell culture was inoculated with 1:100 ratio into fresh LB medium in the absence or presence of 1mM IPTG to induce expression of FrvA. Relative expression of each gene at different growth phases was analyzed by comparing gene expression in the IPTG induced cells versus that in wild-type cells. Full-derepression is considered as the mRNA level (in fold change) of each gene in *perR* null mutant compared to WT (shown as *perR*/WT). In the case of *katA*, *perR fur* double mutant was used to evaluate its full derepression since the *perR* single mutant is not genetically stable and often forms spontaneous suppressors with *katA* null mutation (Faulkner *et al.*, 2012).

We were surprised to note that the two iron uptake systems most important for growth in LB medium (Faulkner *et al.*, 2012), elemental iron uptake (EfeUOB; formerly YwbLMN (Miethke *et al.*, 2013)) and ferric citrate import (FecCDEF; formerly YfmCDEF (Ollinger *et al.*, 2006)) were not highly induced during the course of this experiment (Fig. 4.3). We hypothesized that these operons might be already partially derepressed in the uninduced cells due to mild iron deprivation resulting from leaky expression of FrvA. To test this idea, we monitored the expression of most of the Fur-regulated operons by quantitative PCR (qPCR), including the elemental iron uptake (*efeUOB*), ferric citrate uptake (*fecCDEF*), hydroxamate siderophores uptake (*fhuBCGD*), petrobactin uptake (*fpbNOPQ*), flavodoxins (*ykuNOP*), BB biosynthesis (*dhbACEBF*), BB uptake (*feuABC*), and iron sparing response (*fsrA, fbpAB,* and *fbpC*). Cells were grown in LB amended with 10 µM iron and total RNA was extracted and subjected to cDNA synthesis followed by qPCR. Relative derepression of the first gene in each operon at different time points was analyzed by comparing gene expression in the IPTG induced cells versus that in wild-type cells. The percentage of derepression was evaluated based on the full-derepression observed in a *fur* mutant versus WT, which was set as 100% derepression. Among all the genes tested, three genes, *fpbN*, *efeU*, and *fecC*, were strongly derepressed (30-55% derepression) even at time zero (Fig. 4.5), where only leaky expression of FrvA is present.

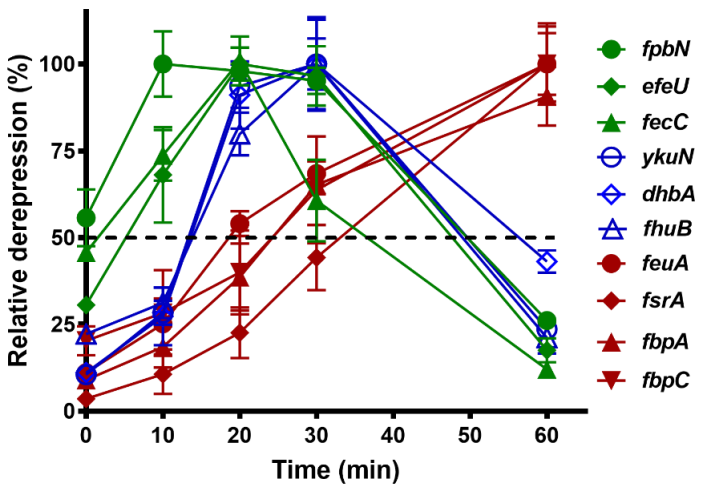

Fig. 4.5 Leaky expression of FrvA induces some genes in the Fur regulon.

Cells were grown at 37^{0}C in LB medium overnight and subcultured with 1:100 ratio into fresh LB medium amended with 10 µM $FeSO_4$. After OD_{600} reaches ~0.25, 1mM IPTG was added to induce expression of FrvA. Relative expression of each gene tested at different time points was monitored by comparing gene expression in the IPTG induced cells (WT P_{spac}-*frvA*) versus that in wild-type cells (WT). The percentage of derepression was normalized based on the full derepression observed in a *fur* null mutant versus WT cells, which was set as 100% derepression for each gene tested.

We hypothesized that a higher concentration of iron in the medium might enable a more complete repression of the Fur regulon. We therefore checked repression in LB medium amended with 25, 50 and 100 µM iron, and determined that 25 µM was sufficient to fully repress Fur-regulated genes. We therefore repeated our qPCR analysis using LB medium amended with 25 µM. For this analysis we used 50% derepression as the threshold to define the order of gene induction. Three waves of derepression were revealed with 50% derepression at ~10, 20, and 60 min (Fig. 4.2). As judged by monitoring of the first gene in each operon, we can resolve early (*fpbN*, *efeU*, *fecC*), middle (*fhuB*, *ykuN*, *dhbA*, and *feuA*), and late genes (*fsrA*, *fbpA*, and *fbpB*) (Fig. 4.6). These results are consistent with the first set of experiments using 10 µM $FeSO_4$ with the exception of *feuA* being assigned as a middle gene (Fig. 4.5 and Fig. 4.6). The late induction of the FsrA/FbpABC iron-sparing response is expected to lead to translational downregulation of a large

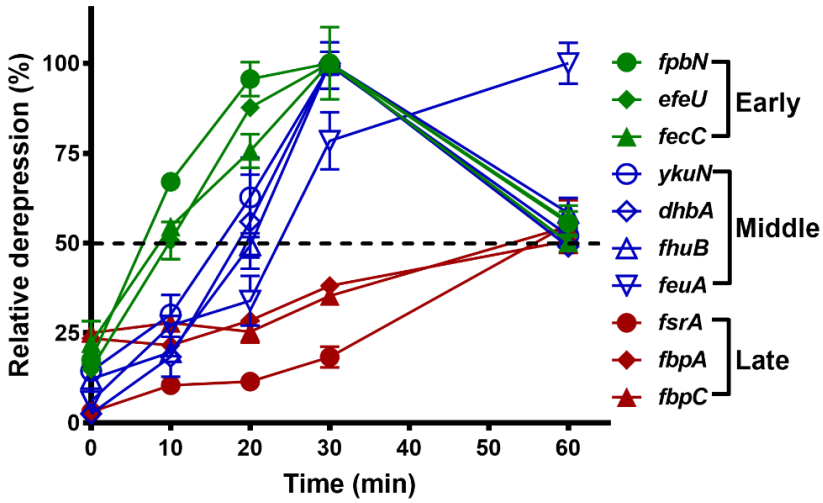

Fig. 4.6 Fur-regulated genes are induced in a stepwise manner as a function of iron depletion.

Cells were grown at 37^{0}C in LB medium overnight and subcultured (1:100 ratio) into fresh LB medium amended with 25 µM $FeSO_4$. At OD_{600} ~0.25, 1 mM IPTG was added to induce expression of FrvA. Quantitative PCR was conducted using a specific primer set for each gene (Table S2). The housekeeping gene 23S rRNA was used as an internal control. Relative expression of the first gene in each operon at different times was analyzed by comparing gene expression in the IPTG induced cells versus that in wild-type cells. The percentage of derepression was normalized based on the full-derepression observed in a *fur* null mutant versus WT cells, which was set as 100% derepression for each gene tested.

number of target genes, which as shown previously is reflected as a reduction of steady-state mRNA levels (Smaldone *et al.*, 2012). Indeed, we also observed a decrease in the mRNA levels of many-FsrA regulated genes at later timepoints (1 h and 2 h) (Fig. 4.7).

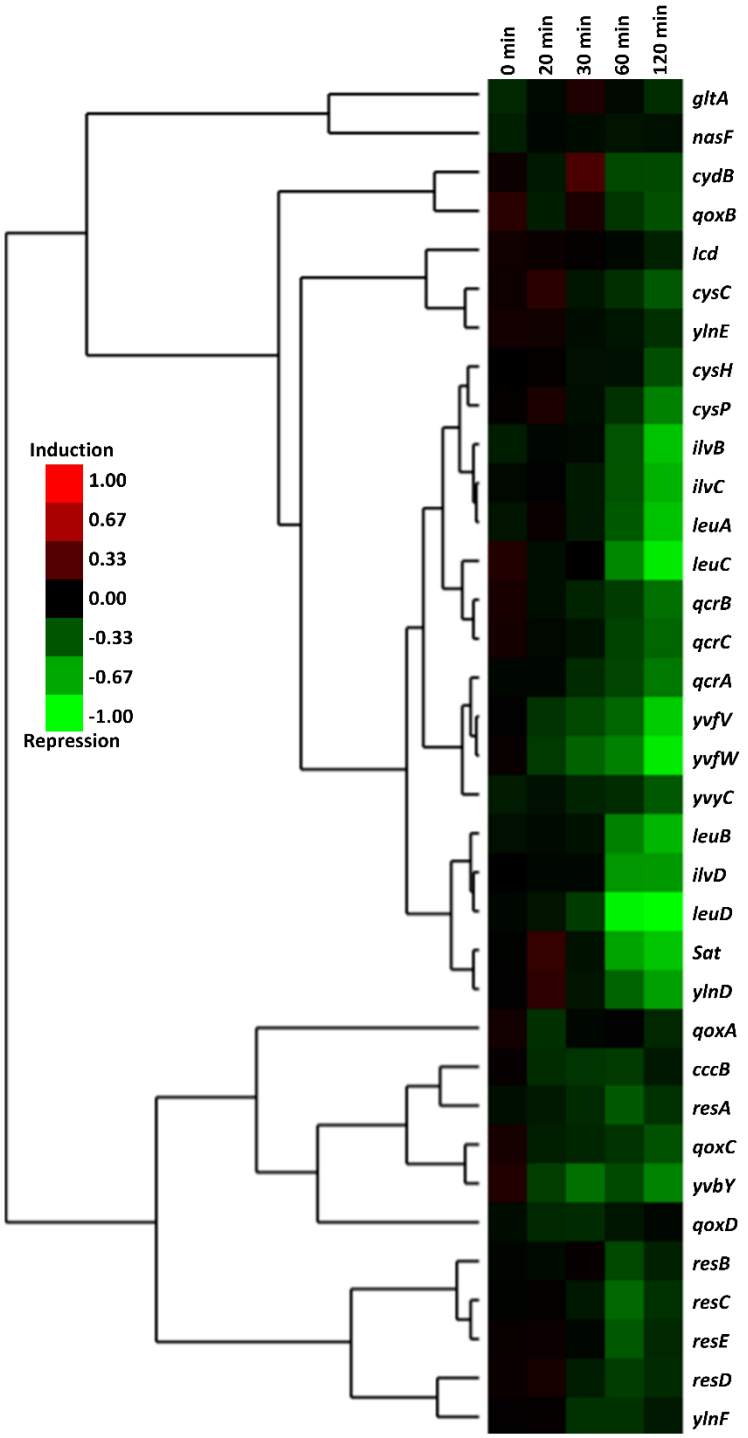

Fig. 4.7 A decrease in mRNA levels of many FsrA-regulated genes is observed at later timepoints in response to iron depletion. Hierarchical clustering was used to generate a heat map of down-regulation (green) of known FsrA-regulated genes at different time points as indicated on the top.

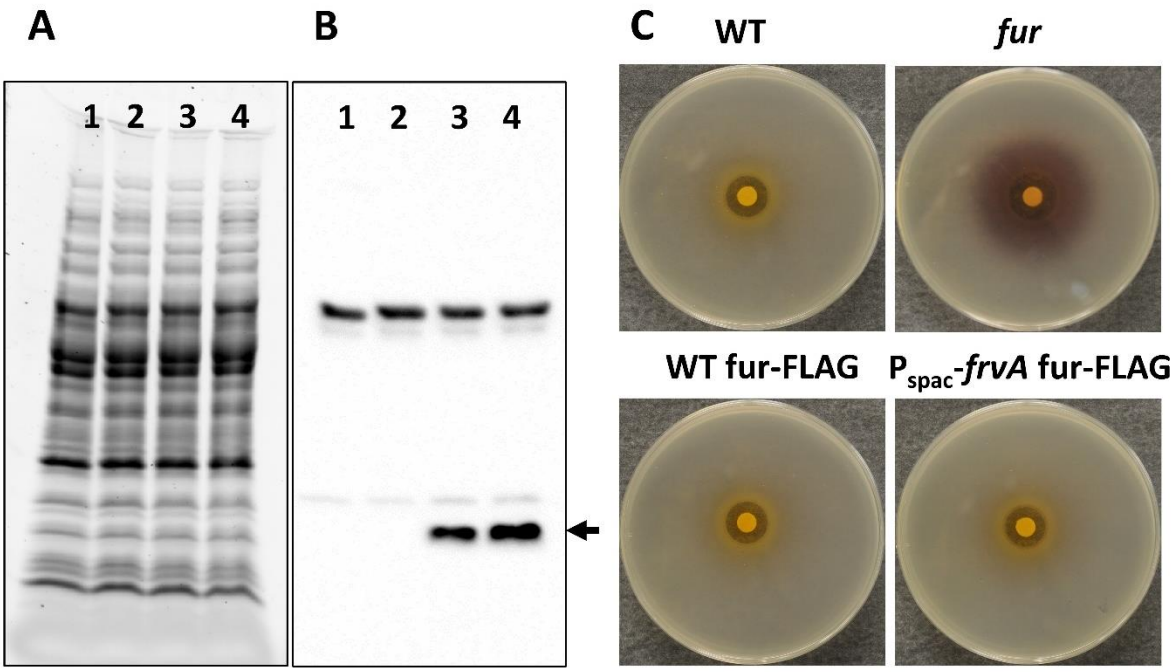

Fig. 4.8 The chromosomal FLAG-tagged Fur is a functional regulator.

A. 20 µg of total protein from the whole cell lysate of each sample was loaded to a SDS-PAGE gel. Strains tested are: Lane 1, WT; Lane 2, WT P_{spac}-*frvA*; Lane 3, WT::Fur-FLAG; Lane 4, WT P_{spac}-*frvA*::Fur-FLAG.
B. The same SDS-PAGE gel as shown in Fig. 4.8A was subjected to Western blot using monoclonal anti-FLAG antibody. The specific signals are indicated by the arrow.
C. A disk diffusion assay was used to confirm the functionality of the chromosomal FLAG-tagged Fur *in vivo*. 10 µl of 1M $FeSO_4$ was applied onto each disk. A purple halo is evident around the inhibition zone in a *fur* null mutant due to derepression of the siderophore bacillibactin biosynthesis (DhbACEBF), which is under regulation of Fur; whereas the FLAG-tagged Fur in both genetic background (WT and P_{spac}-*frvA*) behaves very similarly as WT without FLAG-tagged Fur, indicating the chromosomal FLAG-tagged Fur is a functional regulator.

4.4.3 Stepwise induction of Fur-regulated genes correlates with operator occupancy

The molecular mechanism for the stepwise derepression of Fur regulated genes may simply be that Fur operator occupancy is sequentially affected as a function of iron depletion. To test this idea, we constructed a fully functional chromosomal FLAG-tagged Fur in both WT and P_{spac}-*frvA* (Fig. 4.8). Using chromatin immunoprecipitation (ChIP) coupled with qPCR, we found that occupancy of Fur on the operator sites tested declined rapidly upon iron depletion. Fur occupancy decreased significantly at the

sites of three early genes (*fpbN*, *efeU*, *fecC*) by 1 min; the differences of Fur occupancy among the three sets of genes became evident by 3 min, with only ~ 10% occupancy for early genes (*fpbN*, *efeU*, *fecC*), ~35% occupancy for middle genes (*fhuB*, *ykuN*, *dhbA*, and *feuA*), and ~55% occupancy for late genes (*fsrA*, *fbpA*, and *fbpB*) (Fig. 4.9). More importantly, the three distinct patterns revealed by ChIP (Fig. 4.9) correspond to the same three sets of early, middle, and late genes determined by qPCR (Fig. 4.6). The timescale of Fur dissociation from its operators (Fig. 4.9) appears to be considerably faster than the resulting accumulation of the corresponding mRNAs (Fig. 4.6). However, the ChIP procedure likely underestimates the time required for loss of operator binding since the times noted do not account for the time required to harvest

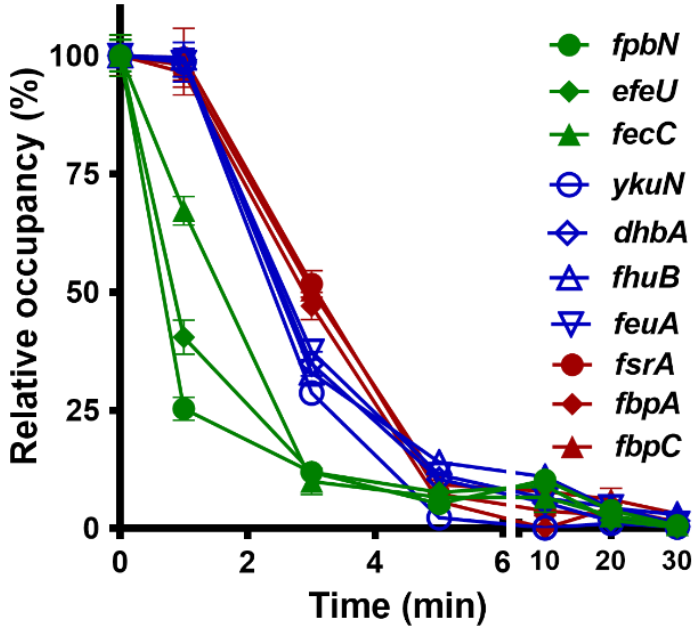

Fig. 4.9 Operator occupancy correlates with stepwise derepression of the Fur regulon.

Fur occupancy on different promoter sites was evaluated by chromatin immunoprecipitation (ChIP) using anti-FLAG antibodies. Co-immunoprecipitated DNA was quantified by qPCR using specific primer sets to the promoter regions of the target genes as listed in Table S2. DNA enrichment was calculated based on the input DNA (1% of total DNA used for each ChIP experiment). Fur occupancy at different sites was set as 100% at time-point 0. Date are presented as the relative percentage (%) of occupancy at different time-points after 1mM IPTG induction (mean ± SD, n=3). No significant DNA Enrichment was observed for *gyrA* that is used as a non-specific negative control.

cells by centrifugation prior to protein-DNA crosslinking. Moreover, the mRNA measurements reflect the cumulative effect of Fur dissociation, RNAP recruitment, and transcription leading to an increase in mRNA levels. Despite the differences in time-scale, these results support the general notion that Fur dissociates from early gene operator sites more quickly as intracellular iron levels decrease.

Table 4.1 Binding affinity of *B. subtilis* Fur to its target promoters

Order of induction	Promoter	K_d *(nM)
Early	*fpbN*	5.6 ± 0.5
	efeU	1.5 ± 0.3
	fecC	3 ± 0.5
Middle	*ykuN*	2.1 ± 0.4
	dhbA	2.1 ± 0.5
	fhuB	0.9 ± 0.2
	feuA	0.8 ± 0.2
Late	*fsrA*	0.6 ± 0.2
	fbpA	0.6 ± 0.1
	fbpC	0.5 ± 0.1

*K_d values were calculated using GraphPad Prism 5 (mean ± SD, n=3) (Fig. 4.10 and 4.11).

4.4.4 Stepwise induction of Fur-regulated genes is correlated with protein-DNA binding affinity

As the FrvA efflux pump gradually depletes iron from the cytosol the concentration of metallated Fur protein is predicted to decrease. We therefore hypothesized that the earliest induced operons in the Fur regulon would correspond to those with operator sites that bind holo-Fur weakly, and, conversely, that the late-induced genes would bind holo-Fur with higher affinity. We determined the biochemical binding affinity *in vitro* using electrophoretic mobility shift assay (EMSA). The equilibrium dissociation

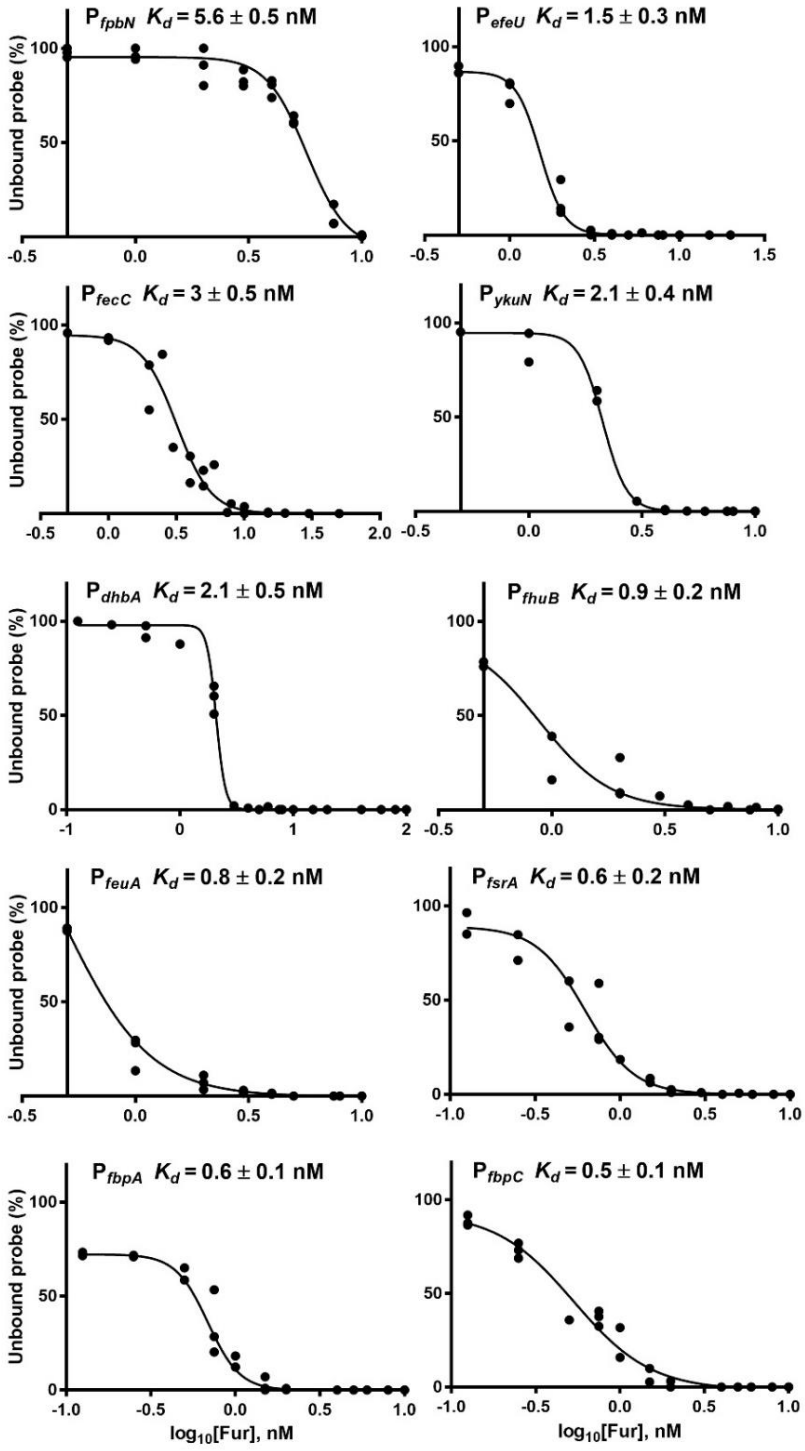

Fig. 4.10 The stepwise derepression of Fur-regulated genes correlates with protein-DNA binding affinity. Fur-DNA binding affinities to different promoter regions are determined by electrophoretic mobility shift assay (EMSA). The band intensity of unbound DNA probe was quantified using GelQuantNET software. All the data points from three independent experiments were plotted and subjected to K_d determination using GraphPad Prism 5.

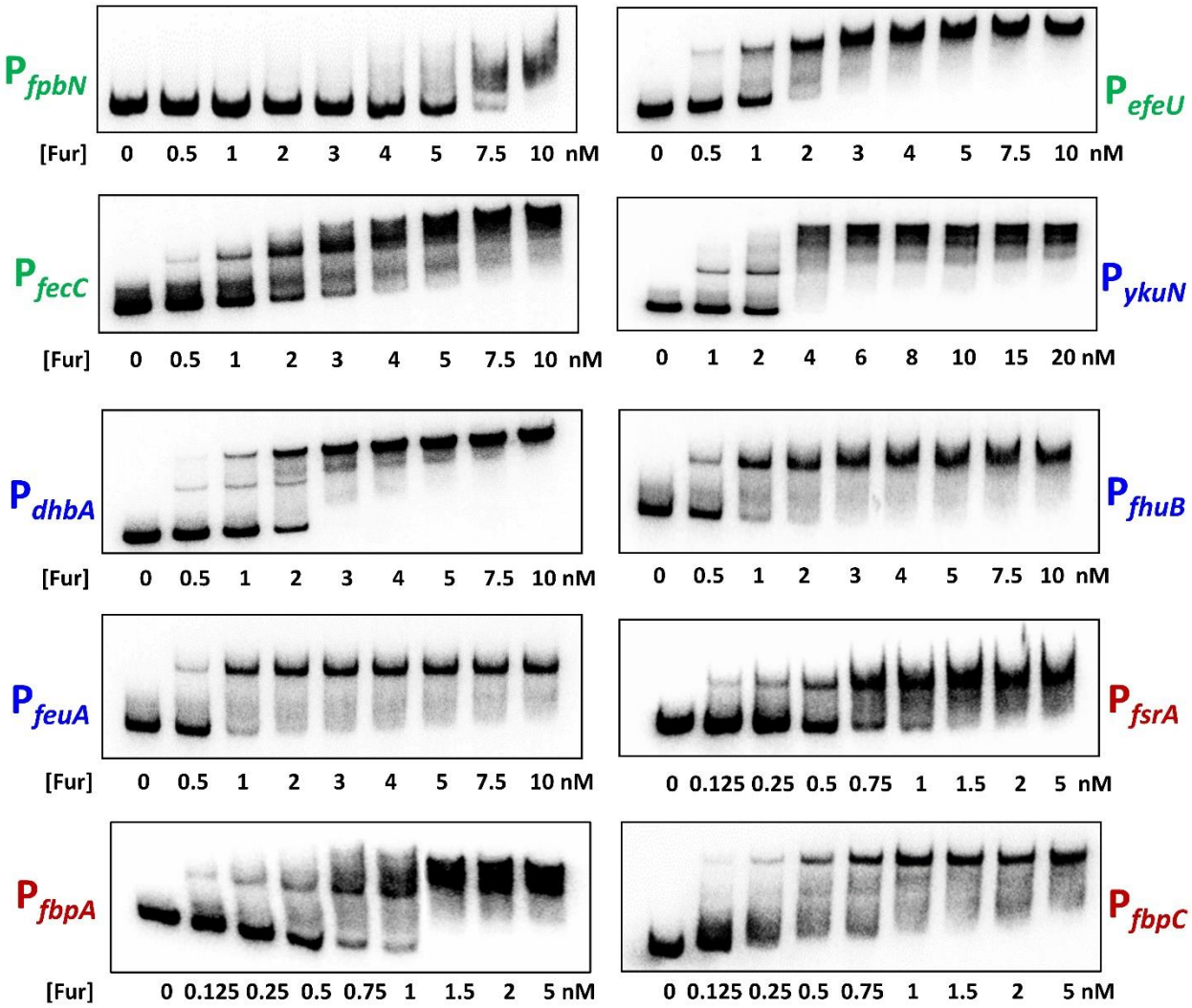

Fig. 4.11 Fur-DNA binding affinities to different promoter regions.

Representative images to show protein-DNA binding affinities to different promoter regions determined by electrophoretic mobility shift assay (EMSA).

constant (K_d) for Fur binding to different target operators provides an estimate of the concentration of active protein required for half-maximal repression. In support of our hypothesis, the stepwise induction of Fur regulon correlates, at least in part, with protein-DNA binding affinity (Table 1 and Figs 4.10, 4.11). For example, Fur binds to the operators of early genes with relatively low affinity (K_d value of ~3 and 5.6

nM for *fecC* and *fpbN*, respectively), to those of middle gene with higher affinity (0.8 nM for *fhuB*, 0.9 nM for *feuA*, and 2.1 nM for *dhbA*), and with highest affinity to those for late genes (0.5-0.6 nM for all three late genes, *fsrA*, *fbpA*, and *fbpB*) (Table 1 and Figs 4.10, 4.11). However, there are some exceptions. For instance, the induction of *efeU*, which binds Fur with high affinity (a K_d value of 1.5 nM), occurs as early as that of *fpbN* (a K_d value of 5.6 nM). Fur binds to some early and middle genes with an affinity difference of 3-4-fold (Table 1 and Figs 4.10, 4.11), suggesting that other factors may also affect the regulation of some Fur target genes. Indeed, previous studies have revealed that multiple transcription factors such as ResD, NsrR, and Fur interact with one another and co-regulate transcription of *ykuN* and other Fur-regulated genes during anaerobic fermentation and nitrate respiration (Henares *et al.*, 2014, Chumsakul *et al.*, 2017). It is also known that the bacillibactin uptake system (FeuABC) is under regulation of both Fur and Btr (Gaballa & Helmann, 2007, Smaldone *et al.*, 2012) (see below).

4.4.5 The stepwise induction of Fur regulon in response to iron limitation in strains expressing bacillibactin

In most environmental isolates of *B. subtilis*, the mature siderophore BB is synthesized and exported by YmfD, a major facilitator superfamily transporter (Miethke *et al.*, 2008). The ferric-siderophore complex (Fe^{3+}-BB) is then imported by the FeuABC-YusV system and hydrolyzed by the BesA esterase to release iron (Miethke *et al.*, 2006). Once imported, BB binds to the Btr transcription activator and stimulates transcription of the *feuABC* operon. BB binds to Fe^{3+} with remarkably high affinity, comparable to the chemically similar enterobactin produced by enteric bacteria (Ollinger *et al.*, 2006, Dertz *et al.*, 2006), and is therefore an effective iron-scavenging agent. Indeed, *sfp*$^+$ strains have higher growth rate and yield in minimal medium amended with either 25 µM (Fig. 4.12A) or 1 mM iron (Fig. 4.12B) compared to *sfp*^{0} strains. Many laboratory strains (based on *B. subtilis* 168) are *sfp*^{0} and therefore only produce the BB precursors DHB(G), which bind Fe^{3+} with only modest affinity (lower than citrate) and may not function as an effective siderophore in natural settings (Ollinger *et al.*, 2006, Chipperfield & Ratledge,

2000). Moreover, DHB(G) is ineffective in activating Btr, although Btr does have significant stimulatory activity even in the absence of siderophore (Gaballa & Helmann, 2007).

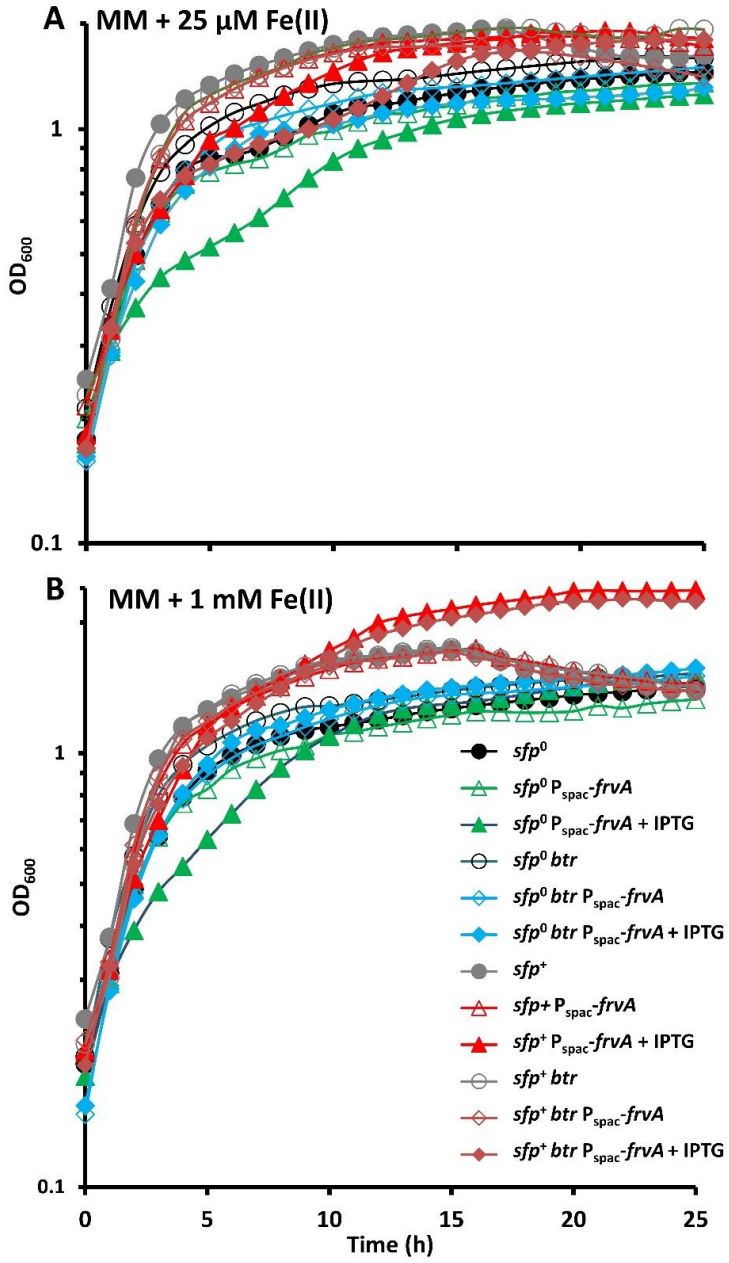

Fig. 4.12 Growth advantage of *sfp*$^+$ strains over *sfp*^{0} strains.

Representative growth curves of *sfp*^{0} and *sfp*$^+$ strains in minimum medium (MM) amended with 5 µM of $MnCl_2$ and different concentration of $FeSO_4$, 25 µM (A) or 1 mM (B). Cells were grown at 37^{0}C in LB medium overnight and subcultured at a 1:100 ratio into MM medium. For IPTG treated cells, 1 mM IPTG was added to cell culture when OD_{600} reaches ~0.2. Cell growth were then monitored for 25 h.

To further explore the graded response of the Fur regulon in strains producing BB, we monitored the induction of Fur target genes in *sfp*$^+$ strains harboring an IPTG-inducible copy of *frvA* (*sfp*$^+$ P_{spac}-*frvA*) as cells transition from iron sufficiency (LB+25 µM iron) to deficiency. Consistent with the studies above (Fig. 4.6), Fur-regulated genes were derepressed in a stepwise manner with early (*ypbN*, *efeU*, *fecC*), middle (*fhuB*, *ykuN*, *dhbA*, and *feuA*), and late genes (*fsrA*, *fbpA*, and *fbpB*) (Fig. 4.13). However, a few changes were notable: induction of all early and middle genes was shifted a little earlier while induction of the late genes (*fsrA*, *fbpA*, and *fbpB*) was shifted later (Fig. 4.13). This suggests that efficient iron acquisition through Fe^{3+}-BB delays proteomic remodeling via the iron sparing response.

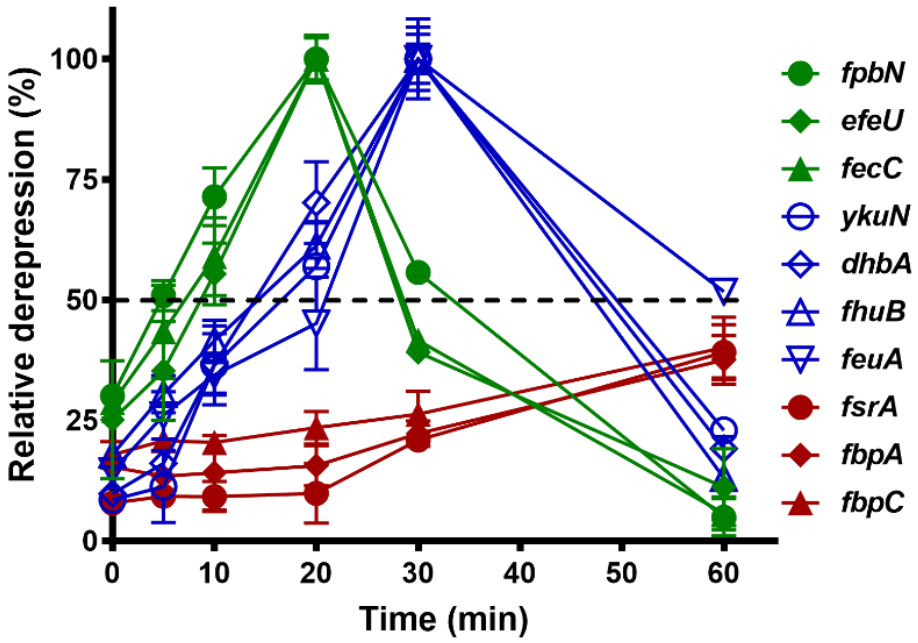

Fig. 4.13 Fur-regulated genes are induced in a similar stepwise manner as a function of iron depletion in strains producing bacillibactin.

Overnight cell culture was inoculated with 1:100 ratio into fresh LB medium amended with 25 µM $FeSO_4$. After OD_{600} reaches ~0.25, 1 mM IPTG was added to induce expression of FrvA. Total RNA was extracted and subjected to cDNA synthesis followed by qPCR. Relative expression of each gene at different times was monitored by comparing gene expression in the IPTG induced cells versus that in *sfp*$^+$ WT cells. The percentage of derepression was evaluated based on the full-derepression observed in *sfp*$^+$ *fur* mutant versus *sfp*$^+$ WT, which was set as 100% derepression.

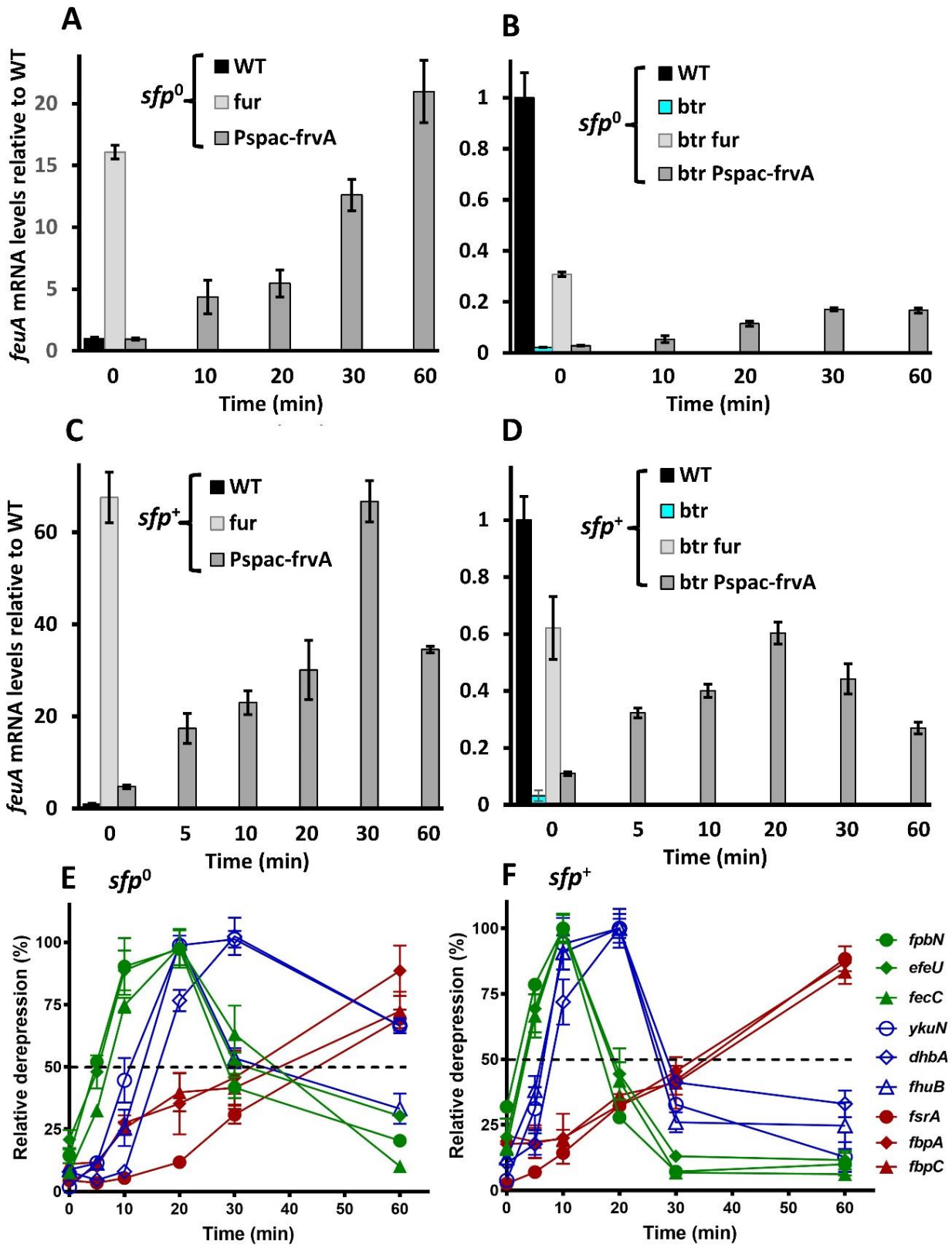
A
B
C
D
E
F
feuA mRNA levels relative to WT
sfp0
sfp+
WT
fur
Pspac-frvA
btr
btr fur
btr Pspac-frvA
Time (min)
Relative derepression (%)
fpbN
efeU
fecC
ykuN
dhbA
fhuB
fsrA
fbpA
fbpC

Fig. 4.14 Inactivation of bacillibactin uptake affects induction of the Fur-regulated gene.

Cells were grown at 37^{0}C in LB medium overnight and subcultured with 1:100 ratio into fresh LB medium amended with 25 µM $FeSO_4$. After OD_{600} reaches ~0.25, 1mM IPTG was added to induce expression of FrvA. Total RNA was extracted and subjected to cDNA synthesis followed by qPCR.

A, B. The expression level of *feuA* in *sfp*^{0} WT cells is set as 1 in both S10A and S10B. Relative mRNA levels of *feuA* in different strains tested compared to that in wild type (*sfp*^{0}) are presented as fold changes (mean ± SD; n=3);

C, D. The expression level of *feuA* in *sfp*$^+$ wild-type cells is set as 1 in both S10C and S10D. Relative mRNA levels of *feuA* in different strains compared to that in *sfp*$^+$ WT are presented as fold changes (mean ± SD; n=3);

E, F. Relative expression of each gene tested was monitored by comparing gene expression in the IPTG induced cells (*i.e.* E, *sfp*$^+$ *btr* P_{spac}-*frvA* + IPTG; F, *sfp*$^+$ *btr* P_{spac}-*frvA* + IPTG) versus that in *btr* null mutants. The percentage of derepression was normalized based on the full-derepression observed in *btr fur* mutant versus a *btr* single mutant, which was set as 100% derepression.

4.4.6 Inactivation of bacillibactin uptake affects induction of the Fur-regulated genes

Expression of *feuA* is induced ~20-fold upon iron depletion in a *sfp*^{0} strain (Fig. 4.14). Previous studies revealed that BB, but not the precursor DHBA, increases binding of Btr to the *feuA* promoter and stimulates transcription (Gaballa & Helmann, 2007, Smaldone *et al.*, 2012). Indeed, the expression of *feuA* was derepressed up to 68-fold in a *sfp*$^+$ strain (Fig. 4.14C), indicating a more than 3-fold activation by BB. In the absence of Btr, *feuA* mRNA levels were reduced >30-fold (Fig. 4.14B and D), although Fur repression of *feuA* is still relieved by iron depletion (Fig. 4.14B and D). This effect can also be observed in disk diffusion assays (Fig. 4.15A). BB and DHB(G) compounds bind to Fe^{3+} and form complexes of purple color apparent around the zone of inhibition resulting from overexpression of FrvA (Fig. 4.15A). As expected, inactivation of bacillibactin uptake by deletion of *btr* leads to clearly visible accumulation of DHB(G) or BB in the medium (Fig. 4.15A). This result was confirmed by quantitation of the secreted Fe^{3+}-DHB(G) or Fe^{3+}-BB complex (Fig. 4.15B-C).

Although deletion of *btr* does not change the order of derepression of Fur target genes (Fig. 4.14E-F), most genes are induced earlier than observed in experiments done in WT cells (Figs. 4.6 and 4.13). In

sfp^0 strains, 50% derepression shifts from 10, 20, 60 min to 5, 14, or 40 min for early, middle, or late genes, respectively (Fig. 4.14E). In *sfp*$^+$ strains, 50% derepression shifts from 8, 15, 70 min to 3, 8, or 35 min for early, middle, or late genes, respectively (Fig. 4.14F). These results suggest that biosynthesis and uptake of BB is critical for maintaining iron homeostasis upon iron limitation. These results also confirm that Btr

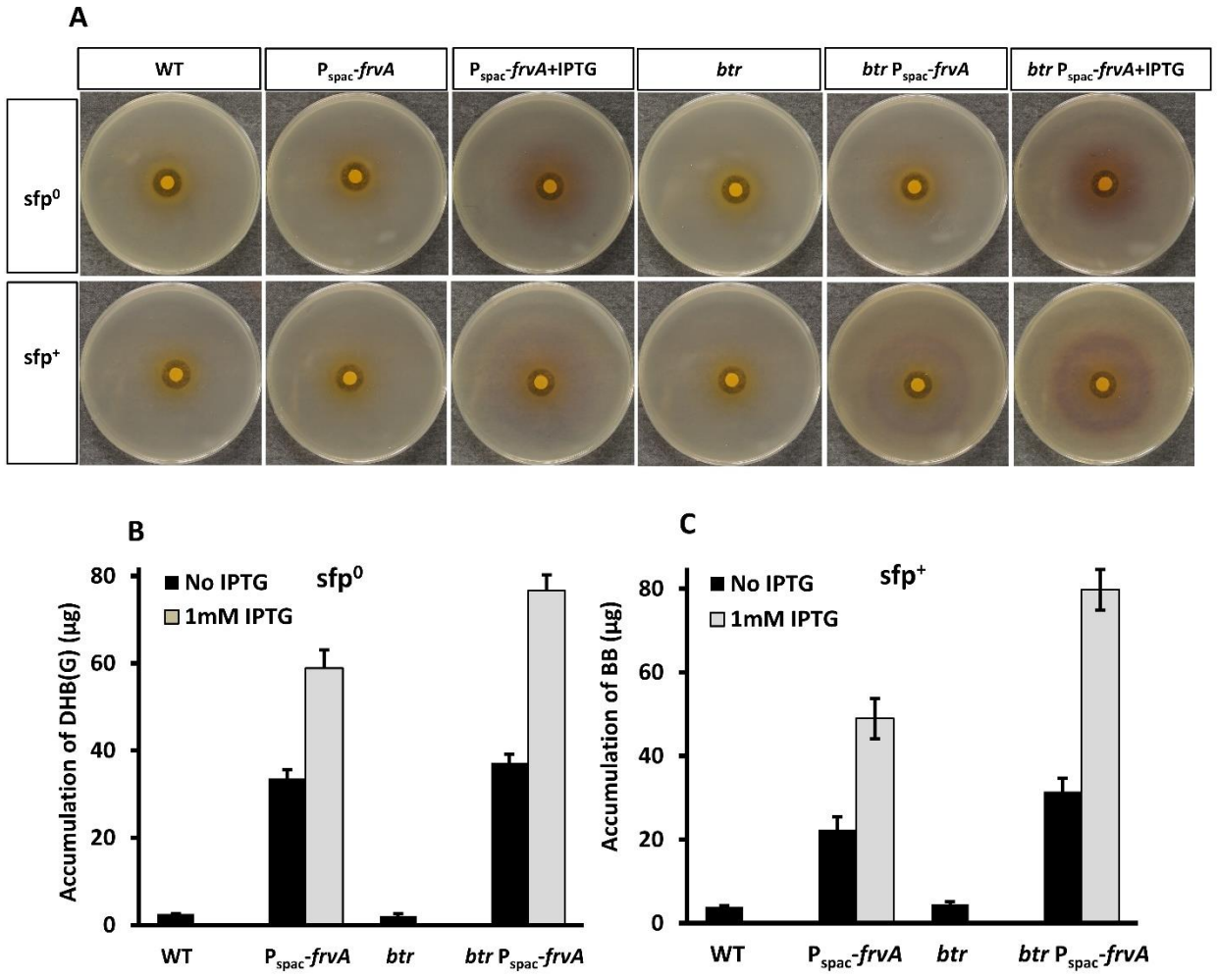

Fig. 4.15 Physiological role of Btr on bacillibactin uptake system in both sfp^0 and sfp$^+$ strains.

A. Representative photographs of a disk diffusion assay performed with *sfp*^{0} (top panel) or *sfp*$^+$ (bottom panel) strains. 10 µl of 1M $FeSO_4$ was added onto each filter paper disk. Accumulation of DHB(G) or bacillibactin (BB) in the medium can be evaluated by comparing the intensity of the purple complexes around the zone of inhibition resulting from overexpression of FrvA;

Quantification of DHB(G) production in *sfp*^{0} strains (B) or quantification of BB production in *sfp*$^+$ strains (C) by measuring the optical density (OD_{510}). An optical density at 510 nm (OD_{510}) of 0.5 is equivalent to 80 µg of DHB(G) or BB per ml.

is required for significant expression of the *feuA* operon, and in the absence of Btr the production of iron chelators (BB or its precursors) that cannot be efficiently imported back into the cell results in a more rapid onset of iron starvation (Fig. 4.14E-F).

4.4.7 The iron sparing response induced by iron depletion leads to an increase in intracellular labile iron

As shown above, when cells experience severe iron limitation the iron sparing response is engaged to modulate cellular proteomes and prioritize the use of limited iron (Figs. 4.5, 4.6, 4.13, and 4.14E-F). Since the translation of many abundant, low-priority iron-utilizing proteins is blocked by FsrA and its coregulators, we anticipated that intracellular labile iron pools might actually increase under these conditions, despite the fact that total intracellular iron is depleted (Fig. 4.1A). Indeed, in *Escherichia coli* expression of the small RNA RyhB, analogous to FsrA in *B. subtilis*, leads to an increase in the intracellular iron pool (Jacques *et al.*, 2006, Gerstle *et al.*, 2012). To test this notion, we monitored the intracellular labile pool by testing sensitivity to streptonigrin (SN), an antibiotic that responds to intracellular labile iron levels (Yeowell & White, 1982). Indeed, when FrvA is expressed, it depletes

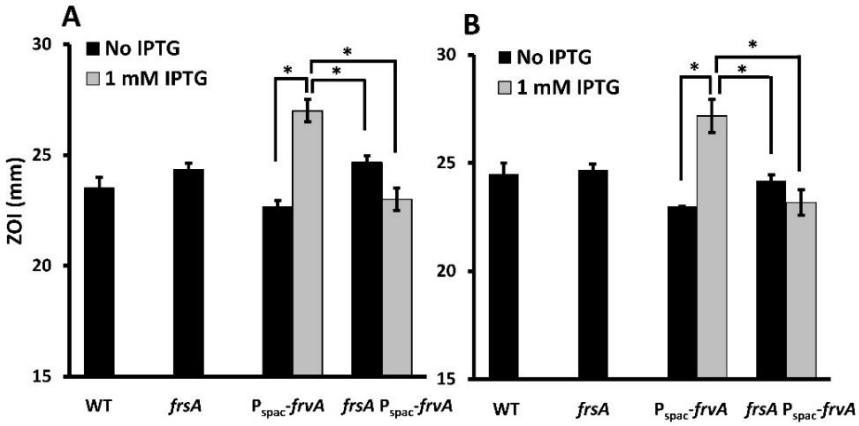

Fig. 4.16 The iron sparing response induced by iron depletion leads to an increase in intracellular labile iron.

Sensitivity to streptonigrin (SN) was monitored using a disk diffusion assay in LB agar plates containing either 0 (A) or 100 µM $FeSO_4$ (B). Strains tested in both panels are wild-type (WT, CU1065), *fsrA* null mutant, P_{spac}-*frvA*, and *fsrA* P_{spac}-*frvA*. The data are expressed as the diameter (mean ±SD; n=3) of the inhibition zone (mm). Significant differences determined by two-tailed *t*-test are indicated: *, $P < 0.05$.

total intracellular iron but the intracellular labile iron level increases, as judged by the higher sensitivity to SN in both LB plates without or with supplementing exogenous iron (Fig. 4.16A-B). In the absence of the FsrA-mediated iron sparing response, this increase in intracellular labile iron no longer occurs (Fig. 4.16A-B), suggesting that the iron sparing response is chiefly, if not solely, responsible for this increase.

4.5 Discussion

Iron homeostasis relies on the ability of bacterial cells to express iron acquisition systems including siderophore(s) synthesis and their uptake systems. In *B. subtilis*, iron limitation activates expression of uptake systems for elemental iron, ferric citrate, and several xenosiderophores, as well as for biosynthesis and uptake of the endogenous siderophore bacillibactin. Our results show that as intracellular iron levels decline Fur-regulated genes are induced in a stepwise manner with three distinguishable waves. The first response to prevent iron starvation is the induction of uptake systems for petrobactin (FpbNOPQ), elemental iron (EfeUOB), and ferric citrate (FecCDEF). Petrobactin (PB), a photoreactive catecholate siderophore, is synthesized by marine bacteria (Barbeau *et al.*, 2002) and some members of the *Bacillus cereus* group (Abergel *et al.*, 2008, Koppisch *et al.*, 2005, Koppisch *et al.*, 2008, Wilson *et al.*, 2006), including *Bacillus anthracis* (Koppisch *et al.*, 2005). PB-mediated iron acquisition may play an important physiological role in cell survival within some ecological niches. For example, in *B. anthracis* PB biosynthesis is required for survival in macrophages and virulence in mice (Cendrowski *et al.*, 2004, Abergel *et al.*, 2006). PB, elemental iron, and ferric citrate likely represent major iron sources generally available in the environment (Frawley *et al.*, 2013, Pi & Helmann, 2017), consistent with the early induction of their uptake systems.

As intracellular iron levels decline further, more efficient siderophore-mediated acquisition systems are needed to support growth. The second wave includes production of BB (DhbACEBF) and expression of several uptake systems: FeuABC for both BB and enterobactin (Miethke *et al.*, 2006), and

FhuBCGD for hydroxamate siderophores (ferrichrome and ferrioxamine) (Baichoo *et al.*, 2002). Both enterobactin and BB exhibit remarkably high affinity to iron, $10^{-34.3}$ or $10^{-33.1}$ M, respectively (Ollinger *et al.*, 2006); while hydroxamate siderophores have lower affinity to iron ranging from $10^{-25.2}$ to $10^{-27.5}$ M (Ollinger *et al.*, 2006). In addition, as part of a common strategy against nutrient limitation, cells replace 4Fe-4S ferrodoxins with alternative iron-independent flavodoxins to help alleviate iron demand (Merchant & Helmann, 2012). *B. subilis* contains two flavodoxins, YkuN and YkuP, which are encoded by the *ykuNOP* operon. They have been shown to function as electron donors for fatty acid desaturation equivalently as ferrodoxin (Chazarreta-Cifre *et al.*, 2011). More generally, flavodoxins have been used as a biological marker for iron limitation in ecological settings (Erdner & Anderson, 1999), indicating this adaptive response is widespread.

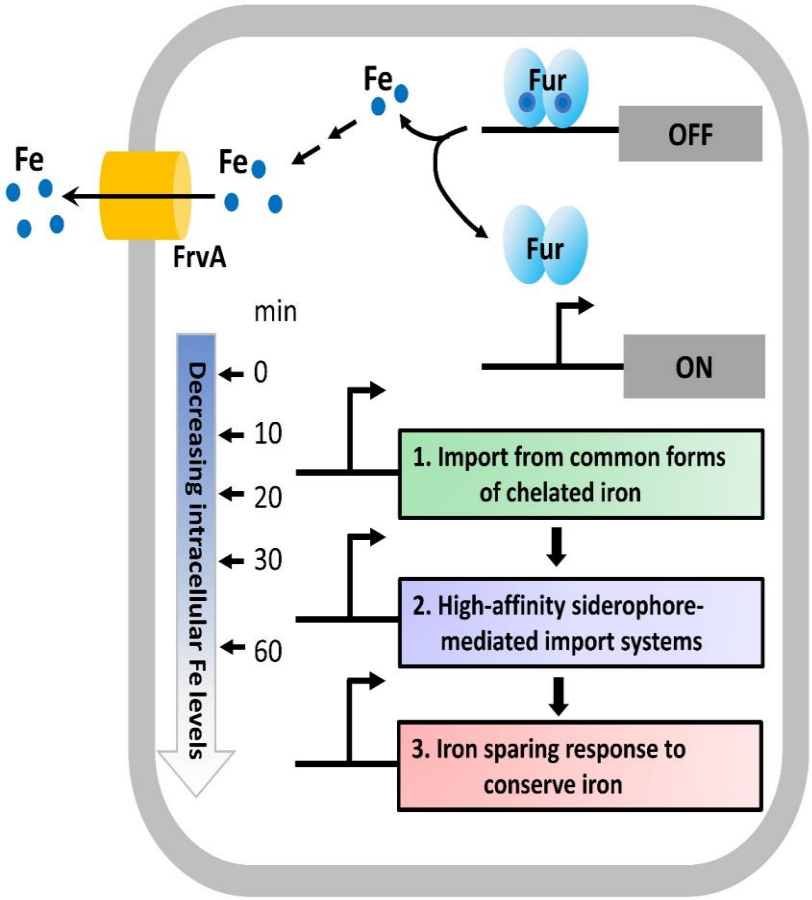

Fig. 4.17 Proposed sequential induction of Fur regulated genes.

We utilized the *L. monocytogenes* ferrous iron efflux transporter FrvA as an inducible genetic tool and monitored the expression changes of the Fur-regulated genes as a function of iron depletion. Three sequential waves are revealed: (i) cells increase their capacity for iron import from common forms of chelated iron in their environment. (ii) cells express high-affinity siderophore-mediated import systems to scavenge iron. (iii) as iron levels fall further cells activate the iron-sparing response to prioritize iron utilization and allow access of iron only to essential iron-requiring enzymes.

As iron bioavailability declines further, the iron sparing response is induced to remodel the proteome and conserve iron. The iron sparing response has been well studied in several microorganisms. In *E. coli*, it is mediated by a small RNA RyhB, which with the assistance of an RNA chaperone blocks the translation of nonessential iron-utilizing proteins (Masse *et al.*, 2007, Masse *et al.*, 2005). In *B. subtilis*, this response is mediated by a small RNA FsrA and its three coregulators FbpA, FbpB and FbpC. FsrA binds target mRNAs through RNA-mRNA base-pairing and blocks translation of its targets to reduce iron demand (Gaballa *et al.*, 2008, Smaldone *et al.*, 2012).

Collectively our results demonstrate that as cells transition from iron sufficiency to deficiency, *B. subtilis* expresses (i) iron uptake systems to prevent deficiency, (ii) alternative non-iron proteins to replace iron enzymes and reduce iron demand and high-affinity siderophore-mediated import systems to scavenge iron, and (iii) a small RNA FsrA and its partner proteins to prioritize iron utilization (Fig. 4.17). Nevertheless, the graded response of Fur regulon to iron limitation may extend further. A recent study using genome footprinting coupled with high-throughput sequencing (GeF-Seq) revealed that under anaerobic conditions *B. subtilis* Fur binds to many DNA sites *in vivo* in addition to the previously established Fur regulon (Chumsakul *et al.*, 2017). *E. coli* Fur has also been shown to play a regulatory role beyond iron metabolism, including DNA synthesis and biofilm formation (Seo *et al.*, 2014). Moreover, a graded response of Fur regulon to iron starvation may also be present in other bacteria. Indeed, a graded response was reported in *Crocosphaera watsonii*, a unicellular diazotrophic marine cyanobacterium (Jacq *et al.*, 2014), however the underlying mechanism was not characterized.

In natural settings, metal limitation may occur gradually as intracellular metal levels fall. As a result, it is unlikely that transcription regulators turn on their regulon all at once, but rather as a graded response. One remarkable example is the derepression of Zur regulon in response to zinc limitation in *Streptomyces coelicolor* (Shin *et al.*, 2011) and *B. subtilis* (Shin & Helmann, 2016). As cells transition from zinc sufficiency to deficiency, Zur regulated genes are also induced in a stepwise manner. In *B. subtilis* it

has been demonstrated that as an initial response to zinc deprivation alternative ribosomal proteins are derepressed to mobilize zinc from intracellular zinc pools. In the second wave, high-affinity uptake systems are induced to import zinc. Finally, as zinc levels decline further, late genes are induced to replace Zn-dependent proteins needed to ensure ribosome assembly and folate synthesis (Shin & Helmann, 2016). Together with the results reported here, this example illustrates how bacterial cells prioritize their responses to metal limitation.

4.6 Materials and methods

4.6.1 Bacterial strains and growth conditions

All strains used in the study are derivatives of *B. subtilis* strain CU1065 (WT) and are listed in Table S1. Cells were grown in LB medium or specified MOPS minimum medium with vigorous shaking or on solid LB agar with appropriate antibiotic selection at 37^0C. The concentrations of antibiotics used are: ampicillin (amp, 100 μg ml^{-1}), spectinomycin (spec, 100 μg ml^{-1}), tetracycline (tet, 5 μg ml^{-1}), chloramphenicol (cm, 10 μg ml^{-1}), kanamycin (kan, 15 μg ml^{-1}), neomycin (neo, 8 μg ml^{-1}), and macrolide lincosoamide-streptogramin B (MLS, 1 μg ml^{-1} erythromycin and 25 μg ml^{-1} lincomycin).

4.6.2 Quantification of intracellular metal ion by ICP-MS

Cells were grown in LB medium amended with 10 μM $FeSO_4$ to an OD_{600} of about 0.25 and 1 mM IPTG was added to induce expression of FrvA where indicated. Aliquots of 4 ml of cell culture were harvested and levels of intracellular metals (Fe, Mn, and Co) were monitored for three hours after IPTG treatment by inductively coupled plasma mass spectrometry (ICP-MS). All samples were washed once with buffer 1 (1X PBS buffer, 0.1 M EDTA) then twice with buffer 2 (1X chelex-treated PBS buffer). Cell pellets were resuspended in 400 μl of buffer 3 (1X chelex-treated PBS buffer, 75 mM NaN3, 1% Triton X-100) and incubated at 37^0C for 90 min to lyse the cells. Lysed samples were centrifuged and the total protein

content was quantified using a Bradford assay. Then, samples were mixed with 600 µl buffer 4 (5% HNO3, 0.1% (v/v) Triton X-100) and heated in a 95^{0}C sand bath for 30 min. The debris was removed by centrifugation and the total metal ions in the diluted samples were analyzed by Perkin-Elmer ELAN DRC II ICP-MS. Gallium was used as an internal standard. The total intracellular ion levels are expressed as µg ion per gram of protein content (mean ± SD; n=3). Mn, and Co levels were not significantly changed over the course of the experiment. Statistically significant differences between WT and induced P$_{spac}$-*frvA* cells are determined by two-tailed *t*-test as indicated: *, $P < 0.01$.

4.6.3 Growth curves

Cells were grown overnight in LB medium and subcultured with 1:100 ratio into fresh LB medium amended with 10 µl of $FeSO_4$ and grown to an OD_{600} of 0.25. For IPTG treated cells, 1mM IPTG was added to induce expression of FrvA. Cell Growth (OD_{600}) was monitored every 15 min for 25 h using a Bioscreen growth analyzer (Growth Curves USA, Piscataway, NJ) at 37^{0}C with continuous shaking. Data shown were representative growth curves and experiments were conducted at least three times with three biological replicates each time.

4.6.4 Microarray analysis

Cells (WT P$_{spac}$-*frvA*) were grown in LB medium amended with 10 µM $FeSO_4$ to an OD_{600} of ~0.25 and divided into two 1 L flasks. To induce expression of FrvA, 1 mM IPTG was added into one flask while the other was left untreated as a control. Aliquots of 40 ml of cell culture were harvested from both flasks at different time-points as indicated and total RNA was extracted using an acidic phenol-based method. All RNA samples were treated with Turbo-DNA free™ DNase (Ambion™) and precipitated in ethanol and sodium acetate at -80^{0}C overnight. RNA samples were washed with 70% ethanol and dissolved in RNase-free water then quantified by NanoDrop spectrophotometer. Twenty microgram of total RNA from each sample was used for cDNA synthesis using the SuperScript indirect cDNA labeling system (Thermo Fisher

Scientific). cDNA from each uninduced control sample or WT sample was labeled with Alexa Fluor® 647 while cDNA from each induced sample or *fur* mutant was labeled with Alexa Fluor® 555. After labeling, cDNA was quantified by NanoDrop spectrophotometer and aliquots of 250 pmol of cDNA were subject to hybridization onto microarray slides that consist of 4,109 gene-specific antisense oligonucleotides (65-mers; Sigma-Genosys). The transcriptome changes were monitored and compared between the IPTG-induced and uninduced cells at the same timepoints as indicated. Only the fluorescence signals well above the background level are considered. The heat maps were generated by using Cluster 3.0 and Java TreeView. The log10-transformed data was subject to hierarchical clustering using uncentered correlation and complete linkage functions. Genes that are upregulated are shown in red and genes that are downregulated are shown in green. The microarray results have been deposited in the NCBI GEO database under the accession number GSE100668.

4.6.5 RNA extraction and real-time qPCR

To monitor mRNA levels of Fur-regulated genes, cells were grown at 37^0C in LB medium overnight and subcultured with 1:100 ratio into fresh LB medium amended with either 10 or 25 μM iron as specified. After OD_{600} reaches ~0.25, 1mM IPTG was added to induce expression of FrvA as indicated. Aliquots of 5 ml of cells were harvested at different time points. To monitor mRNA levels of PerR-regulated genes (Fig. 4.4B), overnight culture was used to inoculate a fresh culture with 1:100 ratio in LB medium. 1mM IPTG was added to induce expression of FrvA in the beginning of inoculum to create severe iron starvation. Aliquots of 5 ml of cells were harvested at timepoints with different optical density (OD_{600}) as indicated for uninduced cells. Total RNA was extracted using RNeasy Mini Kit following the manufacturer's instructions (Qiagen Sciences, Germantown, MD). All RNA samples were treated with Turbo-DNA free™ DNase (Ambion™) and precipitated with 2-3 volume of ethanol and 0.1 volume of 3M sodium acetate at -80^0C overnight. RNA samples were washed with 70% ethanol and dissolved in nuclease-free water then quantified by NanoDrop spectrophotometer. Two hundred nanogram of total RNA from each sample was

subjected to cDNA synthesis using high-capacity cDNA reverse transcription kits (Applied Biosystems, Foster City, CA). Primers used in this study are listed in Table S2. Quantitative PCR (qPCR) was then conducted using iQ SYBR green supermix in an Applied Biosystems 7300 Real Time PCR System. The housekeeping gene 23S rRNA was used as an internal control.

4.6.6 Construction of chromosomal FLAG-tagged Fur

To construct a C-terminal FLAG-tagged Fur at its native locus, the recombinant plasmid pMUTIN::Fur-FLAG was cloned using Gibson assembly and transformed into *Escherichia coli* DH5α. The correct insertion was confirmed by colony PCR and DNA sequencing. The recombinant plasmid was then transformed into *E. coli* TG1. The resulting transformants were confirmed by colony PCR and the recombinant plasmid was extracted, further verified by DNA sequencing and transformed into *B. subtilis* WT (CU1065) and WT P_{spac}-*frvA*. Colony PCR was conducted to verify the presence of FLAG-tag in the C-terminus of Fur of *B. subtilis*.

4.6.7 Western blot analysis of FLAG-tagged Fur

Cells were grown in LB medium to an OD_{600} of ~0.4 and 10 ml of cell culture was harvested. Cell pellets were washed in PBS buffer, resuspended in a lysis buffer (10 mM Tris pH8.0, 100 mM NaCl, 1 mM EDTA, and 5% glycerol) and lysed by sonication. The total protein content was quantified using a Bradford assay and 20 µg of total protein from whole cell lysate of each sample was loaded to a mini-protein TGX stain-free gel. After electrophoresis, the gel was visualized by a ChemiDoc™ MP imaging system (BioRad, Hercules, CA) and transferred to a polyvinylidene difluoride membrane using a Trans-Blot® Turbo™ transfer system (BioRad, Hercules, CA) and then subjected to western blot using a monoclonal anti-FLAG antibody (Sigma-Aldrich, St. Louis, MO) according to the manufacture's protocol. The Fur-FLAG protein has a molecular mass of ∼19 kDa, in accordance with the signals observed in the blot.

4.6.8 Disk diffusion assay

Cells were grown overnight in LB medium and subcultured at 1% into fresh LB medium to an OD_{600} of 0.4. Cell culture (100 µl) was mixed with 4 ml of 0.75% LB agar and poured onto 1.5% LB agar plates. The plates were dried for 15 min in a laminar flow hood at room temperature. Filter paper disks (6.5 mm in diameter) soaked with 10 µl of 1 M $FeSO_4$ (prepared in 0.1 M HCl) or 5 µl of 5 mg ml^{-1} streptonigrin (SN) were placed on the top of the agar plates, and the plates were incubated at 37^0C for 16–18 h.

As shown in Fig. 4.8, a purple halo is evident around the inhibition zone in a *fur* null mutant due to derepression of the siderophore bacillibactin biosynthesis (DhbACEBF) (Baichoo *et al.*, 2002); while the FLAG-tagged Fur in both genetic background (WT and P_{spac}-*frvA*) behaves very similarly as WT without FLAG-tagged Fur, indicating the chromosomal FLAG-tagged Fur is a functional regulator. For experiments done in Fig. 4.51A, overexpression of *L*. *monocytogenes* FrvA induces derepression of Fur regulon in *B. subtilis*, including *dhbACEBF* operon as reported previously (Pi *et al.*, 2016). So effects of Btr on BB uptake can be evaluated by comparing the intensity of the purple complex, DHB(G)-Fe^{3+} or BB-Fe^{3+}. For experiments done in Fig. 4.16, the data are expressed as the diameter (mean ± SD; n=3) of the inhibition zone (mm). Statistically significant differences are determined by two-tailed *t*-test, *, $P < 0.05$.

4.6.9 Quantification of bacillibactin/DHB(G) accumulation in medium

To quantify accumulation of DHB(G) and BB Cells on the plates shown in Fig. 4.15A, cells were grown overnight in LB medium, subcultured with 1:100 ratio into fresh LB. Cell culture (100µl of OD_{600} ~ 0.4) was inoculated into MOPS minimum medium, which is amended with 5 µl of $MnCl_2$ and 1 mM $FeSO_4$. For IPTG-treated cells, 1mM IPTG was added to induce expression of FrvA. Accumulation of DHB(G) and BB was quantified using 1 ml of cell-free supernatant after addition of 50 µl of 10 mM $FeCl_3$ (prepared in 100 mM HCl) and neutralization by 100 µl of 1 M Tris-HCl buffer (pH 8.0). The resulting purple DHB(G)-Fe^{3+} or BB-

Fe^{3+} complex was measured spectrophotometrically. An optical density at 510 nm (OD_{510}) of 0.5 is equivalent to 80 µg of DHB(G) or BB per ml (Ollinger *et al.*, 2006).

4.6.10 Chromatin immunoprecipitation coupled with quantitative PCR (ChIP-qPCR)

To monitor the occupancy of Fur at its target sites in vivo, we performed Chromatin immunoprecipitation coupled with quantitative PCR. Cells were grown in LB medium amended with 25 µM $FeSO_4$ to OD_{600} of ~0.25 and 1 mM IPTG was added to cell culture to induce expression of FrvA as indicated. At different time points, 40 ml aliquots were harvested and the pellets were kept at −80 °C. The pellets were washed and resuspended with buffer CA (10 mM Na2HPO4, 2 mM KH2PO4, pH 7.4, 137 mM NaCl, and 2.7 mM KCl). The samples were incubated with 1% formaldehyde at room temperature for 10 min for crosslinking and then incubated with 133 mM glycine (pH7.5) at 4 °C for 30 min to quench the crosslinking. Cells were spun down, washed twice with buffer CB (50 mM Tris–HCl pH7.4, 150 mM NaCl and 1 mM EDTA), and then resuspended in 0.5 ml buffer CB followed by sonication for cell lysis and DNA fragmentation. Supernatant was collected after centrifugation and the total protein concentration was quantified using a Bradford assay. Aliquots of 400 µg of total protein were kept at −80 °C. Aliquots of 1% volume of the lysate were diluted with CB buffer and kept at −80 °C to serve as the input-control (1% of input DNA). For immunoprecipitation, α-FLAG M2 magnetic agarose beads (Sigma, Cat# M8823) were washed and resuspended in 400 µl buffer CB. Aliquots of 400 µg of total protein were diluted, mixed with the washed magnetic beads, and incubated on a rotation mixer overnight in a cold room (4^0C). The bead slurry was recovered by using a magnetic stand and washed twice with 500 µl of buffer CB. The protein–DNA complexes were eluted with 3X FLAG peptide according to the manufacture's protocol. All samples including 1% input DNA samples were treated at 65^0C for overnight to reverse crosslinking. Co-immunoprecipitated DNA was purified using a PCR purification Kit (Omega Biotek, Norcross, GA), quantified by NanoDrop spectrophotometer, and diluted appropriately followed by quantification using qPCR. Specific primer sets to the promoter regions of the target genes are listed in Table S2. DNA

enrichment was calculated based on the input DNA (1% of total DNA used for each ChIP experiment). The housekeeping gene *gyrA* was used as a non-specific negative control.

4.6.11 Electrophoretic mobility shift assays (EMSA)

The promoter region (~160bp) of each individual Fur-regulated gene tested was amplified by PCR using a specific primer set listed in Table S2. Two hundred nanogram of purified DNA was labelled at 5'-ends with [γ-^{32}P]-ATP using T4 polynucleotide kinase. After labelling, G10 column (NucAway^{TM} spin columns, Invitrogen) was used to remove the unincorporated (γ-^{32}P) ATP and radioactivity of each probe was quantified by a scintillation counter. The binding reactions were conducted as following: ~ 1 fmol of labelled DNA probe, 1 mM $MnCl_2$, varied concentration of Fur protein, and 1X binding buffer (10 mM Tris-HCl, pH 8.0, 5% glycerol, 2 μg ml^{-1} salmon testes DNA, 50 mM NaCl, 1 mM DTT, 50 μg ml^{-1} BSA). The reactions were incubated at room temperature for 20 min and then subject to electrophoresis in a 5% polyacrylamide gel using 40 mM TA buffer (pH 8.0, no EDTA). After electrophoresis, the gels were dried using a gel dryer, exposed to a phosphorimager screen overnight, and scanned by a phosphor image analyzer (Typhoon FLA 7000). The band intensity of unbound DNA was quantified using GelQuantNET software. The K_d values, corresponding to the concentration of Fur that leads to 50% half-maximal shifting of the DNA probe, were calculated using GraphPad Prism 5.

Table 4.2 Strains and plasmids used in this study

Strain	Genotype	Reference
WT (CU1065)	*trpC2 attSPβ sfp^0*	Lab stock
HB19208	*amyE :: P$_{spac}$- frvA* :: *cm*	(Pi *et al.*, 2016)
HB17837	*fur* :: *kan*	(Baichoo *et al.*, 2002)
HB2168	*fur* :: *kan perR* :: *spc*	(Fuangthong *et al.*, 2002)
HB19396	pMUTIN *:: fur-FLAG :: spec*	This study
HB19398	*amyE ::* P$_{spac}$*-frvA*::*cm* pMUTIN *:: fur-FLAG :: spec*	This study
HB8246	*btr* :: *spc*	(Gaballa & Helmann, 2007)
HB19401	*btr* :: *spc amyE :: P$_{spac}$- frvA* :: *cm*	This study
HB8248	*btr* :: *spc fur* :: *kan*	(Gaballa & Helmann, 2007)
HB5800	*sfp$^+$*	(Ollinger *et al.*, 2006)
HB19405	*sfp$^+$ amyE :: P$_{spac}$- frvA* :: *cm*	This study
HB8247	*sfp$^+$ fur* :: *kan*	(Gaballa & Helmann, 2007)
HB8242	*sfp$^+$ btr* :: *spc*	(Gaballa & Helmann, 2007)
HB19409	*sfp$^+$ btr* :: *spc amyE :: P$_{spac}$- frvA* :: *cm*	This study
HB8249	*sfp$^+$ btr* :: *spc fur* :: *kan*	(Gaballa & Helmann, 2007)
HB7384	*fsrA* :: *mls*	Lab stock
HB19411	*fsrA* :: *mls amyE :: P$_{spac}$- frvA* :: *cm*	This study
HB19403	*dhbA :: mls amyE :: P$_{spac}$- frvA* :: *cm*	This study
Plasmid	**Description**	**Reference**
pPL82	Expression of gene under P$_{spac}$ promoter	Lab stock
pMUTIN	FLAG-tagged Fur in native locus	Lab stock

Table 4.3 Primer oligonucleotides

Number	Name	Sequence
Primers used for cloning		
5782	pPL82-check-for	AAGAAAGATATCCTAACAGCACA
5783	pPL82-check-rev	ACGATCTTTCAGCCGACTCA
8095	Fur-Flag-fwd	AGCGGATAACAATTAAGCTTCTCCTGAGATCGGTCTCGCTAC
8096	Fur-Flag-rev	CGATCGATAGCGCTGGTACCTTCAGTTTCTTTTCCGTTACAGC
6541	ybbb-UP-F	ATTGGCTTCACTGTTCAACAA
1452	Spec-check-rev	CGTATGTATTCAAATATATCCTCCTCCTCAC
1451	mls-check-rev	GTTTTGGTCGTAGAGCACACGG
8083	dhbA_CHIP_Fwd	TGACGGACCGCATCTATCAATGG
6439	FrvA-seq1	GTGTTCCAATCGATGGATTGA
6440	FrvA-seq2	CTTGAAGGGCTTTGATCGTAC
Primers used for real-time qPCR		
4368	23S-RT-F	AAAGGCACAAGGGAGCTTGACTGC
4369	23S-RT-R	ATGAGCCGACATCGAGGTGCCAAA
6943	FsrA-RT-F	ATAGAGAGAAGCTACTCTCTGTTC
8053	FsrA-RT-RV2	TTCGGATCTTGATCTGATAGAGG
6524	DhbA-RT-F	ACGCTTGCCAGTCAAGGCGCACAT
6525	DhbA-RT-R	AAAGCTTCTGCATGGCGGGCTTCTGCTTT
8058	YclN-RT-F	TATCGGTGTAGAAGATCTGTCGCC
8059	YclN-RT-R	TGCTGATCTGCTGCATAATCAAACC
6553	FeuA-RT-F	AAGGCAAGCGGCACAGCATCTGAGAAGAA
6554	FeuA-RT-R	AAATTGCGCCTTGCGGATGAACGTCAAGCA
8060	YfmC-RT-F	GATTCCAGAGTGATCCATGACGAA
8061	YfmC-RT-R	GCGTGTGCCTACAGATGTGTAATCA
8062	FhuB-RT-F	GAGCAAGGAATGATCCACCGATA
8063	FhuB-RT-R	GTGTTAAGTCTCGGTGACGATCTG
8064	YkuN-RT-F	CCTTGATTACATATGCCAGCATGT
8065	YkuN-RT-R	TAGGTGCCAATCAGTACATAATCAT
8066	YwbL-RT-F	GATATGGATTCGGCACAACAAACGT
8067	YwbL-RT-R	ATGAGACGCAAGCTCTTCAAGCTG
8070	FbpA-RT-F	GCTGATCCAGGAAAACAAAGAGG
8071	FbpA-RT-R	TTGATGCTTGCGGTCGATCC
8072	FbpC-RT-F	GGTGAAGCAAATGACAATGCTGT
8074	FbpC-RT-R	CATCAAACAGATTTATTAGAGATTCC
8075	AhpC-RT-F	CAATGGAGCGTATTCTGCTTCTAC
8076	AhpC-RT-R	TCAGAGCTGTCATGCCAGCCTT
8077	KatA-RT-F	GCTTGAGTGTAGTGATCGTAGTGA
8078	KatA-RT-R	TTATCAGCGTGATGGGCAAATG
8079	PfeT-RT-F	CGAAGGAAGGAATCGAAGAAACA
8080	PfeT-RT-R	TCTCTGCTGCTTTTATTCATCGTGT
8081	MrgA-RT-F	ATACTCTAAGCTCCACCGTTTCC
8082	MrgA-RT-R	TGATAGATGCATGCTCAGTGTATTC
6697	hemA_RT_FW	TTATGCGGTAGTCGACCAGCTT
6698	hemA_RT_RV	ATCACCATAGAATCAAGTCCGCA

Primers used for synthesis of EMSA probes		
8038	FeuA_fwd	CTATCCGGAGATTGTCCATGAT
8039	FeuA_Rev	GCCGTCAGCGCGAGAAGTAAGA
8040	dhbA_fwd	GTCACTGAAATTATATTTGACTG
8041	dhbA_rev	ATCATCAATTCCTTTCTTCGCTC
8042	YkuN_fwd	TGCTGGATCAGGAAAATCCAT
8043	YkuN_rev	TGCTGGCATATGTAATCAAGGC
8044	fhuB_fwd	GGTTGACACGATATTTTTGCAA
8045	fhuB_rv	GATTTCTTCTGATGCAGTCCGT
8046	ywbL_fwd	GACAGCTTTTTTGCTGTCCATCA
8047	ywbL_rv	CCATCAACAAGCTGAATAGAATA
8048	yfmC_fwd	GAGAAAGCAGTAAAAACGCAGCT
8049	yfmC_rv	AACACTCATGATGGCAATCAAC
8050	YclN_EMSA_fw	TGATAAATGACTAGGTTAATATT
8051	YclN_EMSA_rv	CTGCCTCCTTACATCCTTACA
8052	FsrA_EMSA_fwd	GAGCAGGACGGACTGATTTAA
8053	FsrA_EMSA_RV	TTCGGATCTTGATCTGATAGAGG
8054	FbpAB_EMSA_fwd	GGGAAACTTTTTGTCGATTTGTTG
8055	FbpAB_EMSA_rv	TCTGATTTCTGCAGACTGAGGTG
8056	FbpC_EMSA_fwd	GTGTTGTTAAGCGTCAGAATTCG
8057	FbpC_EMSA_rv	ACAGCATTGTCATTTGCTTCACC
Primers used for ChIP-qPCR		
8083	dhbA_CHIP_Fwd	TGACGGACCGCATCTATCAATGG
8084	dhbA_CHIP_rv	AGCTTCGCCTATTCCTTGGGC
8090	YclN_CHIP_fwd	GTAAACAGCCTAACGTTTTGGGATG
8091	YclN_CHIP_rv	CTGCCTCCTTACATCCTTACAGC
8093	YwbL_CHIP_fwd	GACAAAGGACAGGAACTGGCTATG
8094	YwbL_CHIP_rv	CGAGCCATCATGTTCCTCCTATAA
8092	FsrA_CHIP_fwd	CGATTGACATTGATACTGAGAATCA
8089	FsrA_CHIP_rv	GAACAGAGAGTAGCTTCTCTCTAT
8044	fhuB_fwd	GGTTGACACGATATTTTTGCAA
8045	fhuB_rv	GATTTCTTCTGATGCAGTCCGT
8054	FbpAB_EMSA_fwd	GGGAAACTTTTTGTCGATTTGTTG
8055	FbpAB_EMSA_rv	TCTGATTTCTGCAGACTGAGGTG
8056	FbpC_EMSA_fwd	GTGTTGTTAAGCGTCAGAATTCG
8057	FbpC_EMSA_rv	ACAGCATTGTCATTTGCTTCACC
8038	FeuA_fwd	CTATCCGGAGATTGTCCATGAT
8039	FeuA_Rev	GCCGTCAGCGCGAGAAGTAAGA
8042	YkuN_fwd	TGCTGGATCAGGAAAATCCAT
8043	YkuN_rev	TGCTGGCATATGTAATCAAGGC
8048	yfmC_fwd	GAGAAAGCAGTAAAAACGCAGCT
8049	yfmC_rv	AACACTCATGATGGCAATCAAC

4.7 References

Abergel, R.J., M.K. Wilson, J.E. Arceneaux, T.M. Hoette, R.K. Strong, B.R. Byers & K.N. Raymond, (2006) Anthrax pathogen evades the mammalian immune system through stealth siderophore production. *Proceedings of the National Academy of Sciences of the United States of America* **103**: 18499-18503.

Abergel, R.J., A.M. Zawadzka & K.N. Raymond, (2008) Petrobactin-mediated iron transport in pathogenic bacteria: coordination chemistry of an unusual 3,4-catecholate/citrate siderophore. *Journal of the American Chemical Society* **130**: 2124-2125.

Baichoo, N., T. Wang, R. Ye & J.D. Helmann, (2002) Global analysis of the Bacillus subtilis Fur regulon and the iron starvation stimulon. *Molecular microbiology* **45**: 1613-1629.

Barbeau, K., G. Zhang, D.H. Live & A. Butler, (2002) Petrobactin, a photoreactive siderophore produced by the oil-degrading marine bacterium Marinobacter hydrocarbonoclasticus. *Journal of the American Chemical Society* **124**: 378-379.

Cendrowski, S., W. MacArthur & P. Hanna, (2004) Bacillus anthracis requires siderophore biosynthesis for growth in macrophages and mouse virulence. *Molecular microbiology* **51**: 407-417.

Chazarreta-Cifre, L., L. Martiarena, D. de Mendoza & S.G. Altabe, (2011) Role of ferredoxin and flavodoxins in Bacillus subtilis fatty acid desaturation. *Journal of bacteriology* **193**: 4043-4048.

Chen, L. & J.D. Helmann, (1995) Bacillus subtilis MrgA is a Dps(PexB) homologue: evidence for metalloregulation of an oxidative-stress gene. *Molecular microbiology* **18**: 295-300.

Chipperfield, J.R. & C. Ratledge, (2000) Salicylic acid is not a bacterial siderophore: a theoretical study. *Biometals : an international journal on the role of metal ions in biology, biochemistry, and medicine* **13**: 165-168.

Chumsakul, O., D.P. Anantsri, T. Quirke, T. Oshima, K. Nakamura, S. Ishikawa & M.M. Nakano, (2017) Genome-Wide Analysis of ResD, NsrR, and Fur Binding in Bacillus subtilis during Anaerobic Fermentative Growth by In Vivo Footprinting. *Journal of bacteriology* **199**.

Delany, I., R. Rappuoli & V. Scarlato, (2004) Fur functions as an activator and as a repressor of putative virulence genes in Neisseria meningitidis. *Molecular microbiology* **52**: 1081-1090.

Dertz, E.A., J. Xu, A. Stintzi & K.N. Raymond, (2006) Bacillibactin-mediated iron transport in Bacillus subtilis. *Journal of the American Chemical Society* **128**: 22-23.

Erdner, D.L. & D.M. Anderson, (1999) Ferredoxin and flavodoxin as biochemical indicators of iron limitation during open‐ocean iron enrichment. *Limnology and oceanography* **44**: 1609-1615.

Faulkner, M.J. & J.D. Helmann, (2011) Peroxide stress elicits adaptive changes in bacterial metal ion homeostasis. *Antioxidants & redox signaling* **15**: 175-189.

Faulkner, M.J., Z. Ma, M. Fuangthong & J.D. Helmann, (2012) Derepression of the Bacillus subtilis PerR peroxide stress response leads to iron deficiency. *Journal of bacteriology* **194**: 1226-1235.

Fleischhacker, A.S. & P.J. Kiley, (2011) Iron-containing transcription factors and their roles as sensors. *Current opinion in chemical biology* **15**: 335-341.

Frawley, E.R., M.L. Crouch, L.K. Bingham-Ramos, H.F. Robbins, W. Wang, G.D. Wright & F.C. Fang, (2013) Iron and citrate export by a major facilitator superfamily pump regulates metabolism and stress resistance in Salmonella Typhimurium. *Proceedings of the National Academy of Sciences of the United States of America* **110**: 12054-12059.

Fuangthong, M., A.F. Herbig, N. Bsat & J.D. Helmann, (2002) Regulation of the Bacillus subtilis fur and perR genes by PerR: not all members of the PerR regulon are peroxide inducible. *Journal of bacteriology* **184**: 3276-3286.

Gaballa, A., H. Antelmann, C. Aguilar, S.K. Khakh, K.B. Song, G.T. Smaldone & J.D. Helmann, (2008) The Bacillus subtilis iron-sparing response is mediated by a Fur-regulated small RNA and three small,

basic proteins. *Proceedings of the National Academy of Sciences of the United States of America* **105**: 11927-11932.

Gaballa, A. & J.D. Helmann, (2007) Substrate induction of siderophore transport in Bacillus subtilis mediated by a novel one-component regulator. *Molecular microbiology* **66**: 164-173.

Gerstle, K., K. Klatschke, U. Hahn & N. Piganeau, (2012) The small RNA RybA regulates key-genes in the biosynthesis of aromatic amino acids under peroxide stress in E. coli. *RNA biology* **9**: 458-468.

Guan, G., A. Pinochet-Barros, A. Gaballa, S.J. Patel, J.M. Arguello & J.D. Helmann, (2015) PfeT, a P1B4 -type ATPase, effluxes ferrous iron and protects Bacillus subtilis against iron intoxication. *Molecular microbiology* **98**: 787-803.

Helmann, J.D., (2014) Specificity of metal sensing: iron and manganese homeostasis in Bacillus subtilis. *The Journal of biological chemistry* **289**: 28112-28120.

Henares, B., S. Kommineni, O. Chumsakul, N. Ogasawara, S. Ishikawa & M.M. Nakano, (2014) The ResD response regulator, through functional interaction with NsrR and fur, plays three distinct roles in Bacillus subtilis transcriptional control. *Journal of bacteriology* **196**: 493-503.

Herbig, A.F. & J.D. Helmann, (2001) Roles of metal ions and hydrogen peroxide in modulating the interaction of the Bacillus subtilis PerR peroxide regulon repressor with operator DNA. *Molecular microbiology* **41**: 849-859.

Imlay, J.A., (2003) Pathways of oxidative damage. *Annual review of microbiology* **57**: 395-418.

Jacq, V., C. Ridame, S. L'Helguen, F. Kaczmar & A. Saliot, (2014) Response of the unicellular diazotrophic cyanobacterium Crocosphaera watsonii to iron limitation. *PloS one* **9**: e86749.

Jacques, J.F., S. Jang, K. Prevost, G. Desnoyers, M. Desmarais, J. Imlay & E. Masse, (2006) RyhB small RNA modulates the free intracellular iron pool and is essential for normal growth during iron limitation in Escherichia coli. *Molecular microbiology* **62**: 1181-1190.

Koppisch, A.T., C.C. Browder, A.L. Moe, J.T. Shelley, B.A. Kinkel, L.E. Hersman, S. Iyer & C.E. Ruggiero, (2005) Petrobactin is the primary siderophore synthesized by Bacillus anthracis str. Sterne under conditions of iron starvation. *Biometals : an international journal on the role of metal ions in biology, biochemistry, and medicine* **18**: 577-585.

Koppisch, A.T., S. Dhungana, K.K. Hill, H. Boukhalfa, H.S. Heine, L.A. Colip, R.B. Romero, Y. Shou, L.O. Ticknor, B.L. Marrone, L.E. Hersman, S. Iyer & C.E. Ruggiero, (2008) Petrobactin is produced by both pathogenic and non-pathogenic isolates of the Bacillus cereus group of bacteria. *Biometals : an international journal on the role of metal ions in biology, biochemistry, and medicine* **21**: 581-589.

Lawson, R.J., C. von Wachenfeldt, I. Haq, J. Perkins & A.W. Munro, (2004) Expression and characterization of the two flavodoxin proteins of Bacillus subtilis, YkuN and YkuP: biophysical properties and interactions with cytochrome P450 BioI. *Biochemistry* **43**: 12390-12409.

Lee, J.W. & J.D. Helmann, (2006) The PerR transcription factor senses H2O2 by metal-catalysed histidine oxidation. *Nature* **440**: 363-367.

Masse, E., H. Salvail, G. Desnoyers & M. Arguin, (2007) Small RNAs controlling iron metabolism. *Current opinion in microbiology* **10**: 140-145.

Masse, E., C.K. Vanderpool & S. Gottesman, (2005) Effect of RyhB small RNA on global iron use in Escherichia coli. *Journal of bacteriology* **187**: 6962-6971.

May, J.J., T.M. Wendrich & M.A. Marahiel, (2001) The dhb operon of Bacillus subtilis encodes the biosynthetic template for the catecholic siderophore 2,3-dihydroxybenzoate-glycine-threonine trimeric ester bacillibactin. *The Journal of biological chemistry* **276**: 7209-7217.

Merchant, S.S. & J.D. Helmann, (2012) Elemental economy: microbial strategies for optimizing growth in the face of nutrient limitation. *Advances in microbial physiology* **60**: 91-210.

Miethke, M., O. Klotz, U. Linne, J.J. May, C.L. Beckering & M.A. Marahiel, (2006) Ferri-bacillibactin uptake and hydrolysis in Bacillus subtilis. *Molecular microbiology* **61**: 1413-1427.

Miethke, M., C.G. Monteferrante, M.A. Marahiel & J.M. van Dijl, (2013) The Bacillus subtilis EfeUOB transporter is essential for high-affinity acquisition of ferrous and ferric iron. *Biochimica et biophysica acta* **1833**: 2267-2278.

Miethke, M., S. Schmidt & M.A. Marahiel, (2008) The major facilitator superfamily-type transporter YmfE and the multidrug-efflux activator Mta mediate bacillibactin secretion in Bacillus subtilis. *Journal of bacteriology* **190**: 5143-5152.

Mueller, J.P. & H.W. Taber, (1989) Structure and expression of the cytochrome aa3 regulatory gene ctaA of Bacillus subtilis. *Journal of bacteriology* **171**: 4979-4986.

Ollinger, J., K.B. Song, H. Antelmann, M. Hecker & J.D. Helmann, (2006) Role of the Fur regulon in iron transport in Bacillus subtilis. *Journal of bacteriology* **188**: 3664-3673.

Park, S., X. You & J.A. Imlay, (2005) Substantial DNA damage from submicromolar intracellular hydrogen peroxide detected in Hpx- mutants of Escherichia coli. *Proceedings of the National Academy of Sciences of the United States of America* **102**: 9317-9322.

Pi, H. & J.D. Helmann, (2017) Ferrous iron efflux systems in bacteria. *Metallomics : integrated biometal science*.

Pi, H., S.J. Patel, J.M. Arguello & J.D. Helmann, (2016) The Listeria monocytogenes Fur-regulated virulence protein FrvA is an Fe(II) efflux P1B4 -type ATPase. *Molecular microbiology* **100**: 1066-1079.

Quadri, L.E., P.H. Weinreb, M. Lei, M.M. Nakano, P. Zuber & C.T. Walsh, (1998) Characterization of Sfp, a Bacillus subtilis phosphopantetheinyl transferase for peptidyl carrier protein domains in peptide synthetases. *Biochemistry* **37**: 1585-1595.

Seo, S.W., D. Kim, H. Latif, E.J. O'Brien, R. Szubin & B.O. Palsson, (2014) Deciphering Fur transcriptional regulatory network highlights its complex role beyond iron metabolism in Escherichia coli. *Nature communications* **5**: 4910.

Shin, J.H. & J.D. Helmann, (2016) Molecular logic of the Zur-regulated zinc deprivation response in Bacillus subtilis. *Nature communications* **7**: 12612.

Shin, J.H., H.J. Jung, Y.J. An, Y.B. Cho, S.S. Cha & J.H. Roe, (2011) Graded expression of zinc-responsive genes through two regulatory zinc-binding sites in Zur. *Proceedings of the National Academy of Sciences of the United States of America* **108**: 5045-5050.

Smaldone, G.T., O. Revelles, A. Gaballa, U. Sauer, H. Antelmann & J.D. Helmann, (2012) A global investigation of the Bacillus subtilis iron-sparing response identifies major changes in metabolism. *Journal of bacteriology* **194**: 2594-2605.

Wilson, M.K., R.J. Abergel, K.N. Raymond, J.E. Arceneaux & B.R. Byers, (2006) Siderophores of Bacillus anthracis, Bacillus cereus, and Bacillus thuringiensis. *Biochemical and biophysical research communications* **348**: 320-325.

Yeowell, H.N. & J.R. White, (1982) Iron requirement in the bactericidal mechanism of streptonigrin. *Antimicrobial agents and chemotherapy* **22**: 961-968.

Yu, C. & C.A. Genco, (2012) Fur-mediated activation of gene transcription in the human pathogen Neisseria gonorrhoeae. *Journal of bacteriology* **194**: 1730-1742.

Zawadzka, A.M., Y. Kim, N. Maltseva, R. Nichiporuk, Y. Fan, A. Joachimiak & K.N. Raymond, (2009) Characterization of a Bacillus subtilis transporter for petrobactin, an anthrax stealth siderophore. *Proceedings of the National Academy of Sciences of the United States of America* **106**: 21854-21859.

Zeigler, D.R., Z. Pragai, S. Rodriguez, B. Chevreux, A. Muffler, T. Albert, R. Bai, M. Wyss & J.B. Perkins, (2008) The origins of 168, W23, and other Bacillus subtilis legacy strains. *Journal of bacteriology* **190**: 6983-6995.

Zuber, P., (2009) Management of oxidative stress in Bacillus. *Annual review of microbiology* **63**: 575-597.

Appendix 1 Magnesium-dependent processes are targets of cobalt and manganese toxicity in *Bacillus subtilis*

A1.1 Introduction

About 30% of all proteins require metals as cofactors. The number of metalloproteins that require different metals (e.g. iron, manganese, cobalt, zinc, and magnesium) may differ among bacteria, however, correct metal incorporation into each protein is fundamental to cell growth and survival. Some metals are more competitive than others in protein binding. The relative affinity of divalent metals for protein binding is known as the Irving-Williams Series: Mg=Ca <Mn<Fe<Co<Ni<Cu>Zn (Irving & Williams, 1948). When confronted with a mixed pool of metals, it is very challenging for proteins to single out the correct one. Thus, bacteria have evolved sophisticated mechanisms to ensure proper metal incorporation to maintain the functionality of these metalloproteins, including metal compartmentalization, metal selectivity, metal chaperones, and metal-responsive regulatory control as reviewed in great detail previously (Waldron & Robinson, 2009).

Cobalt is an essential transition metal. It is required as an integral group for cobalamin (vitamin B_{12}) and as a cofactor for eight enzymes (Kobayashi & Shimizu, 1999). Many bacteria (e.g. *E. coli*) require sub-micromolar cobalt for growth and encode specific uptake, efflux, and transcription regulatory systems to maintain cobalt homeostasis (Okamoto & Eltis, 2011). However, *Bacillus subtilis* appears to not require cobalt for growth and the homeostasis systems have not been well characterized. There is no dedicated Co(II) importer reported yet, but two exporters can protect cells against elevated levels of this metal. CadA, a CPx-type ATPase, is the major determinant for Cd(II) resistance and also confers resistance to Zn(II) and

Co(II) (Gaballa & Helmann, 2003). CzcD, a cation diffusion facilitator, confers resistance to Zn(II), Cu, Co(II), and Ni(II) (Moore *et al.*, 2005). Both exporters are under regulation of CzrA, a metal-sensing ArsR/SmtB family repressor. Consistent with the broad selectivity of its regulated transporters, CzrA responds to multiple metals including Zn(II), Cd(II), Co(II), Ni(II) and Cu (Moore *et al.*, 2005).

Cobalt is toxic to cells at elevated levels. Cobalt is redox active and can exist in multiple oxidation states including the two naturally occurring forms Co^{2+} and Co^{3+}. Cobalt intoxication has been well studied in a few bacterial species (e.g. *E. coli* and *Salmonella enterica*) and can take place in various ways: (i) production of reactive oxygen species (Valko *et al.*, 2005), (ii) sulfur assimilation (Thorgersen & Downs, 2007), (iii) reduction of free thiol pool (Thorgersen & Downs, 2007), (iv) competition with iron during Fe-S cluster biogenesis (Ranquet *et al.*, 2007) and metalloporphyrin formation (Majtan *et al.*, 2011). The competition between iron and cobalt is particularly appreciated in *E. coli*. These two metals possess very similar properties such as radii and oxidation states (2+ and 3+), which make mismetallation of iron-requiring proteins possible. Furthermore, cobalt is more competitive than iron in protein binding, and the resulting cobalt complexes would be more stable than iron complexes. In fact, the ligand exchange rate of Co^{3+} is 8 orders of magnitude slower than that of Fe^{3+} (Okamoto & Eltis, 2011), indicating that the mis-incorporation process would be permanent and beyond repair. Indeed, in cobalt-treated *E. coli* cells, many Fe-S enzymes such as aconitase and ferrichrome reductase are inactivated, resulting in drastic growth inhibition (Ranquet *et al.*, 2007). However, cobalt intoxication targets are unknown in *B*. *subtilis*.

Manganese is another essential transition metal. It is required as a cofactor for enzymes that are involved in oxidative stress and DNA replication (Aguirre & Culotta, 2012, Torrents, 2014). The Mn(II) biosensor, MntR, is the key regulator of Mn(II) homeostasis in many bacteria (Baumgart & Frunzke, 2015, Chandrangsu *et al.*, 2017, Huang *et al.*, 2017, Pandey *et al.*, 2015, Waters *et al.*, 2011). It is a member of the diphtheria toxin repressor (DtxR) family. MntR in *B. subtilis* illustrates its dual roles: it functions as a

repressor for two Mn(II) import systems and as an activator for two Mn(II) export systems (Huang *et al.*, 2017).

Like other transition metals, manganese is detrimental to cells when present in excess (Veyrier *et al.*, 2011, Huang *et al.*, 2017). Manganese is redox active and can exist in many oxidation states ranging from −3 to +7 with +2, +3, +4, +6, and +7 being the most common ones. It is relatively uncompetitive compared to iron or cobalt but much more competitive than Mg(II) in protein binding. In *Bradyrhizobium japonicum*, Mn(II) affects Mg(II) dependent processes, probably due to metal competition between these two metals resulting in mis-metalation of Mg(II) requiring enzymes (Hohle & O'Brian, 2014, Barwinska-Sendra & Waldron, 2017). However, its toxicity is largely unknown in other bacteria including *B. subtilis*.

To study competition between these two metal pairs (Fe(II) vs Co(II) and Fe(II) vs Mn(II)) and to identify the toxicity targets of Co(II) and Mn(II) in *B. subtilis*, we utilized FrvA as an inducible genetic tool to deplete intracellular iron pools. FrvA is a high-affinity Fe(II) efflux transporter in *Listeria monocytogenes* and its expression leads to severe iron deprivation in *B. subtilis* (Pi et al., 2016). We found Co(II) very likely outcompetes Fe(II) for binding to Fe-dependent enzymes. More importantly, both Co(II) and Mn(II) affect Mg(II) homeostasis probably due to mis-metalation of some Mg(II) dependent enzymes.

A1.2 Results and discussion

A1.2.1 Effects of FrvA expression on sensitivity to other metals

We tested the effects of iron limitation, imposed by the induction of *L. monocytogenes* high-affinity Fe(II) efflux transporter FrvA, on sensitivity to other metals such as Co(II), Mn(II), and Zn(II) in WT and relevant efflux-deficient mutants. As reported previously, a low-level induction (with 25 µM IPTG) of FrvA confers resistance to Co(II) in a cobalt efflux-defective mutant (*czcD* null) of *B. subtilis* (Pi *et al.*, 2016). Here we observed that different levels of FrvA expression (modulated by various concentration of IPTG) led to different levels of Co(II) sensitivity in both wild type and *czcD* null mutant. The higher the induction

of FrvA, the higher the sensitivity to Co(II). We hypothesized that this increased sensitivity may be due to, at least in part, iron deprivation caused by the high affinity iron exporter FrvA. To test this idea, 100 μM iron was supplemented into the medium. Indeed, the sensitivity to Co(II) intoxication is diminished significantly but not completely. These results suggest that excess Co(II) may result in mismetallation of iron-requiring enzymes under iron deficient conditions, which in turn causes hypersensitivity to Co(II) intoxication (Fig. A1.1).

In parallel, we tested the effects of FrvA expression on Mn(II) intoxication using a *mntR* null mutant, which is very sensitive to Mn(II) (Huang *et al.*, 2017). Induction of FrvA sensitizes cells to Mn(II) intoxication in this mutant. Higher levels of FrvA expression (controlled by varied concentrations of IPTG) leads to higher sensitivity to Mn(II). This phenomenon was only evident in the *mntR* null mutant but not in wild-type cells. These results suggest that iron-dependent processes might be targets of Mn(II) toxicity (Fig. A1.1). We also tested the effects of FrvA induction on Zn(II) intoxication using a double efflux mutant (e. g. *cadA czcD*). Higher resistance but not sensitivity to Zn(II) was observed with higher expression of FrvA. This is consistent with the previous observations that FrvA expression rescues the sensitivity phenotype to Zn(II) in this double mutant (Pi *et al.*, 2016) and that FrvA ATPase activity is stimulated by Zn(II), suggesting that Zn(II) can be exported by FrvA.

Next we asked whether this increase sensitivity to Co(II) and Mn(II) caused by iron limitation are additive. Three pairs of strains were tested by monitoring their growth in either one or both metals: (i) WT vs P_{spac}-*frvA*; (ii) *mntR* vs *mntR* P_{spac}-*frvA*; (iii) *czcD* vs *czcD* P_{spac}-*frvA*. All three pairs showed increased sensitivity when both metals are present compared to either one alone, particularly when FrvA is induced to deprive intracellular iron pools, suggesting that the specific targets of Co(II) and Mn(II) intoxication may be different.

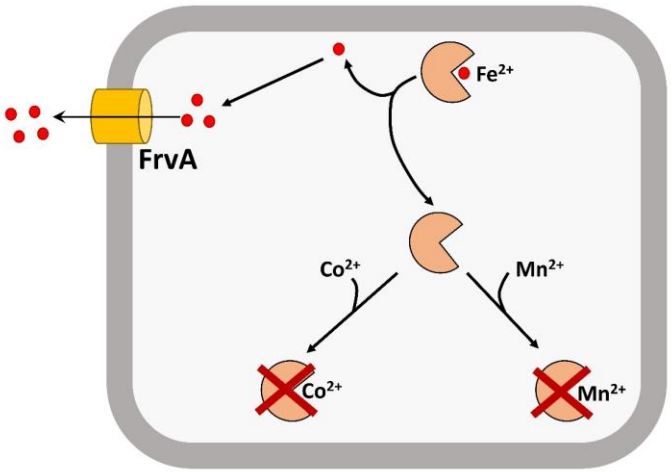

Fig. A1.1 Mismetallation of iron-requiring enzymes by either Co(II) or Mn(II) in case of iron deficiency.
FrvA is a high affinity Fe(II) efflux transporter in *Listeria monocytogenes*. Its expression leads to severe iron deprivation in *B. subtilis*. Some iron-requiring enzymes lose their co-factor in case of iron deficiency. When Co(II) or Mn(II) is present in excess, either metal binds to apo-form of the enzyme resulting in enzyme inactivation or malfunction.

A1.2.2 Isolation of Co(II) resistant suppressors in *czcD* and *czcD* P_{spac}-*frvA* strains

To identify potential targets of Co(II) intoxication and genes involved in Co(II) resistance, we isolated Co(II) resistant mutants in a *czcD* null mutant background without or with different levels of FrvA induction using Mariner transposon mutagenesis. Colonies resistant to toxic levels of Co(II) were isolated and the location of the transposon insertions was identified. In a *czcD* null mutant background, we isolated 12 individual hits in the *yhdQP* operon. The gene *yhdQ* encodes a MerR family transcriptional regulator and *yhdP* encodes a putative magnesium efflux transporter. When a moderate level of FrvA (with 100 µM IPTG) is expressed to deplete intracellular iron pools in the *czcD* null mutant background, multiple suppressors were isolated with transposon insertion in *putP*, *ymfF*, *queF, yhdP*, and *ybaF*. We reasoned higher induction of FrvA (with 1 mM IPTG) would severely deprive the intracellular iron pools and enhance the susceptibility of the *czcD* null mutant to Co(II) intoxication. Then we performed the selection again using 1 mM IPTG to induce higher expression of FrvA in the *czcD* null mutant. Unfortunately, among 16 resistant suppressors isolated, the majority of the transposon mutants (12 out of 16) lost the cm^R cassette along with P_{spac}-*frvA*. A few other suppressors were isolated with transposon insertion in *yhdP*, *yvrB*, *fur*, and *ybcF*.

A1.2.3 Isolation of Mn(II) resistant suppressors

To identify potential targets of Mn(II) intoxication and genes involved in Mn(II) resistance, we isolated Mn(II) resistant mutants in a *mntR* null mutant harboring an ectopic copy of *frvA* with moderate induction (100 µM IPTG) using Mariner transposon mutagenesis. Colonies resistant to toxic levels of Mn(II) were isolated and the location of the transposon insertions was identified. All sixteen resistant suppressors isolated showed transposon insertion at different sites within the *mntH* gene, which encodes the proton-dependent NRAMP family transporter MntH. This is consistent with our previous assignment of MntH as the major Mn(II) transporter under high Mn(II) conditions (Que & Helmann, 2000). A merodiploid construct with a second copy of *mntH* with its native promoter would be useful to identify the targets of Mn(II) toxicity and genes important for Mn(II) homeostasis besides MntH. However, we were unable to make such construct probably due to protein toxicity as the recombinant protein may play an unnecessary and detrimental function in the host *E. coli* cells. We reasoned a *mntR mntH* double mutant would work likewise. Interestingly, among 9 resistant suppressors selected from this double mutant, seven of them showed transposon insertion in the *yhdQP* operon, one in *yeaD*, which encodes an unknown protein, and one in 5' UTR region of *mgtE* riboswitch. Then we performed the selection again in the *mntR mntH* double mutant with moderate expression of FrvA (100 µM IPTG), and found that the majority of the transposon mutants lost the chloramphenicol drug cassette along with P_{spac}-*frvA*. Only two other resistant suppressors were isolated, one has transposon insertion in 5' UTR region of *mgtE* riboswitch (at different site from the one mentioned above) and the other in *yhdQ*.

Altogether, we isolated more than twenty independent suppressors with transposon insertions in the *yhdQP* operon from four different genetic backgrounds under various conditions (Table A1.1). YhdP is a homolog of the putative Mg(II) efflux transporter CorC in *E. coli*. In fact, the mutational disruption of *yhdP* led to an increased level of intracellular Mg(II) and rescued the growth defects caused by the lack of

Table A1.1 Isolated Co(II) and Mn(II) resistant suppressors

Background	Selection conditions	Total # of unique hits	Target gene
czcD P_{spac}-*frvA*	400 μM Co(II) 100 μM IPTG 5 μg ml^{-1} chloramphenicol 15 μg ml^{-1} kanamycin	1	*putP*
		1	*ymfF*
		1	*queF*
		1	*yhdP*
		1	*ybaF*
czcD P_{spac}-*frvA*	400 μM Co(II) 1 mM IPTG 5 μg ml^{-1} chloramphenicol 15 μg ml^{-1} kanamycin	12	*frvA*
		1	*yhdP*
		1	*yvrB*
		1	*fur*
		1	*ybcF*
czcD	400 μM Co(II) 15 μg ml^{-1} kanamycin	12	*yhdQP* operon
mntR P_{spac}-*frvA*	75 μM Mn(II) 100 μM IPTG 5 μg ml^{-1} chloramphenicol 15 μg ml^{-1} kanamycin	16	*mntH*
MntR mntH	200 μM Mn(II) 15 μg ml^{-1} kanamycin	5	*yhdP*
		2	*yhdQ*
		1	*yeaD*
		1	MgtE riboswitch
MntR mntH P_{spac}-*frvA*	200 μM Mn 100 μM IPTG 5 μg ml^{-1} chloramphenicol 15 μg ml^{-1} kanamycin	1	MgtE riboswitch
		1	*yhdQ*
		Note: the majority of the transposon mutants lost the cm^R cassette along with P_{spac}-*frvA*.	

the ribosomal protein L34, indicating that YhdP may function as a magnesium efflux transporter (Akanuma *et al.*, 2014). Indeed, its homolog confers high Mg(II) tolerance in *Staphylococcus aureus* (Armitano et al., 2016). So next we focus on characterizing the physiological role of this transporter and understanding its regulation.

A1.2.4 A *yhdP* transposon suppressor confers resistance to Co(II) in *B. subtilis*

Mutations in metal ion import or export systems often result in decreased or increased sensitivity to the transported metal ions, respectively. To understand the physiological role of YhdP, a disk diffusion assay was performed to check the effects of the *yhdP* transposon-disruption in the wild-type background on sensitivity to various metals. The results revealed that this disruption increased resistance to Co(II) but not other metals (Fig. A1.2). Similar results were observed in *czcD* P_{spac}-*frvA* and *czcD* null mutants, suggesting YhdP might be involved in Co(II) import or efflux of certain metal required for Co(II) intoxication targets (e.g. Mg(II)). It is more likely to be the latter as discussed in the prior section (Akanuma et al., 2014;Armitano et al., 2016). So next we set out to test this idea.

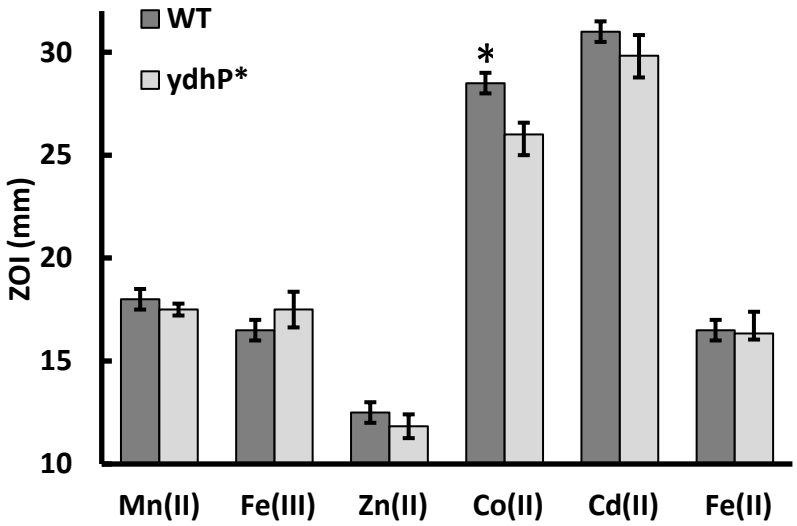

Fig. A1.2 A *yhdP* transposon suppressor confers resistance to Co(II).

Sensitivity of WT and a *yhdP* transposon-disrupted mutant to metal ion stress were monitored using a disk diffusion assay. Data are expressed as the diameter of the inhibition zone (mm).

A1.2.5 YhdP plays an important role in high Mg(II) tolerance

The first gene (*yhdQ*) in the same operon as *yhdP* encodes a MerR family regulator and may regulate transcription of this transporter or work together with YhdP. To evaluate their potential role in Mg(II) efflux, a growth curve assay was performed. Indeed, the results revealed that both *yhdP* and *yhdQ* single mutants are severely compromised in growth under high Mg(II) conditions (300 mM Mg(II)) compared to the wild type cells (Fig. A1.3), suggesting that both of them are involved in high Mg(II) tolerance and YhdQ may function as a positive regulator.

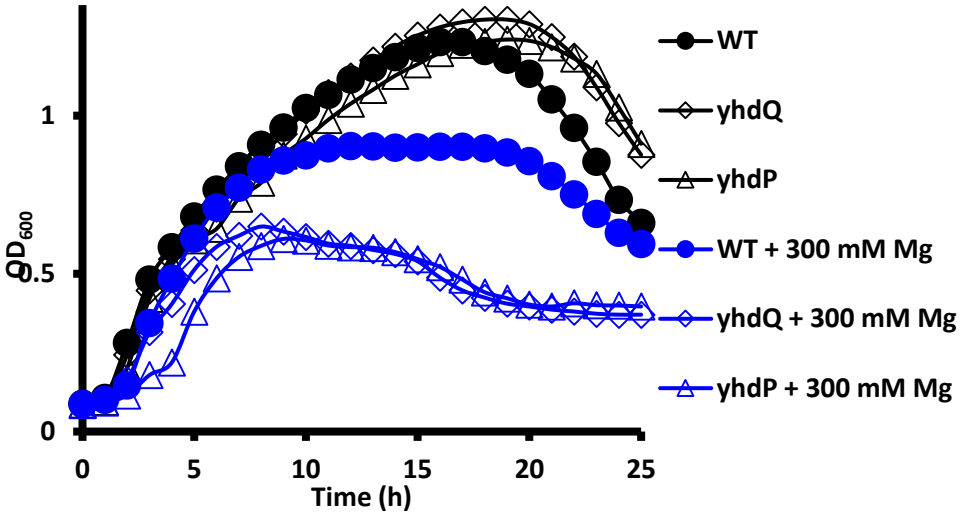

Fig. A1.3 YhdP and YhdQ are involved in high Mg(II) tolerance.
Representative growth curves of WT, *ydhP*, and *yhdQ* single mutants grown in LB without or with addition of 300 mM Mg(II).

A1.2.6 A *yhdP* null mutant accumulates high levels of intracellular Mg(II)

To further understand the physiological role of YhdP, we monitored the intracellular metal levels before and after addition of 10 mM of Mg(II) into LB medium using inductively coupled plasma mass spectrometry (ICP-MS). The *yhdP* null mutant accumulates significantly higher amount of Mg(II) compared to WT during the course of the experiment (Fig. A1.4). However, the difference between the two strains did not change dramatically after addition of 10 mM magnesium, suggesting that 10 mM magnesium

might not be essentially high enough to stress the cells and much higher concentration of Mg(II) should be used for future studies. It is important to note that the intracellular levels of other metals such as Mn, Fe, Zn, Co were also compared between the *yhdP* null mutant and WT but no significant differences were observed during the course of the experiments (Fig. A1.4). These results suggest that YhdP may function as a Mg(II) efflux transporter, although more experiments are needed to confirm its physiological role.

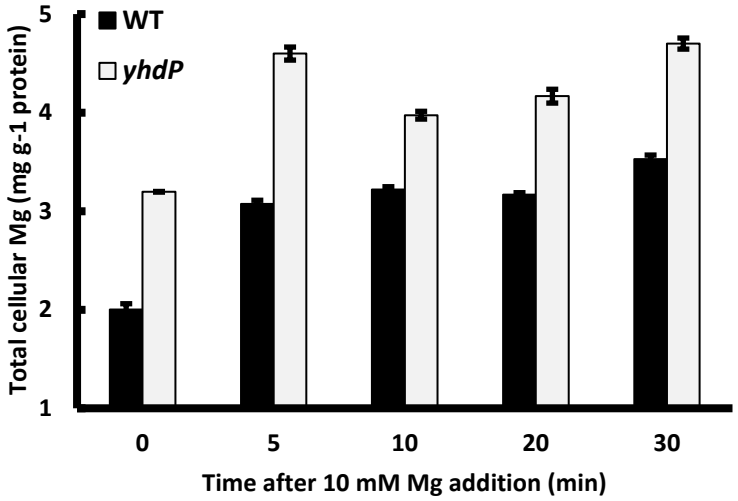

Fig. A1.4 A *yhdP* null mutant accumulates high levels of intracellular Mg(II).
Cells were grown in LB medium to an OD_{600} of ~0.4 and 10 mM Mg(II) was amended into the medium afterwards. Levels of intracellular Mg, Mn, Fe, Co, and Zn were monitored by inductively coupled plasma mass spectrometry (ICP-MS).

A1.2.7 *yhdP* is regulated by YhdQ in response to Mg(II)

If YhdP functions as a Mg(II) efflux, its gene expression would be induced by high Mg(II). Indeed, *yhdP* mRNA levels are elevated 3-fold within 30 min of treatment of 200 mM of Mg(II) and its induction requires the MerR family regulator YhdQ (Fig. A1.5). Its expression was also induced by high levels of Mn(II), Zn(II), and Co(II), implicating that YhdP may be involved in Mg(II) efflux however its metal specificity is rather low. More experiments are needed to confirm its regulation mechanism.

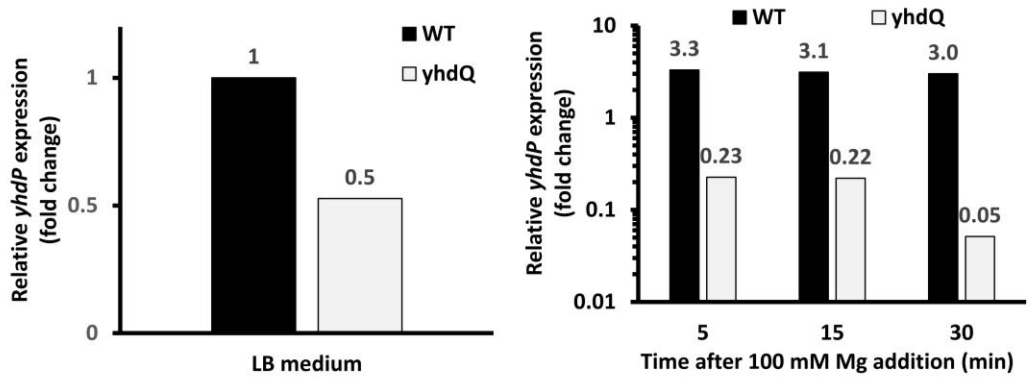

Fig. A1.5 *yhdP* is regulated by YhdQ in response to Mg(II).
Total RNA was extracted from cells harvested at different timepoints as indicated and used for reverse transcription. Quantitative real-time PCR was performed to evaluate mRNA expression levels of *yhdP*.

A1.3 Discussion and future plans

Magnesium is a bulk element and bacteria require millimolar levels of magnesium for growth. However, it is uncompetitive in protein binding compared to many other essential metals (e.g. Zn(II), Co(II), Fe(II), and Mn(II)). So many Mg(II)-dependent enzymes would be at risk in times of elevated levels of other competitive metals such as Co(II) and Mn(II). Indeed, the results show that Mg(II) supplementation in the medium alleviates either Co(II) or Mn(II) intoxication (data not shown). We also show that a *yhdP* null mutant accumulates intracellular Mg(II) and confers resistance to Co(II)/Mn(II) intoxication. These results indicate that Mg(II)-dependent processes may be targets of Co(II) and Mn(II) toxicity in *B. subtilis*. Supportive of this idea, YhdP confers tolerance to high Mg(II) (Fig. A1. 3), suggesting its physiological role as a Mg(II) efflux transporter.

Mg(II) uptake systems are well characterized in many bacteria but it is largely unknown whether bacteria require efflux systems to achieve Mg(II) homeostasis. Future work is needed to (i) to characterize the regulation mechanism of *yhdP* using q-PCR, EMSA, in vitro transcription, and footprinting, (ii) to define the physiological role of YhdP by monitoring intracellular metal levels before and after different metal shock (Co, Mn, and Mg) in WT and *yhdP* null mutant using ICP-MS, and (iii) to understand the roles of

other transposon hits. Some of the hits might be involved in Co(II) homeostasis such as *ybaF* and *yvrB*. YbaF might be a Co(II) importer. YvrB is annotated as a putative vitamin B12 permease. These can be tested using ICP-MS. We also isolated two individual suppressors with transposon insertion in the 5' UTR region of mgtE riboswitch from two different genetic background (Table A1.1). It would be interesting to test whether these transposon-insertion mutations result in upregulation of Mg(II) import using ICP-MS.

It is interesting that one of the suppressors has a transposon insertion in the *fur* gene, resulting in loss of function of this master iron regulator. A *fur* null mutation leads to full derepression of its regulated genes, including various iron uptake systems and the small RNA FsrA that mediates an "iron sparing" response to prioritize iron usage. These suggest that iron-dependent enzymes may be targets of Co(II) toxicity due to competition between these two metals and Co(II) intoxication can be partially rescued by increasing intracellular iron levels. The question is which one, iron uptake or iron sparing, contributes more than the other or whether they are equal contributors. To find out whether competition between Co(II) and Fe(II) is physiologically significant in *B. subtilis*, we can test whether the iron responsive regulator Fur play important role in Co(II) resistance. A metal sensitivity assay can be used to test Co(II) sensitivity in strains: WT, *czcD*, *fur*, and *czcD fur*. If so, we can then dissect the contribution of iron uptake and iron sparing to Co(II) resistance. Overall, this work would provide new insight into homeostasis systems of Co(II) and Mn(II) and intoxication mechanisms of these two metals.

A1.4 References

Aguirre, J.D. & V.C. Culotta, (2012) Battles with iron: manganese in oxidative stress protection. *The Journal of biological chemistry* **287**: 13541-13548.

Akanuma, G., A. Kobayashi, S. Suzuki, F. Kawamura, Y. Shiwa, S. Watanabe, H. Yoshikawa, R. Hanai & M. Ishizuka, (2014) Defect in the formation of 70S ribosomes caused by lack of ribosomal protein L34 can be suppressed by magnesium. *Journal of bacteriology* **196**: 3820-3830.

Armitano, J., P. Redder, V.A. Guimaraes & P. Linder, (2016) An Essential Factor for High Mg2+ Tolerance of Staphylococcus aureus. *Frontiers in microbiology* **7**: 1888.

Barwinska-Sendra, A. & K.J. Waldron, (2017) The Role of Intermetal Competition and Mis-Metalation in Metal Toxicity. *Advances in microbial physiology* **70**: 315-379.

Baumgart, M. & J. Frunzke, (2015) The manganese-responsive regulator MntR represses transcription of a predicted ZIP family metal ion transporter in Corynebacterium glutamicum. *FEMS microbiology letters* **362**: 1-10.

Chandrangsu, P. & J.D. Helmann, (2016) Intracellular Zn(II) Intoxication Leads to Dysregulation of the PerR Regulon Resulting in Heme Toxicity in Bacillus subtilis. *PLoS genetics* **12**: e1006515.

Chandrangsu, P., C. Rensing & J.D. Helmann, (2017) Metal homeostasis and resistance in bacteria. *Nature reviews. Microbiology* **15**: 338-350.

Gaballa, A. & J.D. Helmann, (2003) Bacillus subtilis CPx-type ATPases: characterization of Cd, Zn, Co and Cu efflux systems. *Biometals : an international journal on the role of metal ions in biology, biochemistry, and medicine* **16**: 497-505.

Hohle, T.H. & M.R. O'Brian, (2014) Magnesium-dependent processes are targets of bacterial manganese toxicity. *Molecular microbiology* **93**: 736-747.

Huang, X., J.H. Shin, A. Pinochet-Barros, T.T. Su & J.D. Helmann, (2017) Bacillus subtilis MntR coordinates the transcriptional regulation of manganese uptake and efflux systems. *Molecular microbiology* **103**: 253-268.

Irving, H. & R.J.P. Williams, (1948) Order of Stability of Metal Complexes. **162**: 746.

Kobayashi, M. & S. Shimizu, (1999) Cobalt proteins. *European journal of biochemistry* **261**: 1-9.

Majtan, T., F.E. Frerman & J.P. Kraus, (2011) Effect of cobalt on Escherichia coli metabolism and metalloporphyrin formation. *Biometals : an international journal on the role of metal ions in biology, biochemistry, and medicine* **24**: 335-347.

Moore, C.M., A. Gaballa, M. Hui, R.W. Ye & J.D. Helmann, (2005) Genetic and physiological responses of Bacillus subtilis to metal ion stress. *Molecular microbiology* **57**: 27-40.

Okamoto, S. & L.D. Eltis, (2011) The biological occurrence and trafficking of cobalt. *Metallomics : integrated biometal science* **3**: 963-970.

Pandey, R., R. Russo, S. Ghanny, X. Huang, J. Helmann & G.M. Rodriguez, (2015) MntR(Rv2788): a transcriptional regulator that controls manganese homeostasis in Mycobacterium tuberculosis. *Molecular microbiology* **98**: 1168-1183.

Pi, H., S.J. Patel, J.M. Arguello & J.D. Helmann, (2016) The Listeria monocytogenes Fur-regulated virulence protein FrvA is an Fe(II) efflux P1B4 -type ATPase. *Molecular microbiology* **100**: 1066-1079.

Que, Q. & J.D. Helmann, (2000) Manganese homeostasis in Bacillus subtilis is regulated by MntR, a bifunctional regulator related to the diphtheria toxin repressor family of proteins. *Molecular microbiology* **35**: 1454-1468.

Ranquet, C., S. Ollagnier-de-Choudens, L. Loiseau, F. Barras & M. Fontecave, (2007) Cobalt stress in Escherichia coli. The effect on the iron-sulfur proteins. *The Journal of biological chemistry* **282**: 30442-30451.

Thorgersen, M.P. & D.M. Downs, (2007) Cobalt targets multiple metabolic processes in Salmonella enterica. *Journal of bacteriology* **189**: 7774-7781.

Torrents, E., (2014) Ribonucleotide reductases: essential enzymes for bacterial life. *Frontiers in cellular and infection microbiology* **4**: 52.

Valko, M., H. Morris & M.T. Cronin, (2005) Metals, toxicity and oxidative stress. *Current medicinal chemistry* **12**: 1161-1208.

Veyrier, F.J., I.G. Boneca, M.F. Cellier & M.K. Taha, (2011) A novel metal transporter mediating manganese export (MntX) regulates the Mn to Fe intracellular ratio and Neisseria meningitidis virulence. *PLoS pathogens* **7**: e1002261.

Waldron, K.J. & N.J. Robinson, (2009) How do bacterial cells ensure that metalloproteins get the correct metal? *Nature reviews. Microbiology* **7**: 25-35.

Waters, L.S., M. Sandoval & G. Storz, (2011) The Escherichia coli MntR miniregulon includes genes encoding a small protein and an efflux pump required for manganese homeostasis. *Journal of bacteriology* **193**: 5887-5897.

Appendix 2 Genome-wide identification of Fur-binding sites expands the Fur regulon in *Bacillus subtilis*

A2.1 Introduction

Fur, ferric uptake regulator, is the key regulator of iron homeostasis in many bacteria, including *Bacillus subtilis*, in which the Fur regulon is well defined. However, a few recent studies showed that, besides iron metabolism, the Fur regulatory network might encompass many other biological processes such as DNA synthesis, energy metabolism, and biofilm formation (Seo *et al.*, 2014, Davies *et al.*, 2011, Butcher *et al.*, 2011, Chumsakul *et al.*, 2017), although further experimental work is required for validation. Furthermore, Sang et al. proposed three regulatory modes by Fur: holo-Fur repression, holo-Fur activation, and apo-Fur activation (Seo *et al.*, 2014). Typically, Fur is considered to function as an iron-activated transcriptional repressor for most of its regulated genes, and there are a few examples where holo-Fur functions as a transcriptional activator (Pi *et al.*, 2016, Delany *et al.*, 2004, Nandal *et al.*, 2010), For instance, Fur_{EC} positively regulates expression of the iron storage gene *ftnA* through competing against the H-NS repressor at elevated iron levels (Nandal *et al.*, 2010); Fur positively regulates the ferrous iron efflux transporter FrvA in *Listeria mononcytogenes* (Pi *et al.*, 2016). However, no experimental evidence is supportive of apo-Fur activation yet. These motivated us to obtain a genomic view of the Fur regulatory network in *B. subtilis*.

Here, we identified the genome-wide DNA binding sites *in vivo* by Fur in response to iron availability using chromatin immunoprecipitation coupled with high-throughput sequencing (ChIP-seq) as described in Fig. A2.1. Briefly, proteins are cross-linked to DNA that they are bound to *in vivo* using 1% formaldehyde. After shearing the DNA by sonication, a protein of interest (POI), in this case FLAG-tagged Fur, is extracted

along with the cross-linked DNA fragments from the cell-lysate using α-FLAG M2 magnetic agarose beads and then subjected to reverse crosslinking by incubation at 65 ^{0}C overnight. After DNA library preparation, the short stretches of DNA bound to Fur are identified by high-throughput *seq*uencing. All the Fur-binding sites were then visualized using a shape-based peak caller of the CLC Genomics Workbench.

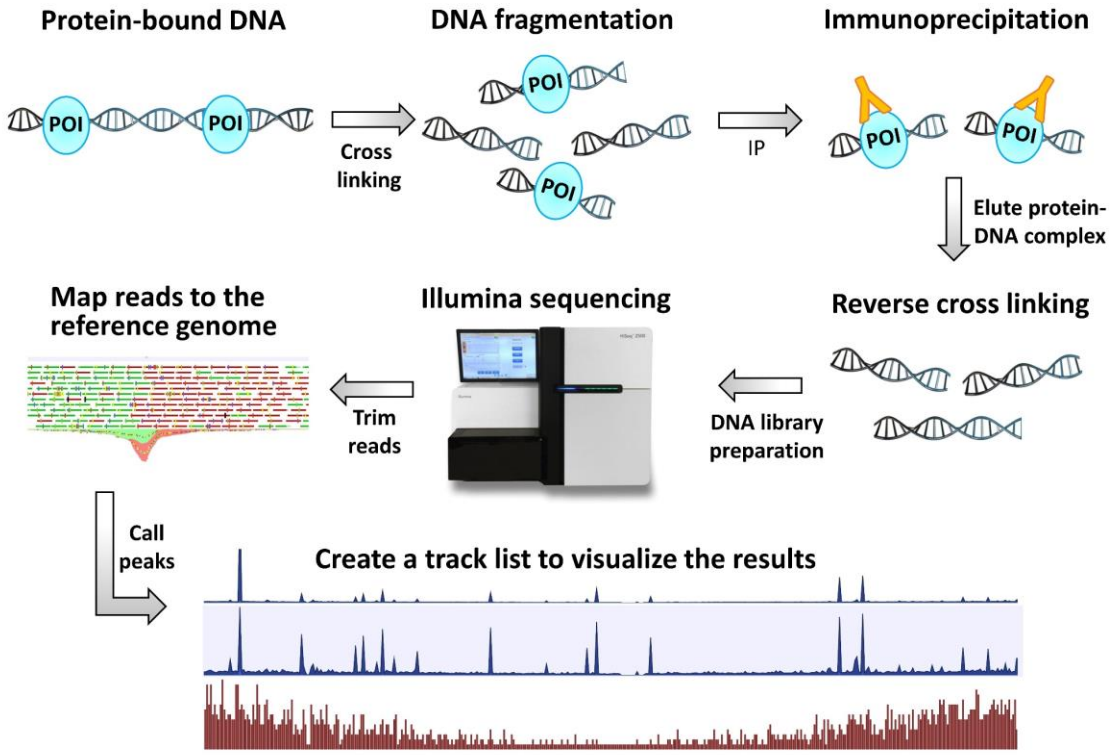

Fig. A2.1 Overview of ChIP-seq (chromatin immunoprecipitation coupled with high-throughput sequencing). α-FLAG M2 magnetic agarose beads (Sigma, Cat# M8823) were used for immunoprecipitation and the protein–DNA complexes were eluted with 3X FLAG peptide according to the manufacture's protocol. POI, protein of interest.

A2. 2 Results and discussion

A2.2.1 Genome-wide identification of Fur-binding sites by ChIP-seq

We utilized FrvA as an inducible iron starvation tool as described previously (Pi & Helmann, 2017). *Bacillus* wild-type cells harboring an ectopic copy of *frvA* were grown in LB medium amended with 25 µM iron to ensure Fur repression (Pi & Helmann, 2017). After the cell culture reaches OD_{600} of ~0.25, an aliquot

of cell culture was harvested to study holo-Fur regulation. Then 1 mM IPTG was added to the cell culture to induce expression of FrvA. Within 30 min of IPTG treatment, FrvA deprives intracellular iron pools, and most of Fur loses its cofactor iron and falls off the target DNA as confirmed by ChIP-qPCR in the prior study (Pi & Helmann, 2017). We thus harvest cells at this timepoint to study apo-Fur regulation. Fur binding sites were mapped in a genome-wide manner in *B. subtilis* using ChIP-seq under iron sufficient (holo) and deficient (apo) conditions as indicated (Fig. A2.2). A large number of peaks were identified for each sample using a shape-based peak caller of the CLC Genomics Workbench.

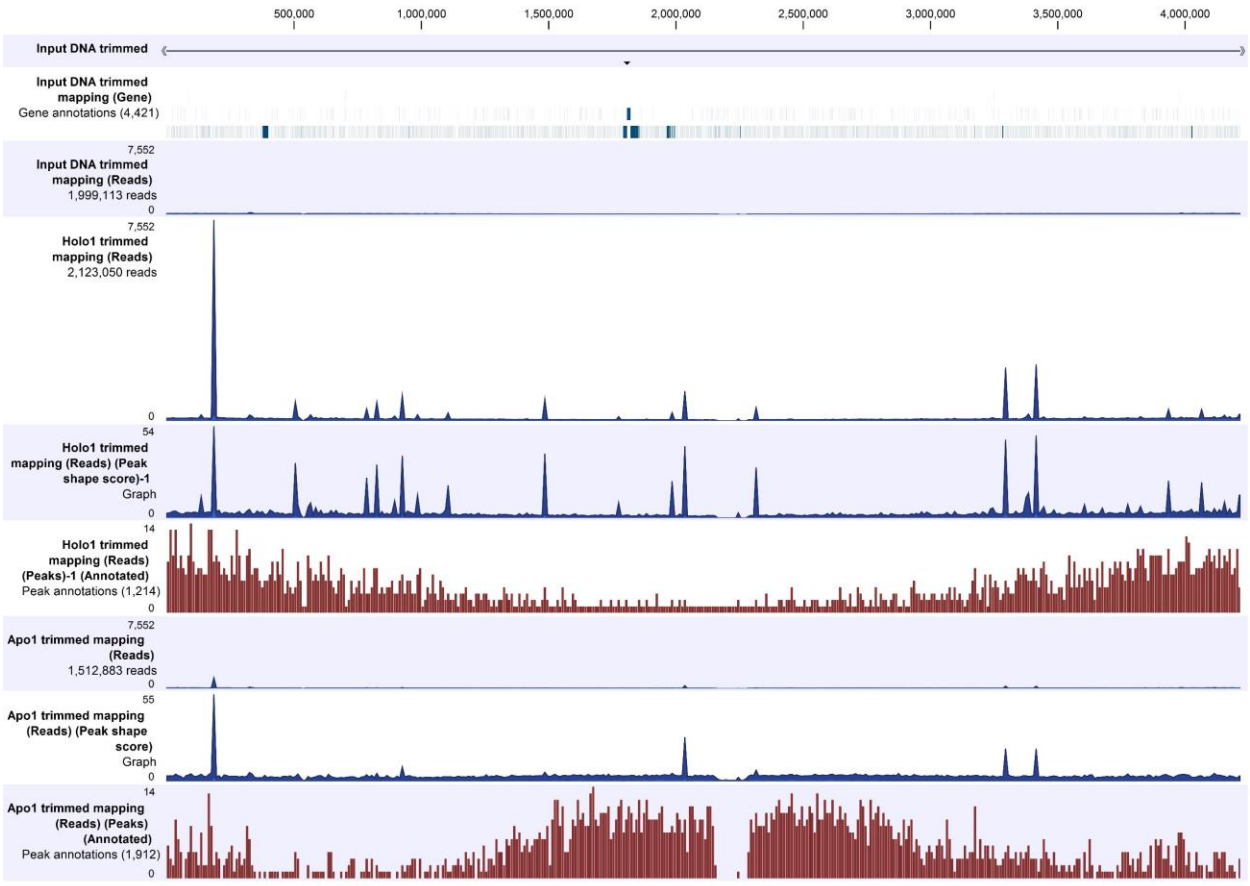

Fig. A2.2 Identification of Fur binding sites by ChIP-seq.
The tracks shown are (from top to bottom): *B. subtilis* genome (input DNA), gene mapping (input DNA), reads (input DNA), reads (holo-fur binding), peak shape score (holo-fur), peak annotation (holo-fur), reads (apo-fur binding), peak shape score (apo-fur), and peak annotation (apo-fur). All the reads are set as the same scale for each individual peak.

Table A2.1. New putative Fur-regulated targets

Genes	Fur box	Relative expression (*fur*/WT)	DP sensitivity	Function
ybaC	Half-boxes	NS	NS	probable aminopeptidase
ydeE ydeF	13/15	NS	NS	YdeF, similar to transcriptional regulator (MocR/ GabR family); YdeE, similar to transcription factor (AraC family)
catD	13/15	5-fold upregulation(qPCR)	More sensitive	Essential for viability in the presence of catechol and may be involved in catechol detoxification
cspB yhcJ	12/15	4-fold downregulation *cspB* (microarray)	More sensitive (both)	YhcJ, unknown, similar to ABC transporter (binding lipoprotein); CspB, major cold-shock protein, RNA chaperone
ymcB	13/15	2-fold down (Microarray)	NS	tRNA maturation, tRNA methylthiotransferase (Fe-S cluster protein)
ppsB	11/15, 10/15	3-fold down (Microarray)	NS	production of the antibacterial compound plipastatin
yufS	12/15, 11/15	NS	NS	unknown
gidA	half-boxes	2-fold down (microarray)	More sensitive	tRNA uridine 5-carboxymethylaminomethyl modification enzyme
yvlA	11/15, 11/15	3-fold down (microarray)	NS	unknown
narJ	10/15, half-boxes	3-fold down (qPCR) 9-fold down (Microarray)	More sensitive	chaperone for the nitrate reductase (NarGHI), under positive regulation of Fnr.
gntR	11/15	3-fold down (Microarray)	NS	transcriptional repressor of the gluconate operon (*gntR-gntK-gntP-gntZ*)
glxK	11/15	NS	NS	putative glycerate kinase
yycE	11/15, 10/15	NS	NS	YycD, unknown; PurA, purine biosynthesis
yybN	12/15, 11/15	NS	More sensitive	unknown, belongs to Rok regulon & DnaA regulon (*yybN-yybM-yybL-yybK-yybJ*)

Note: Sensitivity to high Fe(II) was also tested in all these mutants but no significant phenotype was observed. NS, not significant.

A2.2.2 Identification of new holo-Fur binding sites

The signals from two independent experiments were processed and 40 peaks were selected using a cutoff value of 5 for holo-Fur binding. Most of the known Fur target sites are included with a few exceptions. Twenty-two new sites were identified. The ones I have worked on are listed in Table A2.1. Many of them are quite interesting. Some Fur binding sites are located in the intragenic regions. For

instance, a binding site was identified in the middle of *ppsB*, responsible for production of the antibacterial compound plipastatin. Two putative Fur boxes were identified with 10 or 11 out of 15 bases matching the consensus sequence. Fur binds some small RNAs besides FsrA. For example, Fur binds 5'UTR region of *mrpA*, where a new RNA feature is annotated. MrpA is the Na transporter subunit of the Na /H antiporter and is involved in multiple resistance and pH homeostasis. Two putative Fur boxes were identified in this binding site with 11 or 12 out of 15 bases matching the consensus sequence. It is possible that Fur is involved in pH homeostasis through this small RNA. Some of the putative Fur targets are involved in iron homeostasis, as judged by the high sensitivity to dipyridyl (Table A2.1). These include *catD, cspB, yhcJ, gidA, narJ, yybN*. *catD* is the first gene in a two-gene operon along with *catE*. Future work will be needed to validate each of them.

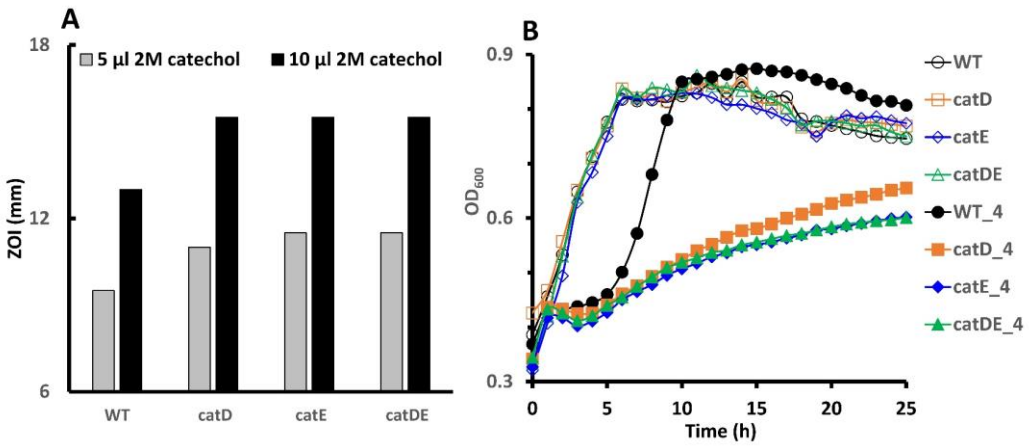

Fig. A2.3 CatDE are crucial for catechol detoxification.
Sensitivity of the wild-type and mutant strains to catechol was evaluated using a disk diffusion assay (A) and bioscreen assay (B).

A2.2.3 Catechol detoxification by CatDE upon iron limitation

CatE encodes a putative catechol 2,3-dioxygenase and require Fe(II) as its cofactor. CatD may be the membrane component. Both are essential for viability in the presence of catechol and may be involved in catechol detoxification, as judged by the sensitivity of either single mutant or double mutant to catechol

intoxication using both disk diffusion and bioscreen growth assays (Fig. A2. 3). A Fur box (13 out of 15 bases match the consensus sequence) is located downstream of the transcription start site, suggesting Fur may act as a repressor. To test this, qPCR was performed. Indeed, expression of *catD* is upregulated 5-fold in the *fur* null mutant compared to wild-type cells (Fig. A2.3). More interestingly, its expression is induced ~2-fold in the presence of dipyridyl. The question is why *catD* is induced under iron limitation. Two possibilities exist: (i) to ensure sufficient enzymatic activity when iron is limiting since *catDE* may encode an Fe(II)-dependent 2,3-dioxygenase; (ii) the enzymatic activity is required to detoxify catechol in times of iron limitation. The latter may connect bacillibactin (a catecholate siderophore) metabolism and catechol detoxification, although further study is needed to dissect the correlation.

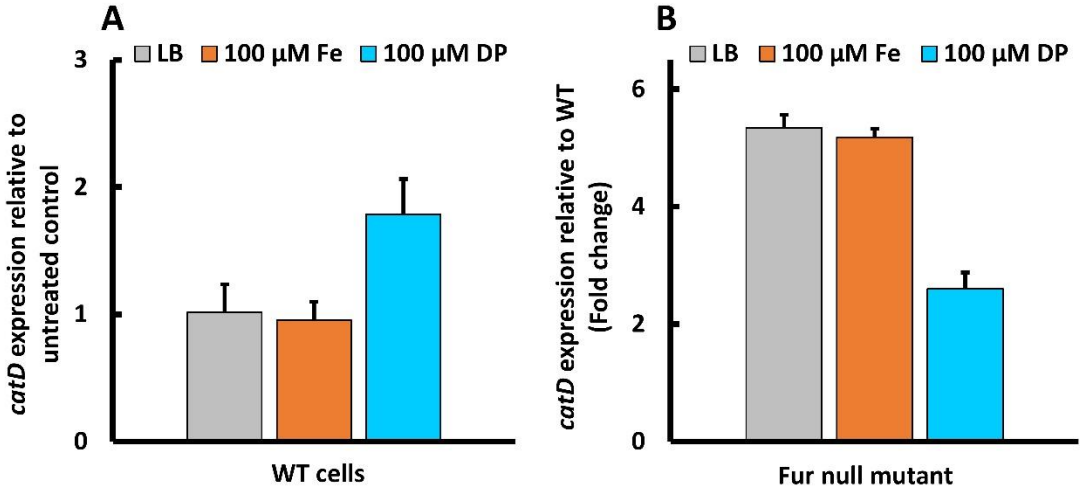

Fig. A2.4 Expression of *catD* is repressed by Fur.

The mRNA levels of *catD* was monitored by qPCR in wild-type (A) and *fur* null mutant cells (B) grown in LB, LB + 100 µM Fe(II), or LB + 100 µM dipyridyl.

A2. 3 Discussion and future plans

The ferric uptake regulator plays a central role in bacterial iron homeostasis and might control other biological processes. A GeF-seq (genome footprinting coupled with high-throughput sequencing) was performed under anaerobic fermentative growth conditions and revealed some new binding sites in

B. subtilis (Chumsakul et al., 2017). However, most of the new binding peaks are indicated as small numbers compared to the known sites. For instance, the binding peak is indicated as 3 for the site in the promoter region of *catD* while 317 for the binding site of *ykuN* (Chumsakul et al., 2017). So it is difficult to tell whether these new sites are significant. Furthermore, no experimental validation was carried out for any of these new sites yet. ChIP-seq is a powerful technique to identify genes regulated by a transcription regulator in a genome-wide manner. Here we identified a list of Fur binding sites *in vivo* under varied iron conditions using ChIP-seq. Initial analysis showed that all the known Fur binding sites are included in the list, validating the modified method of ChIP-seq in *B. subtilis*.

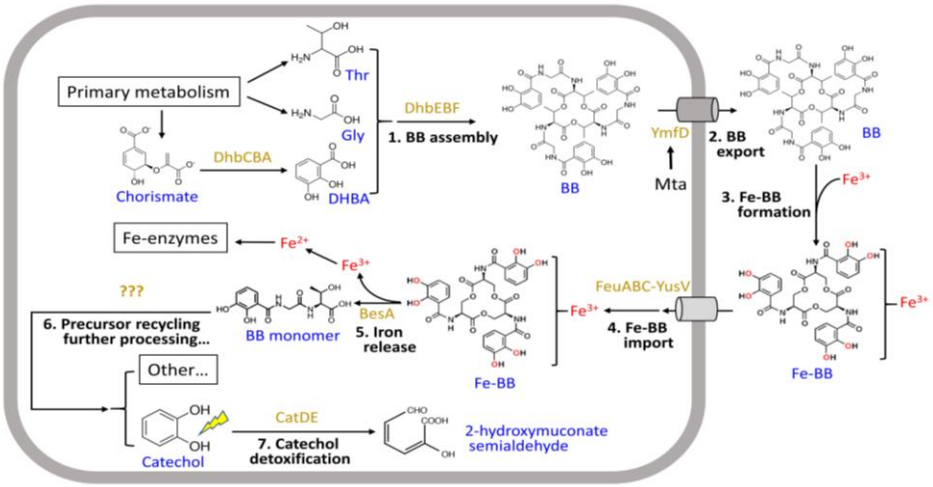

Fig. A2. 5 Correlation between bacillibactin metabolism and catechol detoxification

The endogenous siderophore bacillibactin (BB) is synthesized by an NRPS (non-ribosomal peptide synthetase) assembly system (DhbACEBF) and secreted by YmfD, a major facilitator superfamily transporter. It chelates iron with very high affinity and the resultant ferric-siderophore complex is then imported back into the cytosol by the FeuABC-YusV system and hydrolyzed by the BesA esterase to release iron. It is unknown how the BB monomer is further processed and it might require CatDE for catechol detoxification during this process.

The ultimate goals of this study are to (i) identify new Fur targets, (ii) validate these new sites using a range of assays such as EMSA, 5'-RACE, and in vitro transcription, (iii) characterize the regulation mechanism of these new targets, (iv) further define the physiological roles of these new targets, (v)

comprehensively understand the Fur regulatory network in *B. subtilis*. Among all the new sites detected, the Fur binding site located in the promoter region of the *catDE* operon is of particular interest. It is known that *catDE* is strongly induced by catechol (Tam le *et al.*, 2006). Consistent with this, our results show this operon is critical for catechol detoxification (Fig. A2. 3). This operon is under negative regulation of CatR, a MarR/DUF24 family transcription regulator, and YodB, a regulator important for quinone and diamide detoxification (Chi *et al.*, 2010). Our results show it is also repressed by Fur (Fig. A2. 4). Future work is needed to dissect how these three regulators interact with one another and control expression of this operon under different conditions. A genetic study can be performed using single, double, and triple deletion mutants of these three regulators to understand the interconnections. Furthermore, the *catDE* operon is induced upon iron limitation (Fig. A2. 3) and cells lacking either of these two genes become more sensitive to dipyridyl (data not shown), which very likely links catechol detoxification to metabolism of the catecholate siderophore bacillibactin (Fig. A2. 5). Genetic analysis will be very useful to characterize this correlation. For example, when iron is limiting, cells synthesize bacillibactin (BB) to scavenge iron. BB will accumulate in the cell if the BB efflux transporter YmfD is absent. We can then test whether CatDE is critical for catechol detoxification and cell survival under these conditions.

A2.4 References

Butcher, B.G., P.A. Bronstein, C.R. Myers, P.V. Stodghill, J.J. Bolton, E.J. Markel, M.J. Filiatrault, B. Swingle, A. Gaballa, J.D. Helmann, D.J. Schneider & S.W. Cartinhour, (2011) Characterization of the Fur regulon in Pseudomonas syringae pv. tomato DC3000. *Journal of bacteriology* **193**: 4598-4611.

Chi, B.K., K. Kobayashi, D. Albrecht, M. Hecker & H. Antelmann, (2010) The paralogous MarR/DUF24-family repressors YodB and CatR control expression of the catechol dioxygenase CatE in Bacillus subtilis. *Journal of bacteriology* **192**: 4571-4581.

Chumsakul, O., D.P. Anantsri, T. Quirke, T. Oshima, K. Nakamura, S. Ishikawa & M.M. Nakano, (2017) Genome-Wide Analysis of ResD, NsrR, and Fur Binding in Bacillus subtilis during Anaerobic Fermentative Growth by In Vivo Footprinting. *Journal of bacteriology* **199**.

Davies, B.W., R.W. Bogard & J.J. Mekalanos, (2011) Mapping the regulon of Vibrio cholerae ferric uptake regulator expands its known network of gene regulation. *Proc Natl Acad Sci U S A* **108**: 12467-12472.

Delany, I., R. Rappuoli & V. Scarlato, (2004) Fur functions as an activator and as a repressor of putative virulence genes in Neisseria meningitidis. *Molecular microbiology* **52**: 1081-1090.

Nandal, A., C.C. Huggins, M.R. Woodhall, J. McHugh, F. Rodriguez-Quinones, M.A. Quail, J.R. Guest & S.C. Andrews, (2010) Induction of the ferritin gene (ftnA) of Escherichia coli by Fe(2+)-Fur is mediated by reversal of H-NS silencing and is RyhB independent. *Molecular microbiology* **75**: 637-657.

Pi, H. & J.D. Helmann, (2017) Sequential induction of Fur-regulated genes in response to iron limitation in Bacillus subtilis. *Proc Natl Acad Sci U S A*.

Pi, H., S.J. Patel, J.M. Arguello & J.D. Helmann, (2016) The Listeria monocytogenes Fur-regulated virulence protein FrvA is an Fe(II) efflux P1B4 -type ATPase. *Molecular microbiology* **100**: 1066-1079.

Seo, S.W., D. Kim, H. Latif, E.J. O'Brien, R. Szubin & B.O. Palsson, (2014) Deciphering Fur transcriptional regulatory network highlights its complex role beyond iron metabolism in Escherichia coli. *Nature communications* **5**: 4910-4910.

Tam le, T., C. Eymann, D. Albrecht, R. Sietmann, F. Schauer, M. Hecker & H. Antelmann, (2006) Differential gene expression in response to phenol and catechol reveals different metabolic activities for the degradation of aromatic compounds in Bacillus subtilis. *Environmental microbiology* **8**: 1408-1427.